Imperial College London

Natural Environment Research Council

Valorisation of unconventional lignocellulosic biomass into bioenergy and bioproducts using ionic-liquid based technologies

Louis Henri Marius Hennequin

Thesis submitted for the degree of Doctor of Philosophy (PhD)

Department of Chemical Engineering

Imperial College of London

2022

Supervised by Professor Jason Hallett and Professor Paul Fennell

Science and Solutions for a Changing Planet

Grantham Institute Climate Change and the Environment

Declaration of Originality and Copyright

The entirety of the work described in this thesis was carried out at Imperial College London between June 2017 and December 2021. Unless otherwise stated the work is my own and has not been submitted previously for a degree at this or another university.

Copyright
The copyright of this thesis rests with the author and is made available under a Creative Commons Attribution Non-Commercial No Derivatives licence. Researchers are free to copy, distribute or transmit the thesis on the condition that they attribute it, that they do not use it for commercial purposes and that they do not alter, transform, or build upon it. For any reuse or redistribution, researchers must make clear to others the licence terms of this work.

Publications

The following publications are a result of original work as a PhD candidate during that time:

1. **Hennequin LM**, Levers O, Hallett JP. Ionic Liquids as Solvents for the Production of Materials from Biomass. In: Encyclopedia of Ionic Liquids. Singapore: Springer; 2019. Available from: doi.org/10.1007/978-981-10-6739-6_50-1.
2. Gschwend FJV, **Hennequin LM**, Brandt-Talbot A, Bedoya-Lora F, Kelsall GH, Polizzi K, et al. Towards an environmentally and economically sustainable biorefinery: heavy metal contaminated waste wood as a low-cost feedstock in a low-cost ionic liquid process. Green Chem. 2020 Aug 3;22(15):5032–41. Available from: doi.org/10.1039/D0GC01241F.
3. **Hennequin LM**, Polizzi K, Fennell PS, Hallett JP. Rhododendron and Japanese Knotweed: Invasive species as innovative crops for second generation biofuels for the ionoSolv process. RSC Adv. 2021 May 19;11(30):18395–403. Available from: doi.org/10.1039/D1RA01943K.
4. Sas E*, **Hennequin LM***, Frémont A, Jerbi A, Legault N, Lamontagne J, et al. Biorefinery potential of sustainable municipal wastewater treatment using fast-growing willow. Sci Total. 2021;792:148146. Available from: doi.org/10.1016/j.scitotenv.2021.148146.
5. **Hennequin LM**, Tan S yin, Jensen E, Fennell P, Hallett JP. Combining phytoremediation and biorefinery: Metal extraction from lead contaminated Miscanthus during pretreatment using the ionoSolv process. Ind Crops Prod. 2022;176:114259. Available from: doi.org/10.1016/j.indcrop.2021.114259.
6. **Hennequin LM***, Kim S*, Monroe EA, Eckles TP, Beck N, Mays WD, et al. Reclamation of nutrients, carbon, and metals from compromised surface waters fated to the Salton Sea: Biomass production and ecosystem services using an attached periphytic algae flow-way. Algal Res. 2022;66:102757. Available from: doi.org/10.1016/j.algal.2022.102757.

* *first co-authors*

Award for Best Presentation at the Tsinghua Environmental Remediation Conference 2019.

Abstract

In order to transition energy use away from fossil fuels, the transformation of renewable lignocellulosic biomass needs to be improved and its supply of sustainable bioenergy into a wider bioeconomy increased. Achieving this will require: (1) renewable, cheap and high-quality lignocellulosic feedstocks, (2) a robust process to transform this feedstock into bioenergy and finally (3) a system to recover and use this bioenergy as well as value-added products.

In this PhD, multiple examples were used to explore unconventional feedstocks, novel transformation processes and opportunities for value-added products. Feedstocks ranging from invasive species threatening the UK environment, Rhododendron and Japanese Knotweed (Chapter 3), metal contaminated waste wood (Chapter 4), metal enriched biomass grown on marginal land (Chapter 5), and wastewater irrigated willow, a leading dedicated bioenergy crop (Chapter 6).

While conventional bioenergy systems often burn wood pellets for energy co-generation, the innovative transformation process of ionic liquid-based technologies are explored as flexible enough to fractionate unconventional biomass feedstocks and deliver high yields of sustainable bioenergy and bioproducts. This was allowed by the unique and tuneable properties of protic ionic liquids. Here dimethylbutyl-hydrogen sulphate - [DMBA][HSO_4], a cheap hydrogen sulphate [HSO_4]$^-$ based ionic liquid, and 1-methylimidazolium chloride - [C_1Him][Cl], were used in the ionic-liquid based ionoSolv process. Key efficiency parameters such as temperature, reaction time, biomass to solvent loading and solvent recycling, were explored. The process was also challenged with the presence of diverse metal contamination to determine the potential to extract the metals and produce a fermentable pulp and lignin in parallel.

Bioenergy recovery from the ionoSolv process was explored as well as the potential to recover multiple value-added products. In addition to determination of heating values of isolated lignin as well as hydrolysis and fermentation yields of cellulose rich pulps into bioethanol, interactions of contaminating metals and their impact on yeast fermentation yields were investigated. This investigation highlights the benefits of [C_1Him][Cl] ionic liquid pretreatment for the production of clean bioenergy and bioproducts from highly contaminated feedstocks. As an important property of ionic liquids is that they can act as media for electrochemical reactions, electrodeposition of metals from ionic liquid liquor, metal extraction efficiencies and any detrimental interactions with ionic liquid recycling were assessed. To further diversify system outputs beyond bioenergy alone, production of bio-oils, char and gases from pyrolysis of post-hydrolysis residue was determined, as well as the possibility for recovery of phytochemicals as potential complementary value-added products.

This research highlights that unconventional feedstocks have the potential to support a developing bioeconomy and that the reallocation of waste and reclamation of contaminated soils and waters could act as a financial, social and environmental levers to improve the sustainability of bioenergy production. The studies also showcase how a versatile engineered ionic-liquid pretreatment has the potential to transform environmental burdens into resources that are compatible with the diversification of multiple product streams. Taken together, these findings can serve as a proof-of-concept for integrated scale-up of sustainable ionic-liquid based biorefinery.

Glossary

$[C_1Him][Cl]$	1-methylimidazole chloride
$[DMBA][HSO_4]$	Dimethylbutyl hydrogen sulphate
$[TEA][HSO_4]$	Triethylammonium hydrogen sulphate
AIL	Acid Insoluble Lignin
AIR	Acid Insoluble Residue
ASL	Acid Soluble Lignin
BM	Biomass
CCA	Chromated Copper Arsenate
DM	Dry Matter
DMSO	Dimethyl sulfoxide
DP_n	Degree of polymerisation
EEA	European Environmental Agency
G	Guaiacyl
GPC	Gel Permeation Chromatography
H	*p-hydroxyphenyl*
HHV	Higher heating value
HMF	5-hydroxymethylfurfural
HPLC	High Pressure Liquid Chromatography
HSQC	Heteronuclear single quantum coherence
ICP-MS / OES	Inductively Coupled Plasma Mass Spectrometry / Optical Emission Spectrometry
IL	Ionic Liquid
INNS	Invasive Non-Native Species
IPCC	The Intergovernmental Panel on Climate Change
JPK	Japanese Knotweed
LCA	Life Cycle Assessment
LCC	Lignin-carbohydrate complex
M_n	number-average molecular weight
M_w	weight-average molecular weight
NMR	Nuclear Magnetic Resonance
NREL	National Renewable Energy Laboratory
ODW	Oven-Dried Weight
PDI (Đ)	Polydispersity index
PIL	Protic ionic liquid
ppb / ppm	Part per billion / part per million
RHDN	Rhododendron
RPM	Rotation Per Minute
S	Syringyl
TGA	thermogravimetric analysis
T_{onset}	Temperature of onset of thermal degradation
wt %	weight percentage

Acknowledgements

Before embarking on my journey at Imperial, I used to take my mental health for granted. Therefore, my first acknowledgement goes to my wonderful support team: my sisters, my parents, friends and professionals. Secondly, I would like to thank Jason and Paul and the Grantham institute for giving me this great opportunity, support and funding to carry out this research. In the lab, my hat goes to Aida, one of the bravest and smartest people I know; my buddy Ollie for his energy, advice and uncountable favours; Anton for our endless chats about biomass and HPLC nightmares; Patricia Carry for running the analytical suite like a lioness; and Martin Selby for taking good care of my plants at Silwood Park. Finally, I would like to express a special acknowledgement to the many collaborators, without whom this PhD research would not have been so fruitful: my favourite Zoom willow queen Eszter Sas, for whom I could never be enough grateful for; Elaine Jensen, Harvey Wood, Eric Monroe, Anthe George and Ryan Davis.

Lastly, I dedicate this thesis to Little. I hope I have made the birds proud.

Table of Contents

DECLARATION OF ORIGINALITY AND COPYRIGHT 1

PUBLICATIONS 2

ABSTRACT 3

GLOSSARY 4

ACKNOWLEDGEMENTS 5

TABLE OF CONTENTS 6

LIST OF FIGURES 10

LIST OF TABLES 15

1 INTRODUCTION 17

1.1 THE CHALLENGE OF SUSTAINABLE BIOENERGY 17

1.2 FEEDSTOCKS FOR BIOENERGY 18

1.2.1 The complex structure of lignocellulosic biomass 19

1.2.2 Cellulose 20

1.2.3 Hemicellulose 21

1.2.4 Lignin 22

1.3 DECONSTRUCTION AND PRETREATMENT OF BIOMASS 23

1.3.1 Conventional conversion processes 23

1.3.2 Ionic Liquids for pretreatment 25

1.3.3 Engineered ionic-liquid technologies 30

1.3.4 Ionic liquid recycling 31

1.4 UNCONVENTIONAL FEEDSTOCKS FOR BIOENERGY 32

1.4.1 Unconventional growth environment for biomass: marginal, degraded or contaminated land 32

1.4.2 Unconventional feedstocks grown for metal remediation 33

1.4.3 The choice of feedstock is context specific: hyperaccumulators vs dedicated biofuel crops 34

1.4.4 Agromining and conventional processing of metal enriched biomass 35

1.5 RESEARCH GAPS AND OBJECTIVES 41

1.6 THESIS STRUCTURE 43

2 MATERIALS AND METHODS 45

2.1 OVERVIEW OF EXPERIMENTS AND COLLABORATIONS WITH IMPERIAL CONTRIBUTING TO THIS THESIS 45
2.2 FEEDSTOCK COLLECTION 46
2.2.1 Feedstocks 46
2.2.2 Handling and processing of lignocellulosic biomass 47
2.2.3 Context of feedstock growth 48
2.3 BIOMASS CHARACTERISATION 50
2.3.1 Compositional analysis for structural carbohydrates and lignin in biomass 50
2.3.2 Composition analysis for extractible compounds 52
2.4 IONIC LIQUID LIQUOR PRETREATMENT 54
2.4.1 Ionic Liquid synthesis 54
2.4.2 Fractionation of biomass: the ionoSolv process 55
2.4.3 Ionic Liquid Liquor analysis 57
2.4.4 Recycling of Ionic Liquid 58
2.5 CHARACTERISATION OF PRODUCT OUTCOMES 58
2.5.1 Glucose stream for biofuel production 58
2.5.2 Isolated lignin characterisation 61
2.5.3 Lignin for additional energy production 63
2.5.4 Trace elements analysis and metal recovery 66
2.5.5 Statistical analysis and projected willow biorefinery yields calculation 69
3 INVASIVE SPECIES: BIOLOGICAL WASTE VALORISATION INTO ETHANOL 70
3.1 INTRODUCTION 70
3.2 RESULTS AND DISCUSSION 71
3.2.1 Valuable compositional of selected invasive species 71
3.2.2 IL pretreatment parameters optimisation towards bioethanol production 72
3.2.3 Ionic Liquid liquor analysis for degradation products: potential inhibitors 77
3.2.4 Significant fermentation and bioethanol yields of invasive ionoSolv pulps 78
3.2.5 Unveiling lignin analysis for such unconventional species 80
3.3 CONCLUSION: WASTE INVASIVE SPECIES AS A RESOURCE FOR A BIOREFINERY 88
4 CONSUMER WASTE WOOD: THE CHALLENGE OF HIGHLY CONTAMINATED FEEDSTOCK FOR THE IONOSOLV PROCESS 89
4.1 INTRODUCTION 89
4.2 RESULTS AND DISCUSSION 90
4.2.1 The composition of the waste-wood feedstock is similar to pine 90
4.2.2 Stable fractionation and saccharification of waste wood with recycled liquor 91

4.2.3 Significant metal extraction from the waste wood into the ionic liquid liquor 93
4.2.4 Fate of metals over subsequent recycling: metal mass balance 95
4.2.5 Impact of metals on the fermentation from toxic wood pulp 96
4.2.6 Product diversification: unveiling lignin analysis of waste wood 97
4.2.7 Product diversification: ionoSolv post-hydrolysis solids residue (PHS) 98
4.2.8 Pyrolysis of PHS product: high temperature treatment for further product diversification 99
4.3 CONCLUSION: IONIC LIQUID BASED PROCESS LEADS TO CLEAN BIOFUEL FROM PERNICIOUS WOOD 102
5 REAL LIFE CONTAMINATED FEEDSTOCKS INTO THE IONOSOLV PROCESS: THE VALORISATION OF METAL CONTAMINATED BIOMASS 104
5.1 INTRODUCTION 104
5.2 RESULTS AND DISCUSSION 105
5.2.1 Valuable and alternative supply of biomass: metal-contaminated biomass from phytoremediation processes 105
5.2.2 Dedicated bioenergy crop biomass from controlled-environment trials 111
5.2.3 Biomass loading: an important parameter for process intensification 117
5.2.4 Interaction of metal contaminants in the biomass and ionic liquids 119
5.2.5 Electrochemistry: a way to maintain process performance and recover metals 124
5.3 CONCLUSION: IONIC LIQUIDS CAN BOTH DECONSTRUCT AND DECONTAMINATE BIOMASS GROWN ON MARGINAL, CONTAMINATED LAND 130
6 ANALYSIS AND PROCESSING OF WILLOW FROM A WASTEWATER REMEDIATION IRRIGATION TRIAL FOR THE INOSOLV PROCESS 132
6.1 INTRODUCTION 132
6.2 RESULTS AND DISCUSSION 133
6.2.1 Increased biomass yields and no significant trace element uptake 133
6.2.2 Similarities and differences in biomass composition 135
6.2.3 Impact of stress factor of biomass on the ionoSolv pretreatment 136
6.2.4 Impact of stress factor on the structure of lignin 138
6.2.5 Diversification of products from biomass: valorisation of phytochemicals 139
6.2.6 Effect of preliminary extractive extraction on ionoSolv pretreatment 143
6.2.7 Large scale predictions: integrated biorefinery projected yields 144
6.3 CONCLUSION: WILLOW AS A STABLE AND SUSTAINABLE BIOMASS FEED UNDER STRESS CONDITION 146

7 CONCLUSIONS: IONOSOLV PROCESS FLEXIBILITY TOWARDS A WIDE-RANGING BIOREFINERY ____ 147

7.1 KEY MESSAGES ____ 147

7.2 FUTURE WORK ____ 150

8 BIBLIOGRAPHY ____ 154

9 APPENDIX ____ 191

List of Figures

Figure 1.1: bioethanol production pathways for 1st generation and 2nd generation feedstocks
Figure 1.2: arrangement of cellulose hemicellulose and lignin in the cell walls of lignocellulosic biomass
Figure 1.3: β-1,4 glucosidic bond found in cellulose
Figure 1.4: proposed acid catalysed mechanism for the formation of HMF and levulinic acid from hexoses
Figure 1.5: proposed acid catalysed formation of furfural from xylose
Figure 1.6: three main units forming lignin structure
Figure 1.7: main linkages known to be found in native lignin
Figure 1.8: commonly studied IL anions and cations
Figure 1.9: solubility of lignocellulosic powders in ionic liquids
Figure 1.10: principles of phytoremediation
Figure 1.11: simplified scheme to produce ANSH salt from A.murale biomass
Figure 1.12: current technologies and challenges regarding phytoremediation biomass valorisation
Figure 1.13: visualisation of this this chemical engineering research aims and objectives
Figure 2.1: flow chart of the ionoSolv process
Figure 3.1: compositional analysis of RHDN, JPK and 3 other typical biofuel feedstocks
Figure 3.2: pulp and lignin yields from the time course pretreatments of JPK and RHDN using [DMBA][HSO_4] (20 %wt water) at 1:5 g/g biomass:IL loading
Figure 3.3: enzymatic hydrolysis conversion of untreated samples and the pulp obtained from the pretreated pulps at 150°C (left, dashed) and 170°C (right) for JPK (top, yellow) and RHDN (bottom, blue)
Figure 3.4: A. Compositional analysis of the pulps recovered from the pretreatment (170°C 30 mins for RHDN, 150°C 1 hr for JPK) B. Analysis of the pulp from the pretreatment (170°C 30 mins for RHDN, 150°C 1 hr for JPK). Values are in weight percentage.
Figure 3.5: analysis of the compounds found in the ionic liquid liquor after pretreatment (in mg of compound per g of ionic liquid liquor)
Figure 3.6: ethanol yields from the hydrolysate of pretreated pulps (with the highest glucose release), standardised to the amount of biomass used (dry matter)
Figure 3.7: HPLC analysis of the weak acids found in the solutions after fermentation for JPK and RHDN
Figure 3.8: major sub-units and linkages found in lignocellulosic biomass

Figure 3.9: HSQC NMR results of lignin recovered after pretreatment of RHDN at 170°C for 30 min with [DMBA][HSO_4] and JPK at 150°C 1 hour, biomass to solvent ratio of 1:5 g/g and a final water content of 20 wt%
Figure 3.10: Higher Heating Values (HHV) of the ionoSolv lignins from A. Rhododendron (RHDN) and B. Japanese Knotweed (JPK) at 150°C and 170°C for short reaction times (0.25-1.5 hr)
Figure 4.1: compositional analysis of the CCA treated wood used for the experiments and a virgin softwood pine, for comparison
Figure 4.2: trace element analysis of the CCA treated wood used for the experiments
Figure 4.3: pulp, lignin and saccharification yield of untreated and pretreated CCA wood over 6 cycles
Figure 4.4: A. Metal extractions from IL PT calculated from the metal content found in the pulp B. Metal content found in the IL liquor after pretreatment for n cycles C. Percentage of Cu, Cr as As found in the IL brown liquor after n cycles based on the metal concentration prior to the cycle and the amount of new metal entering the system (fresh biomass)
Figure 4.5: ethanol yields (standardised to the amount of glucan added for the saccharification reaction) from CCA treated wood pulp (CCA), CCA treated wood pulp with added metals back in (CCA +metals), virgin pine pulp (VP-PT), untreated virgin pine (VP-UT) and glucose medium after 48 hours of fermentation
Figure 4.6: HSQC NMR results of lignin recovered after pretreatment of CCA treated wood at 170°C for 30 min with fresh, recycled and 5 times recycled [C_1Him][Cl] with a biomass to solvent ratio of 1:5 g/g and a final water content of 20 wt%
Figure 4.7: A. Compositional analysis of the post-hydrolysis solids (PHS) of the combined CCA pulps from cycles 1-6 after a 5-day enzymatic saccharification and B. properties of the derived PHS
Figure 4.8: pyrolysis product distribution of PHS
Figure 4.9: ^{1}H NMR of liquid products obtained by fast pyrolysis of PHS. Spectra were normalized to the total number of protons after subtracting signals from the region δH 3.0–4.5 ppm
Figure 5.1: illustration of the different parts of the biomass found on the metal contaminated sites: wheat in Market Harborough (left) and maize in Stoke Bardolph (right)
Figure 5.2: trace element analysis of biomass grown on a former mining site in Wales
Figure 5.3: A. key indicators of the outcome of the ionSolv process using contaminated Polish Miscanthus at 150°C for 1 hour with [C_1Him][Cl] and increasing biomass loadings and B. metal extractions from the pretreatment of contaminated Polish Miscanthus at 150°C for 1 hour and different biomass loadings

Figure 5.4: A. compositional analysis of the studied untreated biomasses and the pretreated pulps B. outcome of the pretreatment using an aqueous mixture of 80 % [C_1Him][Cl] 20 % water with a 1:5 g/g biomass/solvent loading at 150°C for 1 hour

Figure 5.5: comparison of biomass pretreatment using [C_1Him][Cl] for 1 hour at 150°C on metal contaminated miscanthus with virgin ionic liquid (cycle 1) and recycled ionic liquid (cycle 2)

Figure 5.6: A. metal extraction from the pretreatment of Miscanthus E and RCG H using [C_1Him][Cl] at 150°C for 1 hour 20 wt% biomass loading in both cellulose pulp and recovered lignin B. final metal concentrations of the ionic liquid liquor after the pretreatment

Figure 5.7: cyclic voltammograms showing the potential cycling of a 3 mm-dia. glassy carbon electrode in 1000 mg kg^{-1} (a) Pb^{II}, (b) Cu^{II}, (c) Fe^{II} and (d) Zn^{II} in [C_1Him][Cl] (40 wt% water). Scan rate was 50 mV s-1.

Figure 5.8: accumulative charge over 1 hr for the electrodeposition of 1000 ppm in [C1Him][Cl], 40 wt% H2O of (a) CuII, potential applied was -0.9 V vs. Ag/AgCl, (b) PbII, potential applied was -0.9 V vs. Ag/AgCl (c) FeII, potential applied was -1.2 V vs. Ag/AgCl, (d) ZnII potential applied was -1.4 V vs. Ag/AgCl

Figure 5.9: A. percentage of recovery by mass and B. charge efficiency of PbII(II), CuII(II), FeII(II) and ZnII(II) recovery from 1000 ppm solutions of [C1Him][Cl], 40 wt% H2O after 1 hr electrolysis with a copper foil electrode. Electrode area = 4.2 cm2. The deposition potential was -0.9 V for Pb and Cu recovery experiments and -1.2 and -1.4 V for Fe and Zn recovery experiments, respectively.

Figure 5.10: A. dissolved metal concentrations determined in IL liquor E during the 1 hour electrolysis of the IL liquor E [C_1Him][Cl] (40 wt% H_20) from the first cycle of pretreatment. Copper foil electrode area = 4.2 cm2, potential applied -0.9V vs Ag/AgCl and B. metal extraction based on pretreated pulps from the ionic liquid pretreatment of metal contaminated miscanthus at 150°C for 1 hr using virgin [C_1Him][Cl] (cycle 1), recycled [H1Cim]Cl and recycled and electrodeposited [C_1Him][Cl] (cycle 2) (standard deviation between parentheses)

Figure 6.1: A. aerial photograph of the Saint-Roch-de-l'Achigan field trial and experimental design B. representative photograph of a control and a wastewater irrigated debarked willow stem C. diagram of the analytical workflow of biorefinery characteristics used here to compare control and wastewater irrigated trees.

*Figure 6.2: A. harvested stem biomass yields from control C and wastewater irrigated W trees, dry matter tons per hectare per year after a three-year harvest cycle. B. Compositional analysis of raw biomass from control and wastewater irrigated trees. Mean values are based on n =3 trees. Significant differences indicated by * (t-test, $p<0.05$)*

Figure 6.3: A. Mass proportion between solid (pulp) and liquid (liquor) fractions after ionic liquid pretreatment. B. Pretreated pulp compositional analysis from control and wastewater irrigated

*trees. C. Inferred biomass composition removed by the ionic liquid pretreatment. D. Glucose release from enzymatic saccharification from control and wastewater irrigated trees untreated samples (before pretreatment) and from the ionoSolv pulps (after pretreatment). E. Lignin solubilised by ionic liquid pretreatment and further precipitated from control and wastewater irrigated trees. Theoretical maximum glucose release and lignin recovery is denoted with dashed lines and are based on initial glucan and lignin content. Significant differences are indicated: * (t-test, p <0.05).*

Figure 6.4: HSQC analysis of lignin from the pretreatment of the willow trees

Figure 6.5: A. Number of phytochemicals identified as not significantly different (NSD) between control and wastewater treatment, and those significantly depleted or enriched by wastewater irrigation with chemical classes shown (Mann-Whitney U test followed by BH FDR correction, p < 0.05) B. Molecular structures of significantly enriched phytochemicals in wastewater irrigated trees.

Figure 6.6: Effect of the extractives extraction with methanol-water (75/25 v/v %) prior to ionoSolv pretreatment for both trees A. key outome parameters of the IL pretreatment for the pulp from control trees and B. wastewater trees C. HSQC analysis of ionoSolv lignins for control trees and D. wastewater trees

Figure 6.7: willow wastewater treatment integrated biorefinery illustration and projected yields, illustrating a proposed biorefinery integrating willow wastewater treatment by phytofiltration, biomass production, lignocellulosic bioenergy and phytochemicals extraction

Figure 7.1: illustrative conclusion of 3 axes of the research objectives: alternative inputs, design of chemical ionoSolv process and diversification of outputs

Figure S0.1: HSQC spectra of lignin from RHDN (top) and JPK (bottom)

Figure S0.2: schematic of experimental set-up for fast pyrolysis experiments using a single-stage fixed-bed reactor; shown here in two-stage configuration though the second stage was not used during experiments

Figure S0.3: plant trial block design at Bwlch glas mine

Figure S0.4: area of interest from CinderHill

Figure S0.5: NMR HSQC spectra of Miscanthus ionoSolv lignin samples A. Miscanthus cycle 1, B. Miscanthus cycle 2 without electrodeposition, C. Miscanthus cycle 2 with electrodeposition

Figure S0.6: percentage recovery of certified trace element reference materials after acid digestion A. algae IAEA 413 B. sludge ERM® CC-144.

Figure S0.7: Differentially abundant phytochemicals between control and wastewater irrigated willows. Differentially abundant phytochemicals between control and wastewater irrigated trees were annotated and grouped by putative phytochemical classes.

Figure S0.8: NMR HSQC spectra of ionoSolv lignin from Canadian willow A. wastewater extractives-free, B. controls extractives free, C. wastewater with extractives, D. control with extractives

Figure S6.1: satellite image of study area of the attached algae flow-way deployment at around the Alamo River, a tributary of the Salton Sea in Brawley, CA.

Figure S6.2: enrichment (top) and contamination factors (bottom) of the sediments at the different points of interest. S1: Upstream Alamo River; S2: Upstream Shank Road Wetland; S3: Inlet of Shank Road Wetland (Inlet ATS); S4: Outlet East Cell (Outlet ATS); S5: Outlet West Cell (no ATS); S6: Downstream Alamo River.

Figure S6.3: pictures of the 900 feet long ATS flow way

Figure S6.4: A. Change in biomass productivity and its ash content over the course of entire cultivation period, B. overall average biomass composition, C. Change in biomass composition on a monthly basis.

*Figure S6.5: Spatial variations in every 30m over the length of the flow-way including: A. biomass productivity in case of the high productivity in top 20 % (T20, dark green), the low productivity in bottom 20 % (B20, light green), and the productivity in between T20 and B20 (Med, green), B. ash content, C. nitrogen (black) and phosphorus (red) removal rate in case of the T20 (dashed), B20 (dotted), and Med (solid), D. composition of the biomass including crude protein (orange), crude carbohydrate (yellow), crude fiber (blue), and total lipid (grey). (Statistical significance in differences in sectional biomass productivities are listed in Table S2, * = $p < 0.05$, ** = $p < 0.01$, ns = not significant)*

Figure S6.6: biplot generated through principle components analysis (PCA) with environmental factors (red) and various dependent variables (blue)

Figure S6.7: comparison between change in biomass productivity, concentration total nitrogen, nitrate/nitrite as nitrogen and total Kjeldahl nitrogen (mg L^{-1})

Figure S6.8: A. Se content of the resident algae biofilm from the ATS taken at 500 ft, B. Heatmap of the Se content in the biofilm along the flow-way taken at 100, 500 and 900 ft and C. Se content in the water sampled from the inlet and outlet and calculated BCF Se factor

Figure S6.9: essential metal content of the algae biofilm from the ATS taken at 500 ft

Figure S6.10: non-essential metal content of the algae biofilm from the ATS taken at 500 ft. Cr, As, Pb (top) and Cd (bottom).

Figure S6.11: BCF for each trace element along the flow way (05.12.2018). log BCF<3: non accumulative, 3< log BCF<3.7: accumulative, 3.7<log BCF: very accumulative. Green algae reference was taken from Lopez i Losada (2020)

Figure S6.12: Average metal uptake along the flow way between spring 2018 and summer 2019 based on metal content and biomass productivity.

List of Tables

Table 2.1: overview of materials, methods and contributions to this PhD thesis

Table 2.2: details of the contaminated sites studied

Table 3.1: GPC results of the lignin. M_n and M_w (Da)

Table 3.2: thermogravimetric analysis of the lignin derived from the pretreated invasive species

Table 4.1: mass closures from ICP-OES analysis of pulp, lignin and brown liquor isolated after each cycle of pretreatment of CCA treated wood

Table 4.2: summary of the elemental analysis and calculated HHV values for the PHS and products the pyrolysis PHS in a downdraft fixed-bed pyrolysis reactor

Table 5.1: chemical characteristics of soil used in this study

Table 5.2: trace element analysis of the biomass found on the sites in Stoke Bardolph and Market Harborough. Standard deviations are displayed between parentheses, bold indicates the values are above the speciation for non woody solid fuels pellets (ISO 17255-6).[232] BDL = Below Detection Limit

Table 5.3: trace element analysis of a tar sample taken from the Cinderhill contaminated site

Table 5.4: trace element analysis of a variety of trees species found in the vegetative areas of the Cinderhill tarpit in mg/kg. Standard deviations are displayed between parentheses, bold indicates the values are above the speciation for non woody solid fuels pellets (ISO 17255-2).[232] BDL = Below Detection Limit

Table 5.5: trace element analysis of the different feedstocks used in pot trials. 'Stoke' indicated biomass samples grown in metal contaminated soil collected from the Stoke Bardolph site in mg/kg. n=number of samples analysed =3, standard deviations omitted for clarity.

Table 5.6: trace element analysis of Miscanthus giganteus grown on lead contaminated land in Poland (Phyto2Energy field trial). The standard deviation is shown between parentheses.

Table 6.1: trace element analysis of the wastewater used for the field trial and the trees harvested used in this study (means of biological replicates, each biological replicate was analysed in triplicate)

Table S0.1: Elemental analysis of lignin from the time course pretreatment of JPK and RHDN

Table S0.2: details of the method developed for ICP-MS analysis. 4 replicates of 100 sweeps for each sample, 2 rinses of 60 seconds between each sample, nebulizer pump speed 0.1/0.3 rps

Table S0.3: phytochemicals annotations, formulas and classes associated.

*Table S6.1: trace elements in the sediments in the Alamo river tributary. TEC= Threshold Effect Concentration from the Sediment Quality Guidelines. * indicates values above the TEC.*

*Table S6.2: trace element analysis of water samples along the Alamo River tributary and Shank Road wetland. * indicates that the value is above the toxicity water quality criteria.*

Table S6.3: monthly change in nitrogen and phosphorus content of the biomass, N/P ratio, N removal rate, P removal rate, and BOD removal rate.

1 Introduction

Current generations are facing multiple challenges, in response to our increasing demands on the planet: feeding both current and future populations and providing sufficient energy with limited resources, while tackling and limiting the effects of human activity on climate change. These needs are only likely to become more pressing. The vast majority of fuels and chemicals are derived from non-renewable resources: in 2020, more than 84 % of the total primary energy supply in the United Kingdom came from non-renewable resources; mainly natural gas and oil.[1] Given the established situation of the limited availability of fossil fuels, their subsequent CO_2 emissions and their dramatic effect on climate change, we need to shift our energy supply towards cleaner and more sustainable sources of energy.

1.1 The challenge of sustainable bioenergy

The Paris Agreement set a global target to limit global warming to well below 2˚C above pre-industrial temperatures and pursue efforts to limit this rise to 1.5˚C.[2] Doing so will require that 'net' human-caused CO_2 emissions are reduced to zero around 2050 or soon after.[3] In 2019, the Committee on Climate Change (CCC) suggested that technologies including afforestation, reforestation and bioenergy will be needed to achieve the statutory UK target of net zero GHG emissions by 2050,[4,5] specifically in Integrated assessment models (IAMs).[6] IAMs are complex models developed by scientists to estimate the most cost-effective scenarios to meet global temperature targets.[3] The models describe the global economy, energy and land use systems to produce 'pathways' that illustrate how the Paris Agreement aims could be met.[7]

However, these IAMs have underpinning assumptions and limitations: cost-effective solutions and readiness of energy transformation technologies, a large increase in biomass yields, but most importantly the amount of land freed by dietary changes and the use of marginal land (such as degraded agricultural land). There is debate about which biomass resources could be used for bioenergy to meet those targets.[8–10] The role of bioenergy, the modelling of available land and biomass and their associated greenhouse gas emissions, sourcing of the biomass used for energy generation, its carbon footprint and overall sustainability are still being researched and discussed.[11–13] Are the implications of increased bioenergy used to meet the net zero target actually sustainable? Estimates of bioenergy by 2050 vary from 100 to 300 exajoules (EJ) per year (equivalent to 17 and 51 % of the global primary energy supply in 2017, respectively).[14,15] The definition of sustainability is often contested, but it is considered to have environmental, economic and social dimensions.[16,17] In practice, the sustainability of bioenergy is often context specific, depending on its location, feedstock, production method and supply chain.[18–21] The International Organization for Standardization has developed

bioenergy sustainability criteria (ISO 13065). These are used to compare bioenergy processes or products, but do not set any thresholds or limits.[22] Moreover, current sustainability schemes do not include emissions from the conversion of biomass itself to an energy vector. The International Energy Agency (IEA) stresses that current sustainability frameworks need to be reinforced to fully integrate the carbon impact of supply chains, understand the interconnections between bioenergy and food security and promote transparency.[23]

Additional to concerns over the sustainability of bioenergy, there are also technological and economic challenges associated with renewable energy production: an engineering challenge from using biomass instead of fossil fuels in power and industrial plants. Moreover, the uses of biomass for energy generation vary depending on the type of raw material and the conversion technology.[24] The main, more "conventional" feedstocks used to produce bioenergy are:

- energy crops, including edible crops and dedicated herbaceous or woody crops;
- forestry resources, e.g., residues from the timber industry (forest bark, thinnings, branches, sawdust);
- waste, i.e. agricultural residues, food waste, sewage sludge, manures.[25–29]

These feedstocks can then be used for power or heat generation by combusting the biomass in a power plant to supply the electricity system or using the heat, for example in a specific industrial plant, e.g. fuel and chemicals production.[26]

1.2 Feedstocks for bioenergy

Bio-derived fuels and chemicals are promising alternatives to those derived from fossil fuels as they can afford carbon savings and are in renewable supply. Bioethanol and biodiesel have the greatest produced volume, with an estimated global biofuel demand of 12 EJ by 2030 according to the IEA Net Zero Scenario.[30] Bioethanol has the advantage of being producible from any type of plant, but its production differs depending on the nature of the feedstock.[31]

First generation biofuels rely on a relatively simple process of convertible edible sugary or starchy biomass, through fermentation of sugars by yeasts into bioethanol. Specifically, growing and importing such biofuel crops can contribute to the extensive use of fertilisers, but also lead to the deforestation and limitation of agricultural soil availability for food crops.[32,33]

Second generation biofuels have been proposed as assisting with addressing this issue. Non-edible lignocellulosic biomass, such as wood or wheat straw are used as a starting material. Present in abundant quantities, this feedstock is cheaper and more environmentally-friendly than alternatives as it does not compete with food or agricultural crops, has a lower fertiliser input and can have a positive effect on soil quality and biodiversity.[32,34] However,

lignocellulosic biomass has a more complex chemical structure, which makes it more recalcitrant to enzymatic hydrolysis required for subsequent fermentation. The composition of the cell wall of the plant, essentially the presence of lignin, has to be deconstructed in order to liberate the sugars within for bioethanol production.[35] The deconstruction of the biomass requires an additional step, called pretreatment as shown in Figure 1.1.[36]

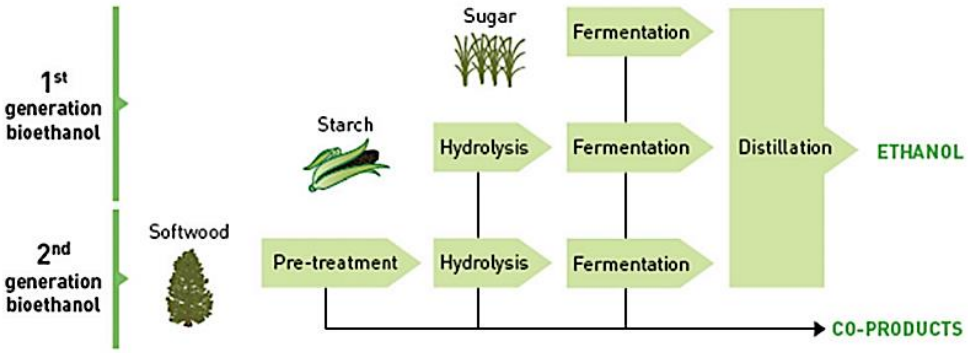


Figure 1.1: bioethanol production pathways for 1st generation and 2nd generation feedstocks

1.2.1 The complex structure of lignocellulosic biomass

The major part of a plant cell is the cell wall. It holds the cytoplasm, vacuole and nucleus of the cell. Lignocellulosic biomass, or 'woody plants', are composite materials. As seen in Figure 1.2, a lignocellulosic cell wall is a complex composite of 3 major polymers: cellulose (35-50 wt%), hemicellulose (25-35 wt%) and lignin (15-25 wt%).[37] The remaining mass of the plant are proteins, lipids, extractives and ash.

There are 3 major different types of lignocellulosic biomass: grasses, softwoods and hardwoods. They differ in chemical composition but also in complexity of the structure (pore size, thickness of cell wall). Generally, hardwoods are deciduous, slower growing species such as willow, poplar or beech. Their structure is complex due to their large water conducting pores. Softwoods, such as pine or spruce, have needles instead of leaves. Their lignin content is higher than those of hardwoods. The lignin is highly cross-linked which makes it more recalcitrant to deconstruction. They also differ from the other types by having mannose as their main hemicellulose monomer.[38] Finally, grasses are relatively easy to deconstruct because of their cell structure and lower lignin content.[39]

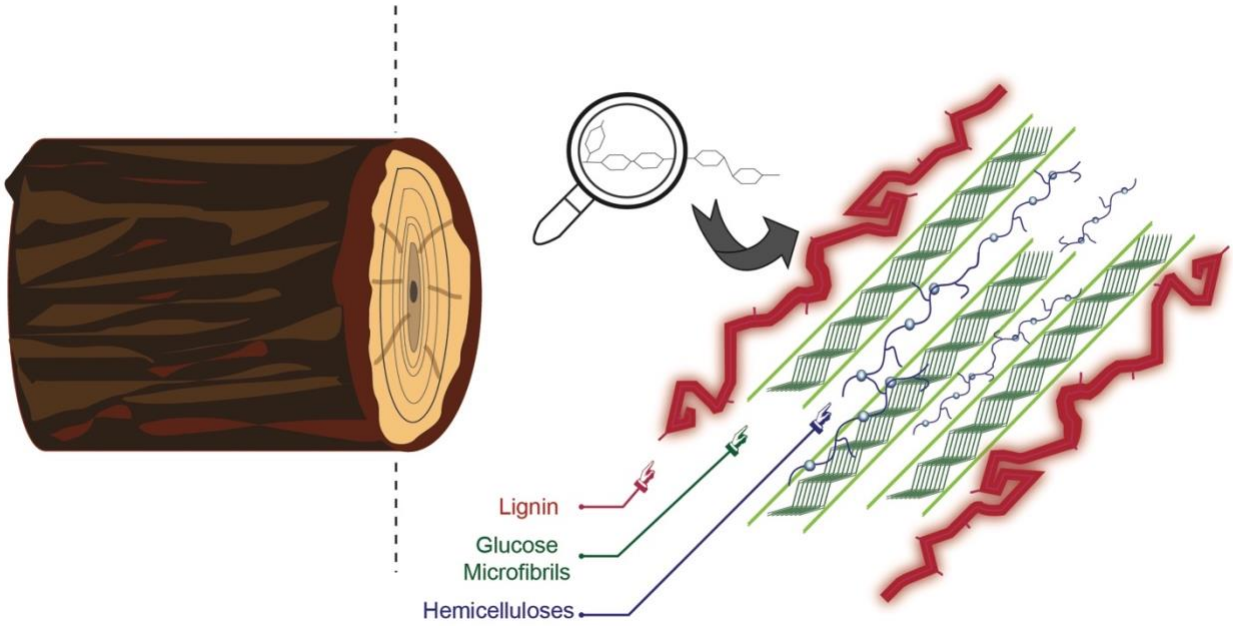


Figure 1.2: arrangement of cellulose hemicellulose and lignin in the cell walls of lignocellulosic biomass

1.2.2 Cellulose

Cellulose is the most abundant polymer on Earth. This chemical is a homopolymer of D-glucose units as shown in Figure 1.3. The β-1,4 bond between each monomer introduces a 180-degree angle between each sugar, so that the polymer backbone organises itself as a strong micro fibril. These micro fibrils are held together via hydrogen bonds and Van der Walls interactions to form the very backbone of the cell wall, a cellulose micro fibril. Each chain from the micro fibril is highly aligned, rigid and ordered, which gives cellulose a crystalline structure. Due to its high molecular weight and high degree of polymerization (reaching a DP_n of 10 000 or higher), cellulose is insoluble in water and most of organic solvents. Only some solvents can dissolve cellulose: metal complexes solvents such copper(II)-ethylenediamine complex (cuen or CED), *N*-methylmorpholine-*N*-oxide (NMMO) or *N,N*-dimethylacetamide/lithium chloride (DMAc/LiCl);[40] some ionic liquids also have proven to dissolve cellulose with small, hydrogen bond accepting anions.[41]

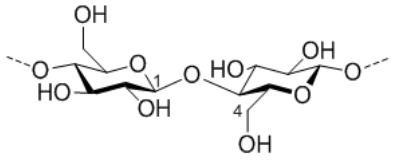


Figure 1.3: β-1,4 glucosidic bond found in cellulose

Cellulose represents a starting chemical for a large number of various applications (e.g. paper, paperboard, membranes and textile[42,43]).

The hydrolysis of cellulose gives glucose, which can be converted into variety of chemicals such as bioethanol, levulinic acid, lactic acid and 5-hydroxymethyl furfural (5-HMF).[44,45] 5-HMF, as shown in Figure 1.4,[46] is considered as a versatile platform of chemicals and it is in fact listed as one of the most important renewable chemicals that can be obtained from lignocellulose biomass.[44,46]

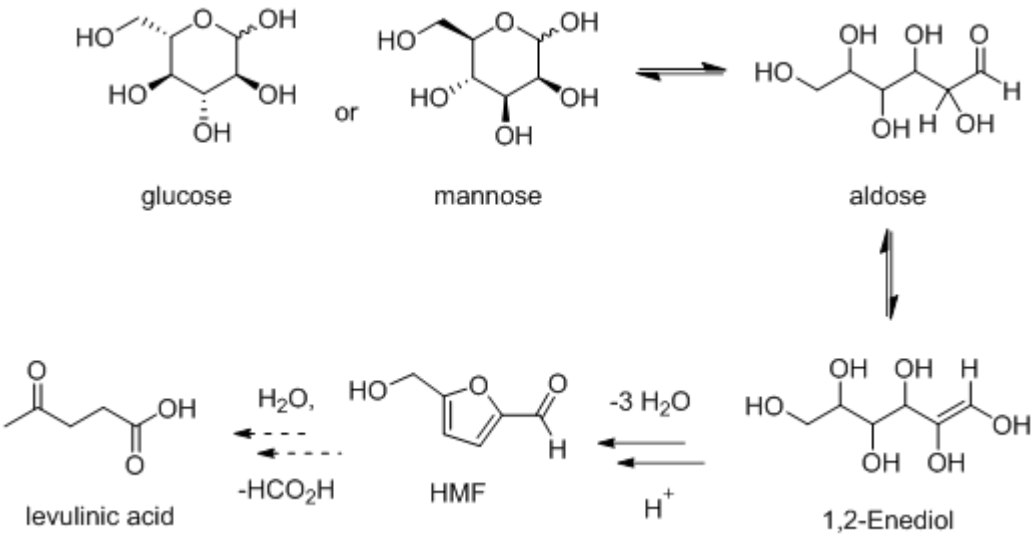


Figure 1.4: proposed acid catalysed mechanism for the formation of HMF and levulinic acid from hexoses

1.2.3 Hemicellulose

Hemicellulose is a low molecular weight polysaccharide heteropolymer: made of hexoses (glucose, mannose and galactose) and pentose (xylose and arabinose) sugars. The exact composition of the hemicellulose component depends mainly on the species of the plant.

The amorphous hemicellulose binds non-covalently to the cellulose micro fibrils, increasing its overall stiffness.[35] Moreover, polysaccharides in the hemicellulose can be functionalised with groups such as acetyl, methyl cinnamic, glucuronic or galacturonic acids. It has been proposed that the acetylation of some of the hemicellulose sugars increases its affinity to lignin, which increases the overall cohesion of the lignocellulose biopolymer matrix.[39] During pretreatment processes, especially fractionation processes, these lignin-carbohydrates complexes bonds are cleaved.[47] Hemicellulose polysaccharides are branched and made of lower degrees of polymerization than glucose, of around 100 to 200 units, which makes them easier to hydrolyse compared to cellulose. The sugar monomers can be converted to furfural

as shown in Figure 1.5, a promising platform chemical for the replacement of many commodity petro-chemicals.[48]

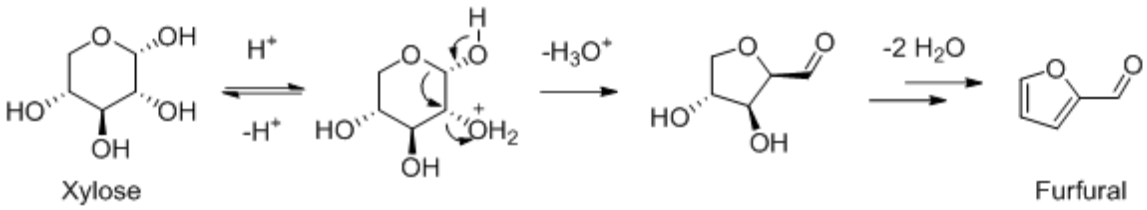


Figure 1.5: proposed acid catalysed formation of furfural from xylose

1.2.4 Lignin

Cellulose, hemicellulose and pectin are the main components of what is called the primary cell wall. After the growth of a plant cell, it differentiates according to its role and place in the plant. This differentiation is often determined by the composition of its cell wall. Among the last termination stages of differentiation, a secondary wall is secreted within the primary cell wall by synthesising new molecules in the membrane. For all lignocellulosic plants, this secondary cell wall contains large amounts of lignin as well as other polysaccharides in variable proportions. Lignin is a complex hydrophobic aromatic heteropolymer, which acts as a water-proof mechanical support and physical and chemical barrier to climate conditions and microbiological attacks.

The biosynthesis of lignin involves the random radical polymerisation of three monomers: coniferyl, sinapyl and p-coumaryl alcohols.[47] The monomers are identified based on their aromatic structure as guaiacyl (G), syringyl (S) and p-hydroxyphenyl (H) subunits respectively, as shown in Figure 1.6. The proportion of these subunits is different from one lignocellulosic biomass to another.[45] Lignin found in softwoods is made almost exclusively of G units, while hardwood lignin has equal proportions of G and S units and all three units are found in grasses.[49]

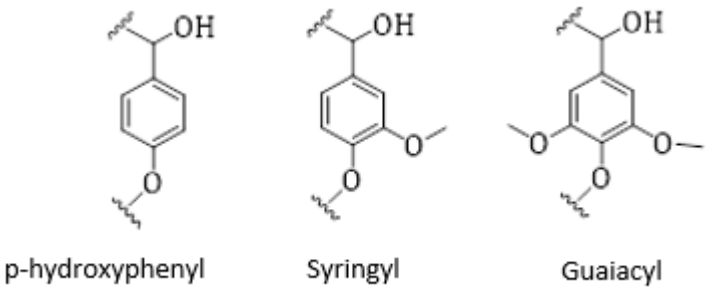


Figure 1.6: three main units forming lignin structure

The exact structure of native lignin is not fully known because of its complexity, still unknown degree of polymerisation or linkages and numerous bonding patterns. However, it is known that the C-O-C linkages are predominant in the lignin structure, whether as ether bonds or furan rings.[50] Specifically, the β-*O*-4' ether bonds account for about 50 % of the linkages in lignin polymers.[51,52] Figure 1.7 shows the most common linkages found in native lignin, including the 4-*O*-5 ether bonds, less present than the β-*O*-4', as well as highly present C-C bonds.[53]

The presence and the nature of lignin is considered to be the main barrier to the utilisation of lignocellulosic biomass for biorefinery. Lignin acts as a shield against the hydrolysis of cellulose and hemicellulose sugars. This is why the biomass needs a pretreatment step prior to any valorisation of the chemical components of the biomass and one of the major deconstruction approaches of the biomass is delignification to enhance enzymatic digestibility and sugar release.

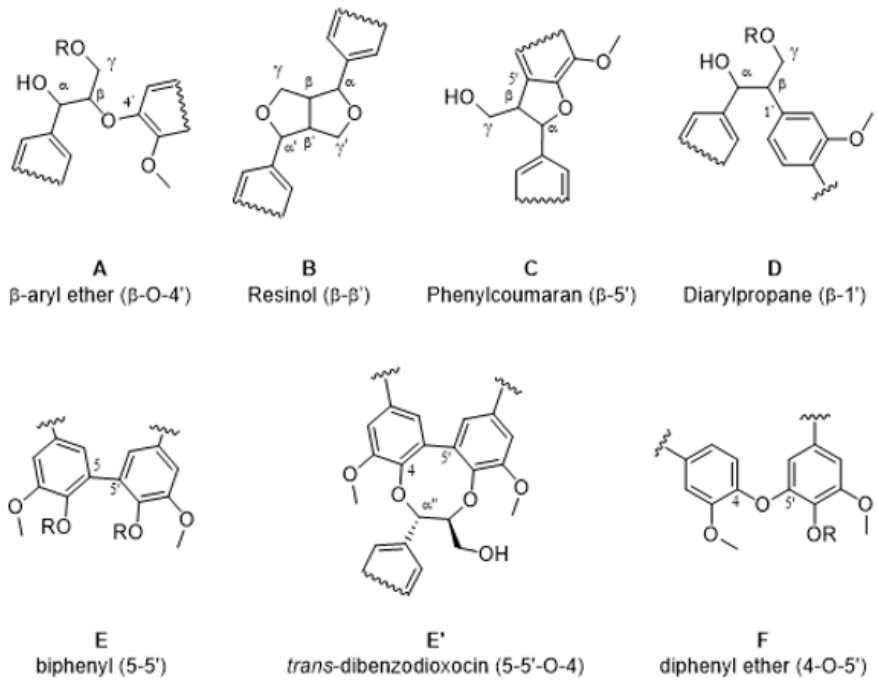


Figure 1.7: main linkages known to be found in native lignin

1.3 Deconstruction and pretreatment of biomass

1.3.1 Conventional conversion processes

There are essentially two possible routes to using lignocellulosic biomass as a fuel: thermal and bioconversion. Thermal conversions include the gasification of biomass into syngas (a mixture of CO_2, CO and H_2) and conversion into hydrocarbons via Fischer-Tropsch synthesis

using metal-based catalysts. Pyrolysis is another way to convert biomass at elevated temperature in the absence of oxygen, but product recovery is challenging.[54] Bioconversion is sensible to the structure of the biomass as it aims at separating the different components and converting them into valuable chemicals and/or energy. However, because of the nature of lignocellulosic feedstock, the bioconversion includes four steps as shown in Figure 1.1: pretreatment of the biomass, enzymatic hydrolysis, microbiological fermentation and distillation. As seen previously, the secondary cell wall of biomass forms a robust molecular matrix. In order for the hydrolysis of the sugars to occur, the enzymes need to access the cellulose and hemicellulose of the cell wall.[55] The presence of lignin prevents the hydrolases (enzymes) from accessing and breaking down the polysaccharides, while deconstructed forms of lignin can also cause inefficient binding of the enzymes. To achieve a realistic and efficient hydrolase activity, the lignin can be removed from the sugar components of the cell wall during an additional step called pretreatment. In the context of a biorefinery, the pretreatment enables subsequent recovery of high-quality sugar yields (C_6 and C_5) as well as other possible value-added product streams in a way that it is sustainable and economically viable. Pretreatment processes can be classified into physical, chemical, physico-chemical and biological methods, depending on how the changes in the biomass are achieved.

Physical pretreatments (e.g., milling/crushing, extrusion, microwave, ultrasound and high-energy radiation) modify the lignocellulosic biomass structure without the need of chemical or biochemical reactions. They prevent chemical degradation of biomass, avoiding loss of sugars and other compounds, but suffer from high energy consumption and insufficient biomass destruction. To overcome these disadvantages, they are usually performed in combination with chemical, physicochemical or biological methods.[56]

Chemical methods use acids, alkalis, oxidants and organic solvents to perform the biomass degradation. They lead to extensive chemical changes in the biomass and can be more efficient than physical and biological methods.[57–59] However, these chemical changes lead to the production of undesired by-products.[57] Other disadvantages are the amounts of chemicals consumed and the need to remove them from the biomass.[57–59] In order to achieve better pretreatment results, combinations between chemical and physical pretreatment methods have been largely studied: liquid hot water pretreatment,[60,61] steam explosion[62,63] and ammonia fibre expansion.[64–66]

Biological pretreatments are considered safer and more environmental-friendly, as they do not require chemicals or high temperature/pressure conditions. However, they are usually expensive and slow in comparison to other methods due to the high cost of enzymes and hydrolysis rates.[58] Biological pretreatments can be divided in two different processes: bio-delignification, which aims to remove lignin from the biomass; and saccharification which aims to hydrolyse cellulose and hemicellulose in sugars.[57,58] Enzymes and microorganisms have

been evaluated to perform biomass delignification, while saccharification is normally performed using enzymes.[56–58]

The extra pretreatment processing step adds complexity, cost and energy to the bioenergy production process. Some studies show that cost of the pretreatment step can reach 18-20 % of the total biorefinery process,[67,68] although capital investment of the plant itself and waste water treatment are also expensive (15-20 % of the Capital Expenditures).[69] Furthermore, the production cost of the chemicals is very much dependant on the composition of the biomass (amount of carbohydrates, lignin and extractives content) and the chemicals used in the process. Each pretreatment approach has its own advantages and drawbacks. However, the real challenge of pretreatment technologies today is their techno-economic effectiveness. In order to be viable, they need to meet large-scale process goals of low operating and capital and energy costs.[70]

1.3.2 Ionic Liquids for pretreatment

Ionic liquids are a class of 'designer' solvents, which are made of two components: a mobile anion and a cation. They are essentially molten salts that are liquid at or near room temperature (< 100°C). Ionic liquids have high thermal stability and many of them have negligible vapour pressure under standard process conditions, which makes them very attractive for reducing atmospheric pollution from the classic volatile organic solvents. Moreover, there is a wide range of possible combinations of ions, which makes ionic liquids tuneable and task specific.[71,72]

In practice, only a relatively small number of anionic and cationic structures have been commonly studied such as alkylated nitrogenous cations, e.g., imidazolium, pyrridinium, or ammonium – as shown in Figure 1.8.

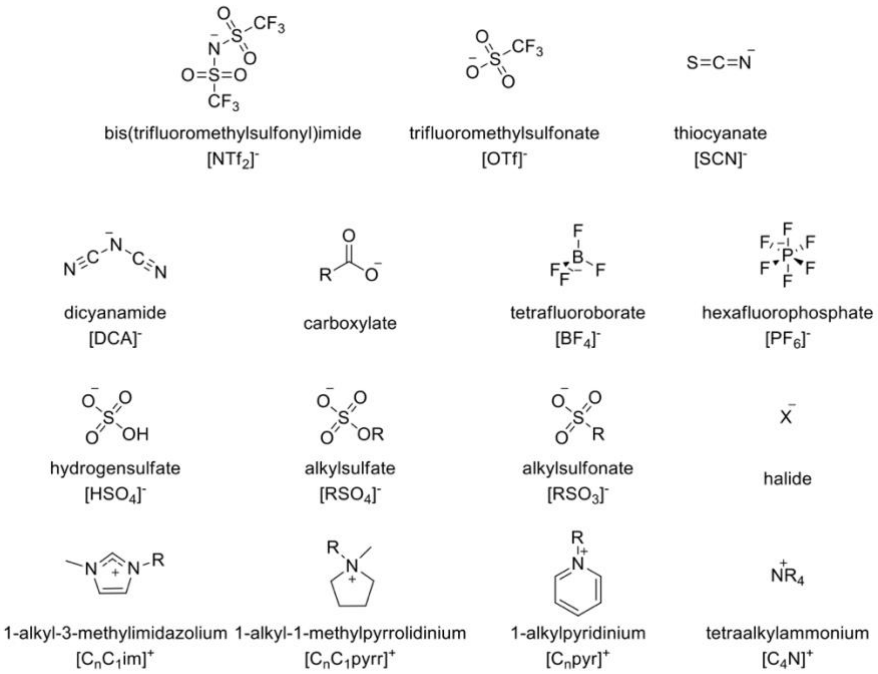


Figure 1.8: commonly studied IL anions and cations

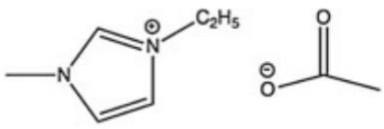
1.3.2.1 Dissolution vs fractionation processes using ionic liquids

1.3.2.1.1 The dissolution process of cellulose

There are two approaches to lignocellulosic biomass processing using ionic liquids. The first one is dissolution of the biomass, where the whole biomass is non-selectively dissolved in the ionic liquid.[35] The solubility of the cellulose component has been attributed to the strong hydrogen bond basicity of its anion: in this case the halide, chloride, carboxylate and alkylphosphate anions.[73] The hydrogen of the anion forms bonds with the hydrogen of the cellulose, disrupting the interactions of the macromolecule. These anions are often combined with imidazolium, pyridinium, ammonium-based cations (Figure 1.8). The dissolution process involves dissolution of the entire lignocellulosic matrix, followed by precipitation of a more easily hydrolysable solid pulp, often carbohydrate-enriched, using an antisolvent such as water or water/acetone in order to retain more lignin in solution.[74,75] Cellulose dissolution requires a solvent with high hydrogen-bond basicity (β).[35] It has been estimated that dissolution of the cellulose fraction needs a β value above 0.8,[76,77] whereas for lignin dissolution a β value above 0.4 is needed.[78] More recently this concept has been extended to take into account the net hydrogen bond basicity of the solvent. It has been suggested that in order to dissolve cellulose a difference between hydrogen bond acidity and basicity needs to be higher than 0.35.[77] Therefore, the choice of IL is a decisive factor that affects which process will take place. The solvent properties of the IL tend to be dominated by the anion,[79] leading to a relatively low number of different anions being used for each process. ILs containing

dialkylimidazolium cations and chloride and acetate anions have been shown to have high β values (*i.e.* over 1).[79,80] As a result, the most common ILs employed for dissolving the whole biomass are aprotic, such as $[C_2C_1im][OAc]$ and $[C_4C_1im][Cl]$. On the other hand, protic ILs (PILs) usually do not have sufficient hydrogen bond basicity to dissolve cellulose even when dry.[35] Nevertheless, there are a number of exceptions such as a small number of carboxylate and chloride protic ionic liquids (PILs);*i.e.* $[N_3(CH_2)_2OH][HCOO]$ and $[C_2im][Cl]$.[81] To date, dissolution of biomass has been studied with a wide range of conventional, typical lignocellulosic feedstocks and ILs, as seen in Figure 1.9. Usually, dissolution processes change the cellulose structure from cellulose I to cellulose II, with a reduction in cellulose crystallinity. Lignin and hemicellulose removal depend on the biomass and IL evaluated. The precipitation procedure, usually by the addition of an anti-solvent, also influences the content of both lignin and hemicellulose in the regenerated biomass.[82–84]

Water content also play a major role in the dissolution process. Water has a low β, and thus dilution of the IL leads to a decreasing hydrogen bond basicity.[85,80] Therefore, in order to optimally dissolve the entire biomass structure in a dissolution type process, the water content needs to be minimized.[35] As a result, certain ILs can behave as either dissolution or fractionating solvents depending on their water content. Additional factors, such as the temperature and biomass loadings used in pretreatment can also affect the process due to solubility limits.[86]

Ionic Liquid	Structure of Ionic Liquid	Feedstock	Temperature and time	Biomass loading (%wt)	Solubilisation %	References
1-ethyl-3-methylimidazolium acetate		Pine	170 °C, 30 min	5	92.2	87
		Pine	185 °C, 7 min	5	42.8	
		Pine	110 °C, 16 h	5	93.5	88
		Oak	110 °C, 16 h	5	98.5	
		Beech	115 °C, 24 h	5	75	89
		Beech	115 °C, 72 h	5	95	
		Spruce	115 °C, 24 h	5	40	
		Spruce	115 °C, 72 h	5	75	

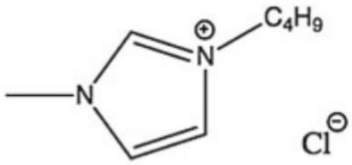
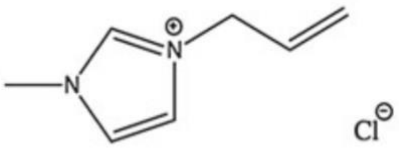
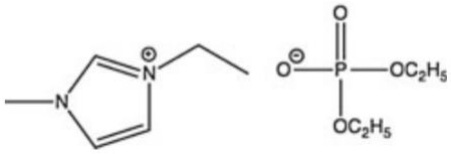
1-butyl-3-methylimidazolium chloride		Pine	110 °C, 16 h	5	26	[88]
1-allyl-3-methylimidazolium chloride		Spruce	110 °C, 8 h	8	95	[90]
		Pine	100 °C, 15 h	5	26	[91]
		Pine	110 °C, 2 h	3	50	
		Spruce, Eucalyptus	75 °C, 48 h	10	100	[92,93]
1-ethyl-3-methylimidazolium diethyl phosphate		Wheat Straw	100 °C, 1 h	4	not determined	[94]

Figure 1.9: solubility of lignocellulosic powders in ionic liquids

1.3.2.1.2 The fractionation process to separate cellulose and lignin

The second ionic liquid strategy for the pretreatment of biomass is the fractionation process. These processes are meant to fractionate and therefore produce fragments of lignocellulosic chemicals: cellulose, lignin and to a certain extent, hemicellulose. To achieve fractionation, lignin and hemicellulose are selectively solubilised in the ionic liquid, leaving a cellulose rich pulp. Ionic liquids do not need to exhibit high hydrogen basicity to solubilise lignin. Ionic liquids with anions such as halides (chlorides, bromides)[72,95], acetate, triflate $[OTf]^-$ methyl sulphate $[C_1SO_4]^-$, xylenesulfonate[96] $[XS]^-$ and hydrogen sulphate $[HSO_4]^-$ have been used.[97] Imidazolium cations can also solubilise lignin by interacting with its phenyl groups via the aromatic ring.[35]

Brandt *et al.* designed a method called the ionoSolv process for the pretreatment of lignocellulosic biomass using a mixture of ammonium-based ILs with $[HSO_4]^-$ anion in 20 wt% water (avoiding the need to work under strict anhydrous conditions).[98,47] This process can successfully dissolve lignin - by breaking some of its ether bonds - and partially dissolving hemicellulose. It does not solubilise the cellulose component of the biomass, which stays in the solid phase as a cellulose pulp. The lignin can be recovered by the addition of an anti-solvent from the ionic liquid liquor. This ionoSolv fractionation process has been studied using

conventional feedstocks, for consistency and study of inherent chemical reactions: grasses (Miscanthus, sugarcane bagasse), softwoods (Pine), hardwoods (Willow) and Eucalyptus.[99–104] While the process is still being developed at bench-scale, the research on the ionoSolv fractionation currently focuses on the production and purity of the cellulose pulp and the recovered lignin (readily available fractionation products);[99,105,106] with one study investigating the ionoSolv process from 10 mL to 1L.[107]

The most common ILs employed for ionoSolv pretreatments can be broadly divided into two categories: acidic and basic. Protic ionic liquids (PILs) due to their easy synthesis consisting of an acid/base reaction, usually exhibit a lower cost, and lower hydrogen bond basicity, allowing cellulose to remain undissolved.[108] The economic assessment of $[HSO_4]$ based protic ionic liquids showed that the prices of these solvents are very competitive compared to traditional solvents, at a price range of \$0.78 to \$5.88.kg^{-1}.[109,110]
Acidic ILs dissolve and hydrolyse both the lignin and the hemicellulose, leaving a solid cellulose-rich pulp. High-purity cellulose can be obtained, often with an increased degree of crystallinity due to removal of amorphous cellulose fragments, lignin and hemicellulose,[111] opening pathways for high value cellulosic materials applications. Valorisation of hemicellulose and its constituent sugars is not always possible due to their rapid hydrolysis and degradation in solution. The most commonly employed acidic ILs are based on the $[HSO_4]^-$ anion, although other anions such as $[Cl]^-$, and $[MeSO_4]^-$ have also been used.[98] Regarding cations, studies on ionoSolv pretreatment have been gradually moving away from alkylimidazolium-based cations (e.g. $[C_4im]^+$)[112] to cheaper alkylammonium cations (e.g. $[N_{2220}]^+$ and $[N_{1140}]^+$).[100,103,104] Due to the low basicity of the anion,[113] these ILs are not able to solubilise the cellulose with dialkylimidazolium-based cations (such as $[C_4C_1im][HSO_4]$ and $[C_2C_1im][HSO_4]$)[78,98] and under anhydrous conditions.[78] Acidic PILs using a chloride anion, e.g. $[C_1im][Cl]$ has been used and shown to dissolve cellulose and lignocellulose when dry (as has $[C_2im][Cl]$),[74,75,81,114]

Even though ionoSolv research has been typically focussed on acidic PILs, more recently there have been several studies investigating the use of basic PILs. Basic PILs may still dissolve and depolymerise lignin due to their alkaline nature, while broadly preserving the hemicellulose fraction in the pulp. Basic PILs usually use on carboxylate anions (*e.g.* acetate, propionate, butyrate, pentanoate, hexanoate, lactate) combined with alkylammonium, pyridinium, or pyrrolidinium cations.[113,115–119] Although other ILs based on these anions tend to be cellulose-dissolving, the protic nature of the IL reduces its basicity sufficiently that some of them have been found not to dissolve cellulose or lignocellulose when dry. Protic alkylimidazolium acetate and formate ILs (*i.e.* $[HC_1im][OAc]$ and $[HC_2im][HCOO]$) have not

been substantially studied in terms of pretreatment efficacy but had been reported as not dissolving lignocellulose or cellulose when dry,[75,119] although one study has reported [HC_1im][OAc] as being able to dissolve up to 4 wt % of cellulose and lignocellulose at 115°C.[120] Additionally, a number of studies have added water to the pretreatment mixture in order to reduce viscosity, which also reduces the β of the solvent.[115,118]

1.3.2.2 The one pot process

In recent years, another IL based pretreatment alternative, the "one pot process", directly hydrolyses biopolymers and recovers the hydrolysis products. This approach aims to perform pretreatment, saccharification and fermentation without carrying out an exhaustive biomass fractionation and IL removal. Additionally, no washing step of the pulp is needed before saccharification and fermentation. One-pot processes have been reported to produce sugars,[121–128] lactic acid,[129] levulinic acid,[130–132] alcohols,[133–137] biofuels,[138–141] furans,[142] furfural related compounds,[143–145] and lignin byproducts.[146,147] Several ILs have been used in the pretreatment step leading to high sugar recovery after enzymatic saccharification.[123,124,134,135] Like the dissolution process, pretreatment conditions strongly affect one-pot process performance because an optimum pretreatment improves enzyme accessibility to cellulose and hemicellulose.[136] Additionally, saccharification and fermentation also need to be optimized. In this regard, the most challenging issue is the performance of enzymes and microorganisms at high IL concentrations. Enzyme inactivation by the IL significantly affects sugar recovery, even more than pretreatment performance. Therefore, the selection of IL type and its concentration, as well as enzyme and microorganism are highly relevant. Detrimental effects of an increment of IL concentration during saccharification and fermentation have been reported for several ILs and biomasses.[137] Consequently, to improve saccharification and fermentation performance, dilution of the pretreated medium is usually conducted. However, the use of a large amount of water to dilute the medium negatively affects operating costs of the process.[148–151] Several groups have screened enzymes and microorganisms, or studied how to improve enzymes stability, in order to enhance sugar hydrolysis and fermentation in media containing high IL concentrations.[152–156]

1.3.3 Engineered ionic-liquid technologies

According to the Douglas Methodology of Conceptual Chemical Engineering, basic experimental research is needed to study the variables that will have the greatest economic impact on the process. In the technical research of the process, the efforts should be focused on the ways to improve an existing process. Douglas suggests a hierarchy of decisions as follows: nature of the batch (batch vs continuous), **input and output structure**, **recycle**

structure, general structure of the separation system and heat-exchanger network.[157] Because ionic liquids are designer solvents, the development of ionic-liquid based technologies can be tailored to fit one or several task-specific applications.

There only has been very little research carried out on ionic liquid-based process for unconventional feedstocks; the ionoSolv process is solely focused on grasses, softwoods and hardwoods to produce a cellulose-rich pulp and a lignin stream. Furthermore, the presence of metals in the biomass adds another layer to the "onion" of the process of engineering design: managing metals, their extraction and their recovery. The ionic character of ionic liquids makes them efficient agents for heavy metal extraction in aqueous phases.[158] Ionic liquids behave as hydrophobic media, which can incorporate and dissolve charged compounds such as metal complexes. The ionic liquid anion, chloride or thiocyanate based for example, can strongly coordinate or dissolve metals in an aqueous phase through the formation of chelating complexes so that the metal ion binds with the ionic liquid media.[159] Protic ionic liquids have recently been used for metal extraction from sewage sludge.[160] Designing an ionic liquid-based process, which could both pretreat and deconstruct lignocellulosic biomass, but also solubilise and recover metals in the solvent phase, has not been reported in the literature yet. ILs can also be used for the electrodeposition of metals or micro/nanomaterials.[161–164] By applying an electric current, dissolved metal ions can be electroplated on an electrode. Most electrochemical applications have been done using APILs, while the use of PILs have been limited and done for a few of metals such as silver and copper. Their thermal stability, low vapour pressure and tuneable properties with anion/cation combinations add to the flexibility in redox potentials for a wide electrodeposition of metals and alloys. Moreover, some ILs do exhibit wider electrochemical windows (4-6 V) compared to water (1.4 V) and conventional organic solvents, which means that they allow highly electronegative metals to be electrodeposited using IL phases – for example Aluminium, Molybdenum or Tantalum.[165–167] It should be noted that the corrosion and toxicity aspects of ILs can be major drawbacks from using such solvents for a process application.[137]

1.3.4 Ionic liquid recycling

Ionic liquid recovery and recycling are key aspects for the success of an ionic liquid-based process. The price of the ionic liquid and the amount of ionic liquid make-up will drive the process economics and operating costs.[168] Even if the cost of the ionic liquid is low, at least 94 % recovery of the solvent should be reached for the solvent cost not to be become limiting.[97] Despite the interest of ionic liquid and their recycling properties under process conditions, only a few studies looked into this aspect of the process in the literature. Brandt-Talbot *et al.*

investigated the recyclability over 4 cycles of [TEA][HSO_4] for the ionoSolv process using *Miscanthus giganteus* on a variety of parameters and 2 process outputs: the composition and digestibility of the cellulose rich pulp, the yield and changes in the lignin (as well as liquor analysis - degradation products, presence of organic salts).[97] The study showed no negative impact of recycling on the process performance (glucose yields increased over 3 cycles) and a recovery of ionic liquid of 98-99 %. A few other studies investigated the recycling of ionic liquids for a dissolution process. However, the biomass loadings used are relatively small for an industrial process (5 wt %). Auxenfans *et al.* used 1-ethyl-3-metylimidazolium acetate 7 times for the pretreatment of hardwood and softwood sawdust without loss of efficiency.[169] Using the same ionic liquid, Qiu *et al.* investigated the recycling the ionic liquid for bagasse pretreatment and managed to tune the treatment parameters (temperature and time) to improve to the pretreatment efficiency over the subsequent cycles.[170]

1.4 Unconventional feedstocks for bioenergy

1.4.1 Unconventional growth environment for biomass: marginal, degraded or contaminated land

A contaminated site is "a land where substances could cause significant harm to people or protected species and significant pollution of surface water or groundwater".[167,171,172] The main causes of land contamination are the treatment and disposal of waste and industrial and commercial activities such as mining, oil refining and electricity generation.[173] As a result of the causes of contamination, organic substances account for more than 50 % of the soil pollutants such as hydrocarbons, polycyclic aromatic hydrocarbons, halogen solvents or mineral oils. According to the latest data from the European Environment Agency, 35.5% of these contaminants are metalloids: Pb, Cd, Hg, As, Cu, Cr, Zn, Ni and Cd. The different contents and importance of each metal differ amongst sites, origin of the contamination and nature of the soil.[174] Agriculture is still one of the major sources of metal pollution of soil. Efforts to increase agricultural productivity have increased the use of inorganic fertilisers, pesticides, and sewage sludge application. Superphosphate fertilizers for example contain not only plant nutrients but also impurities such as Cd, Pb or Hg.[175] In many areas of the world, industrial and municipal wastewaters have been used for irrigation due to the scarcity of fresh water for agriculture. It is estimated that half of the vegetables grown in Asian and African cities are currently irrigated with wastewater.[176] Mining and metal extraction from the Earth's crust are equally responsible for the metal contamination of soil since the industrial revolution. In the UK, the most extensive areas with the highest values of metal contamination are located in the Pennines, the South-West and in the North Midlands. These can be historical areas of intense industry and metalliferous mining (South West and Cornwall, steelworks in South

Wales) or local areas associated with atmospheric deposition of Pb from coal and derived fuels for road transport and urbanisation near London and Glasgow for example.[177–179]
If some metals have essential biological functions, their presence in certain fine quantities not only causes a major issue for the quality and health of the soil but these contaminants are also prone to human intake. Heavy metals are harmful substances because they are non-biodegradable and have long biological half-lives.[176] They can be directly ingested (children playing on the ground or working farmer for example) or indirectly transferred from soil to surface groundwater leading to significant water contamination, food crops and animals.

Currently, there is still a predominance of *ex situ* treatments for dealing with metal contaminated land: excavation of the soil and disposal or landfill of the contaminated material off-site. This method, called 'dig and dump' is the most economically competitive on the market compared to *in situ* techniques (e.g. chemical/physical isolation and immobilisation of the metals).[180] Excavation is essentially more time-efficient than *in situ* methods as the soil can be used for another purpose after digging up the superficial layer of contaminated soil, which can be treated in a second process.[173] The 'dig and dump' methods are still very expensive and highly energy intensive. 93 % of the remediation techniques used in the UK include excavation and disposal off-site. For England and Wales only, the government reported that £20.5 million had been spent on remediation techniques up to the end of March 2007 and £62 million would be the estimated remaining cost to complete full remediation of contaminated sites within the country.[179] Moreover, these methods can only be used on localised, relatively small contaminated areas. More importantly, these are not environmentally friendly techniques regarding the soil itself. Excavation leads to total disruption of the soil functionality as an ecosystem and the groundwater system within.[180]

1.4.2 Unconventional feedstocks grown for metal remediation

Phytoremediation is a process that uses plants to decontaminate or stabilise a pollutant from its growing medium (water, soil). This is an *in situ* remediation solution for large, contaminated sites, aesthetically appealing, and relies on technologically simple agronomic methods. In contrast to current remediation technologies, it can sustain biodiversity and coherence of the soil without producing large quantities of chemical waste. A wide range of organic and inorganic pollutants can be phytoremediated, especially heavy metals: As, Cd, Cu, Au, Pb, Mn, Ni, Zn, etc.[181–183] While physiological and biological relevance of metal accumulation in plants is still being investigated, it is believed that the metal accumulation could be a genetic adaptation of the species to the type of soil they are initially growing in. Accumulating metals in their organs could be a mechanism for the plants to fight off competition of non-metal

resistant species, unable to grow in its surroundings. This optimises the nutrient availability for the metal accumulating species, which can thrive under such conditions.[184]

There are several sub-processes of phytoremediation depending on the interaction of the plant with the contaminant. Plants can either stabilise, degrade, extract, or even evaporate hazardous substances from the soil, as shown in Figure 1.10. The phytochemistry of phytoremediation is complex and depends on the contaminant (each metal will be loaded/transported/unloaded/stored under different conjugated forms), the mechanism adopted dependant on the species (genetics, tolerance of the metal, tissues available) and the type of soil (toxicity level of metals, tolerance thresholds of plants).[185] The use of marginal and contaminated land (MaCL) for successful phytoremediation is challenging because of the complexity of the biological mechanisms associated.[186,187]

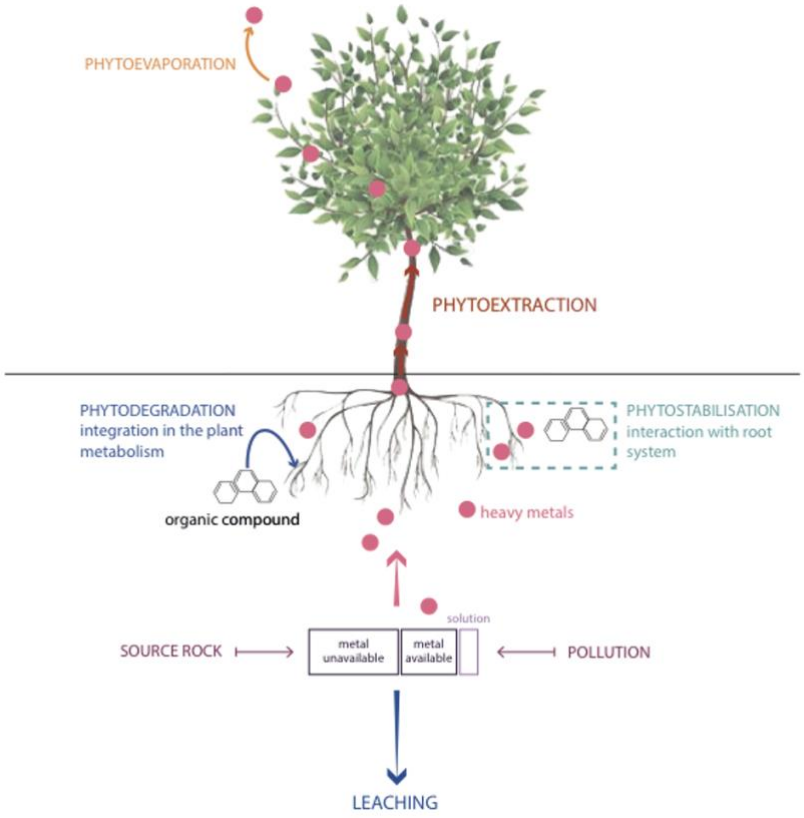


Figure 1.10: principles of phytoremediation

1.4.3 The choice of feedstock is context specific: hyperaccumulators vs dedicated biofuel crops

Many studies have been carried out using hyperaccumulators for phytoremediation. They are plant species that can hyperaccumulate metals in their natural habitat, 50 to 100 times more than non-accumulating plants depending on the metal – 1 mg metal per kg dry mass for Au/Cd

for example and up to 10 000 mg metals per kg dry mass for Zn, Ni, As.[188] There are more than 500 hyperaccumulating species known today, of which 2/3 hyperaccumulate for Nickel.[189,190] These plants, usually native of an area with a natural occurrence of metals in the soil, are largely from the *Brassicaceae* family. However, most hyperaccumulators have biological drawbacks: only native in certain areas of the world (naturally ultramafic soils) and commonly exhibit low biomass yields.[191,192]

Some studies have focused their attention on plants that are non-accumulating species but present significant biomass yields. The robust nature of second generation biofuel crops (i.e., the presence of lignin) makes them potential candidates for crops grown on land unsuitable for food-based agriculture, such as low to MaCL; and can tolerate some amounts of metals in their growing environment. Plants from the *Salicaceae* family (e.g. willow, poplar), but also rape seed, sunflowers, tobacco, miscanthus, sorghum have been investigated.[167,193–197] *Miscanthus spp*. are species native to Asia, over a wide range of climates and challenging soil conditions (including abandoned mines and low pH soils).[198–200] Within the *Miscanthus* genus are highly productive perennial energy types that have low requirements for agricultural inputs and have shown tolerance for growth on MaCL, providing the potential for environmental and economic benefits.[201–203] Miscanthus hybrids have even demonstrated differences in metal uptake.[204–207] Some metals are easier to remediate, especially if they are taken up naturally as nutrients in small quantities such as Zinc.[208–210] Growing feedstocks on MaCL could have a positive impact on land-use but raises the issue of the safety and fate of trace element and pollutants in the biomass after harvest. Because of their potentially hazardous nature, these feedstocks are very often burnt for heat and the ash subsequently treated. Moreover, the choice of species to use for phytoremediation depends on other several factors: the concentration and extent of the contamination (toxicity thresholds), the bioavailability of metal in the soil (dependent on a number of factors including pH, clay content and cation exchange capacity [180,211–215]) and finally the technology available/to be used for the valorisation of the biomass.[189,216]

1.4.4 Agromining and conventional processing of metal enriched biomass

The phytoextraction of metals followed by the recovery of metal from the plant is called phytomining.[217] It is an interesting technology to subsidise the cost of phytoremediation on a contaminated site. It requires a plant which can extract a significant amount of metal, an agronomic technology to achieve high biomass yield and a final process to efficiently recover the metal to a valuable form.[218–222] The term agromining is also used because of the multidisciplinary aspect of phytoremediation: the plant can be engineered or factors influencing metal uptake can be altered to achieve a more successful phytoremediation.[223,224]

Therefore, the challenge of phytomining is to combine a phytoremediation with a technology that would turn this trace element enriched biomass into a profit. This would provide a cheap and new renewable feedstock for the bio-based economy and a recovery of metal(s), while improving ecosystem services.

1.4.4.1 Phytoexclusion: no significant metal uptake but valorisation of marginal land

Phytoremediation technologies can produce a waste stream: a metal enriched biomass, which cannot be released into the environment.[225–227] To avoid producing and dealing with contaminated biomass, phytoexclusion (or phytostabilisation) can be used: the biomass grown on MaCL is unable to take up any contaminant from the soil and therefore, free from contaminants.[228] This is the case for a large number of non-extracting energy crops. This feedstock can undergo regular biomass conversion: gasification for syngas generation,[229] biodiesel/bioethanol production[230] or anaerobic digestion for biomethane and compost production.[231] However, this needs to be closely and regularly monitored as to which extent the biomass does not extract hazardous substances. The species might change their behaviour by adapting to the soil environment. Moreover, even if the process has a positive impact on the functionality of the soil and can provide a valuable source of energy/chemicals, the site in question is not remediated. The pollutants remain and the land will not improve in value or ever be converted into an agriculture site. This area of research is only at trial stage.[232]

1.4.4.2 Metallurgy for hyperaccumulators

The potential end-use of contaminated biomass from phytoextraction is the current challenge for the success of the technology for clean-up, especially on the fate of trace elements during biomass conversion. Hyperaccumulating species exhibit low biomass yields but high metal bioaccumulation factors. Because of these features, the most traditional conversion route for hyperaccumulating biomass is extractive metallurgy for metal recovery, i.e., the process of removing valuable metals from its source and refining the extracted raw metals into a purer form. There are two types of extractive metallurgy. Pyrometallurgy is the most widely used pathway to deal with contaminated phytobiomass because it is easily scaled-up, it is an efficient way to concentrate the metals from the biomass into the ash, it lowers the transportation costs of the bio-ore and the scale of the downstream process used to extract the metals from the resulting ash.[233] The biomass is ashed at temperatures at 550°C to effectively remove organics - but not above as certain elements may be lost to volatilisation along the process. Once the ash is produced, the metals are leached out for recovery. This is usually done in aqueous solutions using hydrochloric or sulfuric acid. It is a relatively cheap process, and the effluent can be neutralised with quick lime. The leachate is further partly evaporated to concentrate and refine the final product (see below for the case study of Nickel).

Because the majority of hyperaccumulating species accumulate for Nickel and there is relatively high economic value for this metal, the focus of phytomining within the past twenty years has been attributed to the profitability of Nickel from hyperaccumulating plants.

Some researchers have successfully recovered Nickel salts as a valuable product of the process.[220,234,235] A patent had been submitted for the hydrometallurgical process of ammonium nickel sulphate hexahydrate (ANSH) from a contaminated site in Albania using the plant *Alyssum Murale* as shown in the simplified scheme of the process in Figure 1.11.[234,236] The process has more than 10 steps, divided in 3 stages: leaching of Ni from the ash to the aqueous phase, crystallisation of the Ni salt and purification/separation of the salt. This process is still under optimisation, but they estimated the value of the crop at 16 000$.ha^{-1} using this process. Using similar technologies, they also used other families of plants such as *Thlaspi Caerulescens* for Cadmium and Zinc decontamination.[237] Researchers have also investigated turning phytoextracting biomass into metal-based catalysts. This is usually done by leaching the ash with hydrochloric acid, followed by deposition on clay (montmorillonite). Two French start-ups, Stratoz and Econik, are investigating hyperaccumulators ash to produce Lewis acid catalysts and show good performance in 'green organic synthesis' (e.g. Diels-Alders reactions).[233,238]

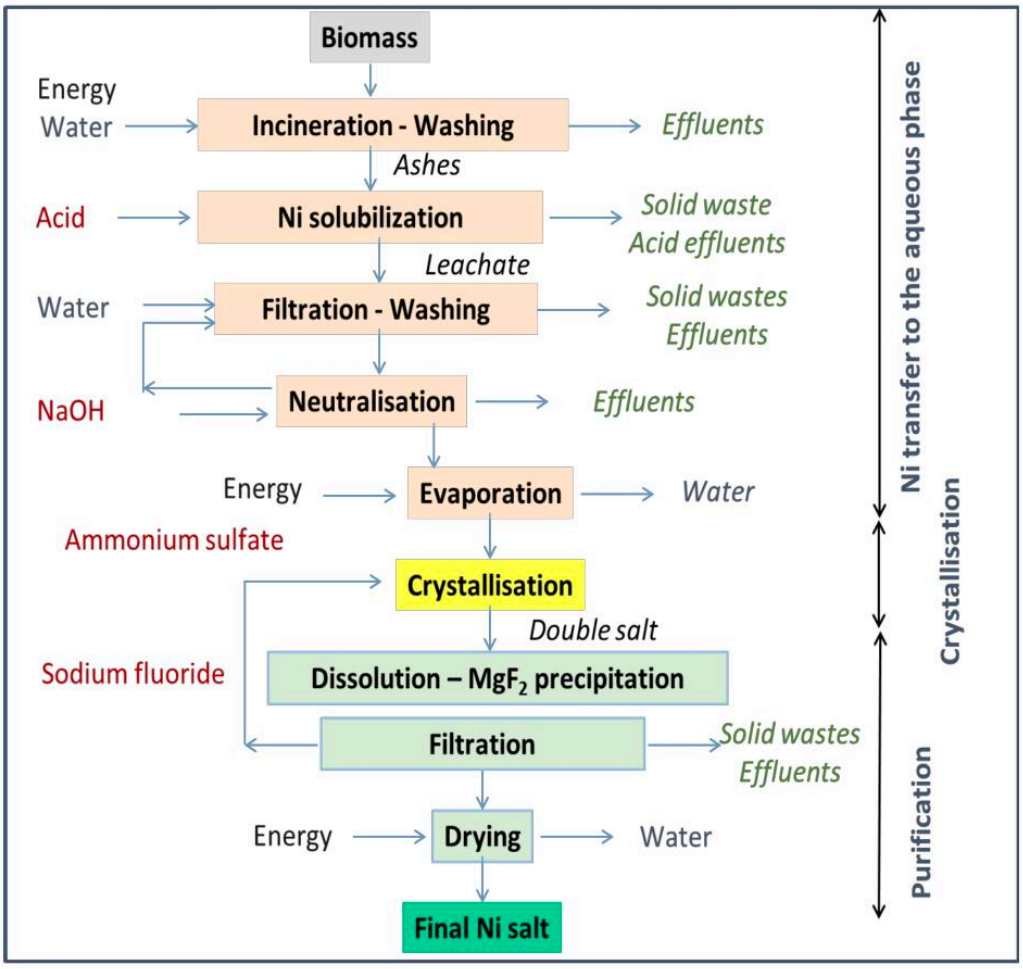


Figure 1.11: simplified scheme to produce ANSH salt from A.murale biomass

Provided the metals' concentrations in the ash are low enough and the ash not used for metal leaching, the product can be used for fertiliser (depending on the regulations), added to sewage sludge, or even landfilled.

Finally, hydrometallurgy is a process by which the biomass does not undergo ashing before metal leaching. This method only uses hot compressed water between 200°C and 375°C at 25 MPa; for a significant energy demand and produces a metal contaminated water stream.[236] Metals such as Ni, Zn, Pb, Cu have been recovered by hydrothermal treatment from hyperaccumulators. Unlike pyrometallurgy, the leachate contains organic compounds, which adds complexity to the refining of the metals.

1.4.4.3 Biorefinery of compromised biomass

When dealing with metal enriched energy crops, the feedstocks could undergo regular biomass conversion to biofuels but the fate of the metals during processing is still being investigated or even unknown as it depends on the technology used. They can also go through incineration for valorisation of their metal content (like hyperaccumulators).[239,240] First and

second generation of biofuel crops have been studied, such as miscanthus, maize, rape seed, wheat, poplar, and woody species like willow.[241,242]

However, there is a gap between the metallurgy and biorefinery technologies, or more specifically how to integrate/couple/articulate both to make the most of the biorenewable energy and metal stream[243–247]; and illustrated in Figure 1.12. The biochemicals and biofuels need to be produced while simultaneously extracting the metals from the biomass.

Only a few researchers are looking into producing clean, metal-free products: one study investigated the fate of trace elements in tobacco, birch and willow feedstocks after different pretreatment methods - ethanol Organosolv, soda and dilute acid pretreatments or even ionic liquid.[227,248] It seems that alkaline pretreatment does not exhibit any metal extraction from the biomass; soda pretreatment maintains the metals in the cellulose pulp, leaving a clean lignin and effluent stream; and acid pretreatment shows high metal extraction in the cellulose pulp and lignin for valorisation but still leaves a metal contaminated water effluent afterwards.[225,249]

Another study has investigated a tandem phytoremediation/biorefinery process for the valorisation of Nickel contaminated sunflowers and white mustard. The first step is an aqueous metal extraction (hydrothermal, agitation and homogenisation were studied) followed by solid state lignocellulose degradation by the fungus *Phanerochaete chrysosporium* for sugar and phenols release. The aqueous metal extraction reaches 80 % using hydrothermal extraction and can subsequently produce bio-derived chemicals but there is no indication on the treatment of the contaminated waste stream effluents nor actual yields in % of the bio-derived chemicals.[250]

Pyrolysis and thermochemical conversion of contaminated crops have been also researched.[225,251] As, Cd, Zn and Pb tend to transform to their gaseous forms at relatively low temperatures (<1000 °C), thus their potential emission is of significant concern. Operating at high pressure significantly increases the starting temperature for phase transformation of heavy metals. After completion of pyrolysis, more than 98.5 % of the metal in the product stream was present in the char stream, which could be considered as a metal concentrate to be subsequently processed for metal extraction.[252] Incineration of contaminated plant material in special dedicated smelters seems to be less time consuming, and being an environmentally sound and economically acceptable alternative.[253] This requires special furnaces and filters for the different metals (especially for Arsenic, which will volatilise in a variety of oxygenated forms).

Finally, contaminated biomass can be digested for the production of biogas and compost.[254] The metal contents of the biomass (Al, Cd, Cu, Ni, Zn, Co) does not seem to affect the anaerobic fermentation and can be a source of methane for direct heating or further utilisation for generation of electricity. However, the residue of the digestion is still metal contaminated

and needs to be treated. The further decontamination step(s) obviously depends on the nature and quantity of the metals: sludge application, special waste treatment facility or even landfill.

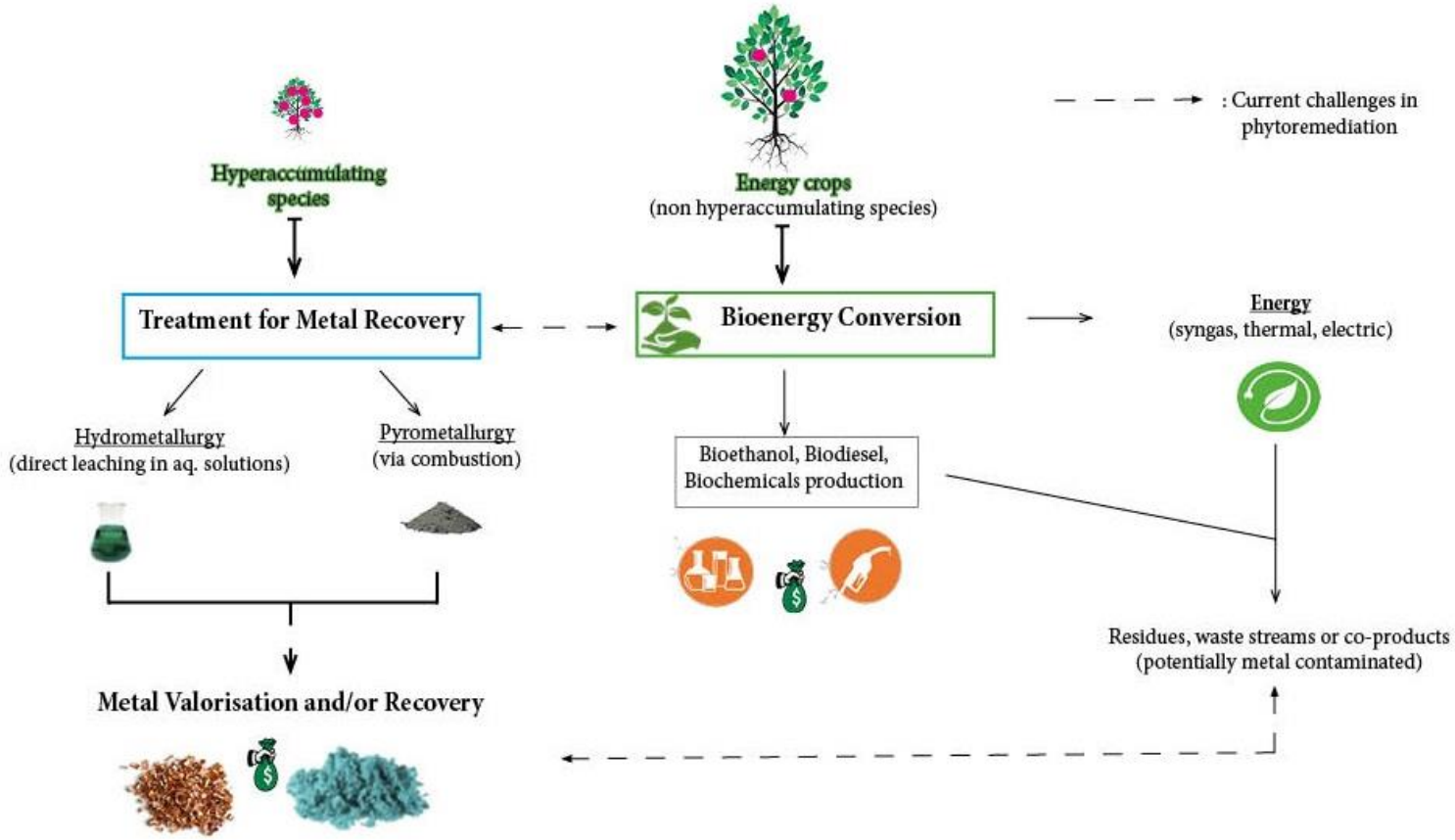


Figure 1.12: current technologies and challenges regarding phytoremediation biomass valorisation

In summary:

- Sustainable bioenergy is not clearly defined and often context specific,
- Lignocellulosic biomass is, by its chemical nature, more complex to valorise and requires a pretreatment step,
- Ionic liquids are tuneable, recyclable solvents, some used in the deconstruction of lignocellulosic biomass,
- Some other ionic liquids also exhibit metal coordinating properties, however combining several of these ionic liquid properties in one process has not been extensively studied,
- Ionic liquid based pretreatment of biomass is binary in terms of product outcomes, i.e., carbohydrates, lignin,
- Marginal, degraded and contaminated land can be used to grow renewable lignocellulosic feedstock under the right conditions,
- Waste and contaminated biomass are mostly incinerated into bio-ash for valorisation in conventional metallurgical or biorefinery processes.

1.5 Research gaps and objectives

As it has been explored in this literature review, research is still to be carried out on the sourcing, processing and delivery of bioenergy and bioproducts to support a sustainable biorefinery. One of the key reasons hindering the energy and chemical transition is the lack of research on scalable bioenergy processes, which can integrate all type of lignocellulosic feedstocks in a cost effective manner and produce a wide range of chemicals and energy to feed the expanding bioeconomy. Moreover, the use of marginal, degraded contaminated land for bioenergy production has been raised as a sustainable alternative for bioenergy; nevertheless, using such areas for biomass production and valorisation needs to be investigated in terms of variety of feedstocks, nature of contaminants in feedstocks and derived products. Currently, the main product stream from integrating metal contaminated feedstocks is metal enriched ash, as the process always involves burning of the biomass, a bio-conversion step too often used, which completely overlooks the potential for bulk biochemicals from lignocellulosic biomass. This PhD researches, for the first time, the combination of phytoremediation inputs with IL-based pretreatment processes to simultaneously produce clean renewable energy as well as a recoverable metal stream for the valorisation of marginal areas.

The ionoSolv process is a promising approach, which has made significant progress in the past ten years, developing low-cost protic ionic liquid water mixtures, to produce high purity cellulose and a lignin stream; using conventional biomass feedstocks. In this thesis we will test the hypothesis that the ionoSolv is flexible enough and study the design of the process to pretreat unconventional feedstocks. Here unconventional feedstocks are defined in two different ways: (1) unconventional nature of feedstocks, lignocellulosic matter which has not been studied for a pretreatment process such as waste (invasive species and construction wood) and (2) unconventional growth environment (metal contaminated soil and irrigation with wastewater).

In order to prove that such process is in fact ‘feedstock agnostic’, a wide range of waste and innovative materials need to be investigated and characterised to be integrated into a larger scale ionoSolv biorefinery, or any other biorefinery. Furthermore, the product outcomes of the ionoSolv process have remained exclusively binary: cellulose pulp and lignin. Here, the solubility of metals in some protic acidic ionic liquids offers an opportunity to treat metal contaminated biomass and study the solubility and fate of metals during the process. Using such ionic liquids, the ionoSolv process would combine both valorisation of biomass and detoxification of the feedstock and its product streams, without the need to burn the biomass. The diversification stream of products could be even further expanded by determining if it is

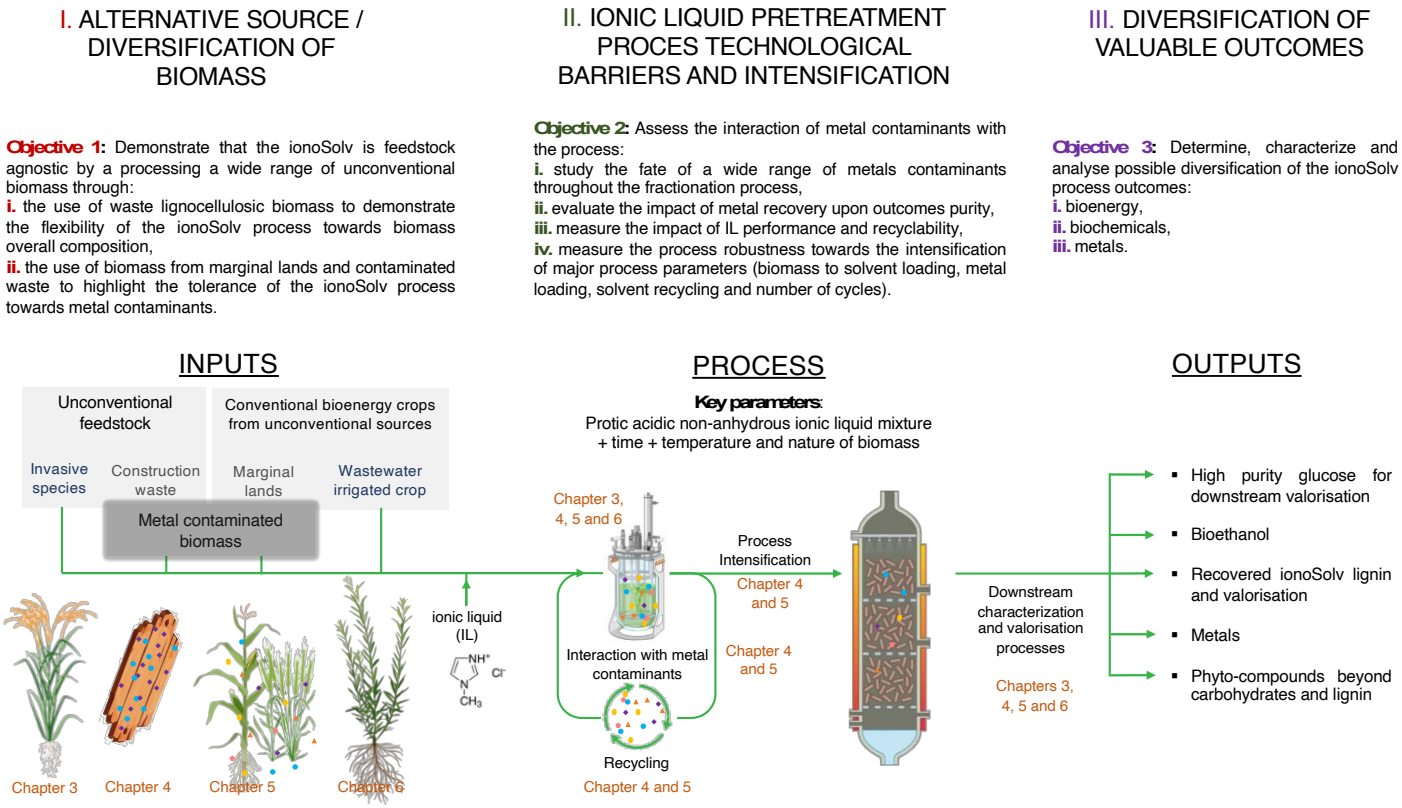
possible to produce a bioethanol, as a proof of biofuel production, along with bioheat, recovered metals and extractives. Diversification of products is at the core of the biorefinery concept, where all possible chemicals can be investigated and extracted from one starting material: lignocellulosic biomass. This thesis aims to investigate the chemical engineering aspects of the process; while economic and ecological aspects shall be investigated by others.

Using state-of-the-art trace element analysis, this chemical engineering piece of research aims at investigating new and alternative sources of biomass for the ionoSolv pretreatment, study the technological barriers and process intensification for using such unconventional feedstocks, and diversify the valuable outcomes from the ionoSolv pretreatment using marginal, degraded contaminated land. The boundaries of study of this research are the supplied biomass, the ionic liquid process and separation into selected product outputs, as well as the recycle aspect of the solvent (referring to Douglas design methodology in 1.3.3.).

The objectives of this project are illustrated in Figure 1.13 and described as follows:

- demonstrate the value of unconventional feedstocks for an ionic-liquid based technology,
- measure the transformation yield of those new type of feedstocks, without burning or ashing the whole plant,
- evaluate the flexibility and the feedstock agnostic property of the process towards biomass overall composition, solubility of lignin and fractionation of lignocellulosic components,
- study the impact of metal contamination associated with some of those feedstocks, and investigate the technological barriers of pretreating such feedstocks in ionic liquid media,
- track the fate of a wide range of metal contaminants through the process,
- determine the impact of process parameter intensification and metals on the process and the recycling of the ionic liquid,
- Study other valuable outcome products from the ionoSolv process in order to diversify and valorise its waste streams, but also enhance the process economics, by carrying out deep lignin analysis, post-hydrolysis solids conversion, extraction of phytochemicals and recovery of metals.

Figure 1.13: visualisation of this this chemical engineering research aims and objectives



1.6 Thesis structure

This thesis is structured into 7 chapters, outlined as follows:

- Chapter 1 aims to provide a background regarding sourcing sustainable renewable lignocellulosic biomass, the use of ionic liquids for such feedstocks, the challenges behind the utilisation and valorisation of marginal and contaminated areas,
- Chapter 2 describes the materials and experimental methods used to carry out this research,
- Chapter 3 investigates the integration of two UK invasive terrestrial biomass species and its implication for the ionoSolv pretreatment process development, varying process conditions, the characterisation of its raw biomass and product outcomes,
- Chapter 4 focuses on using post-consumer Chromated Copper Arsenic treated waste wood as a highly pernicious feedstock for clean renewable bioethanol and products, studying the fate and management of metals through recycling of the ionic liquid and valorisation process of its waste streams,
- Chapter 5 researches the sourcing of various feedstocks from real-world marginal contaminated land and larger phytoremediation trials, carrying out state-of-the-art

trace element analysis and tracking of metals throughout the ionoSolv process, up until recovery of metals in ionic liquid media via electrodeposition,

- Chapter 6 expands the supplying of ionoSolv process with a biofuel crop grown with the addition of a stress condition, namely the irrigation of Willow with diverted municipal wastewater, analysing the quality of the biomass as a biorefinery feedstock and the impact of phytoextraction of specialty compounds on the process,
- lastly, the key conclusions and findings are summarised in Chapter 7, along with future work aspects and limitations of this research.

2 Materials and methods

2.1 Overview of experiments and collaborations with Imperial contributing to this thesis

Thesis Chapter		Sourcing of biomass	Laboratory experiments performed at Imperial by Hennequin (unless specifically stated otherwise)	Laboratory experiments performed outside Imperial from collaborations	Analysis of the results
Invasive species		External: companies, relatives	all experiments described in this chapter performed by Hennequin	None	Hennequin
CCA treated wood		External: company in China	all experiments described in the chapter including all product analysis, except running the pyrolysis reactor (Dr Clementine Chambon)	None	Hennequin
Feedstocks from MaCL by site of origin	Wales	Dr Jenssen	processing of biomass, trace element analysis, compositional analysis, pretreatment (from IL synthesis to product streams analysis), recycling, electrochemistry	XRF and pH measurements of the contaminated soil in Wales	Hennequin
	Poland	Dr Pogrzeba and Kryzak	processing of biomass, compositional analysis, trace element analysis, pretreatment (from IL synthesis to product streams analysis)	None	Hennequin
	Market Harborough	collected by Hennequin	processing of biomass, trace element analysis	None	Hennequin

	Stoke Bardolph	collected by Hennequin	processing of biomass, trace element analysis	None	Hennequin
	Cinderhill	collected by Dr Wood	processing of biomass, trace element analysis	None	Hennequin
	Silwood Park (pot trials)	Hennequin, cuttings purchased from *Willow Bank*	pot trials, processing of biomass, trace element analysis	None	Hennequin
Wastewater Willow		Trial led by Dr. LaChapelle	pretreatment (from IL synthesis to product streams analysis), compositional analysis, trace element analysis	Phytochemicals extraction and untargeted metabolite data by Sas	Hennequin and Sas

Table 2.1: overview of materials, methods and contributions to this PhD thesis

2.2 Feedstock collection

2.2.1 Feedstocks

- Invasive species

Japanese knotweed dried stems were supplied by Japanese Knotweed Ltd. Rhododendrons were collected by Mrs T. Dancey from a public area at a roadside in Dorset.

- Waste wood

Pine (*Pinus sylvestris*) was obtained from Metla (Finish Forest Research Institute). CCA treated wood was received from Tianjin Dongli District Yilin wood preservative processing plant in China.

- Biomass samples from real life contaminated sites

  - Miscanthus and Reeds feedstocks from Wales were obtained from Dr Elaine Jensen, Aberystwyth University, UK. They were grown in an abandoned mine area: Bwlch Glas Mine, Talybont, Ceulanymaesmawr, Wales, UK (52° 28' 20" North , 3° 54' 3" West).[255] The 2 year old biomass was harvested in winter 2019 and oven dried at 60°C. Further information on the planting trial and quality of the soil is available in the Appendix. Upon reception at Imperial College, all samples from each row were pooled together.

- Miscanthus feedstocks from Poland were obtained from Dr Marta Pogrzeba and Jacek Kryzak at the Institute for Ecology of Industrial Areas (IETU), a Polish research centre acting under the Minister of Climate & Environment. Samples were obtained from the field trield 'Phyto2Energy' grown on a heavy metal degraded local area: *Miscanthus x giganteus* winter harvest of a 4 year old plantation. [256]

- Canadian Willow for wastewater remediation

A four-hectare willow plantation was established in 2008 at Saint-Roch-de-l'Achigan (45° 50′ 50″ N–73° 38′ 27″ W) using *Salix miyabeana* 'SX67' at a density of 16,000 trees ha^{-1}. Three plots (10 x 10 meters each) were left unirrigated as controls while three others were irrigated with primary municipal wastewater effluent. Irrigation rate was 29.5 million litres of wastewater per hectare and per year. The detailed composition of the wastewater used was carried out and reported by Lachapelle et al. and Jerbi et al.[257,258] At the end of a three-year coppice cycle, three willow trees were randomly selected within each plot (control / wastewater) and the entirety of the aboveground biomass was harvested. Leaves were removed and stems from each tree were air dried to a constant mass. All samples were analysed in three biological replicates (each tree individually for each treatment). Each of these samples were carried out in technological triplicates, as a way to observe any differences between each treatment (control / wastewater) and laboratory experiments (standard deviation between the same sample).

2.2.2 Handling and processing of lignocellulosic biomass

All material was air-dried to a moisture content below 12 wt % to avoid any microbial growth. A Heavy Duty Cutting Mill SM2000 was used to ground the biomass, which was subsequently sieved using an analytical sieve shaker to a particle size between 180 and 850 μm.

The moisture content of biomass was determined using the National Renewable Energy Laboratory (NREL) protocol 'Determination of Total Solids in Biomass and Total Dissolved Solids in Liquid Process Samples'.[259] Samples were weighed into a tared piece of aluminium foil, which was folded and placed in a VWR Venti-Line convection oven at 105°C overnight. The following day, the sample folded in aluminium was removed from the oven and placed in a desiccator for 20 minutes to cool down and the final mass was recorded. The moisture content of the sample was calculated on air-dried basis according to the equation:

$$Moisture\ content\ (\%) = mc = \frac{m_{air-dried} - m_{oven-dried}}{m_{air-dried} - m_{al\ foil}} \times 100$$

where $m_{air-dried}$ is the air-dried mass of the foil and biomass, $m_{oven-dried}$ is the mass of the foil and biomass on the following day and $m_{al\ foil}$ is the mass of the aluminium foil on its own.

2.2.3 Context of feedstock growth

2.2.3.1 Contaminated soil sample collection

Three sites had been accessed for this study and soil was collected to carry out pot trials (using the one from Stoke Bardolph). Further details are available in the Appendix.

Origin of soil sample	Description	Purpose	Contamination	Biomass feedstock found on site	Site Contact
Market Harborough, UK	Pigeon clay shooting site highly contaminated with Pb.	Site to be treated via current remediation technologies (stabilisation).	High Pb concentrations up to 4000 $mg.kg^{-1}$ in the soil.	*Triticum aestivum* (wheat)	Simon Coffey (GRM Development Solutions Ltd)
Stoke Bardolph, UK	Historical agricultural land site from Severn Trent used for sewage sludge disposal.	Site used for energy production from anaerobic digestion.	Heavy metals and metalloids: Cd, Cu, Pb, Ni, Zn, F, Hg, Mo, Se, As, Cr.	*Zea mays* (maize)	John Jackson (Severn Trent Energy and Crop Plant Manager
Cinderhill, Derbyshire, UK	Tar pit (more details in the Appendix)	Historical contaminated site[260,261]	Heavy metals (Pb) and hydrocarbons	Variety of softwoods and hardwoods	Harvey Wood (Clean Rivers Trust)

Table 2.2: details of the contaminated sites studied

2.2.3.2 Pot trials

Pot trials were conducted at Imperial Silwood Park campus in the Impact Greenhouse space. John Innes compost N°2 was used for the controls, while the contaminated soil used was the one obtained from the Stoke Bardolph site.

Willow cuttings were supplied from the Willowbank, Gloucestershire, UK. The cuttings were 30 cm long and consisted of *Salix Viminalis,* cultivated variety (cv) BG1, Gaston and Rocket. Tobacco seeds were purchased from Chiltern Seeds Ltd: *Nicotiana tabacum*, cv Tobacco Rosa.

The plants were placed in clean plastic pots and placed into plastic trays. Watering was done from the tray in order to avoid washing out of the soil. Biomass feedstocks were harvested after senescence (when the leaves have fallen off) ~ 3-4 months.

2.2.3.3 Soil analysis: pH and cation exchange activity

The cation exchange capacity of soil samples was measured based on the modified silver-thiourea method developed by Dohrmann.[262] Each sample was done in triplicates, along with blanks. 15.2 g of thiourea were dissolved in 1400 mL of ultra-purified de-ionised water and sonicated for a few minutes. 3.397 g of $AgNO_3$ were dissolved in 300 ml of de-ionised water. The silver solution was added slowly to the thiourea solution while stirring. Finally, 200 ml of 1M ammonium acetate solution for a final solution of AgTU (silver thiourea solution) 2L and used straight away for the cation exchange measurements of the soil.

50 mL of AgTU is added to the 1 g of soil (<2mm) and the suspension was shaken for 2 hours in a 250 ml volumetric flask. 25 mL of trace element grade of 0.5 M HNO_3 was added to the sample. The solution was centrifuged for 20 minutes at 3000 RPM. The supernatant was poured into a flask and washed out with 50 mL of de-ionised water. The solution was centrifuged and washed with another 25 mL of de-ionised water before chemical analysis.

The cation exchanged capacity (CEC) is the determined difference between the initial and remaining silver content, measure using an Agilent 7800 ICP-MS.

The pH of the soil was measured according to the *Kellogg Soil Survey Laboratory Methods*.[263] 20g of soil was sieved (< 2mm) and mixed with 20 mL of ultra-purified water (1:1 w:v). The sample is allowed to stand 1 hour with occasional stirring before the 1:1 water pH is measured. Results are available in the Appendix.

2.3 Biomass characterisation

2.3.1 Compositional analysis for structural carbohydrates and lignin in biomass

For the compositional analysis of untreated biomass samples, the extractives content of the biomass was measured first using 150mL of absolute ethanol for 24 hours in a Soxhlet apparatus, following the NREL protocol 'Determination of extractives in biomass'.[264]

Compositional analysis was carried out according to a published procedure by the NREL 'Determination of Structural Carbohydrates and Lignin in Biomass'.[265] Briefly, 300 mg (calculated on dry matter basis) of biomass or recovered pulp was incubated with 3 mL of 72 % sulfuric acid at 30°C for 1 hour and then diluted with 84 mL distilled water before being autoclaved for 1 hour at 121°C. The samples were then filtered through ceramic crucibles of a known weight. Two aliquots of the filtered samples were then prepared in 15 mL falcon tubes. One is used to determine the acid soluble lignin content (ASL) by UV analysis at 240 nm on a Perkin Elmer Lambda 650 UV/Vis spectrometer according to the equation:

$$ASL\ (\%) = \frac{A \times V_{filtrate}}{\varepsilon \times ODW_{sample} \times l} \times 100$$

where A is the absorbance at 240 nm, l is the path length of the cuvette in cm (1 cm), ε is the absorptivity of biomass at specific wavelength (L/g cm), ODW is the oven-dried weight of the sample (mg) and $V_{filtrate}$ is the volume of the filtrate (mL).

The other aliquot was used to determine the carbohydrate concentrations of the sample via HPLC. The samples were neutralised to a pH of 5-6 using calcium carbonate to be match the working range of the HPLC column. The samples were filtered through a 0.2 μm syringe filter for HPLC analysis. Sugar concentrations were determined using a Shimadzu HPLC system with a Refractive Index Detector (RID) and a micro-guard deashing column (BioRad), 30 x 4.6 mm, to avoid any contamination of the system. The HPLC system was serviced each week with a routine maintenance consisting of a 30 % acetonitrile wash (HPLC grade) for 4 hours to offer optimum resolutions. The column used was an Aminex HPX-87P from Bio rad, 300 x 7.8 mm, purified water as mobile phase at 0.6 ml/min, column temperature 85°C, 25 minute run. The samples were systematically run along with sugar standards in different concentrations (0.1, 1, 2, 4 and 8 mg/mL): glucose, xylose, galactose, arabinose and mannose.

The crucibles were oven dried at 105 °C overnight before weighing to determine acid insoluble lignin (AIL) and then incubated at 575 °C in a muffle furnace to determine ash content, using the following equations:

$$AIL\ (\%) = \frac{m_{crucible+AIR} - m_{crucible+ash}}{ODW_{sample}} \times 100$$

$$Lignin\ (\%) = \%\ AIL + \%\ ASL$$

where $m_{crucible\ +\ AIR}$ is the weight of the oven-dried crucible plus the acid insoluble residue (AIR), $m_{crucible\ +\ ash}$ is the weight of the crucible after ashing to constant temperature at 575°C and ODW_{sample} is the weight of the sample used (mg). The total lignin content is the sum of the *AIL* and the *ASL*.

From the compositional analysis results of both untreated and pulp samples, glucan recovery, hemicellulose removal and lignin removal were calculated according to the following equations:

$$Glucan\ recovery\ (\%)\ = \frac{Glucan_{pulp}\ x\ Yield_{pulp}}{Glucan_{untreated}} \times 100$$

where $Glucan_{pulp}$ is the glucan content in the cellulose pulp, $Yield_{pulp}$ is the yield of the pulp after ionoSolv processing relative to untreated biomass, and $Glucan_{untreated}$ is the glucan content in the untreated biomass. The glucan content is the total glucose derived from either cellulose or hemicellulose.

$$Hemicelluose\ removal\ (\%) = \frac{Hemicellulose_{untreated} - Hemicellulose_{pulp} \times Yield_{pulp}}{Hemicellulose_{untreated}} \times 100$$

where $Hemicellulose_{untreated}$ is the hemicellulose content of untreated biomass calculated as the sum of all sugars (except glucose) and $Hemicellulose_{pulp}$ is the hemicelluloses content in the cellulose pulp. The hemicellulose content is the sum of the following carbohydrates: xylose, galactose, arabinose and mannose.

$$Delignification\ (\%)\ = \frac{Lignin_{untreated}\ -\ Lignin_{pulp} \times\ Yield_{pulp}}{Lignin_{untreated}} \times 100$$

where $Lignin_{untreated}$ is the lignin content in the untreated biomass and $Lignin_{pulp}$ is the lignin content in the recovered cellulose pulp after the ionoSolv pretreatment.

2.3.2 Composition analysis for extractible compounds

2.3.2.1 Willow phytochemicals extraction

Persistent phytochemicals were extracted using a Dionex ASE 350 Accelerated Solvent Extractor (ASE) system equipped with 11 mL extraction cells. Briefly, 1.2 g (calculated on DM basis) ground stem material was extracted with a methanol-water solution (75-25 % v/v) at 100°C (under ~1500 psi). ASE conditions were a 5-minute heating phase, 3 cycles of 7-minute static extraction phases, 150 % flush volume and 120 seconds purge.[264] Extracts were made up to 50 mL with the solvent, centrifuged at 5000 RPM for 5 minutes, filtered at 0.2 μm porosity, diluted with ultra-high purity water (1:1) and stored at -70°C prior to LC-MS/MS analysis. The extracted biomass was oven-dried at 105°C for 24 hours to measure mass loss.

2.3.2.2 Liquid chromatography-tandem mass spectrometry (LC-MS/MS) acquisition

Chromatographic separation was performed using an Agilent 1260 Infinity system, where 10 μL of extract was injected onto a Zorbax Eclipse Plus C18 column (4.6 x 100 mm, 3.5 μm) at 30°C. Mobile phase was solvent A (water, 5 % methanol, 0.1 % formic acid) and solvent B (methanol, 0.1% formic acid) with a flow rate of 0.4 mL min^{-1} and an 80-minute elution gradient: 100 % A hold for 20 min, then a linear increase from 0 % to 100 % B over 50 min and 100 % B hold for 10 min.

Untargeted full-scan (100-1300 Da) MS1 acquisition was performed on extracts from all biological samples (18 trees in total) and blanks (extraction solvent and mobile phase) using an Agilent Q-TOF 6530B mass spectrometer equipped with an Agilent Jet Stream ion source operating in negative ion mode (ESI (-)). Gas temperature was 300°C, drying gas flow was 5 L min^{-1}, and the nebulizer pressure was 45 psig. Sheath gas temperature was 250°C with a gas flow of 11 L min^{-1}. MS2 acquisition was performed on 3 biological replicates per treatment (from 6 trees in total) and blanks (samples extraction solvent and mobile phase). Tandem mass spectra were acquired with a collision energy of 20 and 35 V. UV spectra were also acquired from 200 to 550 nm with 10 nm increments.

2.3.2.3 Untargeted metabolite data analysis

Raw LC-MS data were processed using by Sas by the open-source software package MZmine 2.37/53 (http://mzmine.github.io/).[266] After detection, features were deconvoluted, their isotopic peaks grouped, and alignment was performed across samples before dereplication of phytochemicals detected as multiple features. Background noise cut-off was set to an

intensity threshold of 5000 for MS1 spectra and 1000 for MS2 spectra with a minimum 10,000 peak intensity threshold for feature detection. Deconvolution used the local minimum search algorithm and isotopic features were grouped with 20 ppm mass tolerance, 0.4 min retention time tolerance. Features were aligned with 20 ppm mass tolerance (weighing for 80 %) and 0.4 retention time tolerance (weighing for 20 %) across samples. Only features detected in >5 samples, with an isotope pattern, a blank:sample average ratio <50 % and within 5-74 min retention time were retained. Features eluting within < 0.2 min retention time and with peak shape correlated by >85 % (MZmine metaCorrelate algorithm) were assigned to a feature correlation group and used for curation of adducts, complex formation, and in source fragments.[267]

Principal component analysis (PCA) and differential abundance analysis of features were performed with the MetaboAnalyst platform (www.metaboanalyst.ca).[268,269] Significant differential abundance analysis compared mean peak areas calculated per plot (3 trees per plot) for each treatment (3 plots) using the univariate non-parametric Mann-Whitney U-test followed by Benjamini-Hochberg false discovery rate (FDR) correction ($p<0.05$). Permutational multivariate analysis of variance (PERMANOVA) used Benjamini-Hochberg false discovery rate correction and permutations set to 9999 (Adonis function, R package vegan).[270]

Putative chemical formulas of differentially abundant features were generated *in silico* with 14 possible ESI (-) adducts and 5 ppm m/z tolerance using CEU Mass Mediator (http://ceumass.eps.uspceu.es)[271], before comparison to an in-house Salicaceae Metabolite Library (including Populus Metabolite Database from the Plant Metabolic Network plantcyc.org/databases/poplarcyc/11.0).[272] Feature annotation was further refined by MS2 fragmentation where possible using published spectra as well as the Global Natural Product Social Molecular Network (GNPS) platform and SIRIUS 4 computational prediction.[273–275] For molecular networking, the minimum cosine similarity score was set to 0.7 and clusters were visualised with Cytoscape version 3.8.0 within GNPS. Each feature was annotated using either MS1 and MS2, MS1 only, or as an unknown feature, and categorised using standard confidence levels.[276] Features with multiple potential candidate metabolites or poor identification are annotated as derivatives of the most specific chemical class (*de novo* class prediction). Chemical classifications were based on Classyfire ontology included in Canopus MS/MS molecular fingerprint prediction within Sirius 4 and the literature.[277] All annotation should be considered as putative even when confirmed using matched MS2 fragmentation patterns as untargeted identification methodologies and database records are subject to change.

2.4 Ionic Liquid liquor pretreatment

2.4.1 Ionic Liquid synthesis

- *N,N,N*-dimethylbutylammonium hydrogen sulphate

N,N,N-Dimethylbutylamine (purity >99 %) and 5 M sulfuric acid were purchased from Sigma Aldrich. All commercial reagents and solvents were used as received. *N,N,N*-dimethylbutylammonium hydrogen sulphate, [DMBA][HSO_4] was synthesised in a one-step acid-based reaction under equimolar conditions. One mole of the amine, *N,N,N*-dimethylbutylamine (101.19 g), was weighed into a 500 mL round-bottom flask and cooled with an ice bath. Under stirring, an equimolar amount of the required acid (200 mL of 5 M H_2SO_4), was added dropwise. Excess water was removed using a rotary evaporator (Büchi). The water content of the ionic liquid was determined using a volumetric Karl Fisher titrator (V20 Mettler-Toledo), standardised using Hydranal water standards.

^1H and ^{13}C NMR spectra were recorded on a Bruker 400 MHz spectrometer by dissolving 20 mg of ionic liquid in 500 µl of DMSO-d_6. The solution was transferred to an NMR tube for analysis. All NMR spectra were analysed employing MestReNova software. All spectra were referenced to the DMSO peak at 2.500 ppm (^1H) and 39.520 ppm (^{13}C).

^1H NMR: δH (400 MHz, DMSO-d6)/ppm: 9.24 (s, ^1H, N−H), 3.02 (dt, *J* = 12.9, 5.0 Hz, 2H, N−CH_2), 2.76 (d, *J* = 4.3Hz, 6H, N−$(CH_3)_2$), 1.64−1.51 (m, 2H, N−CH_2−CH_2), 1.30 (h, *J* =7.4 Hz, 2H, N−CH_2−CH_2−CH_2), 0.89 (t, *J* = 7.4 Hz, 3H, N−CH_2−CH_2−CH_2−CH_3). ^{13}C NMR δC (101 MHz, DMSO-d^6)/ppm: 56.62 (N−CH_2), 42.48 (N−CH_3), 25.82 (N−CH_2−CH_2), 19.40 (N−CH_2−CH_2−CH_2), 13.71 (N−CH_2−CH_2−CH_2−CH_3).

- 1-methyimidazolium chloride

The minimum purity of the starting material for 1-methylimidazole was 99%. HCl was obtained as a concentrate containing 1 mole FIXANAL (Fluka Analytical). 3 moles of the ionic liquid 1-methyimidazolium chloride [HC_1im][Cl] was synthesised at once in order to always use the same batch of ionic liquid for all experiments. 3 moles of 1-methylimidazole (246.3 g) were cooled with an ice bath in a 2 L round-bottom flask. Under stirring, 3 moles of aqueous HCl (FIXANAL ampoules) were added dropwise. Excess water was removed using a rotary evaporator until a water content of below 20 wt % was obtained. The ionic liquid water mixture was recovered as a light yellow liquid.

^{1}H NMR: δH (400 MHz, DMSO-d_6)/ppm: 9.16 (s, 1H, H-2), 7.71 (s, 1H, H-4/ 5), 7.64 (s, 1H, H4/5), 4.5–3.5 (br, H2O, N-H+), 3.87 (s, 3H, N-CH3). ^{13}C NMR: δC (101 MHz, DMSO-d6)/ppm: 135.63 (C-2), 123.21 (C-4/5), 119.55 (C-4/5), 35.48 (N-CH3).

Acid-base ratio of the ionic liquids was determined using a G20S Compact Titrator (Mettler-Toledo) by titration with 0.1M of NaOH, standardised using hydrogen phthalate.

2.4.2 Fractionation of biomass: the ionoSolv process

The pretreatment of the biomass was conducted as described by the ionoSolv standard operating procedure from the Hallett laboratory.[278] A flow diagram of the experiments and process studied here are shown in Figure 2.1 below.

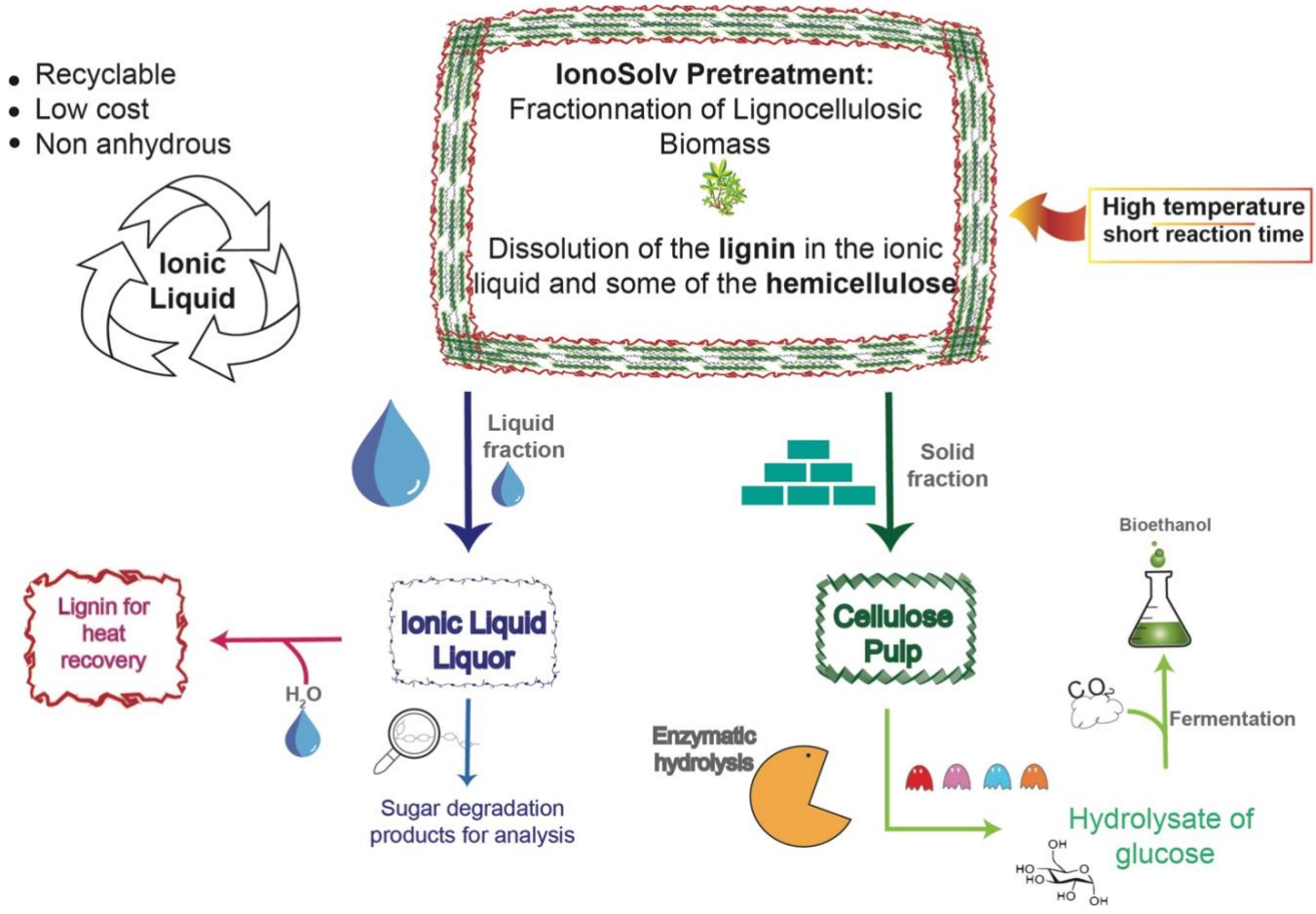


Figure 2.1: flow chart of the ionoSolv process

All samples were run in triplicate. The lignocellulosic biomass was pretreated with the ionic liquid with a final water content of 20 wt %, taking into account the water content of the IL and the moisture content of the biomass according to the equation:

$$Water\ content\ (\%) = \frac{m_{IL} \times wc_{IL} + m_{biomass} \times mc_{biomass} + m_{water}}{m_{IL} + m_{water}}$$

where m_{IL}, $m_{biomass}$, m_{water} are the masses of ionic liquid (IL) used, air-dried biomass and water added respectively. wc_{IL} refers to the water content of the IL and $mc_{biomass}$ is the moisture content of the biomass.

The solvent to biomass ratio used was 1:5 g g^{-1} or 20 wt % on an oven dried basis, according to the following equation:

$$Biomass\ loading\ (\%) = \frac{m_{biomass} \times (1 - mc_{biomass})}{m_{biomass} \times mc_{biomasss} + m_{IL} + m_{water}} \times 100$$

The desired biomass and IL mixture were transferred into 15 mL ACE pressure tubes, sealed with a Teflon cap and a silicone O-ring. The tubes were vortexed until homogeneity of the biomass/IL mixture was achieved.

The pressure tubes were placed into a Thermo Scientific convection oven for the pretreatment for a set time and temperature. After the pretreatment, the pressure tubes were allowed to cool down at room temperature. The pretreated slurry was transferred into a 50 mL falcon tube using 40 mL of absolute ethanol (VWR). The falcon tubes were vortexed and left to stand for one hour before being vortexed again and put into a VWR Mega-Star 3.0 centrifuge for 40 minutes at 3000 RPM. The supernatant was decanted into a round bottom flask. This ethanol wash was repeated three times, after which the resulted pulp fraction was transferred into a cellulose thimble and washed by Soxhlet overnight (20-24 hours) to remove any residual ionic liquid. The residual liquid fraction from the Soxhlet was added to the round bottom flask.

The pulps were not air-dried after the Soxhlet step, to avoid hornification.[279] Drying the cellulose pulps can induce physical changes in fibre structure, called hornification or pore collapse, that reduces enzyme accessibility to cellulose.[280,281] In a scaled-up or industrial process, pulps would be saccharified directly after washing, as an additional drying step would add an unnecessary step, here for analytical purposes only.
The wet pulps recovered from the Soxhlet were placed into a falcon tube with 40 mL of water, vortexed and centrifuged for 25 minutes at 3000 RPM. The supernatant was removed, and the pulps were kept in the falcon tube at 4°C to avoid any microbial growth.

The moisture content was determined in duplicate. The pulp yield was calculated on an oven dried basis, following the equation:

$$Pulp\ Yield\ (\%) = \frac{m_{pulp} \times \left(1 - mc_{pulp}\right)}{m_{untreated} \times \left(1 - mc_{untreated}\right)} \times 100$$

where *m* refers to the weight of the substance, *mc* its moisture content and the subscript *untreated* refers to the untreated biomass used.

The ethanol collected to wash the ionic liquid from the pulp from the 3 ethanol washes and Soxhlet extraction in the round bottom flask was evaporated using a rotary evaporator under reduced pressure (40-50 mbar) at 40°C. The lignin dissolved within the ionic liquid liquor fraction was precipitated by the addition of an anti-solvent: 1 g of water for 3 g of IL used. After centrifugation, the ionic liquid liquor was recovered and separated from the lignin. The lignin was dried using a freeze dryer (LabConco FreezeDry Benchtop) and the lignin yield by mass was calculated according to the following equation:

$$Lignin\ Yield\ (\%) = \frac{m_{lignin}}{m_{untreated} \times \left(1 - mc_{untreated}\right)} \times 100$$

The IL liquor was analysed directly after the pretreatment, prior to any washing by taking an aliquot of the IL liquor (200 mg) into a tared micro centrifuge tube. The aliquot was diluted with 700 mg of purified water and centrifuged to remove any water-insoluble material at 13.3 g for 20 minutes at 4°C. The supernatant was analysed using a Shimadzu HPLC system with both RID and UV detectors, an Aminex HPX-87H Bio rad column, 300 x 7.8 mm, with 0.005 M H_2SO_4 as the mobile phase (0.6 ml/min). The column temperature was 55°C and the time acquisition was 45 min. Calibration was carried out for each set of runs, using standards of 0.01, 0.02, 0.1, 0.4, and 1 mg/mL of furfural, 5-HMF, levulinic acid, glacial acetic acid, and formic acid, and 0.2, 1, 2, and 4 mg/mL of glucose, xylose, and arabinose.

2.4.3 Ionic Liquid Liquor analysis

The IL liquor was analysed directly after the pretreatment, prior to any washing by taking an aliquot of the IL liquor (200 mg) into a tared micro centrifuge tube. The aliquot was diluted with 700 mg of purified water and centrifuged to remove any water-insoluble material at 13.3 g for 20 minutes at 4°C. The supernatant was analysed using a Shimadzu HPLC system with both RID and UV detectors, an Aminex HPX-87H Bio rad column, 300 x 7.8 mm, with 0.005 M H_2SO_4 as the mobile phase (0.6 ml/min). The column temperature was 55°C and the time acquisition was 45 min. Calibration was carried out for each set of runs, using standards of

0.01, 0.02, 0.1, 0.4, and 1 mg/mL of furfural, 5-HMF, levulinic acid, glacial acetic acid, and formic acid, and 0.2, 1, 2, and 4 mg/mL of glucose, xylose, and arabinose.

2.4.4 Recycling of Ionic Liquid

For recycling experiments, the IL liquor from cycle *n* was recovered after pretreatment and subsequent lignin washes into a pre-weighted round bottom flask. The water was evaporated using a rotary evaporator. The weight of the flask was recorded, and the water content of the IL was measured (Karl Fisher titrator). For the cycle n+1 of pretreatment, the water content of the IL liquor was adjusted with the addition of water to achieve 20 wt % and the solution was stirred until homogeneous. The recovered IL was transferred into a pressure tube for cycle n+1 and raw biomass was added accordingly for the next cycle.

For recycling experiments, the IL liquor from the 1st cycle was recovered after pretreatment and subsequent lignin washes into a pre-weighted round bottom flask. The water was evaporated using a rotary evaporator. The weight of the flask was recorded and the water content of the IL was measured (Karl Fisher titrator). For the 2nd cycle of pretreatment, the water content of the IL liquor was adjusted with the addition of water to achieve 20 wt % and the solution was stirred until homogeneous. The recovered IL was transferred into a pressure tube for cycle 2 and raw biomass was added accordingly for the next cycle.

2.5 Characterisation of product outcomes

2.5.1 Glucose stream for biofuel production

2.5.1.1 Enzymatic saccharification assay

Enzymatic saccharification was carried out according to an adapted version of the NREL protocol: 'Low solids Enzymatic saccharification of lignocellulosic biomass'.[282] Samples were run in triplicates, along with blanks. 100 ±10 mg of pretreated and un-pretreated samples were incubated in a medium consisting of 5 mL of 0.1 M sodium citrate buffer at pH 4.8, 40 µL of a tetracycline antibiotic solution (10 mg/mL in 70 % ethanol), 30 µL of a cycloheximide antibiotic solution (10 mg/mL in purified water), 40 (hardwoods, softwoods) or 20 µL (grasses) of CTec2 enzyme mix from Novozymes and purified water to obtain a final volume of 10 mL. Blank samples used 100 µL of water instead of biomass to correct for any sugar background concentration. The saccharification was carried out at 50°C and 250 RPM for 7 days. Sugar concentrations were obtained after filtering 1 mL of the hydrolysate through a 0.2 μm PTFE syringe filter. Samples were run on a Shimadzu HPLC system (RID, Aminex HPX-87P Bio rad

column, 300 x 7.8 mm) with purified water as the mobile phase (0.6 mL/min) at 85°C for 20 minutes. The conversion of glucose was then calculated following the equation:

$$Saccharification\ yield\ (\%) = Glucose\ release\ (\%)$$
$$= \frac{(C_{sample} - C_{blank}) \times V_{sample} \times corr_{anhydro} \times Pulp_{yield}}{m_{sample} \times (1 - mc_{sample}) \times Glucan_{untreated}} \times 100$$

where C_{sample} is the glucose concentration of the hydrolysis sample determined by HPLC, C_{blank} is the glucose concentration of the blank control determined by HPLC, V_{sample} is the volume of the hydrolysis sample, $corr_{anhydro}$ is a correction factor accounting for the increase in mass of sugars during hydrolysis (0.9 for glucose). Other parameters have been described previously.

Enzymatic saccharification assays were carried out according to an adapted NREL procedure[282] as previously described on three biological replicates (trees, one per plot) per treatment and three technical replicates per tree and included both substrate and enzyme blanks. Ethanol equivalent of released glucose was calculated based the following equation:

$$V_{ethanol} = \frac{2}{density_{EtOH}} \times \frac{m_{glucan}}{ACF} \times \frac{M_w(ethanol)}{M_w(glucose)} \times Fermentation\ yield$$

where *ACF* is the anhydrous correction for the mass increase during hydrolysis of glucan to glucose, m_{glucan} is the mass of glucan, M_W the molecular mass and the fermentation yield set at 90 %.[37]

2.5.1.2 Biological fermentation

- Invasive species

Solutions with sufficient concentration of glucose (around 20 mg.mL^{-1}) were obtained by carrying out enzymatic saccharification over 24 hours with high enzyme loading. 330 mg of pulp samples or 1.6 g untreated samples of invasive species (dry matter) were incubated with 4 mL of sodium citrate buffer at pH 4.8, 4 mL of purified water and 400 µL of CTec2 enzyme mix from Novozymes. Saccharified samples were then centrifuged to remove the solids and the resulting glucose-containing solutions were used to make a medium by mixing with 1X yeast nitrogen base (YNB) with amino acids. The concentration of the resulting solutions was checked using the HPLC system (Shimadzu, RID detector, Aminex HPX-87P from Bio rad). Single colonies (OD_{600} of 0.1) of Saccharomyces cerevisiae BY4741 [MATa his3Δ1 leu2Δ0 met15Δ0 ura3Δ0] were used for the fermentation studies on the hydrolysate solutions. The fermentation was carried out in triplicate at 30°C with shaking at 250 RPM for 48 hours in an incubator (Labnet International). After the fermentation, the optical density of the cultures was

measured to check for any abnormally high density due to bacterial development. The supernatant was analysed using an HPLC system (RID detector, Aminex HPX-87H Bio rad column, 300 x 7.8 mm, 0.005 M H_2SO_4 as mobile phase, 0.6 ml/min for 35 minutes at 55°C) for ethanol concentration. Yields of ethanol were standardized to the amount of biomass used for each sample to obtain the hydrolysates.

- Waste wood

Saccharomyces cerevisiae BY4741 [MATa his3Δ1 leu2Δ0 met15Δ0 ura3Δ0] was used for the fermentation studies using CCA treated wood. Single colonies were used to inoculate 10 mL of YPD medium in 250 mL baffled flasks in triplicate and grown for 24 hours at 30 °C with shaking at 250 RPM. The optical density (absorbance) of these cultures was measured and used to inoculate 3 mL of YPD containing varying concentrations of metal salts (Cr^{III},Cu^{II} and As^{V} ranging from 128 mM to 100 nM) at an initial optical density of 0.1. 3 mL of the medium containing cells was then transferred to individual falcon tubes. The cells were cultured anaerobically at 30 °C, 250 RPM for 48 hours. The cultures were pelleted by centrifugation and the supernatant was retained for HPLC analysis. Fermentation of hydrolysed wood samples was carried out in 10 mL centrifuge tubes (Falcon). Saccharification was carried out to obtain sugar solutions concentration of around 20 $mg.mL^{-1}$: around 330 mg of pretreated samples and 1.6 g of non-pretreated samples were incubated in a medium consisting of 4 mL of 5 M sodium citrate buffer, 4 mL of DI water and 400 µL of CTec2 enzyme mix (Novozymes). It should be noted that the enzymatic hydrolysis was run using an excess of enzymes in order to achieve high enough glucose concentrations from the non-pretreated biomass (VP-UT). Saccharified wood samples were centrifuged to remove the solids and the resulting glucose containing solution was used to make a medium by mixing with 1X yeast nitrogen base with amino acids (Sigma Aldrich). Samples were standardized to the amount of glucan added to the saccharification reaction. Controls containing metals (Cr, Cu, As from chromium sulphate, copper sulphate and arsenic(V) in water respectively – all purchased from Sigma) were prepared as follows: for samples of CCA-treated wood that had undergone extraction, the metal content was readjusted to the amount of Cr, Cu and As in the pulp after pretreatment if no extraction had occurred (as a non-extracted control); in regard to the pulp yield after pretreatment. All liquid samples were analysed in triplicate through the ICP-OES to check the concentration of metals. For the assay, single colonies were used to inoculate YPD medium as described above. After 24 hours of growth, cultures were diluted to an OD600 of 0.1 in PBS. 3 mL was transferred to each centrifuge tube, cells were pelleted by centrifugation, the supernatant was removed, and the cell pellet was resuspended in 3 mL of the appropriate wood medium. Cells were grown at 30 °C with shaking at 250 rpm in a Vortemp ™ 56 shaking incubator (Labnet International) for 48 hours. The OD600 of cultures was measured against a

blank of the same type of medium and then the cells were pelleted by centrifugation and the supernatant retained for HPLC analysis. The supernatant was pipetted into a HPLC vial and submitted for analysis on a Shimadzu HPLC system (RI and UV/Vis detector, Aminex HPX-87H column BioRad, 300 × 7.8 m, mobile phase 0.005 M H_2SO_4 as mobile phase, 0.6 mL.min^{-1}, column temperature 55 °C, acquisition run 35 min). Calibration was carried out using standards with concentrations of 0.1, 0.4, 1, 2, 4, 10, 20 and 30 mg.mL^{-1} of HPLC grade ethanol. Ethanol concentrations in the HPLC sample were calculated using the resulting calibration curves.

2.5.2 Isolated lignin characterisation

2.5.2.1 Heteronuclear Single Quantum Coherence Spectroscopy Nuclear Magnetic Resonance (HSQC NMR)

40 mg of lignin was dissolved in 0.5 mL of DMSO-d_6 and the solution transferred to an NMR tube. HSQC NMR spectrum was recorded on a Bruker 600 MHz spectrometer (pulse sequence hsqcetgpsi2, spectral width of 10 ppm in F2 (^{1}H) with 2048 data points and 160 ppm in F1 (^{13}C) with 256 data points, 16 scans and 1s interscan delay). Spectra were analysed using MestReNova 12.0.4, referenced to the central DMSO-*d_6* solvent peak (δ*C* 39.520 ppm, δ*H* 2.500 ppm) and the assignment of the HSQC spectra based on the relevant literature, specific to a species/feedstock.[47,99,100,103,104,283–286] Relevant HSQC spectra are found in the Appendix. For ether linkages, the C-H$_\alpha$-signals were integrated, for PCA and H the 2,6-signals were integrated. All integrals were normalised to the sum of the G_2 + $G_{2\ cond}$ volume integrals. The S/G ratio of lignin was determined as follows:

$$S/G = \frac{0.5 \times S_{2,6} + S_{2,6\ cond}}{G_2 + G_{2\ cond}}$$

where *S* is the volume integral of the relevant syringyl sub-unit, and *G* is the volume integral of the relevant guaiacyl sub-unit. Subscripts *2* and *6* refer to the position of the protons on the aromatic ring of the measured sub-unit, and subscript *cond* refers to condensed sub-units.

2.5.2.2 Thermogravimetric analysis - TGA

Thermogravimetric analysis of lignin was conducted on a TA Q500 (TA Instruments, USA) TGA fitted with a gas switching system, using a platinum pan, with N_2 as the purge gas (50 mL/min). 3±2 mg of freeze-dried lignin was loaded per run. For proximate analysis of sample composition, a drying step at 105 °C for 15 min was carried out before linearly ramping the temperature at 60 °C/min over a temperature window of 105 to 600 °C. The sample was held at 600 °C for 15 min before a burn-off step was initiated by switching the purge gas to 10 %

air and 90 % nitrogen to remove all organic material and determine the ash content. Proximate analysis was performed using TA Universal Analysis software using the weight loss curve against temperature to determine moisture content, volatile matter, fixed carbon and ash contents.

For thermal analysis, the TGA weight loss curves and their first derivatives, i.e., the differential thermogravimetric (DTG) curves with respect to temperature for lignin were plotted and used to identify the temperature at which the DTG curve showed the maximum rate of thermal composition - DTG_{max}. DTG_{max} is the temperature at which rate of weight change (i.e., gradient of differential thermogravimetric curve) with respect to temperature is the steepest.

2.5.2.3 Elemental analysis

The Carbon, Hydrogen, Nitrogen and Sulphur (CNHS) elemental analysis was performed using a Vario Micro tube supplied by Elementar, consisting of a dynamic flash combustion analysis and thermal conductivity detection. Accuracy is +/- 0.30 % absolute. Oxygen content was obtained by difference.

The Higher Heating Value (HHV) in $MJ.kg^{-1}$ was estimated according to the Demirbas formula (an adaptation of Dulong's formula)[287] on a dry ash free basis, according to the equation:

$$HHV = 33.5 \times C + 142.3 \times H - 15.4 \times O - 14.5 \times N$$

where C = carbon content, H = hydrogen content, O = oxygen content, and N = nitrogen content.

2.5.2.4 Gel Permeation Chromatography (GPC)

GPC measurements were performed using an Agilent 1260 Infinity instrument equipped with a Viscotek column set (AGuard, A6000M and A3000M). The Agilent 1260 Infinity RID was used for detection. HPLC grade DMSO containing 1 g/L of Lithium Bromide was used as the eluent at 0.4 mL/min at 60°C. Samples were prepared by dissolving 20 mg lignin in 1 mL eluent and filtered through a 0.2 μm syringe filter. Ten pullulan polysaccharide standards (Agilent calibration kit, from 180 to 780 000 g/mol) were used for calibration. GPC was used on the lignin to determine their molecular distributions and absolute molar masse M_w and M_n respectively; and polydispersity Đ, where:

$$Đ = M_w / M_n$$

2.5.3 Lignin for additional energy production

2.5.3.1 Post Hydrolysis Solids (PHS) production

PHS residues were produced using a mixture of wet pretreated CCA-treated wood pulps and subjecting them to enzymatic hydrolysis. The pulp mixture consisted of a combination of 11.65 g of pulp (on an oven-dried basis) from all 6 pretreatment cycles in equal quantities, each having been treated at 170 °C for 30 min using [HC_1im][Cl] solutions. The enzymatic hydrolysis conditions used are described by the NREL in a recent techno-economic study.[288,289] 31.3 mg protein per g of cellulose in feedstock, using cellulase enzymes from *Trichoderma reesei* (Sigma), the saccharification master mix as described in Section 2.2.7 and a solids loading of 5 wt % at 50°C and 250 RPM. After a residence time of 5 days, the residual solids were collected by centrifugation, washed twice with deionized water and freeze-dried. The dried post-hydrolysis solids (PHS) were then ground and sieved to a narrow size fraction (106-150 µm) and stored in air-tight vials before further analysis.

2.5.3.2 Fast pyrolysis experiments

2.5.3.2.1 Fixed-bed reactor description

Pyrolysis experiments of PHS were performed by a Dr Clementine Chambon, using a pyrolysis reactor designed and built by Dr Matthew E. Boot-Handford from the Fennell Group. The description of the reactor can be found in the Appendix and has been reported both in the literature and in Boot-Handford's doctoral thesis.[290] The reactor is a single-stage fixed-bed downdraft, which allows pre-loaded sample from a solid fuel feeder in a batch wise manner. The reactor body consisted of a high temperature BN Incoloy 800HT alloy working tube with an internal quartz liner. Sand was loaded into the quartz liner reactor to provide an inert bed and heat sink for the K-type thermocouple to be placed in. A sintered quartz disk acted as a bed support to retain the ash and residual char. Gases are introduced through a T-piece at the top of the reactor, N_2 first so the sample could be pyrolyzed generating the different pyrolysis products (bio-oils, char and detected gases). During the reaction, the exhaust gas and volatiles were swept downstream into the main tar trap. The tar trap was packed with glass wool to increase the surface area for the condensation of the bio-oils formed. A secondary line diverted the gas flow from the tar trap to the reactor outlet, using two ball valves so that the tars could be isolated from the hot gas flow after the reaction time (90s) and sealed off from the atmosphere prior to recovery. Two smaller quartz wool traps were placed after the main tar trap outlet and at the diversion line outlet respectively to condense any remaining tars. A refrigerant solution (30 wt % ethylene glycol in distilled water; -2 °C) was used to cool the gases and condense the tars and water vapour contained in the reactor flue gas for

analysis. Concentration of CO, CO_2, CH_4 and H_2 were measured via an online multi-gas infrared detector and analyser (MGA3000, ADC Analyzer) connected after the pressure control valve. The gas exiting the analyser was vented in the fume cupboard. A control program written in Agilent VEE automated the entire process including fuel feeding, temperature control and switching, gas flow rate control and switching, pressure control and data monitoring and collection.

2.5.3.2.2 Pyrolysis conditions

Experiments were done in triplicate. Gas calibration was performed using a certified calibration mixture (29.9 vol % CO_2, 9.7 % CO, 10.1 % CH_4, balance N_2) supplied by BOC. The reactor was heated up to 500±5 °C under N_2 and the temperature was allowed to stabilize for at least 30 min. Prior to feeding, the loaded sample cylinder was purged for 5 minutes with a 10 $ml.s^{-1}$ flow of N_2 to displace any air that could interact with pyrolysis results. The biomass sample (0.10 g – particle size 106–150 μm) was then fired into the reactor from a pressurized 50 mL double-ended sample cylinder, pressurized to 0.5 bar above the reactor pressure (1.5 bara). During sample feeding, 20 $ml_N.s^{-1}$ of flow was diverted to the feeder for sweeping the biomass particles from the sample feeder into the reactor. After the sample was fed, the reactor was held at the set point temperature for 900 s to ensure complete pyrolysis was achieved. The pyrolysis tube was flushed with N_2 gas with a superficial velocity of 0.25 ms^{-1}(60 $ml_N\ s^{-1}$ at 500 °C) to sweep evolving volatiles from the sample bed downstream to the tar trap. After this time had elapsed, following the isothermal phase, the char combustion step was initiated by switching the gas composition to 10 vol % O_2 (balance N_2) causing the organic content of the char bed to combust. The char combustion step was allowed to continue for a further 10 min. Following the char combustion step, the heating was switched off and the reactor allowed to cool. All pyrolysis experiments were conducted in duplicate measurements.

2.5.3.2.3 Product recovery

After cooling down below 60 °C, the reactor and traps were dismantled and each of the reactor components (including all three quartz wool samples) was carefully washed with a 4:1 (v/v) solution of chloroform and methanol (~300 mL) to collect any liquid products. The washings were filtered (Whatman no.1 filter paper) to collect any solid debris. The bulk of the solvent was removed under vacuum on a rotary evaporator (Büchi) at 60 °C. The concentrated bio-oil/solvent solution was then transferred to a pre-weighed aluminium beaker to be further dried for 2 hours in a circulating oven at 35 °C under a N_2 purge to ensure complete solvent removal from the samples. The bio-oil was then weighed to determine the gravimetric yield as a percentage of the initial dry weight of the biomass sample. After the bio-oil yield was

determined, the bio-oils were transferred to sealed and N_2 purged glass vials using ~3 mL of 4:1 v/v chloroform:methanol solvent. The oils were stored in this solvent in the refrigerator (-4 °C) before analysis.

The char was recovered from the bed and analysed for its carbon content to calculate the char yield. The char yield was determined was determined via the following equations:

$$C_{char,g} = Q_{out,293K} \times Ar_C \left(\frac{x_{CO_2}}{MR_{CO_2}} + \frac{x_{CO}}{MR_{CO}} + \frac{x_{CH_4}}{MR_{CH_4}} \right)$$

$$W_{char,g} = \frac{C_{char}}{Ar_C \times x_{C,char}}$$

$$W_{char,\%} = \frac{W_{char,g}}{W_{feedstock,g}} \%$$

where $C_{char,g}$ is the carbon content of the char from the combustion step, as determined from the concentrations of CO_2, CO and CH_4 measured at the reactor outlet; $Q_{out,298K}$ is the total flowrate at the outlet of the reactor at 293 K and 1 bara (temperature and pressure of the gas analysers); Ar_C is the atomic mass of carbon; x_i is the mole fraction of gaseous species *i* in the gas stream exiting the reactor; MR_i is the relative molecular mass of gaseous species *i*; $W_{char,g}$ is the total calculated weight of char, including ash; $W_{char,\%}$ is the total yield of char relative to the dry feedstock fed into the reactor; $x_{C,char}$ is the mole fraction of carbon in the char where $Ar_C \times x_{C,char}$ is the fraction of carbon in the char as determined by elemental CHN analysis of the char.

To determine the gaseous product distribution, the concentrations of CO_2, CO and CH_4 were measured in the outlet gas of the reactor after the tar trap via online gas detectors. The total gas yields were determined by integrating the signals from the IR detector with reference to the gas calibration conducted prior to each experiment.

2.5.3.3 NMR analysis of bio-oils

Bio-oil sample was analysed within 3 days of production. 30 +/-10 mg of dried bio-oil was dissolved in 0.25 mL DMSO-d_6 and the solution transferred to a Shigemi tube. ^{1}H NMR spectra were acquired on a Bruker 600 MHz spectrometer using 1D pulse sequence zg30 and a 30° flip angle; the spectral width was 16 ppm; the acquisition time was 1.7 s and the number of scans was 16. The integral values of selected regions of the spectra were calculated on a percentage basis after subtracting the region with significant water resonances, which interfered with the spectra (δH 3.0–4.5 ppm). Chemical shifts assignments were as follows:

alkanes δ*H 0.5–1.5 ppm* / aliphatics δ*H 1.5-2.0 ppm* / methoxy, carbohydrate δ*H 4.5-6.0 ppm* / aromatics δ*H 6.0-8.5 ppm* / aldehydes δ*H 8.5-10.0* ppm.

2.5.3.4 Energy recovery calculations

The energy and carbon efficiency of the pyrolysis were calculated based on the input and output streams of the pyrolysis products and feed as a system boundary, without including the gaseous products and volatiles. Higher Heating Values (HHV) were calculated based on the ultimate analysis of the samples (CHNS) using the Demibras formula as previously described. The energy requirement for the reactor heating was estimated as 20 % of the HHV of the feed.[291]

The energy recovered in the char and bio-oil from the pyrolysis of the feed (fuel) is calculated following the equation:

$$Energy\ recovery(\%) = \frac{HHV_x \times \gamma_x}{HHV_{reactor\ heating} + HHV_{feed}} \times 100$$

where HHV_x is the energy in the product x (char, bio-oil) (MJ.s^{-1}) and γ_x is the yield of the product x.

The carbon recovered in the char and bio-oil from the pyrolysis of the feed (fuel) is calculated following the equation:

$$Carbon\ recovery\ (\%) = \frac{C_x \times \gamma_x}{C_{feed}} \times 100$$

where C_x is the carbon content of x (wt%) and γ_x is the yield of the product x (char, bio-oil).

2.5.4 Trace elements analysis and metal recovery

2.5.4.1 Trace element analysis of waste wood using ICP-OES

ICP-OES measurements were performed on a Perkin Elmer Optima 2000 for CCA treated wood samples. All samples were done in triplicate.

Standards were prepared using Multielement standard solution 4 for ICP in 10 % nitric acid (TraceCERT). The standard solution was diluted with 5 % nitric acid as required to obtain at least 4 different concentrations for calibration (maximum 25 ppm).

Ionic liquid liquors were diluted to approximately 1 % ionic liquid (by mass) concentration with 5 % nitric acid. In the case of IL liquors with high concentrations of metals, this solution was further diluted (maximum concentration of each metal < 25 ppm). All solutions were filtered through a 0.22 µm syringe filter prior to analysis. For the analysis of the recycled IL, a blank IL without any biomass was subjected to the same experimental procedures as the working IL to account for eventual accumulation of metals from external sources, such as metallic dust

found on stirrer bars and chromium leaching from stainless steel spatulas. It was used as a blank in the ICP-measurements and its metal concentrations (below detection limit for As and Cu, <1 ppm for Cr) subtracted from the ones measured for the working ILs. For analysis of solid samples (biomass, pulp and lignin), approximately 300 mg of sample was weighed out and the exact weight recorded (±0.1 mg, Mettler Toledo NewClassic MS). The samples were digested in 1 mL 69 % nitric acid in a closed PTFE vessel (MARSXpress) vessels and microwave with power/time control by CEM with the following sequence: 300 W at 83 % power for 5 min, 600 W at 66 % power for 5 min and 1200 W at 58 % power for 6 min. The obtained solution was cooled in a freezer for one hour before diluting to 10 mL with 5 % nitric acid and filtration through a 0.22 μm PTFE syringe filter.

Percentage recovery of metal *M* in the pulp was calculated according to the following equation:

$$M_{pulp}\ (\%) = \frac{C_{M,pulp}}{C_{M,UT} \times r_{pulp}} \times 100$$

Extraction of metal *M* (%) from the biomass is then calculated as 100 − M_{pulp}(%).

Percentage recovery of metal *M* in IL liquor according to equation:

$$M_{IL,n}\ (\%) = \frac{C_{M,IL,n}}{C_{M,BM} \times ODW_{BM} \Big/ \left(m_{IL} \times (1 - wc_{IL})\right) + C_{M,IL,n-1}} \times 100$$

Percentage recovery of metal M and in lignin according to equation:

$$M_{lignin}\ (\%) = \frac{C_{M,lignin}}{C_{M,BM} \times r_{lignin}} \times 100$$

where $C_{M,x}$ is the concentration of metal M in component x as measured by ICP, $IL_{,n}$ is the ionic liquid liquor at cycle n, BM is the raw biomass, r_x is the recovery of component x after pretreatment with respect to the initial biomass weight on an oven-dried basis, ODW_{BM} is the oven-dried weight of the biomass used in pretreatment, m_{IL} is the initial weight of IL solution used for pretreatment and wc_{IL} is the water content of this solution.

2.5.4.2 Trace element analysis of other lignocellulosic samples using ICP-MS

The trace element analysis was determined by ICP-MS for all other lignocellulosic samples by closed microwave digestion followed by ICP-MS, as adapted from the US EPA 3051a protocol. All samples were run in triplicate on a dry biomass basis. For each sample, 9 mL 67-69 % HNO_3 (trace element grade, Fischer Scientific) and 3 mL of 35-37 % HCl (trace element grade, Fischer Scientific) were added to 400 mg of sample in PFA digestion vessels. The

samples were digested using a microwave reactor, whereby the samples were heated to 180 °C and held for 10 min before cooling down at room temperature. After cooling, the digested samples were diluted using ultra-pure 18 MΩ Milli-Q® water and passed through a 0.22 µm Whatman syringe filter for ICP-MS (7900 Agilent). The details of the Agilent ICP-MS method developed is described in the Appendix. Five calibrated solutions were prepared by mixing and diluting single-element and multi-element standards (Inorganic Ventures) of known concentrations. The matrix effects of the dilution mixture were corrected using internal standards. Certified reference materials for trace elements were systematically digested in duplicate using the same procedure in order to validate the results: Sewage Sludge reference material ERM® CC144 from Sigma Aldrich[292] and Algae reference material 413 from the International Atomic Energy Agency.[293] The recoveries of the reference materials and detailed ICP developed instrumental methodology are presented in the Appendix.

Percentage recovery of metal *M* in the pulp, lignin and IL liquor and extraction of Metal *M* (%) from the biomass were calculated as described in the previous section.

2.5.4.3 Electrochemical Measurements

Metal doped-IL solutions were prepared by using chloride metal salts $CuCl_2$, $FeCl_2$, $PbCl_2$ and $ZnCl_2$. Solutions of 1000 $mg.kg^{-1}$ in $[H_1Cim][Cl]$ (40 wt % water, Millipore Milli-Q purification system, resistivity ca. 18.2 MΩ cm at 25 °C) were used.

An Autolab PGSTAT302A potentiostat (Metrohm) with NOVA software was used for all electrochemical experiments.

For all cyclic voltammetry experiments, a glassy carbon disc electrode (1.5 mm radius) served as the working electrode. Prior to use, the working electrode was polished with a slurry of 0.05 µm alumina particles on a soft microfibre polishing pad (MicroCloth, Buehler Ltd.) and then on a clean wet microfibre pad. A platinum coiled wire acted as the counter electrode and the reference electrode comprised a Ag/AgCl (3 M NaCl) glass-fritted electrode.

Electrolysis experiments were conducted with a copper foil (Goodfellow, 99.9 %) substrate acting as the working electrode. The surface area of the copper foil electrode is 8.4 cm^2 (7cm length x 0.6 cm width both sides). The counter electrode was a platinum coiled wire inserted into a glass tube fritted with CoralPor™ (7.8 nm pore size). This served to separate the anolyte solution from the catholyte. The reference electrode comprised a Ag/AgCl (3 M NaCl) glass-fritted electrode. The electrolysis experiments were carried out for 1 hr at varying potentials (-0.9 V vs Ag/AgCl for Pb and Cu deposition and -1.2 V and -1.4 for Fe and Zn deposition, respectively). During the electrolysis, small aliquots of the catholyte were taken (0.1 mL) and the concentration of metals were determined using ICP-MS.

The charge efficiency η from the electrolysis was calculated using the following equation:

$$\eta = \frac{Q_{th}}{Q_{acc}} = \frac{n \times \mathcal{F} \times m}{Q_{acc}}$$

where Q_{th} is the theoretical charge calculated from the change in solution concentration, n is the number of electrons, $\mathcal{F}$ is the Faraday constant, m is the number of moles converted from the electrolysis solution and Q_{acc} is the accumulative charge passed during the electrolysis experiment.

2.5.5 Statistical analysis and projected willow biorefinery yields calculation

Experiments were carried out on three biological replicated (trees, one per plot) per treatment and three technical replicates per tree. Significant difference was assessed on biological replicates by using the Student's t-test ($p<0.05$).

3 Invasive species: biological waste valorisation into ethanol

3.1 Introduction

While most of pretreatment technologies are designed for a specific type of feedstock and end-product, we test the hypothesis that the ionoSolv process is flexible enough to integrate two selected invasive species. To become a promising feedstock, we focus on the pretreatment step and the valorisation of this unconventional biomass and fractionation products. In this chapter, we will investigate the potential to supply the ionoSolv process with discarded, biologically hazardous terrestrial invasive species. Terrestrial plant invasive species are diverse, but they do exhibit one common chemical characteristic: (1) they are comprised of lignocellulosic biomass, (2) they produce a high yield of biomass, and (3) they do not compete with agricultural land use, as they tend to grow in marginal areas (e.g., acidic soils, road-sides, discarded agricultural areas). Three characteristics pursued for bioenergy production. Japanese knotweed (JPK) and Rhododendrons (RHDN) are two famous example of UK's most invasive species that mobilize significant financial resources towards their eradication and which residues once teared out are considered as waste.[294] Despite the potential environmental positive impact of using waste and/or marginal land for renewable energy, little research has been given to using such species as an innovative renewable energy source.[295–297] Most studies revolving around invasive species focus on African and North American species and their safety practises.[298,299]

In this chapter, we investigate for the first time, the composition in structural carbohydrates and lignin of invasive species such as JPK and RHDN and valorisation of these products. Once their composition revealed, it led to the question: can an ionic liquid-based process experimentally produce renewable energy from such invasive species? Possible synergies between integrating an unconventional feedstock to the ionoSolv feedstock supplier chain, and the chemical engineering barriers are studied here: time and temperature of pretreatment for optimised glucose release, and subsequently fermentation into ethanol. Established dedicated bioenergy crop (i.e. grasses, softwoods, hardwoods) will be used alongside as a reference against JPK and RHDN, to weigh those alternative crops and guide pretreatment parameters adjustments.

3.2 Results and discussion

3.2.1 Valuable compositional of selected invasive species

The composition in structural carbohydrates and lignin has not been reported in the literature for invasive species such as JPK and RHDN. However, in order to optimise a pretreatment technique and its desired outcomes, it is crucial to determine the composition of the biomass input. The ionoSolv process has been successfully applied to a variety of lignocellulosic feedstocks already such as pine (softwood), miscanthus (grass) and willow (hardwood). Compositional analysis for glucan, hemicelluloses and lignin was performed on JPK and RHDN, along with typical biofuel feedstocks, as seen in Figure 3.1. The results show that JPK is richer in glucan and lignin compared to RHDN with 40.2 % and 42.7 % and 32 % and 32.6 % respectively, with a lower hemicellulose content than RHDN. Rhododendron exhibits a higher hemicellulose content than JPK of 26.9 %. If we compare these values to established typical biofuel feedstocks, JPK would be closer in composition to a softwood such as pine: a high glucan (above 40 %) and lignin contents (30-40 %), with lower hemicelluloses content. RHDN exhibits a similar composition to a hardwood such as willow with a more evenly distributed portions of the polymers. These results show that these invasive species exhibit a composition comparable to those suitable for second generation biofuels. Moreover, comparing the compositional analysis results of these new feedstocks with the ones that have already been extensively studied for the ionoSolv process, gives an indication of the range of pretreatment parameters that would be successful using low-cost acidic ionic liquids. The ionoSolv process is a fractionation process, where the lignin is solubilised in the ionic liquid by the breakage of bonds between the lignin and the hemicellulose-glucose backbone, leaving behind a cellulosic pulp.

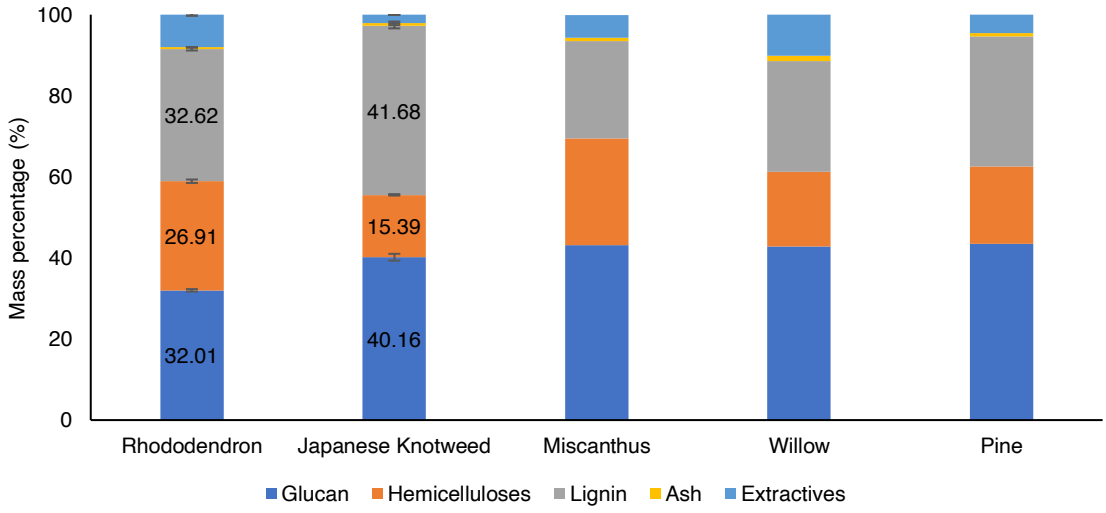


Figure 3.1: compositional analysis of RHDN, JPK and 3 other typical biofuel feedstocks

3.2.2 IL pretreatment parameters optimisation towards bioethanol production

3.2.2.1 Glucose release over time and temperature to tune the pretreatment

The severity of the ionic liquid pretreatment conditions (temperature, time) is a trade-off between the prevention of extensive cellulose degradation and sufficient lignin solubilisation and recovery, which depends on the initial lignin content of the biomass.

The parameters of the ionoSolv pretreatment can be tuned depending on the biomass and the preferred outcome of the pretreament: mostly the time and temperature of the treatment, but also the biomass loading (for process intensification purposes). Time course pretreatments (varying of time and temperature of the biomass – ionic liquid reaction) were performed to investigate how these invasive species responded to ionoSolv fractionation. The glucose release after pretreatment from the pulp was selected as an assessment of the success of the pretreatment, in order to produce fermentable glucose solutions for conversion into bioethanol.

N,N,N-dimethylbutylammonium hydrogen sulphate [DMBA][HSO_4] is a low-cost protic ionic liquid. This ionic liquid was selected for its easy synthesis consisting of an equimolar acid-base reaction between two cheap starting chemicals; but also for its performance for quantitative sugar release from pine compared to other protic ionic liquids.[103] The price range of $[HSO_4]^-$ based ionic liquids was estimated between \$0.78 to \$5.88.kg^{-1}, which is competitive with organic solvents such as acetone or ethyl acetate.[109,110]

Time courses at 150°C and 170°C were performed, based on the compositional analysis of the feedstocks studied here, and previous research carried out for woody samples, involving high temperatures above 120°C combined with shorter reaction times (less than 2

hours).[97,100,103,104] The yields of the pretreatment fractionation process into a cellulose rich pulp and a lignin stream are shown in Figure 3.2.

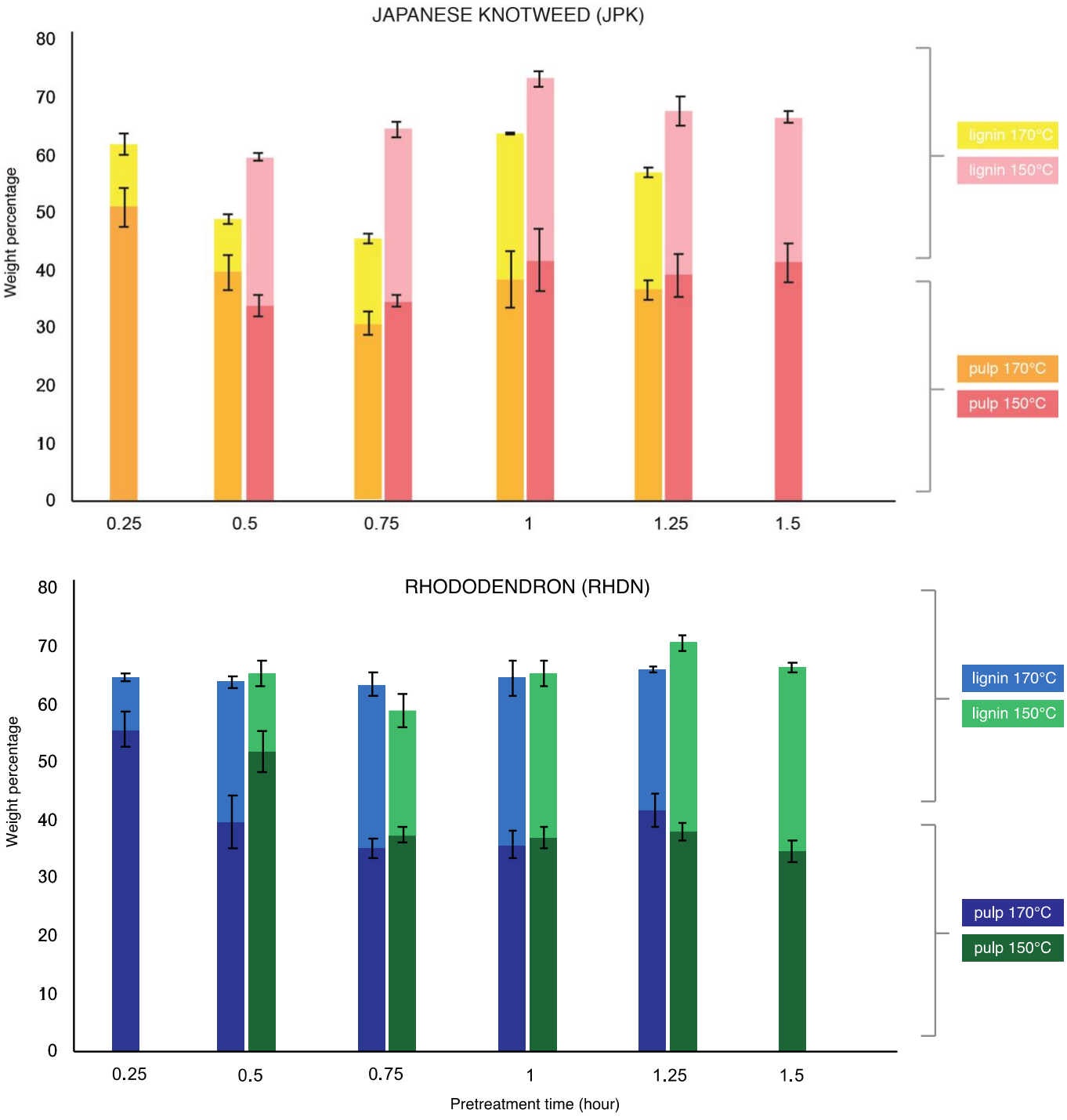


Figure 3.2: pulp and lignin yields from the time course pretreatments of JPK and RHDN using [DMBA][HSO_4] (20 %wt water) at 1:5 g/g biomass:IL loading

Figure 3.2 shows two trends concerning the pulp and the lignin yield that are characteristic to the pretreatment. The pulp yields decrease as the pretreatment time increases; this is due to the amount of hemicellulose and lignin solubilised in the ionic liquid. On the other hand, the lignin recovered from the ionic liquid liquor increases as the pretreatment time increases: the lignin is hydrolysed and extracted at longer pretreatment times as more lignin ether linkages are being cleaved. However, little information can be interpreted from the pulp and lignin recovery yields; the success of the pretreatment is often measured by the enzymatic glucose release from the cellulose rich pulp, also known as saccharification yield. This is a key value in determining the accessibility of the glucose by enzymes and therefore the deconstruction of the lignocellulosic matrix from the pretreatment (as lignin hinders glucose accessibility). Given the nature of the feedstocks (waste invasive species), the glucose release from the pulp will be optimised here, as we have selected fermentation of glucose into bioethanol for this study as an end-use example of the cellulose rich pulp. Other routes of valorisation such as cellulose crystallinity or cellulose fibres properties required for cellulose-based materials have more complex routes, best to be kept for 'textbook' typical biofuel feedstocks which have been extensively studied.

The results of the enzymatic saccharification of the cellulose pulps are shown in Figure 3.3. The enzymatic hydrolysis of non-treated samples for the two invasive species only yielded 12.6 % and 9.2 % of glucose for RHDN and JPK respectively. This shows that the presence of lignin does hinder the access of enzymes to the cellulose and the need for pretreatment prior to subsequent utilisation of the cellulose. The maximum glucose release for RHDN was achieved after 30 minutes at 170°C with 75.6 % glucose (a 6-fold increase compared to the untreated tests) and 71.5 % after 45 minutes at 170°C. This is similar to what has been reported with pretreatment of pine using [DMBA][HSO_4] with sugar releases over 70 % at high temperature and short reaction time (170°C, 30 min).[103] After reaching the optimal value, the glucose yields decrease at both temperatures. This indicates either degradation of the cellulose, charring of the pulp at harsher pretreatment conditions, or re-deposition of pseudo-lignin (hydrolysed smaller fragments of lignin, possibly re-condensed with degradation products) onto the surface of the pulp during the process.[100] Shorter reaction times are preferable for a pretreatment process (since this reduces equipment size and cost); this is why the optimal pretreatment condition was subsequently considered to be 170°C for 30 minutes for RHDN for further analyses.

The glucose release from JPK at 170°C after pretreatment was consistently lower than at 150°C. This indicates that 170°C is too harsh for pretreating JPK. This is consistent with the composition of the biomass and differences between the two feedstocks. JPK has a greater

glucan content than RHDN; higher temperatures would degrade the glucan faster, while solubilising the lignin is achieved at lower temperatures. The highest glucose release for JPK was observed at 150°C for 1 hour at 85 %, a 7.7-fold increase compared to untreated samples. The pulps at 150°C for 1 hour and 170°C for 30 minutes were selected for further compositional analysis for JPK and RHDN respectively.

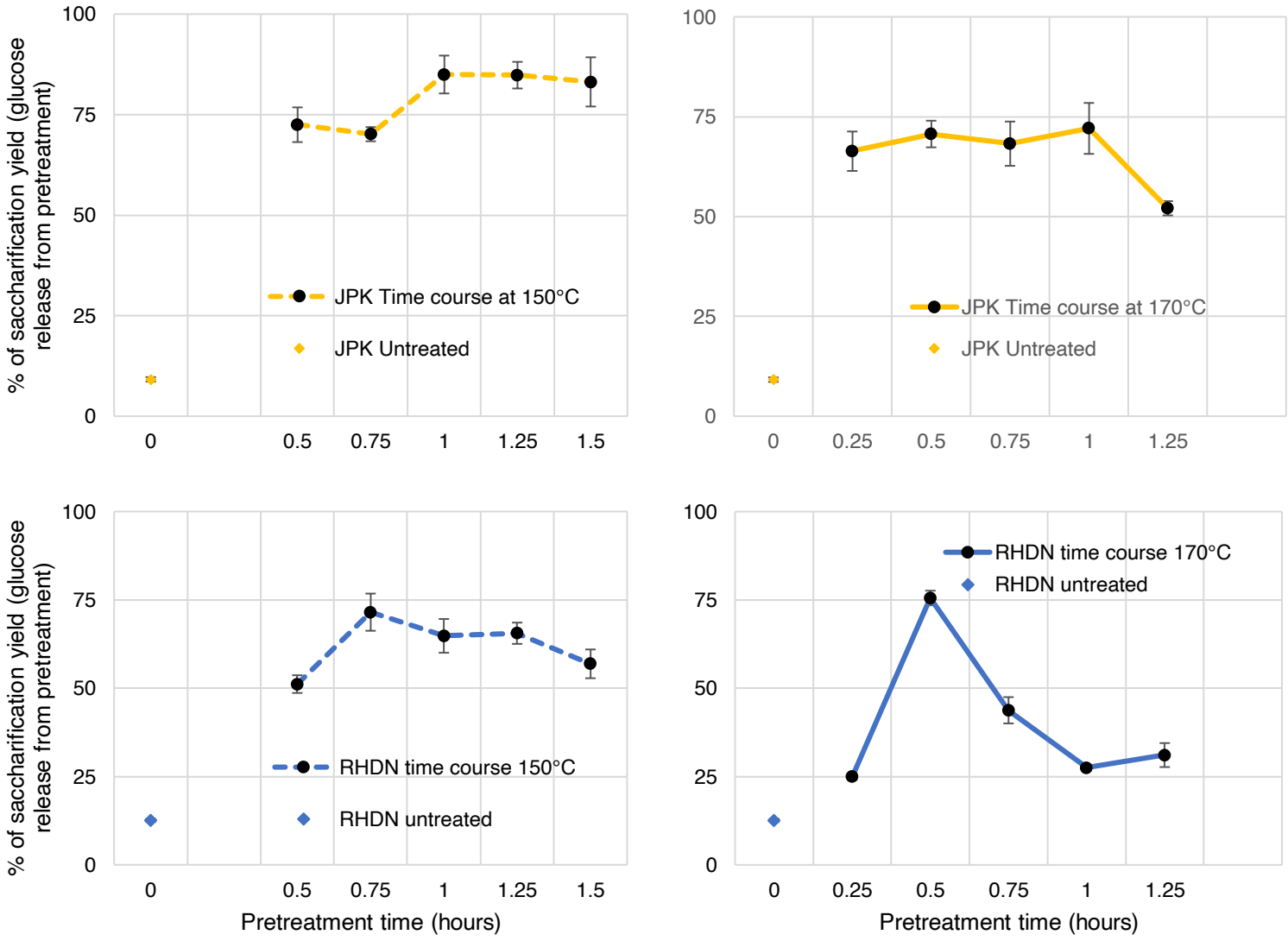


Figure 3.3: enzymatic hydrolysis conversion of untreated samples and the pulp obtained from the pretreated pulps at 150°C (left, dashed) and 170°C (right) for JPK (top, yellow) and RHDN (bottom, blue)

At lower temperature (150°C), the effect of time has only a lower impact on saccharification yield, than at a higher temperature (170°C) where an optimal duration of pretreatment needs to be respected before the drop of the saccharification yield, especially for RHDN.

If a more universal / feedstock agnostic condition is to be chosen, a lower temperature (150 °C) but longer pretreatment (45-60 mins) seems to be the most interesting consensus, reaching out 70% of saccharification yield for both invasive species.

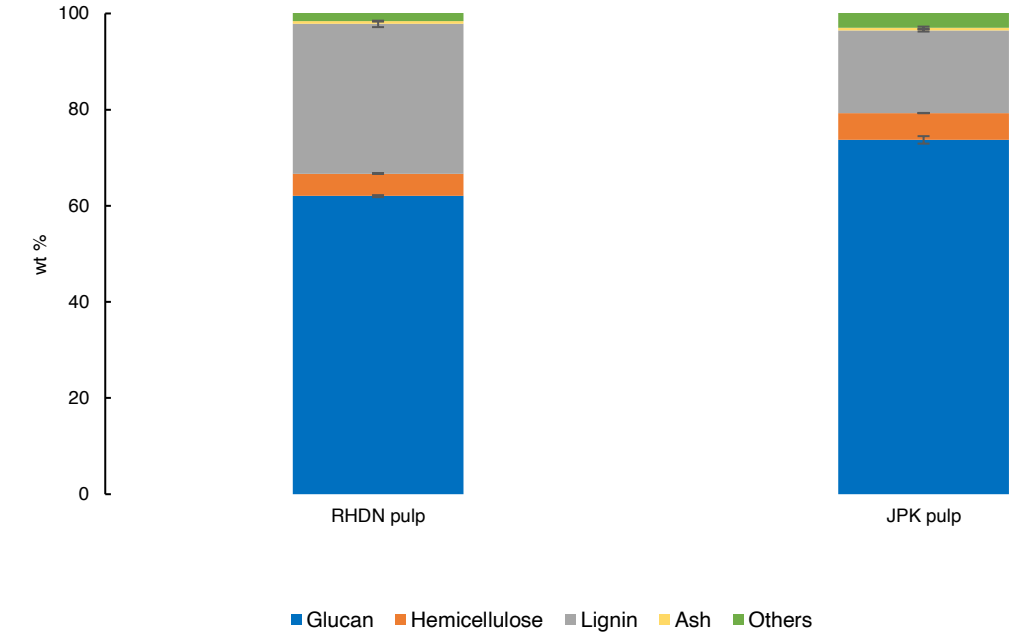
3.2.2.2 Optimised pulp composition for cellulose purity

The pulps were analysed for their cellulose purity and the effect of the ionic liquid pretreatment on the lignocellulosic matrix using compositional analysis, as shown in Figure 3.4. The pulps still retain some lignin since the delignification rates are just below 90 %. This level of lignin extraction in the pulps is enough to deconstruct the biomass and achieve significant saccharification yields as shown in Figure 3.2 (85 % for JPK, 75.6 % for RHDN). The lignin content of the RHDN pulp is higher than in the untreated samples. This could be due to the deposition of a condensed lignin oligomers (pseudo-lignin), which are water soluble, on to the cellulose-rich pulp at harsh pretreatment conditions (170°C for RHDN compared to 150°C for JPK).[286,300]

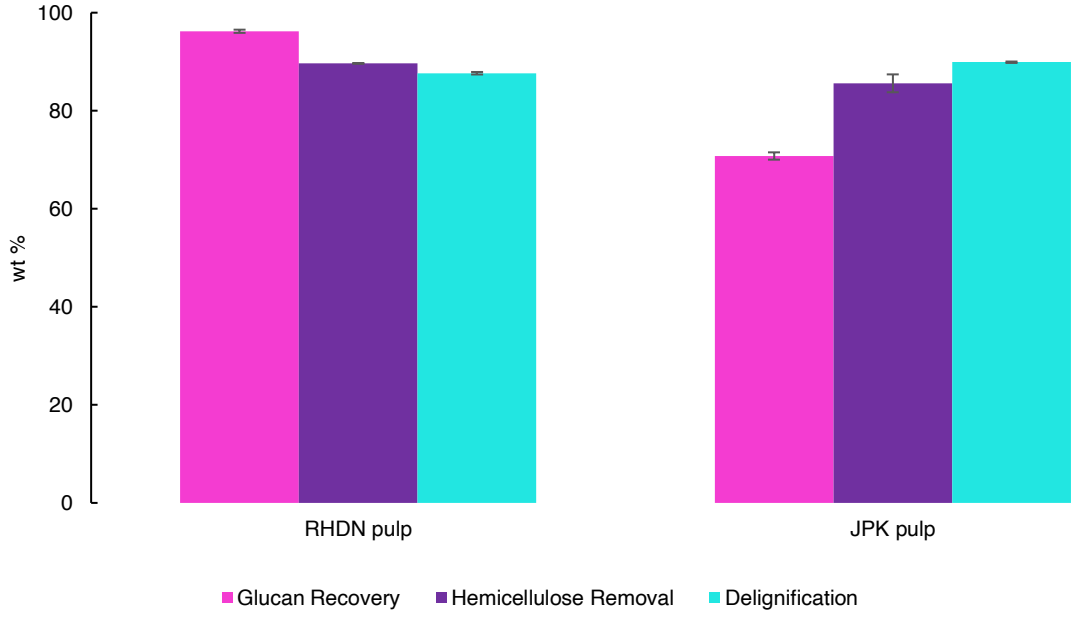
The pretreatment yields high cellulose purity of the pulps: 62 % for RHDN and over 73 % for the JPK, which represents glucose recoveries of 96.2 % and 70.8 % respectively. Even though the glucose recovery is lower for the JPK, which has a higher initial glucan content (Figure 3.1), the cellulose purity of the pulp is higher. This could be due to hydrolysis of the less crystalline regions of cellulose during pretreatment, or better delignification.[106] Overall, the ionic liquid fractionated the biomass during the pretreatment, leaving a rich cellulose pulp with around 5 % of hemicelluloses and some lignin, which has been disrupted.

Figure 3.4: A. Compositional analysis of the pulps recovered from the pretreatment (170°C 30 mins for RHDN, 150°C 1 hr for JPK) B. Analysis of the pulp from the pretreatment (170°C 30 mins for RHDN, 150°C 1 hr for JPK). Values are in weight percentage.

A.



B.



3.2.3 Ionic Liquid liquor analysis for degradation products: potential inhibitors

Before the precipitation of the lignin with the addition of water, the ionic liquid liquor or 'black liquor' can be analysed to assess the concentration of sugar degradation products from the biomass fractionation, as more than 80 % of the hemicelluloses were removed from the biomass (Figure 3.4B). Moreover, liquor analysis can reveal the presence of valuable by-

products, which can be recovered; or potential inhibitors for subsequent biorefinery steps, i.e., here fermentation. The results are presented in Figure 3.5 for the ionic liquid liquors derived from the 'optimum pulps' (170°C 30 min for RHDN and 150°C 1hr for JPK). The two main chemicals found in the liquor are acetic acid and furfural for both feedstocks. The glycosylic bonds from the hemicelluloses and cellulose are hydrolysed in the acidic ionic liquid, leaving monomers in liquor.[301] This explains the presence of glucose and hemicelluloses (arabinose, mannose, galactose) in the IL. These monomers can then go through further transformation in the IL at such temperatures: the dehydration of sugars lead to the formation of furfural and HMF.[61] The removal of acetyl groups from sugars lead to the formation of acetic acid in relatively important concentrations. More than 8 mg/g for acetic acid and furfural were found in the liquor for both feedstocks. Other degradation products are also observed in the liquor in smaller concentrations: levulinic and formic acid – from the further degradation of HMF.[301] Degradation products found in the liquor could be recovered via distillation to maximise the biorefinery products. However, recovery was not in the scope of this study, but this analysis was used to understand which compounds are found in the liquor and their impact on the subsequent stages of the process, such as enzymatic saccharification and fermentation.[302]

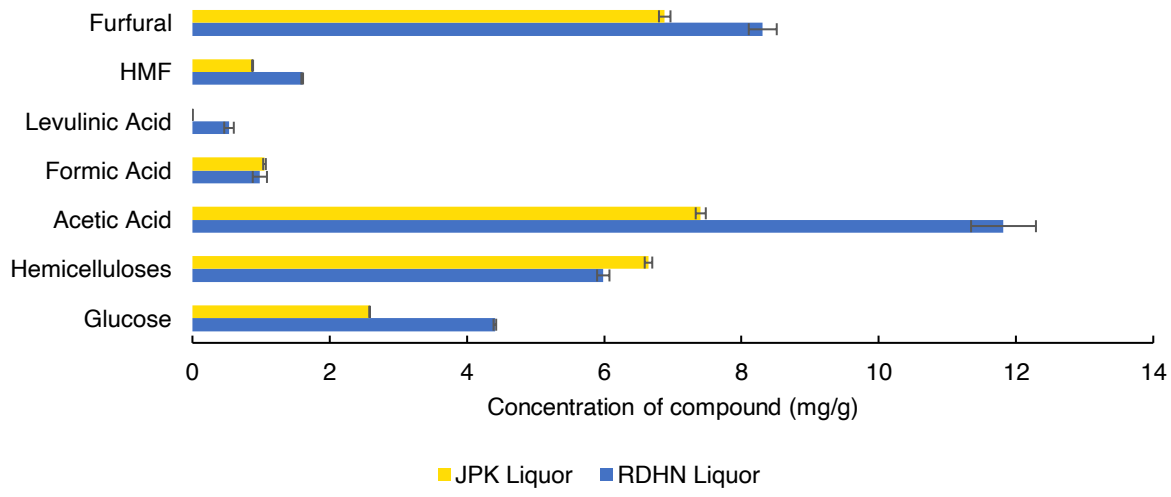


Figure 3.5: analysis of the compounds found in the ionic liquid liquor after pretreatment (in mg of compound per g of ionic liquid liquor)

3.2.4 Significant fermentation and bioethanol yields of invasive ionoSolv pulps

To demonstrate potential valorisation of the hydrolysate, fermentation of the glucose solutions into bioethanol was performed. The obtained hydrolysates which released the highest glucose yields were used to grow yeast cells (*Saccharomyces cerevisiae*) for ethanol production. Ethanol production was observed for the two feedstocks, as shown in Figure 3.6.

The ethanol yields observed for the untreated invasive species are below 2 %, much lower than the ones obtained from the pretreated samples, as a result of the high amount of biomass necessary to achieve a sufficient sugar concentration for the fermentation. This further demonstrates the necessity of pretreatment for lignocellulosic biomass and subsequent valorisation into a fuel. The yield of glucose conversion into bioethanol from pretreated RHDN reached 75.7 % showing that this feedstock is suitable for fuel production under these conditions. The yield of ethanol from pretreated JPK is slightly below 25 %, which is a 67-fold increase compared to untreated JPK.

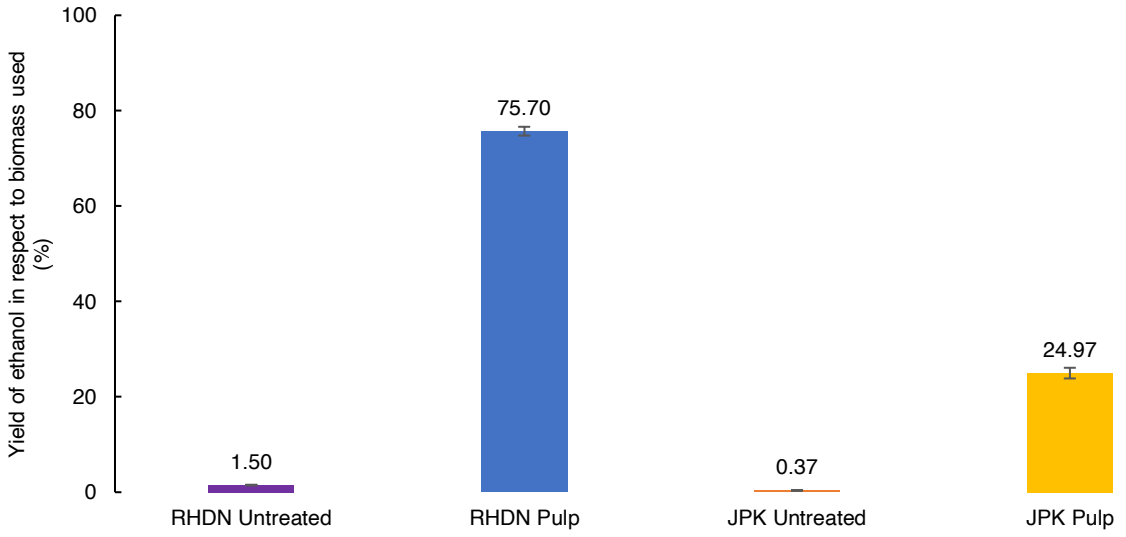


Figure 3.6: ethanol yields from the hydrolysate of pretreated pulps (with the highest glucose release), standardised to the amount of biomass used (dry matter)

The significant difference between the fermentation of RHDN and JPK can be explained by the presence of fermentation inhibitors in the hydrolysate.[303] The presence of degradation products from the pretreatment such as furans and carboxylic acids can hinder the fermentation of yeasts.[304] In fact, the HPLC analysis of solutions after fermentation shown in Figure 3.7 exhibits higher concentrations of acetic and levulinic acids for the JPK than for the RHDN; with the presence of formic acid only in the JPK fermentate. These compounds were also found in the IL liquor right after pretreatment (Figure 3.5), showing that removing and/or recovering such compounds before fermentation could have a positive impact on the bioethanol yields. Looking at the value for fermented JPK pulp, it looks like the feedstocks did not perform as well. However, it needs to be taken into consideration that the fermentation process is not optimised, but merely used at a proof of concept of biofuel production derived from ionoSolv pulp. Perhaps a threshold of minimum of bioethanol yield could be established,

using this fermentation protocol and ionSolv pulps; however, the optimisation of the fermentation process is out of scope for this thesis.

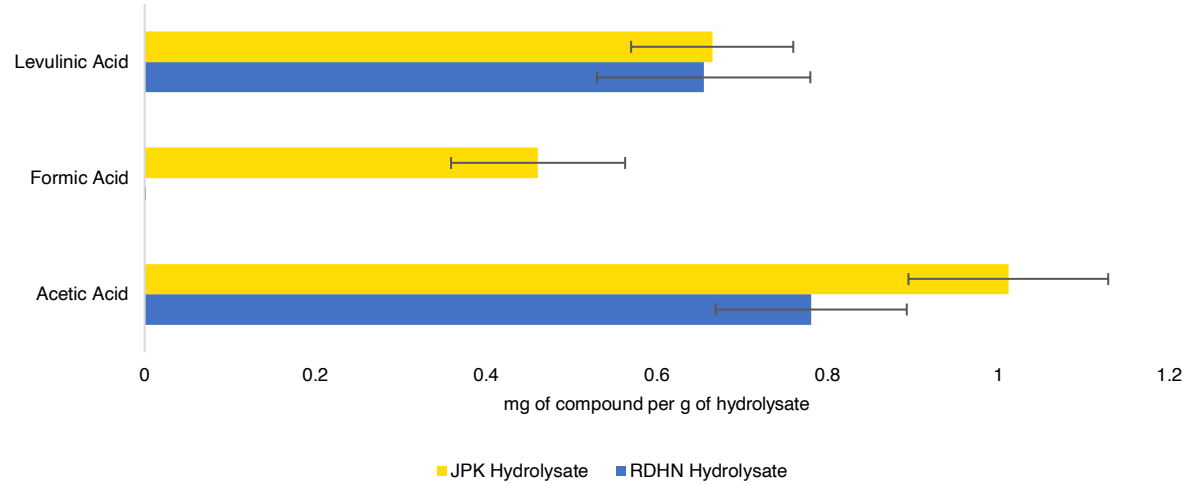


Figure 3.7: HPLC analysis of the weak acids found in the solutions after fermentation for JPK and RHDN

We have shown here that these invasive species samples can be deconstructed using a low-cost innovative solvent and that the cellulose pulp derived from the process can be converted into a biofuel with significant yields, especially for RHDN. Such biomass can be used as a resource to feed into the ionoSolv process and could have a significant positive environmental impact. Instead of being burned as contaminated waste, this biomass could be used to yield renewable and financially attractive compounds using an innovative technology that has proven successful on other feedstocks (softwoods, hardwoods, grasses).

3.2.5 Unveiling lignin analysis for such unconventional species

The lignin stream was studied for its value as a fuel, and the lignin structure of the lignin was analysed using 2D HSQC NMR, and to further analyse ionoSolv product streams. Elemental analysis was performed to assess the higher heating value of the ionoSolv lignin compared to untreated biomass. Thermogravimetric analysis was used to study the thermal stability of the lignins from the pretreatment, while gel permeation chromatography (GPC) was used to determine the molecular size and weight of the lignin extracted from the pretreatment.

3.2.5.1 Lignin solubilisation over time from the protic acidic ionic liquid mixture treatment

2D HSQC NMR was employed here to gain insights on the structure of the isolated lignins obtained at optimum conditions (170°C 30 min for RHDN and 150°C 1hr for JPK). HSQC NMR analysis is a two-dimensional NMR technique that resolves signals that otherwise overlap in

one-dimensional spectra. The resulting NMR spectra can be analysed into two sub-sections: the aromatic region showing cross-signals of the aromatic sub-units (*p*-hydroxyphenyl H, guaiacyl G and syringyl S as well as *p*-coumarates) and the region representing cross-signals for the linkages between these aromatic subgroups as seen in Figure 3.8 (taken from reference 52). The structural changes in isolated lignin from miscanthus have been previously reported using acidic ionic liquid water mixtures.[47] Lignin extracted from invasive species has not yet been reported in the literature and therefore the assignments of $^{13}C–^{1}H$ cross signals in the HSQC spectra were performed based on the existing literature for a range of lignocellulosic feedstocks.[283,284,305–307] The structure of lignin changes depending on the extraction or isolation method applied. HSQC NMR here is not used to determine the native structure of the lignin from such invasive species, as its structure has been altered by chemical modification from the pretreatment, but to look into the aromatic sub-units and side chains linkages present in the ionoSolv lignin from RDHD and JPK. Softwoods are made predominately from guaiacyl (G) sub-units, while hardwoods are made of G and a large amount of syringyl (S) sub-units and grasses are made of all three S, G and smaller amounts of *p*-hydroxyphenyl (H) sub-units.[35] Some biomass lignins may also contain *p*-coumaric acid (PCA) and ferulic acid (FA) units. The S/G ratio is used to characterise the lignin type of feedstock and is known to have an impact on the delignification of hardwoods, as well as hydrolysis of the cellulose and hemicellulose.[308–311] Moreover, HSQC NMR technique is used to semi-quantity the major linkages between these units: β-*O*-4' aryl ether, phenylcoumaran β-5' and β-β' resinol linkages.

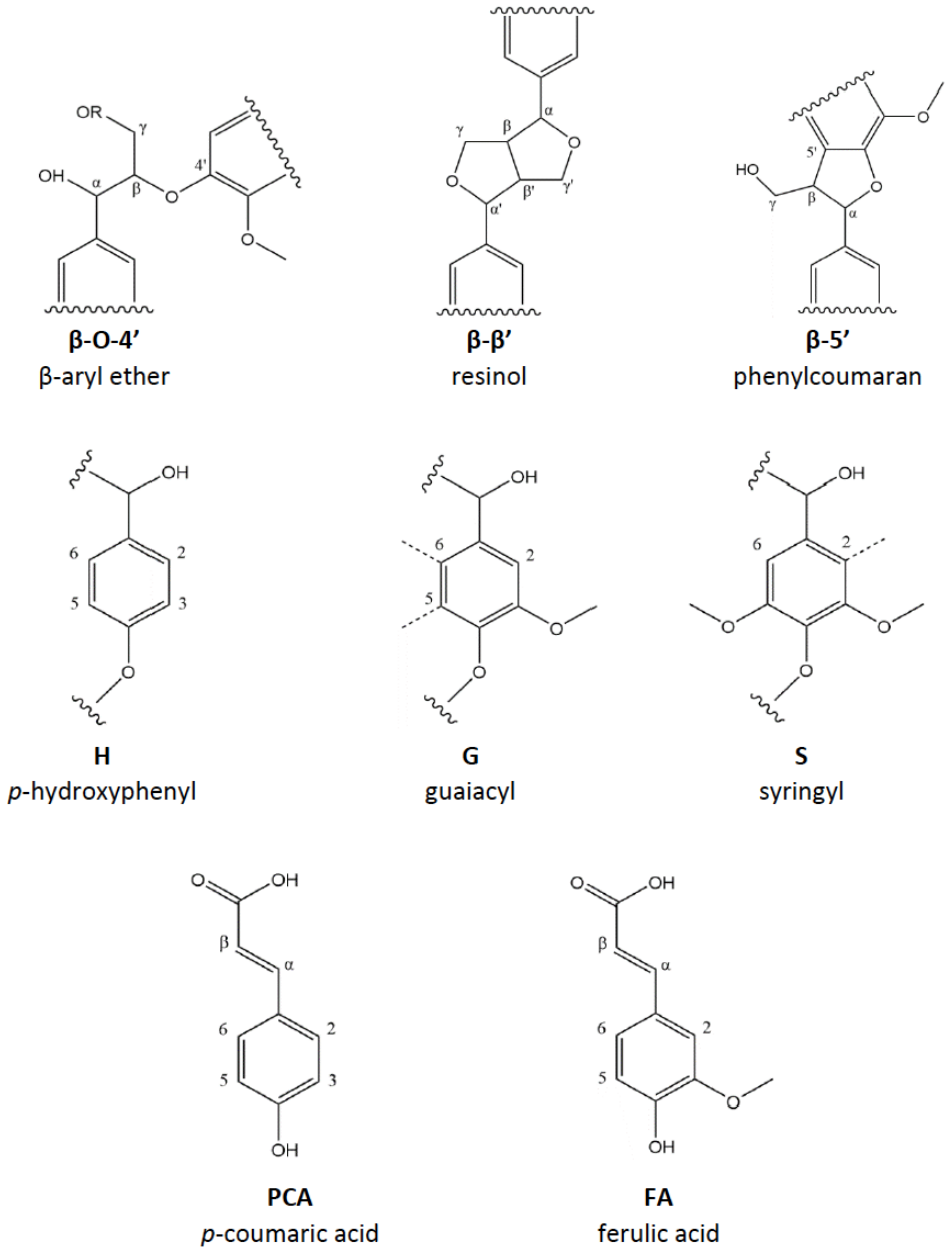


Figure 3.8: major sub-units and linkages found in lignocellulosic biomass

The results of the HSQC of the lignins are presented in Figure 3.9. Neither feedstock showed any signal for H sub-units in their lignin HSQC. The S/G ratio of the recovered lignin was determined as 0.5 and 0.8 for JPK and RHDN, respectively. These results are in agreement with the compositional analysis of the untreated biomass. These species are not considered grasses due to the absence of H sub-units. The ionoSolv lignin from RHDN showing higher amounts of S aromatic units is closer to that of hardwoods such as willow, while the lignin extracted from JPK has a lower S/G ratio with lower S units.[103,104] Since the degree of condensation of G_2 units is similar between the two feedstocks, it could also be that a greater

amount of S sub-units were extracted from JPK than RHDN. S-rich lignins are easily extracted in mild pretreatment conditions, as G sub-units are more prone to condensation, forming C-C bonds between units and resulting in cross-linking of the aromatic ring. In fact, JPK lignin exhibits fewer β-*O*-4' linkages than RHDN, which adds to the evidence that JPK lignin is more condensed (nucleophilic attack of the G sub-units onto the alpha carbon of the β-*O*-4' linkage in acidic conditions). JPK lignin was found to show PCA linkages, which are usually in grasses and believed to be involved in cross-coupling with lignin monomers and the formation of lignin carbohydrates-complexes (LCCs).[83]

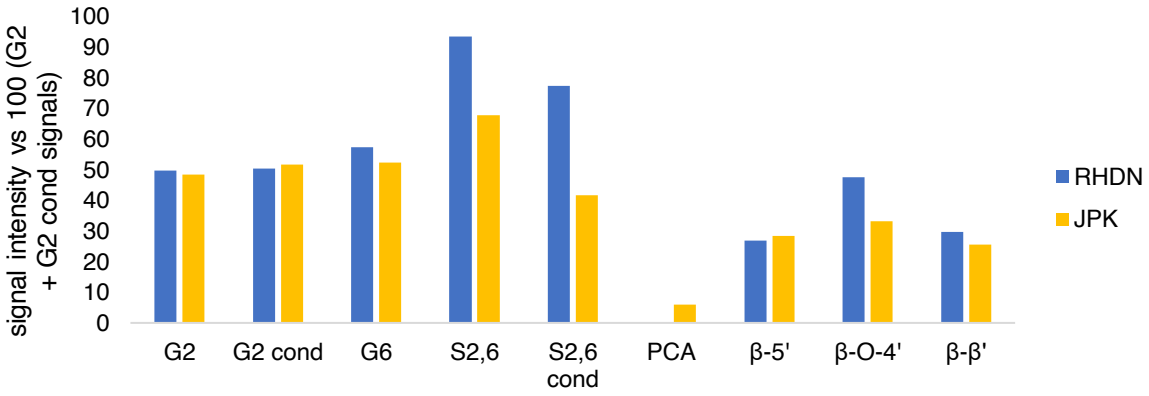


Figure 3.9: HSQC NMR results of lignin recovered after pretreatment of RHDN at 170°C for 30 min with [DMBA][HSO$_4$] and JPK at 150°C 1 hour, biomass to solvent ratio of 1:5 g/g and a final water content of 20 wt%

3.2.5.2 Invasive ionoSolv lignin properties over time via Gel Permeation Chromatography

Lignin can also be used as a precursor for value added chemicals, for which characterisation of the lignin is often needed.[45,312] The GPC results determined the weight average molecular weight (M_n), the number average molecular weight (M_w) and the dispersity (Đ) of the lignin extracted from the pretreatment (Table 3.1). Pretreatment conditions such as temperature, time, acid/base ratio of the IL, have an impact on the molecular distribution of the ionoSolv lignins.[97,104] However, the relation between pretreatment conditions and impact on the lignin structure and weight is not always straightforward. The ionoSolv pretreatment utilises an acidic ionic liquid to deconstruct and react with the lignin from the biomass. At the molecular stage, there is a balance between lignin condensation reactions and depolymerisation of lignin through the cleavage of β-*O*-4' linkages into smaller lignin fragments.[47] These phenomena have been observed for other lignocellulosic feedstocks such as miscanthus and willow with protic ionic liquids and similar pretreatment conditions.[100,104] M_w decreases through lignin depolymerisation, while M_w increases as lignin condensation reactions are favoured, resulting in longer chains of cross-condensed lignin.

The pretreatment of RHDN at 150°C yielded larger lignin chains than at 170°C because lignin hydrolysis is favoured at higher temperatures based on the M_w values. For RHDN at 150°C, the highest M_w and M_n was observed at 0.5 h. This is the early extraction stage, where the lignin is extracted with remaining cleavable ether bonds and low polydispersity. M_w increases with pretreatment time due to the continued extraction of lignin; and later condensation of G sub-units with longer residence time within the ionic liquid, while M_n and Đ decrease due to further hydrolysis of already extracted shorter chain lignins. At 170°C for RHDN, M_w increases from 0.25 to 0.75 h of pretreatment, and decreases at even longer reaction times. This shows that beyond 0.75 h at 170°C, lignin extraction has ceased, resulting in the coexistence of more heterogenous condensed lignin and smaller lignin fragments.

The extracted lignin from JPK have lower M_w and M_n compared to RHDN. It is interesting that JPK at 170°C seems to follow the same trend as RHDN at 150°C. Mw and Đ increase as the pretreatment time increases, showing that the lignin is continuously extracted at 170°C but Mn decreases from 3.90 to 5.96 between 0.25 h and 1.25 h respectively. While lignin is extracted and smaller fragments are being hydrolysed, lignin condensation is accelerated within the G sub-units, with other fragments of lignin and possibly degradation products (pseudo-lignin and LCCs). At 150°C, M_w reached its maximum at 5040 Da for 1 hour of pretreatment, then decreases, while M_n remains fairly constant. It seems that the lignin extraction stage ceased after this point and the presence of PCA linkages confirmed by HSQC NMR (Figure 3.10) could be further evidence of pseudo-lignin formation and interaction with residual carbohydrates.

Sample	RHDN - 150°C			RHDN - 170°C			JPK - 150°C			JPK - 170°C		
Time (h)	M_n	M_w	Đ	M_n	M_w	Đ	M_n	M_w	Đ	M_n	M_w	Đ
0.25	-	-	-	1272	6130	4.82	-	-	-	1274	4672	3.90
0.5	1436	6824	4.97	1291	6321	5.10	1218	4544	3.59	842	4067	4.95
0.75	1311	7204	5.14	1201	6666	5.56	1050	4063	3.96	824	4322	5.48
1	1187	7386	6.02	1166	6226	5.36	1064	5040	4.67	990	5484	5.68
1.25	1113	7798	6.83	1131	6287	5.56	1077	4063	4.12	857	5332	5.96
1.5	1037	7893	7.48	-	-	-	1019	4371	4.46	-	-	-

Table 3.1: GPC results of the lignin. M_n and M_w (Da)

Differences in molecular weight of the lignin are inherent to the species of the biomass itself, but also to the pretreatment technology used, and its severity.[104,313] The desired properties of ionoSolv lignin from invasive species would depend on its end application. Lignin with higher

molecular weight, high aromaticity and increased C-C bonds is preferrable for composite materials such as fillers, carbon fibres or resins,[314,315] while lower molecular weight lignin is proposed in biological valorisation routes.[316–318]

3.2.5.3 Proximate analysis of lignin: invasive ionoSolv lignin as a fuel

Thermogravimetric analysis (TGA) was used to assess the thermal properties of the lignin extracted from the invasive species, as the application of lignin in fast pyrolysis could be an interesting end application. Proximate analysis was conducted employing an incremental heating process up to 600°C to quantify the composition, moisture, volatile matter, ash and fixed carbon components of the lignin and raw biomass. DTG_{max} is the peak in the DTG curve, which correlates to the temperature at which the sample exhibits the maximum rate of degradation and is used to compare the relative thermal stability between samples.

Similarly to the molecular weight of lignin, the thermal degradation of lignin is inherently linked to the chemical structure of the extracted lignin. Lignin linkages begin to break where the bond dissociation energy is relatively low, mainly hydroxyl groups and in a second instance ether bonds (including β-*O*-4 linkages). It was found that the thermal stability of lignin (DTG_{max}) increases with incrementally higher molecular weight.[319] Moreover, the thermal behaviour of lignin is driven by the presence of highly crossed linked and condensed lignin: with a greater degree of condensation of the lignin macromolecule, the thermal energy needed for bond cleavage increases.[320,321]

Table 3.2 shows the thermal stability parameters of the lignin from the time course using invasive species. The proximate analysis data is coherent with the GPC analysis of lignins for the invasive species. As the severity of the pretreatment increases, more ether bond linkages are broken during pretreatment and fewer are left in the resulting lignin. Hence the gradual increase of DTG_{max} with pretreatment time for all lignin samples. Harsher pretreatment conditions lead to more hydrolysed and more condensed lignin: this results in an increase in fixed carbon content during thermal decomposition, corresponding to the remaining volatilized lignin due to the formation of highly condensed aromatic structures; and decrease in volatile matter from less oxygenated lignins.

Sample	RHDN - 150°C				RHDN - 170°C			
Time (h)	DTG_{max} (°C)	VM (%)	FC (%)	VM/FC (%)	DTG_{max} (°C)	VM (%)	FC (%)	VM/FC (%)
0.25	-	-	-	-	315	69.1	30.9	2.2
0.5	332	64.1	35.9	1.8	320	60.2	39.8	1.5
0.75	331	61.4	38.6	1.6	327	60.1	38.9	1.5
1	332	58.6	41.4	1.4	329	57.8	42.2	1.4
1.25	336	58.0	42.0	1.4	337	56.6	43.4	1.3
1.5	342	58.7	41.3	1.4	-	-	-	-
Sample	JPK - 150°C				JPK - 170°C			
Time (h)	DTG_{max} (°C)	VM (%)	FC (%)	VM/FC (%)	DTG_{max} (°C)	VM (%)	FC (%)	VM/FC (%)
0.25	-	-	-	-	328	65.6	34.4	1.9
0.5	335	66.2	33.8	2.0	338	60.0	40.0	1.5
0.75	336	71.7	28.3	2.5	341	60.5	39.5	1.5
1	344	59.4	40.6	1.5	347	55.6	44.4	1.3
1.25	329	59.6	40.4	1.5	346	57.4	42.6	1.3
1.5	343	57.0	43.0	1.3	-	-	-	-

Table 3.2: thermogravimetric analysis of the lignin derived from the pretreated invasive species

The Higher Heating Values (HVV) of the lignin for the two time courses performed were calculated according to the Demirbas formula,[287] based on the elemental composition of the samples (values shown in the Appendix); and shown in Figure 3.10. The HHV for the untreated biomass is 16.3 $MJ.kg^{-1}$ for both feedstocks. This is within the range of the values reported in the literature for other biomass feedstocks (8-20 $MJ.kg^{-1}$) or bio oils (16-19 $MJ.kg^{-1}$).[322,323] The highest energy value of lignin was obtained from of RHDN at 170°C for 15 minutes (25.7 $MJ.kg^{-1}$), a 1.5-fold increase compared to untreated raw biomass. This is due to the higher carbon and lower oxygen contents of the lignin compared to untreated biomass.[324,325] For RHDN, HHVs range between 23.7 $MJ.kg^{-1}$ and 25.7 $MJ.kg^{-1}$, with slightly higher values for pretreatments conducted at 170°C compared to 150°C, due to the higher degree of condensation of lignin at harsher pretreatment conditions. We can observe an opposite trend for JPK, with values ranging from 22.9 to 24 $MK.kg^{-1}$; with higher values at 150°C than 170°C. These differences could be due to the reaction of lignin with more oxygenated compounds

such as pseudo-lignin and carbohydrates; as the presence of LCCs was already suspected from the HSQC NMR.

The N and S content between 1-3 % in the lignin indicate residual IL contamination; nitrogen is representative of the dimethylbutylammonium cation and sulphur is representative of the hydrogen sulphate anion. Further washing of the lignin could be investigated to remove any contamination such as a Soxhlet ethanol extraction overnight as it is performed on the pulp at bench scale.

IonoSolv lignin can be burned for energy as a fuel, with more energy liberated per unit mass than untreated biomass, contributing to the valorisation of all products derived from the pretreatment of the biomass.

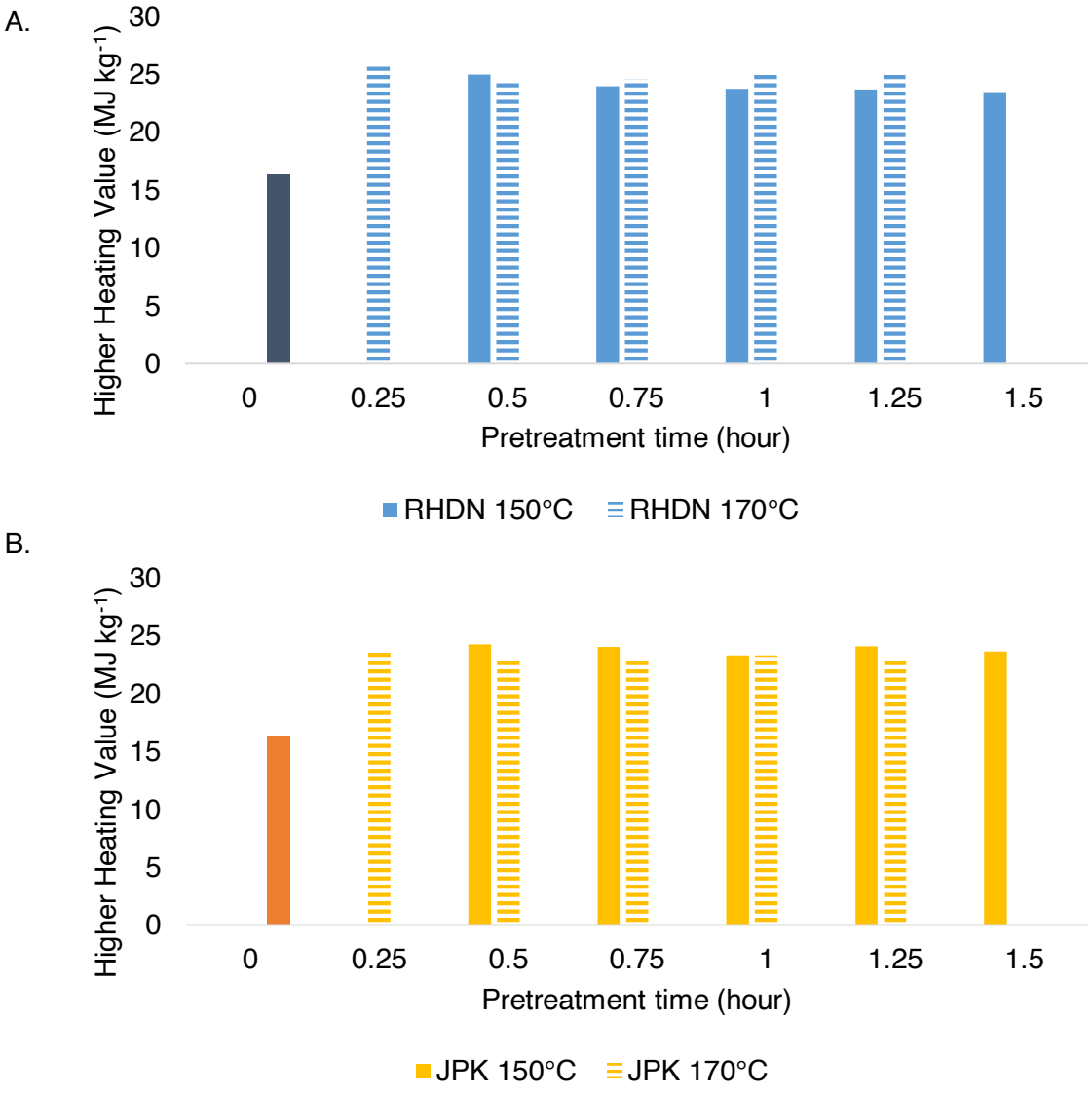


Figure 3.10: Higher Heating Values (HHV) of the ionoSolv lignins from A. Rhododendron (RHDN) and B. Japanese Knotweed (JPK) at 150°C and 170°C for short reaction times (0.25-1.5 hr)

The structures and properties of lignin differ between feedstocks and are affected by the delignification chemistry and its severity in biomass fractionation using ionic liquids.[326] The conditions of the pretreatment will essentially depend on the desired outcome of the process, whether it is bioethanol production from the pulp, or high purity of cellulose for nanocellulose production, or even specific properties for extracted lignins for carbon fibres. Nonetheless, this study demonstrates that the ionoSolv pretreatment can be feedstock agnostic and applied for a variety of different lignocellulosic feedstocks, such as UK invasive species, to extract high quality lignin and generate a cellulose rich pulp, which was fermentable into bioethanol.

3.3 Conclusion: waste invasive species as a resource for a biorefinery

To the authors' knowledge, this is the first time UK invasive species such as JPK and RHDN were investigated as biofuel feedstocks. The composition of these two invasive species was determined and found to be similar to typical biofuel feedstocks, such as pine and willow. The ionoSolv process was able to integrate such biomass for lignocellulosic fractionation at high temperature and short reaction times into value-added bioproducts, demonstrating potential as an energy feedstock. This pretreatment process proves that it is flexible regarding the biomass feed, yielding a cellulose rich pulp from these two invasive species, as well as a lignin stream. The cellulose was hydrolysed and successfully fermented into bioethanol, while the lignin was isolated and valorised into bioheat. While JPK seemed a more promising feedstock based on compositional analysis; RHDN lead to higher yields after transformation mainly due to a higher pulp yield. This highlights the non-linearity between glucose composition and bioethanol yields, as well as the importance of inhibitors derived from the during the biomass fractionation process. However, the optimisation of fermentation was out of the scope of this thesis and merely served as a proof of concept for biofuel production.

In Great Britain, the estimated total cost of removal and disposal of JPK alone stands at £165 million per year, whereas the current control efforts against RHDN species are estimated to cost over £8 million per year.[55,327,328] Through this study, we have shown that a chemical engineering process for biomass can be an alternative to waste disposal and that these invasive species can instead be a source of useful products and fuels. In combination with strict management practises to avoid further spreading of invasive species (i.e., transport, harvest), they could be fed into the ionoSolv process. Such a strategy could lead to creating renewable energy from these species and generate a revenue, allowing eradication at a lower cost. Moreover, as these feedstocks are easily available and not agriculturally grown on purpose, they have the advantage of taking the pressure off land use and land availability for

the production of bioenergy. This represents an upgrading of an underutilised biomass, extremely hard to eradicate by conventional chemical and physical means.[329–332]

The results should be leveraged with accurate biomass yields and of course, biomass availability on the short, medium and long term. With RHDN taking up 3.3 % of Britain's woodland (98 700 ha),[333] this feedstock could represent a market for a biorefinery; and a significant increase in land used for bioenergy without competing with food or forests. JPN would still have value and could be used in co-processing with RHDN. If the goal is to both supply the ionoSolv process with biomass and exterminate the threat of such invasive species, one should agree that the supply of such invasive species will be decreasing over time. The biomass supplied for the ionoSolv biorefinery should not be only from one source, but from a myriad of feedstock solutions. In the next chapter, we will further investigate the ability and chemical engineering barriers to integrate another type of waste, metal contaminated waste wood, into the ionoSolv supply chain and test the ability of the ionic liquid solvent to dissolve metal species in the wood.

4 Consumer waste wood: the challenge of highly contaminated feedstock for the ionoSolv process

4.1 Introduction

While invasive species offer a promising alternative for sourcing lignocellulosic feedstock to the ionoSolv process, their availability and potential misuse raise long-term complexities. In this chapter, we investigate using another alternative waste feedstock, which availability is directly induced from human activities and demographic growth: construction waste wood. We test both the flexibility of the ionoSolv process to pretreat unconventional feedstocks and its ability to treat a waste with imbedded metals. What happens to waste wood after its shelf life? Waste wood is associated with a major environmental burden, often landfilled, or incinerated in specialised burners. Copper Chromated Arsenate (CCA) wood is a type of construction wood that has been extensively used all around the world.[334–336] It is being phased out by the Environmental Protection Agency and production has been banned but scientists agree that dealing with the disposal of waste CCA wood will remain an environmental challenge for the coming decades.[337]

In the effort of finding innovative feedstocks for the ionoSolv process, this chapter investigates the use of post-consumer and hazardous waste wood as a biorefinery feedstock. Similarly to invasive species, using such waste is more sustainable than using conventional biofuel crops for two reasons: it uses waste as a resource in the context of a circular bioeconomy and it diverts a waste from landfill, freeing land and avoiding contamination of the environment from

metals. Moreover, this chapter capitalises on the unique properties of ILs as designer solvents. Here we suggest that some PILs can both deconstruct the lignocellulosic feedstock and decontaminate the waste by extracting its metals within the wood. Thanks to their ionic nature, ILs have been studied for their ability to dissolve various metals.[166,338–341] Moreover, PILs often show higher solubility of metal salts than their aprotic analogues.[161,162]

In the effort of further enhancing the process' recyclability and separation system, the following aspects are investigated in this chapter: the fractionation of waste wood for the ionoSolv supply chain, the metal extraction from its solvent, the impact of metals on subsequent fermentation and recycling of the solvent over 6 cycles. Finally, the diversification of by-product valorisation is widened beyond the binary of glucose and lignin based products, with analysis and valorisation of a waste stream: post hydrolysis solid residues via pyrolysis.

4.2 Results and discussion

4.2.1 The composition of the waste-wood feedstock is similar to pine

Compositional analysis was conducted, showing 43.5 % glucose, 20.1 % hemicelluloses (xylose, galactose, arabinose and mannose), 30.9 % lignin and 1.4 % ash – as seen in Figure 4.1. Structural carbohydrates and lignin are similar to those of a softwood such as pine, displayed along with the results for CCA. The main differences between the two feedstocks are the ash content and small differences in lignin and hemicellulose contents, which can vary even from within the same species of tree.

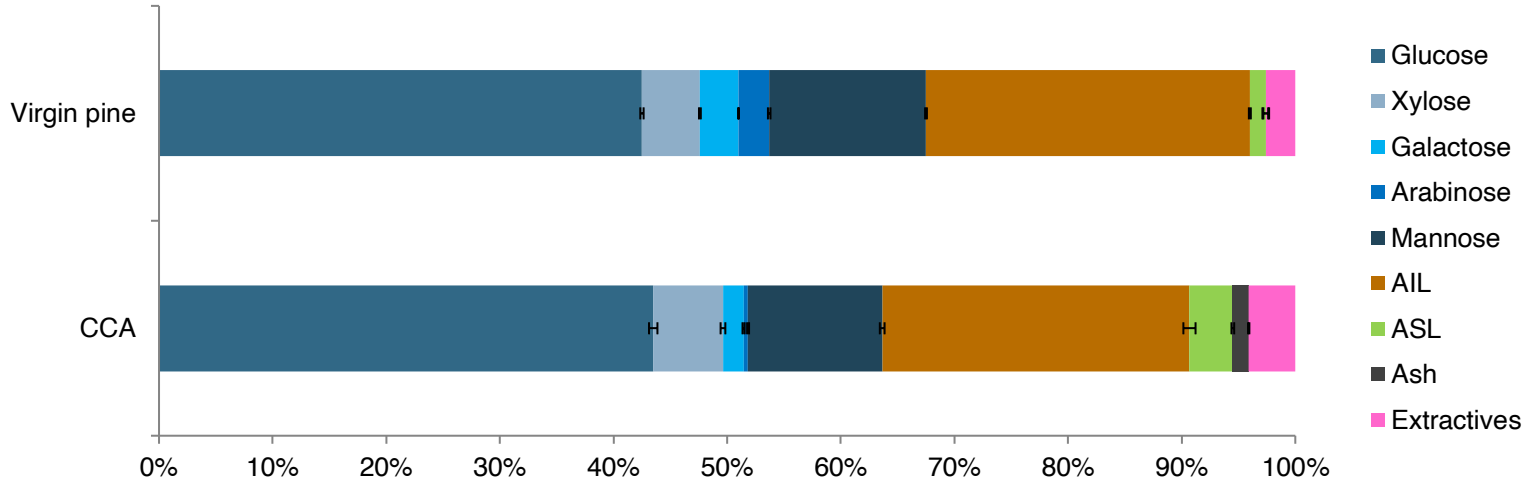


Figure 4.1: compositional analysis of the CCA treated wood used for the experiments and a virgin softwood pine, for comparison

The ash content is due to the presence of metals in the biomass in very high concentration and confirmed by ICP-OES, as shown in Figure 4.2. The CCA treated wood contains nearly

4000 mg.kg^{-1} of Cr and As, as well as 2000 mg.kg^{-1} of Cu. As explained in the methodology section, the error bars shown refer to a single standard deviation value from the technical triplicate experimental measurements. The metal content of the untreated CCA wood shows some variability even within the same sample, especially for As. Even homogenised after grounding, the CCA wood could exhibit some small variations in metal owning to the metal impregnation process.

Its metal content categorised CCA treated wood as Grade D waste and its waste poses an environmental issue: it is either necessary to dispose of it using special expensive burners, or in specialised landfills to avoid metal leaching in the soil and groundwaters.

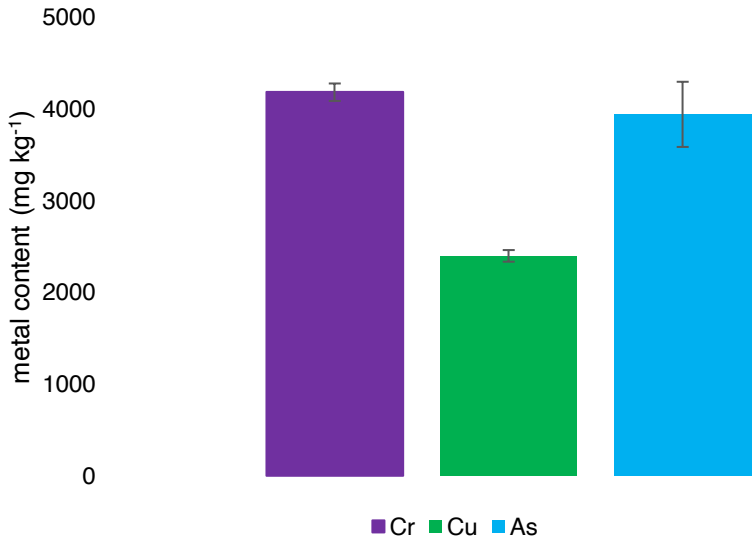


Figure 4.2: trace element analysis of the CCA treated wood used for the experiments

4.2.2 Stable fractionation and saccharification of waste wood with recycled liquor

Based on the compositional analysis results of the treated wood and previous studies published using the ionoSolv process, CCA samples were pretreated as a softwood feedstock: 170°C for 30 minutes, 20 wt % biomass loading.[103] The IL [C_1Him][Cl] was selected for its imidazolium cation to deconstruct lignocellulosic biomass and its chloride anion known to coordinate with metals in aqueous phases.[35,158,342] In order to investigate the process economics of this feedstock, the same pretreatment conditions were used but the ionic liquid solvent was recycled over the course of 6 cycles. IL recovery was found to be 99.06 ± 0.72 % overall, showing it can be recycled with minimal losses. After each cycle of pretreatment, the isolated wet pulps were subjected to enzymatic hydrolysis and the lignin was recovered by the addition of an anti-solvent into the ionic liquid liquor. Finally, the water from the ionic liquid

liquor was evaporated and the liquor was analysed and recycled for the subsequent pretreatment. The impact of the recycling of the ionic liquid was studied using key performance indicators for this pretreatment: the theoretical maximum glucose release, also called saccharification yield (Figure 4.3).

The analysis of pulp and lignin yields are limited as they are only quantitative weight measurements by mass of the products recovered from the pretreatment. However, in the case of recycling of the ionic liquids, these pretreatment values can be insightful. The pulp yields were stable along the different cycles, between 53-54 % (n=1 and n=5 respectively) and 62 % (n=6), with standard deviations increasing with the number of cycles. This indicates that the variability of the cellulose pulp recovered increases with the repeated recycle of the IL.

On the other hand, lignin yields increased from 12.1 % of the whole initial biomass in cycle 1 to almost double, with a lignin yield of 21.5 % in cycle 6. As lignin is being dissolved in the ionic liquid over the course of each pretreatment, a significant amount of lignin in the form of small water-soluble fragments (also called pseudo-lignin) can stay dissolved in the liquor from one cycle to another. These small lignin fragments can also re-condense during the following cycles until they eventually precipitate out, though they may stay in the liquor for a few cycles before precipitating. Those fragments are likely to have had more of their ether bonds broken and a significant amount of condensation occurs between aromatic units over the repetitive recycling of the IL. This can explain the monotonic increase in lignin yield over a number of cycles: more lignin can be precipitated from the liquor as the cycle number increase and the pulp yields increase as some of this pseudo-lignin fragments can also redeposit on the cellulose pulp during pretreatment.[106,343]

Glucose release, or percentage of saccharification yields are key parameters to assess the performance of the pretreatment, recycle, and overall valorisation of the biomass. Comparing the values for saccharification of the ionoSolv pulp (n=1) and the untreated biomass (n=0), a 14-fold increase compared between the two samples, showing the crucial importance of this specific [HC_1im][Cl] pretreatment step for any subsequent chemical valorisation.

Saccharification yields, starting at 67 % after the first cycle, gradually decreased over the subsequent 3 cycles to 55 % in cycle 4 before increasing to 75 % in the 6th cycle. Again, this could be due to the amount of lignin accumulating as water soluble fragments on the surface of the pulp over the cycles 2-4. After cycle 4, these fragments finally condense and are able to be precipitated in cycle 5, which improves the accessibility of enzymes for the saccharification. We can note that the standard deviation between samples at cycle 6 is higher than for the previous ones, showing that the recycling of the IL can introduce variability.

However, we can conclude that the pretreatment is efficient and robust for at least 6 cycles providing a significant glucose release from such waste wood, with minima impacts on the performance of the process from the recycling of the solvent.

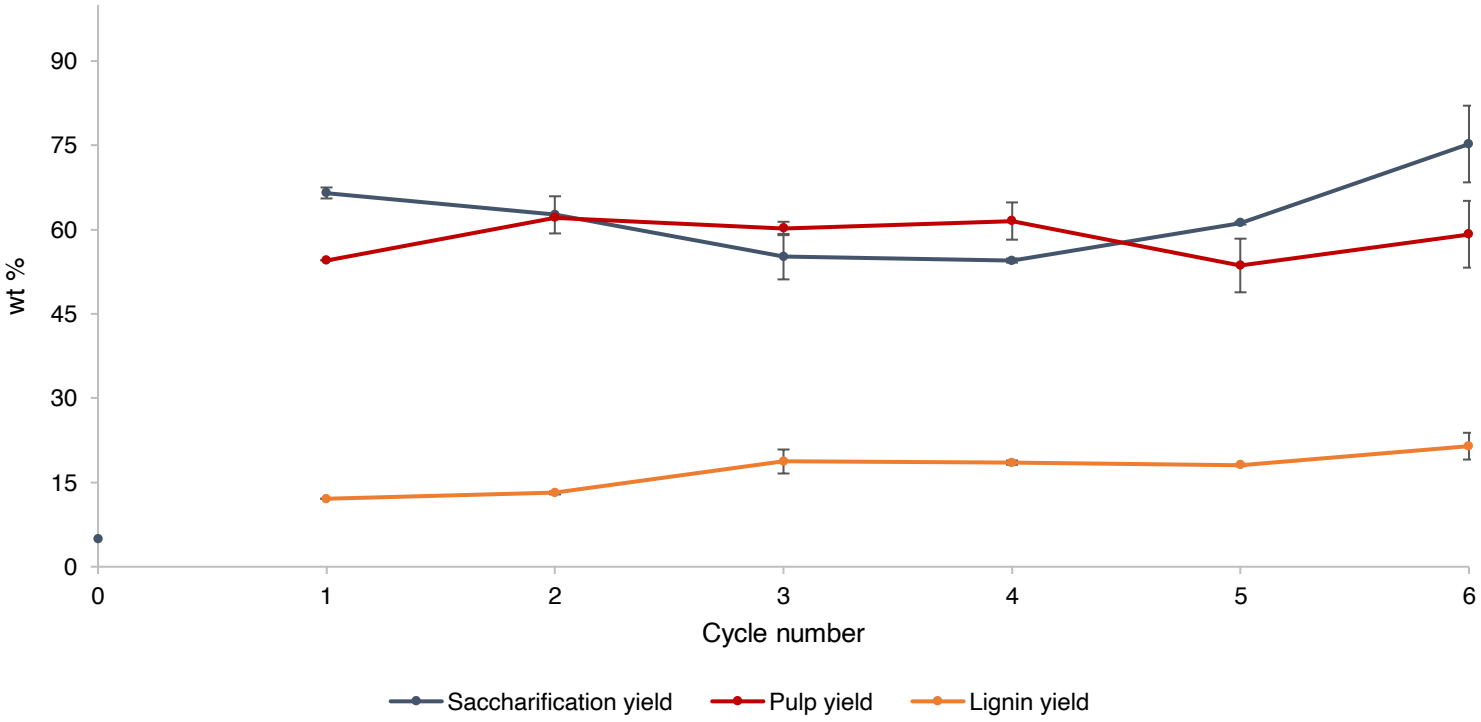


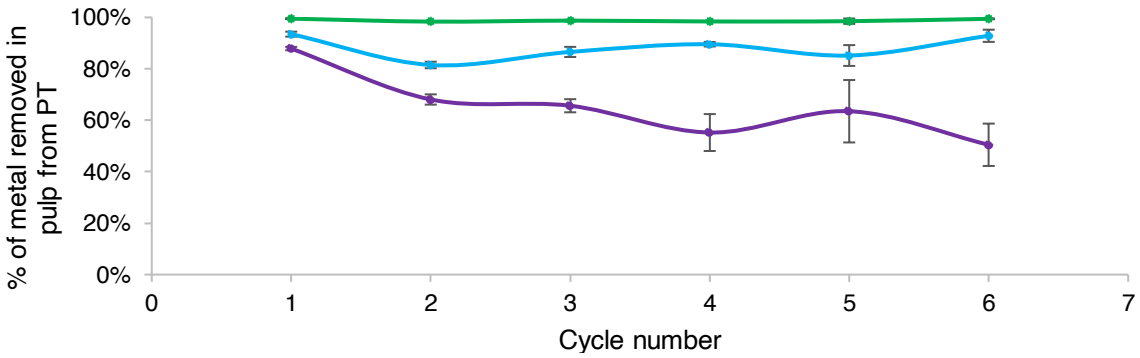
Figure 4.3: pulp, lignin and saccharification yield of untreated and pretreated CCA wood over 6 cycles

4.2.3 Significant metal extraction from the waste wood into the ionic liquid liquor

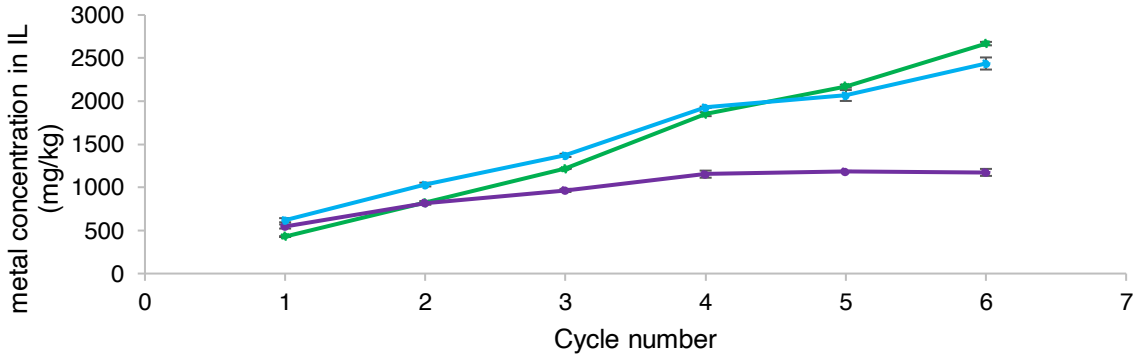
Given the concentration of metals from the trace element analysis of the wood, it is crucial to assess the fate of metals along the process explored, i.e., the second aspect of the pretreatment step, which is the removal of metals within the biomass using [HC_1im][Cl]; and explore the opportunity to recover them as a by-product.

Cu^{II}, Cr^{III} and As^{V} are potent biocides, which could not only hinder a biological fermentation of the sugar solutions derived from the pretreated pulp but would kill any yeast cultures in the process.[250,344] Therefore, it is crucial that these metal contaminants at such levels be removed from the cellulose pulp. The metal extractions results are presented in Figure 4.4.

A.



B.



C.

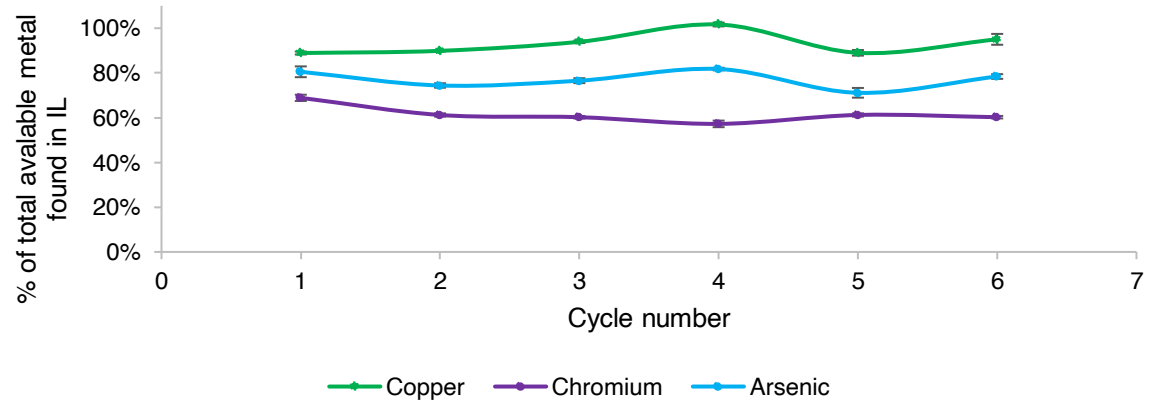


Figure 4.4: A. Metal extractions from IL PT calculated from the metal content found in the pulp
B. Metal content found in the IL liquor after pretreatment for n cycles
C. Percentage of Cu, Cr as As found in the IL brown liquor after n cycles based on the metal concentration prior to the cycle and the amount of new metal entering the system (fresh biomass)

In the first instance, trace elements were carried out on untreated biomass and ionoSolv pulps to assess the metal removal from the ionic liquid pretreatment. [C_1Him][Cl] was found to be an excellent agent to solubilise impregnated metals present in the biomass, to the extent that the metals were extracted in the ionic liquid liquor. Copper extraction was very high through the 6 cycles, consistently above 98 %. Chromium and Arsenic extraction were not as linear. Cr extraction decreased from an initial 88 % to 55 % after the cycle 4, slightly increased again during cycle 5 and went back down to 51 % at cycle 6. Arsenic extraction fluctuated between 80 and 94 %. As and Cr extraction behaved in opposite ways from cycle 2 onwards, with As

extraction increasing with a decreasing Cr extraction and vice versa. Competition for ligands is likely an underlying cause, i.e. the addition of recycled solvent might cause some lignin precipitation, leading to adsorption of metals to the pulp. An altered washing protocol where less wash solvent is used, or where recycled IL that contains less lignin is used, may yield better metal extractions over many cycles.

As can be seen from Figure 4.4B, Cu and As concentrations steadily increased in the IL over the 6 cycles. Despite there being almost twice as much As in the wood as Cu, concentrations in the IL were found to be similar. Cr concentration however only increased slightly over the first 4 cycles and then remained stable at around 1200 $mg.kg^{-1}$. These results suggest that a large proportion of Cr and smaller amounts of As and Cu could precipitate out during the lignin recovery, as lignin is known to be a sorbent for transition metals.[345]

Figure 4.4C shows the percentage of the different metals found in the IL after each stage, taking into account the metal in the IL from the previous cycle. Cu recovery into the IL was initially ~ 90 %, rising to ~ 95 %. As extraction started off at 81 % and subsequently fluctuated at around 75 %. Despite the deviation within the triplicate experiments being fairly small, a spike is observed at cycle 4 where 102 % of Cu appeared to have been found in the IL liquor; while the As percentage in the liquor showed an increase. Inhomogeneity in the untreated sample (Figure 4.2), metal contamination or instrumental accuracy could be one the reasons. An apparently higher concentration of As and Cu in one cycle would then reflect negatively on the next cycle, where the concentration of the IL in the earlier cycle is the baseline for the consecutive cycle. Cr appeared to be unaffected by this outlier, quite possibly due to the system having reached a saturation limit (1100-1200 $mg.kg^{-1}$) as we saw in Figure 4.4B where Cr concentration in the IL stagnated after cycle 4.

4.2.4 Fate of metals over subsequent recycling: metal mass balance

The isolated pulps, recycled IL and lignin precipitates were analysed for Cu, Cr and As content and the metal balance was calculated, as seen in Table 4.1. For As and Cu the mass closures are more or less close to 100 % for the various cycles, taking into account the standard deviations. As we have seen for metal extraction, Cu is the most consistent metal from all 3, with a mass balance around 100 (± 5 %). The numbers were consistently below 100 % for As. Volatilisation of As compounds is a possible explanation for this, however it is unclear whether this would have happened during the biomass pretreatment or during the sample preparation for ICP analysis (acid digestion). As and Cr mirrored each other for metal extraction, Cr metal mass balance is often above 100 %, with significant variations between the triplicate

experiments. While all numbers are corrected for a blank IL which went through the same process steps of ethanol and water addition and evaporation, it cannot be excluded that minor Cr contamination was introduced to one or more of the samples, as explained in the previous section.

Cycle n	Cr	Cu	As
n = 1	95.1 ± 4.3 %	94.7 ± 4.3 %	92.3 ± 3.0 %
n = 2	111.4 ± 2.9 %	93.8 ± 0.7 %	98.1 ± 0.8 %
n = 3	125.9 ± 0.2 %	99.0 ± 2.4 %	97.6 ± 1.8 %
n = 4	133.1 ± 26.4 %	105.4 ± 2.9 %	99.6 ± 6.7 %
n = 5	109.7 ± 19.6 %	98.9 ± 7.2 %	92.9 ± 6.3 %
n = 6	128.9 ± 4.2 %	105.4 ± 2.3 %	97.8 ± 0.9 %

Table 4.1: mass closures from ICP-OES analysis of pulp, lignin and brown liquor isolated after each cycle of pretreatment of CCA treated wood

4.2.5 Impact of metals on the fermentation from toxic wood pulp

To assess the impact of the metal removal from CCA pulp on a biological process, i.e., fermentation, Cu, Cr and As were added to CCA treated pulp to mimic the original metal content in the waste wood. Following saccharification, the obtained sugar hydrolysates were used to grow yeast cells for ethanol production, together with controls consisting of enzymatic hydrolysates of non-pretreated virgin pine (VP-UT), pretreated virgin pine (VP-PT), pretreated CCA treated wood (CCA) and glucose solutions of equivalent concentrations. Ethanol production was observed for all feedstocks, as shown in Figure 4.5. The findings are most significant for the potential valorisation of waste wood. Heavy metals are clearly detrimental to fermentation using Saccharomyces cerevisiae: 10.1 % ethanol yield was obtained for CCA wood pulp, compared to 1.3 % from CCA treated wood pulp in the presence of metals. This shows that CCA treated wood would not be suitable for the production of bioethanol or other fermentation products without an additional decontamination/detoxification process. The decrease of only 1.2 % in ethanol yield for CCA treated wood pulp compared to pretreated virgin pine (VP-PT) demonstrates that the difference in the quality of the pulp for fermentation is minimal between ionoSolv pulps from CCA wood and a typical biofuel feedstock. The ethanol yields obtained from lignocellulosic hydrolysates are higher than the ones from untreated pine (VP-UT) and glucose medium. This might be due to the presence of other sugars (e.g. mannose) and other carbon and nitrogen compounds from the hydrolysate of the pretreated pulp, that enhance the growth and fermentation of the yeasts. Finally, the untreated

virgin pine showed a low yield of 3.2 % due to the high amount of biomass that was necessary to achieve a sufficient sugar concentration for the fermentation (details in the materials and method section).

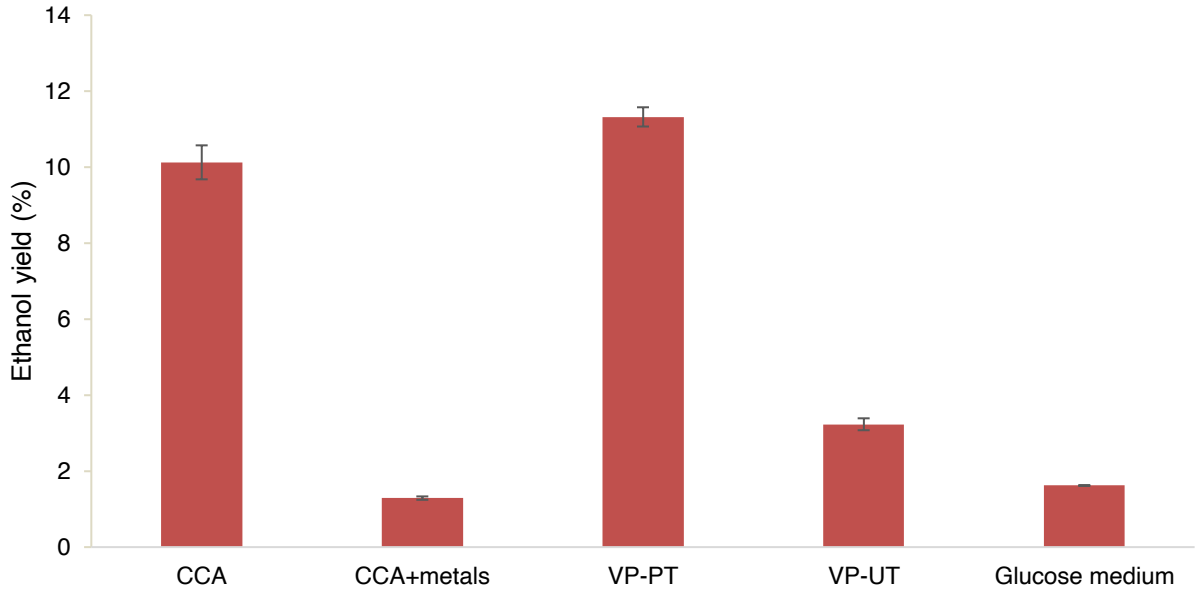


Figure 4.5: ethanol yields (standardised to the amount of glucan added for the saccharification reaction) from CCA treated wood pulp (CCA), CCA treated wood pulp with added metals back in (CCA +metals), virgin pine pulp (VP-PT), untreated virgin pine (VP-UT) and glucose medium after 48 hours of fermentation

4.2.6 Product diversification: unveiling lignin analysis of waste wood

Changes occurring in the lignin structure during ionoSolv pretreatment have been reported for miscanthus[47] and pine and for up to 4 cycles of IL use.[97,103] Here the lignins obtained after the 1st, 2nd and 6th cycle were analysed via 2D HSQC NMR to gain insight on the sub-units and main linkages present in the extracted lignins. The results are displayed in Figure 4.6. The data indicate that recycling of the IL has a similar effect on lignin properties as have been reported for prolonged pretreatment, mainly relying on condensation reactions and formation of higher chains of lignins.[12-14, 25] We can observe an increase in condensation as evidence by a shift of the G_2 signal (see G_2 vs. G_2 condensed) and a decrease in G_6 signal intensity, accompanied by a weaker signal for ether bonds in the isolated lignin. Indeed, part of the lignin precipitating from the liquor at the second cycle will have been in the IL for two cycles but was in the form of water-soluble fragments after the first cycle. Precipitating after the 2nd cycle, those fragments are likely to have had their ether bonds broken and a significant amount of condensation between aromatic units, resulting in a decreased signal intensity in the ether and G_2 areas, and an increase in signal in $G_{2,cond.}$ The same, but in a more pronounced way,

can be observed for lignin precipitated after cycle 6. The signal intensities for β-*O*-4' and G_6 have changed significantly between cycles 2 and 6, potentially indicating that lignin fragments can spend several cycles in the IL before precipitating. This is consistent with the analysis of the previous saccharification yields of the pulp with recycled IL. The G_5 signal remained relatively stable, indicating that the incorporation of carbohydrate degradation products increases signal intensity in this area while the condensation occurring in G_6 decreases it in a complementary fashion.

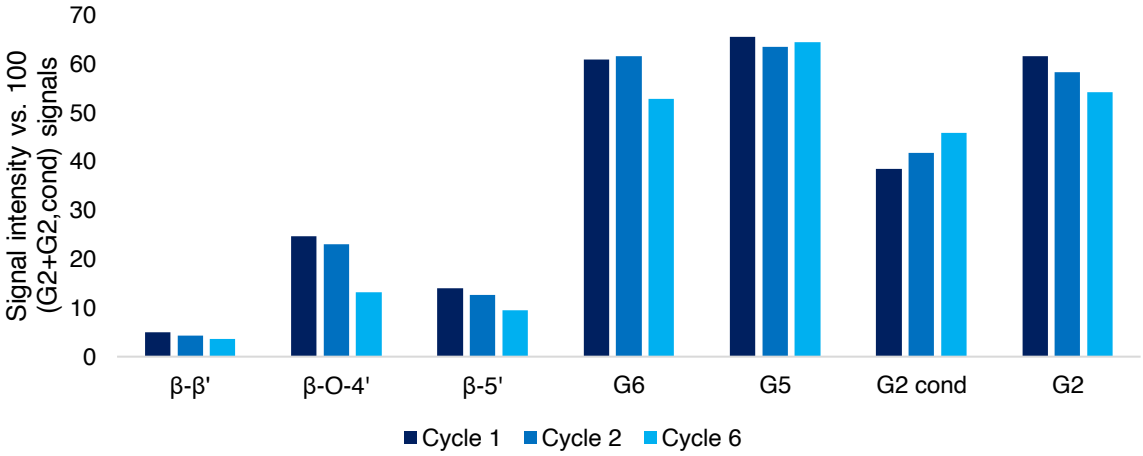


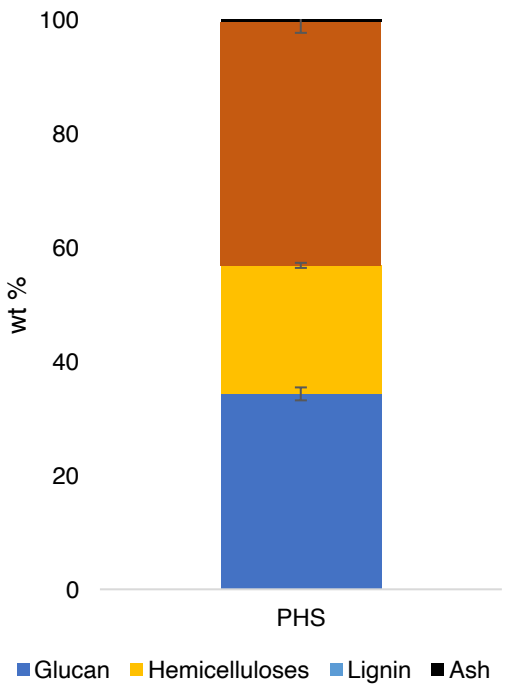
Figure 4.6: HSQC NMR results of lignin recovered after pretreatment of CCA treated wood at 170°C for 30 min with fresh, recycled and 5 times recycled [C_1Him][Cl] with a biomass to solvent ratio of 1:5 g/g and a final water content of 20 wt%

4.2.7 Product diversification: ionoSolv post-hydrolysis solids residue (PHS)

The saccharification yields from the ionoSolv pulps over the average of the 6 cycles was 62.5 %, with an overall metal extraction (3 metals 6 cycles) of 85.6 %. This suggests that a post-hydrolysis solids (PHS) residue remains after the hydrolysis of the cellulose rich pulp and this residue still retains some metals. In order to enhance the techno-economics of a potential biorefinery and valorise CCA wood waste streams, the PHS from CCA wood pulp was analysed and valorised through pyrolysis and the fate of the metals was investigated throughout the process. The results are shown in Figure 4.7.

The saccharification yield obtained from the pulp mixture after 5 days of enzymatic hydrolysis was 45.5 ± 0.4 % of theoretical maximum sugar release, an acceptable result given the average value of glucose yields from all six cycles was 54 % (7-day saccharification). The yield of recovered solids following enzymatic hydrolysis relative to the amount of pulp mixture present before hydrolysis, was 61.2 % on a dry basis. The compositional analysis of the residue shows that it consists of 56.7 % carbohydrates and 45.5 % lignin, with a remaining 0.36 % ash content. The trace element analysis of the residue is consistent with the extraction results from the ionoSolv pulp, with Cr remaining the main metal present in the pulp and PHS at 806 mg.kg^{-1} (with significant fluctuation between samples also observed for metal extraction), followed by 198 mg.kg^{-1} of As and only 25.6 mg.kg^{-1} of Cu. The trace element analysis of the hydrolysate solution did not detect any metal, showing that the metals present in the pulp did in fact stay in the pulp and did not dissolve into the enzymatic solution.

A.



B.

Properties of PHS	
Solids recovery	61.2 %
Saccharification yield	45.5 ± 0.4 %
Carbohydrate content	56.7 %
Volatile matter (wt% daf)	75.79 % ± 0.14
Fixed carbon (wt% daf)	24.95 % ± 1.30
Ash	0.40 % ± 0.20
Cr content	806 ± 173 mg.kg^{-1}
Cu content	25.6 ± 5.5 mg.kg^{-1}
As content	198 ± 13 mg.kg^{-1}

Figure 4.7: A. Compositional analysis of the post-hydrolysis solids (PHS) of the combined CCA pulps from cycles 1-6 after a 5-day enzymatic saccharification and B. properties of the derived PHS

4.2.8 Pyrolysis of PHS product: high temperature treatment for further product diversification

Solid residues from the production of cellulosic ethanol are lignin-rich solids, which represent 10-30 wt % of the feed.[346,347] Since their composition is variable and often contain residues enzymes and hydrolysis products, they are often used as fuel in a boiler for the cogeneration

of steam process and electricity or utilised in a thermochemical process such as pyrolysis or gasification.[288,348] In this study, fast pyrolysis was used to valorise the residue to enable to maximisation of liquid (bio-oils) products rather than char by using shorter residence time and moderate temperature (400-500°C).[349–353]

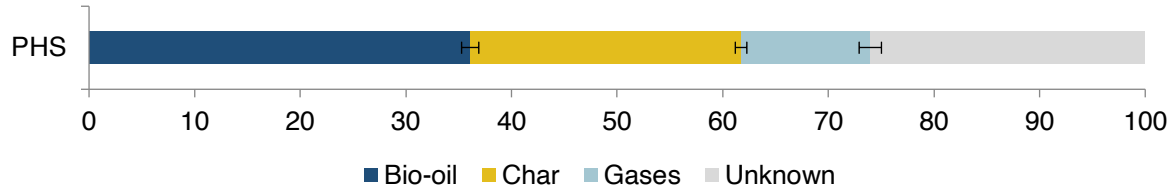


Figure 4.8: pyrolysis product distribution of PHS

It was found that the fast pyrolysis of PHS gave 36 % bio-oil, 26 % char and 12 % detected gases, as shown in Figure 4.8. The yield of bio-oil is fairly low for such a lignin-rich and carbohydrate sample, which composition resembles lignocellulosic biomass, compared to typical biofuel feedstocks. Herbaceous biomass samples were reported to have bio-oil yields with ranges of 40-60 % and woody feedstocks 60-95 % respectively.[354–356] However, it was reported that bio-oils yields from agricultural residues are typically lower than the ones for woody feedstocks due to the catalytic effect of inorganic ash content.[357,358] ^{1}H NMR was used as a means of obtaining approximate ratios of the chemical environments of protons present in the PHS bio-oil. Changes in the hydrogen type distribution in the bio-oil in terms of the structural assignments are shown in Figure 4.9. The majority of protons are in alkane or unsaturated aliphatic compounds, followed by a significant proportion of methoxy/carbohydrate protons. This is similar to the bio-oils from biomass such as switchgrass reported in the literature.[359–361] The presence of aromatics shows that some aromatic rings were not destroyed during pyrolysis at 500 °C. Only 5 % of protons are attributed to aldehydes, which is expected. Aldehydes can arise from multiple reaction pathways, including α-*O*-4', β-*O*-4' and β-1' cleavage.[362] As we have seen from the HSQC NMR (Figure 4.6), the number of such bonds are significantly reduced in the lignin over the recycling of the liquor, and we would expect the same from the residual lignin in the PHS.

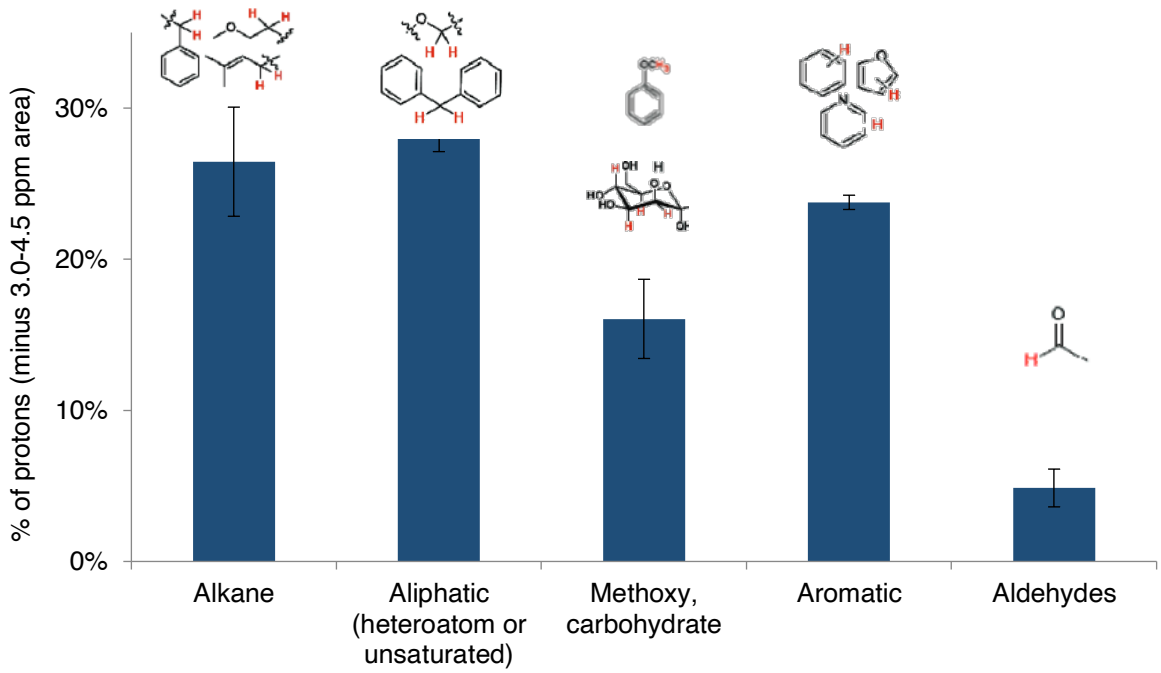


Figure 4.9: ^{1}H NMR of liquid products obtained by fast pyrolysis of PHS. Spectra were normalized to the total number of protons after subtracting signals from the region δH 3.0–4.5 ppm

The pyrolysis of the PHS resulted in 26 % char. Given the nature of the fuel derived from metal contaminated waste wood, it is interesting that the char is not the main product of the fast pyrolysis process by mass (char being essentially the metals and non-volatile elements in the ash). Only 12 % of gases (CO_2, CO and CH_4) were detected from the exhaust gas, while 26 % of pyrolysis products were not accounted for. Heavy metals can volatilise during pyrolysis in samples with high ash content such as sludge.[363,364] Studies have found that Cr can volatise in the form of chromium chloride when chloride is present in sludge samples.[365,366] Given the nature of the ionic liquid used for pretreatment, the PHS derived from the pretreatment could certainly contain residual chloride-based ionic liquid. As being volatile below 500°C, it was not detected in any of the products and was released into the fume cupboard. Other products unknown/unaccounted for are likely to include losses during drying and recovery steps, as well as light molecular weight compounds such as alcohols, water and hydrogen.

Proximate analysis of the PHS and the pyrolysis yields are consistent: total volatile yields of 75 % did not exceed the sum of the bio-oils and gas quantified (48.3 %); and fixed carbon content of 24. 9 % given the char yield of 25.6 %. This demonstrates that some compounds were not able to condense in the tar trap during fast pyrolysis. Some of the yields observed can also be reduced due to technical difficulties recovering products from the reactor and handling of such small quantities of samples (0.1 g initial feed).

Table 4.2 showed that the bio-oil (23.5 $MJ.kg^{-1}$) is more energy dense than PHS feed itself (19 $MJ.kg^{-1}$) and char even more so (26.5 $MJ.kg^{-1}$). The table shows that 80.1 and 79.9 % of energy and carbon recovery respectively are in the detected pyrolysis products (without gases); with 40-45 % of energy and carbon in the bio-oil only.

A trace element analysis on the bio-oil and chars was conducted but given the very small amounts of sample, the likelihood of contamination and detection limitation of the ICP-OES instrument used, the results were inconclusive.

Sample	Ultimate analysis (wt% daf)				Atomic ratio		**HHV**	Energy recovery	Carbon recovery
	C	**H**	**N**	**O**	H/C	O/C	($MJ.kg^{-1}$)	(wt%)	(wt%)
PHS	49.6	6.2	2.3	41.9	2.02	0.63	19.0	-	-
PHS oil	55.8	7.0	3.6	33.6	2.01	0.45	23.5	44.5	40.6
PHS char	73.1	3.7	2.0	21.2	0.81	0.22	26.5	35.6	39.2

Table 4.2: summary of the elemental analysis and calculated HHV values for the PHS and products the pyrolysis PHS in a downdraft fixed-bed pyrolysis reactor

4.3 Conclusion: ionic liquid based process leads to clean biofuel from pernicious wood

We have shown that CCA waste wood is capable of being integrated into the ionoSolv process, with yields similar to those of virgin pine wood, a conventional biofuel crop. Moreover, impregnated metals in the wood are not a process barrier, but can be extracted from the wood using PILS: the ionoSolv process is capable of efficiently decontaminating and extracting the cellulose contained in heavy metal-contaminated waste wood. With 99 % of the ionic liquid solvent being recovered and recycled 6 times with retention of its dual efficacy for deconstruction of biomass and metal extraction, we have shown the robustness of the ionoSolv process and its sustained yields with recycling of the liquor. The resulting sugar hydrolysate was readily fermentable to bioethanol at levels commensurate or even higher than with sugars derived from traditional biomass sources. These results would be highly relevant for assessing the techno-economics of such waste wood as a biofuel feedstock.
In the effort of valorising biorefined waste streams, the potential of ionoSolv PHS from waste wood was assessed for the first time via pyrolysis to yield yet another set of bioproducts.

Approximately 4.5 million tonnes of waste wood are produced in the UK annually (and collected, transported and stored, without any need for silage) and would be ready to be pretreated.[367] According to a study on the economic viability of the ionoSolv process at scale, with an ionoSolv biorefinery plant size of 770 000 tons of biomass per year, UK waste wood alone would be enough to feed this scale-up ionic-liquid technology.[97] Nevertheless, even if this supply is plentiful, such CCA waste wood is meant to be eradicated and therefore the ionoSolv plant would need to be feed with more long term oriented biomass supply.

Moreover, metals in consumer waste wood are impregnated chemically in the biomass. Would the metal extraction process wood, which had been metal contaminated from natural means, i.e., the environment? The fate of the metals and build-up in the liquor during the recycle is still a chemical engineering aspect of the process to consider, to separate them from the stream but also potentially recover such metal species. In the next chapter, we look an another, but yet different alternative feedstock for the ionoSolv process in long term supply, and investigate further the process intensification at bench scale.

5 Real life contaminated feedstocks into the ionoSolv process: the valorisation of metal contaminated biomass

5.1 Introduction

We have shown that contaminated waste wood and invasive species can be biorefined for the production of energy and bulk chemicals on a chemical engineering level. However, being waste feedstocks, they could be challenging in terms of long term availability and therefore, dedicated crops could still be required in the supply chain to reach the minimum of biomass input for a profitable biorefinery. Growing dedicated biofuel crops raises the question of not only land use, but also the choice and screening of a food crop on a given land. Land use is of huge concern when it comes to bioenergy, to the extent that it generated research from 1st to 2nd to 3rd generation of biofuels.

As presented in Chapter 1, the use of marginal and contaminated land (MaCL) can offer opportunities for crops and land use, but is particularly challenging because of the complexity and case-specificity of the process of growing biomass on MaCL. Metal contaminated soil from a 'real-life' contaminated area was used to screen a variety of crops in such an environment to gain insight on potential trace element uptake/contents and showcase how discarded metal contaminated sites can still be suitable for the growth of renewable biomass. Results from the previous chapters have shown that metal impregnated waste wood and invasive species can be biorefined for the production of energy and bulk chemicals. In this chapter, we investigated the combination of larger phytoremediation trials with the ionoSolv process to process 'real-life' metal contaminated biomass to act simultaneously as a biorefining (access to carbohydrates and a lignin stream) and decontamination (extraction and recovery of the metals from the biomass) process, without extractive metallurgy. Process intensifications are also studied with increased biomass loading, recycling of the liquor and diversification of product outcomes with the recovery of metals via electrodeposition.

5.2 Results and discussion

5.2.1 Valuable and alternative supply of biomass: metal-contaminated biomass from phytoremediation processes

5.2.1.1 Highly diverse feedstocks collected on real life contaminated soil

5.2.1.1.1 Description and means of contamination of Stoke Bardolph and Severn Trent sites

The site located in Stoke Bardolph, Nottinghamshire is owned by Severn Trent, a sewage treatment plant. Despite being composed of mostly water, wastewater can still contain less than 0.1 % total dissolved solids. As the sewage is treated, the process produces an insoluble solid residue, referred to as sewage sludge, which needs to be disposed of. Landfill and land applications have been found to be the most economical methods for sewage disposal, but are of growing major environmental concern.[368] The benefits of such methods are soil fertilisation and enhancement of soil properties, as sewage sludge contains significant amounts of organic carbon, nitrogen, phosphorous and other plant nutrients for agriculture. However, sludge can also contain non-essential hazardous and toxic trace elements such as Cd, Zn, Cu, Ni, Pb and Hg. Sewage sludge from the Nottingham treatment works had been disposed of onto the land for several decades. The amounts of sludge applied has declined to conform with new sewage sludge application regulations, as the amounts of trace elements in the soil in the southern area of the site have been found to increase significantly since their first soil survey in 1987.[369] The latest survey performed on the soil in 2003 revealed levels of heavy metals in top layers of the soil reaching 932 $mg.kg^{-1}$ of Cu, 1922 $mg.kg^{-1}$ of Zn, 387 $mg.kg^{-1}$ of Ni, 722 $mg.kg^{-1}$ of Pb and 38.7 $mg.kg^{-1}$ of Cd.

In such areas of the estate, the land is not considered suitable for agriculture as metals can be taken up by the crops and may end up accumulating in the human body via the food chain. Severn Trent put in practise polyculture crops for energy generation. Maize was grown that year for anaerobic digestion. This bioconversion process also produces a sludge, while providing for energy (biomethane). The sludge is then reapplied onto the metal contaminated soil, as a way to maintain biomass production on the site but avoiding any human contamination via agriculture food crops.

The second site accessed is located in Market Harborough, in Leicestershire. The site used to be a pigeon clay shooting site and this resulted in very high contamination from shotgun pellets, with Pb concentration in the topsoil ranging from 50 to 4000 $mg.kg^{-1}$. The site has been found contaminated since 2014 and the land had been used to grown wheat until the company started the remediation work and clean-up of the soil. The soil had been ploughed for the wheat crops, resulting in a homogeneous concentration of Pb within the top 0.4 meters of the topsoil.

5.2.1.1.2 Analysis of the soil: cation exchange capacity and pH

Both soil and biomass samples found on these contaminated sites were collected and analysed to assess the trace metal content and study the soil properties. The results are of the analysis of the soil are presented in Table 5.1. The soil from Stoke Bardolph has the highest carbon and nitrogen contents - even compared to commercial topsoil- from the continuous sewage sludge application, making this soil a fertile environmental for plant growth. Other soil parameters are key for phytoremediation purposes, such as pH and cation exchange capacity (CEC). These soil characteristics play a role in metal bioavailability and therefore metal uptake from the plant. Ideally, the soil should be rather acidic for phytoremediation purposes as heavy metal cations are most mobile in low pH environments.[177,370] The soil collected from Market Harborough is more acidic than the other samples, but also less fertile with the lowest carbon and nitrogen contents of all three.

The CEC of the soil sampled at Stoke Bardolph is 20.29 centimoles kg^{-1}, with the dominant exchangeable cation being K^+, followed by Ca^{2+}, Na^+ and Mg^{2+}. This value is higher than the ones from the topsoil and soil from Market Harborough at 17.22 and 14.41 centimoles.kg^{-1} respectively; with the dominant cation for the topsoil and the soil from Market Harborough being K^+, followed by Na^+, Ca^{2+} and Mg^{2+}.

Sample	pH (1:1 H20)	C (%)	H(%)	N(%)	CEC (centimoles kg^{-1})
Stoke Bardolph soil	6.58	14.3 ± 2.6	1.92 ± 0.3	1.24 ± 0.3	20.29 ± 0.6
Topsoil (John Innes #2)	7.08	6.6 ± 0.4	0.75 ± 0.02	0.29 ± 0.03	17.22 ± 0.7
Market Harborough soil	5.91	2.73 ± 0.2	0.83 ± 0.1	0.19 ± 0.02	14.41 ± 0.8

Table 5.1: chemical characteristics of soil used in this study

5.2.1.1.3 Screening of metal contaminants in agricultural biomass

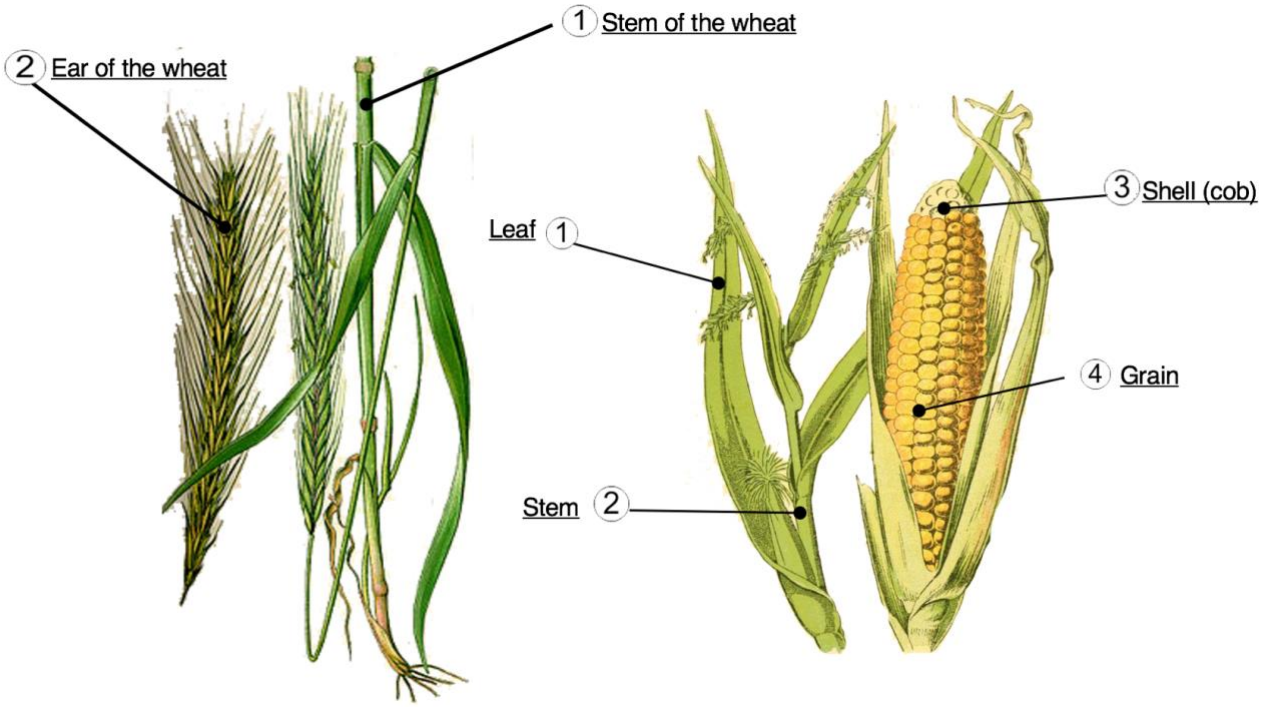
Biomass samples found growing on the contaminated sites of Stoke Bardolph and Market Harborough were analysed for their trace element contents. The analysis was carried out for the different parts of the plant, as seen on Figure 5.1, to study if some contaminants would preferably concentrate in certain locations of the biomass. The trace element analysis of the feedstocks is shown in Table 5.2, and were compared to the acceptable limits for metals for

commercial or residential use of the resultant biomass pellets if they were to be used as solid biofuels.

The wheat from Market Harborough shows levels of Pb contamination in both parts of the biomass studied, more than 3 times above the criteria for lead concentration of non woody pellets for biofuels. The level of As is also above the ISO 175255 criteria and Cu in the ear of the wheat. This demonstrates that the soil is contaminated with Pb and As and that the contaminants can be taken up by a food crop such as wheat.

The maize collected from Stoke Bardolph is above the ISO 175255 for Zn in both the leaf and the stem of the plan, as well as Cu for the leaf. These metals would be found in the sludge after the process. The trace element assessment from food crops such as maize and wheat reveals the environmental dispersion of soil contamination through the food chain, which represent a risk for human and animal health.[371,372]

Figure 5.1: illustration of the different parts of the biomass found on the metal contaminated sites: wheat in Market Harborough (left) and maize in Stoke Bardolph (right)



Location	Market Harborough		Stoke Bardolph				**Graded non woody pellets for Solid Biofuels Criteria**
Sample	Ear of wheat	Wheat Stem	Maize Shell	Maize Leaf	Maize Cob	Maize Stem	ISO 17255-6
Analyte (mg/kg)							
Cr	1.65 (0.1)	4.12 (0.5)	0.73 (0.2)	6.28 (1.5)	0.46 (0.03)	3.67 (0.1)	50
Ni	1.09 (0.03)	2.06 (0.2)	0.61 (0.2)	1.72 (0.5)	0.97 (0.01)	1.57 (0.01)	10
Cu	**13.6** (0.4)	6.73 (0.5)	3.98 (0.7)	**16.7** (1.2)	2.50 (0.01)	7.56 (0.7)	10
Zn	45.7 (3.5)	26.0 (2.1)	25.5 (3.1)	**107.2** (9.5)	18.4 (5.3)	**139.2** (6.5)	100
As	**1.05** (0.1)	**1.97** (0.2)	BDL	0.53 (0.1)	BDL	0.42 (0.1)	1
Cd	BDL	0.04 (0.1)	0.09 (0.01)	0.25 (0.1)	BDL	0.42 (0.1)	0.5
Pb	**18.61** (2.4)	**31.98** (2.7)	BDL	1.48 (0.37)	0.15 (0.07)	2.10 (0.05)	10

Table 5.2: trace element analysis of the biomass found on the sites in Stoke Bardolph and Market Harborough. Standard deviations are displayed between parentheses, bold indicates the values are above the speciation for non woody solid fuels pellets (ISO 17255-6).[232] BDL = Below Detection Limit

5.2.1.2 Cinderhill tarpit marginal contaminated land

5.2.1.2.1 Description and means of contamination of the site

In 2007, the Borough of the Amber Valley identified the site of Cinderhill in Derbyshire as a contaminated land under the Environmental Protection Act of 1990.[260] In the 1970's, the site was used to tip tar waste, ash, saturated oil and foundry sand. The acid tar pit deposition activities ceased in the late 1970's and the pits were covered with a range of waste materials. The industrial activity in the area left very large water logged and partially vegetated lagoons and numerous acid tar pits; with significant risks of groundwater contamination.[261] A project of

restauration of the area has been initiated via the Environmental Agency, Atkins Limited and the Clean Rivers Trust; around phytoremediation using a horizontal planting of willow to stabilise the area.

Several native species occurring in and around the tar pits were collected, along with a sample of the tar pits, for trace element analysis. A sample of the raw tar pit was digested and analysed for its metal contaminants; the results are shown in Table 5.3. The major metal contaminant is Pb, with a concentration of 4612 mg kg^{-1}, from the oil refining process. The focus of this study was trace elements but the tar pits must also contain hazardous hydrocarbons from the oil recycling industry in great quantities.

Analyte	Cr	Fe	Ni	Cu	Zn	As	Cd	Pb
Concentration ($mg\ kg^{-1}$)	19.8 ± 2.3	1873 ± 89	3.73 ± 0.5	372.8 ± 31.8	34.1 ± 2.5	3.14 ± 0.05	0.18 ± 0.001	4612 ± 228

Table 5.3: trace element analysis of a tar sample taken from the Cinderhill contaminated site

5.2.1.2.2 Screening for metal contaminants in native biomass

A variety of softwood and hardwoods species have been growing in the vicinity of the tar pits on the Cinderhill contaminated land. Woody biomass has been studied for the ability to either stabilise contaminants or extract them from the soil. The trace element analysis of representative tree species is shown in Table 5.4. The opportunities for woodland on metal contaminated sites have been reviewed and showed that species from the *Betulaceae* and *Salicaceae* families have potential to accumulate metal contaminants in the below-ground biomass (roots).[196,240,373–377] The results show that only species from the *Betulaceae* family, Hazel and Silver Birch, have Pb above the criteria only for commercial or residential use of derived woody pellets from the trees. The Cd content of above-ground biomass of goat willow, from the *Salicaceae* family, is also above the same criterion for this contaminant. This shows the ability of a variety of tree species to grow on contaminated land, mainly excluding metal contaminants from translocation from the roots to the shoots. Other tree species, from the *Fagaceae*, *Oleaceae*, *Platanaceae* and *Rosaceae* families, exhibited an ability to tolerate contaminants in the soil and the environment without translocating them to the stems.

Family	Specimen	Cr	Ni	Cu	Zn	As	Cd	Pb
Betulaceae	Hazel (*Corylus avellana*)	0.294 (0.04)	0.301 (0.02)	2.97 (0.90)	5.06 (1.01)	BDL	BDL	**12.07** (0.10)
	Silver Birch (*Betula pendula*)	0.206 (0.05)	0.129 (0.03)	2.74 (0.41)	43.6 (1.46)	BDL	0.153 (0.003)	**13.01** (0.35)
Fagaceae	Oak (*Quercus sp.)*	0.491 (0.03)	0.38 (0.02)	2.37 (0.26)	20.62 (2.24)	0.028 (0.004)	0.05 (0.002)	2.19 (0.06)
Oleaceae	Ash (*Fraxinus americana*)	0.202 (0.02)	0.343 (0.01)	4.68 (0.68)	3.37 (0.43)	0.056 (0.003)	BDL	0.33 (0.03)
Platanaceae	Sycamore (*Platanus occidentalis*)	0.933 (0.06)	0.541 (0.02)	3.01 (0.18)	21.41 (1.06)	0.023 (0.005)	0.072 (0.003)	6.8 (0.09)
Rosaceae	Blackthorn (*Prunus spinosa*)	0.129 (0.07)	0.319 (0.03)	1.86 (0.33)	31.87 (6.71)	BDL	0.098 (0.01)	2.06 (0.19)
	Hawthorn (*Crataegus sp.*)	0.50 (0.03)	0.61 (0.19)	3.59 (0.29)	41.78 (5.23)	BDL	0.1 (0.01)	0.34 (0.1)
	Damson (*Prunus domestica*)	0.34 (0.03)	0.32 (0.05)	2.53 (0.27)	50.87 (2.06)	BDL	0.11 (0.01)	0.54 (0.05)
	Crab Apple (*Malus sylvestris*)	0.42 (0.04)	0.72 (0.03)	2.60 (0.16)	17.12 (3.38)	BDL	BDL	0.58 (0.01)
Salicaceae	Field Maple (*Acer campestre*)	0.467 (0.04)	0.542 (0.09)	4.78 (2.39)	23.96 (1.14)	0.024 (0.004)	0.12 (0.01)	5.06 (0.40)
	Goat Willow (*Salix caprea*)	0.487 (0.11)	0.851 (0.11)	2.15 (0.13)	102.31 (7.85)	0.017 (0.006)	**1.018** (0.07)	0.8 (0.09)
	Poplar (*Populus tremula*)	0.13 (0.01)	0.34 (0.02)	4.58 (0.33)	17.16 (4.75)	BDL	0.07 (0.01)	0.64 (0.01)
	Aspen (*Populus alba*)	0.154 (0.01)	0.285 (0.03)	4.37 (1.30)	55.97 (2.88)	BDL	0.143 (0.01)	7.14 (0.20)
Graded woody pellets for commercial and residential / industrial use (ISO 17255)		10 / 15	10	10 / 20	100 / 200	1 / 2	0.5 /1.0	10 / 20

Table 5.4: trace element analysis of a variety of trees species found in the vegetative areas of the Cinderhill tarpit in mg/kg. Standard deviations are displayed between parentheses, bold indicates the values are above the speciation for non woody solid fuels pellets (ISO 17255-2).[232] *BDL = Below Detection Limit*

5.2.2 Dedicated bioenergy crop biomass from controlled-environment trials

Artificially metal contaminated soils are often used for pot trials in order to assess the viability of plant species growing in media with contaminants. However, working with 'real' life soil from contaminated land benefit from the results for a specific case study. Since the phytoremediation potential of a feedstock depends on the soil parameters, the clay content, its microbiome, the mobility of the metal ions in the soil (redox potential, pH, metal concentration, cation exchange capacity, etc). This is why pot trials with soil collected from recognised contaminated land were carried out. The potentials of various feedstocks are investigated:

- willow as an emerging crop for phytoremediation for its high biomass yield and resilience for contaminants,[378,379]
- sunflowers as a biofuel feedstock with rapid growth and tolerance for Pb,[380–383]
- tobacco for its ability to extract a variety of contaminants at significant levels.[384,385]

The results of the trace element analysis of the plants are shown in Table 5.5. Even within the same soil (the one collected from Stoke Bardolph in this study), the different species were found with various amounts of trace elements in their upper organs. Firstly, 3 species of Willow hybrids were analysed for their phytoremediation potential. From all the willow species studied, BG1 contains the highest amount of metals: Cr, Cu, Pb. Cd reached 6.18 $mg.kg^{-1}$ in the BG1 grown in the Stoke Bardolph soil, compared to 8.22 $mg.kg^{-1}$ in the controls (compost soil). This shows the ability of this species to extract and translocate metal species from the soil to its upper organs. However, the controls and samples grown in metal contaminated soil show similar levels of these trace elements.

The hybrids Gaston and Rocket grown in the Stoke Bardolph soil have extracted more than the controls for Ni, Cu, Zn, Cd and Pb. It seems that this species is a candidate for phytoremediation of Cd in particular, with levels reaching 11.2 $mg.kg^{-1}$. The wood ash of willow has been reported to reach 70 $mg.kg^{-1}$, and its reported tolerance for metals made it a great candidate for the remediation of a wide range of metals.[386]

The metal content of giant sunflowers grown in metal contaminated soil exhibited higher metal concentrations than the controls for Cr, Ni, Zn and Cd. Zn and Ni being essential nutrients, it is possible that these elements were simply taken up in higher quantities for the metabolism and photosynthesis of the plant only and not a result of a higher contamination from the soil. Sunflowers had been used in previous studies for the remediation of Cd-polluted soils, which is consistent with the content of 0.93 $mg.kg^{-1}$ in Stoke sunflower samples compared to 0.04 mg of Cd per kg of plant in controls.[386]

Tobacco leaves and stems were separated for analysis, as the leaves had not yet fallen off at the time of harvest. Several studies reported the ability of tobacco to translocate metal contaminants such as nickel from the shoots to the leaves.[387,388] Considering the totality of the trace metals, tobacco is the species that exhibits the highest contamination of metals, particularly for Ni and Cd. The leaves in the Stoke samples have a 7.2-fold increase in Ni concentration compared to controls and 43-fold for Cd; a 10.9-fold increase in the stems for Ni compared to controls and 12.7-fold increase for Cd. In the context of a biorefinery, flowers would not be necessarily separated from the stems during harvest and most likely lost during transport / processing.

This study showed that the soil from Stoke Bardolph has both suffered from historical repeated trace metal application from sewage sludge application but also gained in fertility from the application of the organic components. A variety of feedstocks, whether they are typical biofuel crops such as willow, or accumulators like tobacco, are able to thrive on such soil. The small differences in some metal uptakes between controls and samples grown in the soil from Stoke Bardolph can be explained by an insufficient growth time and cropping of the biomass material (rotations for willow), where the plants did not have sufficient time to bioactivate metals or transfer them from roots to shoots; the roots were too constricted in the pot trials and the bioactivation of the rhizosphere was limited; this was caused by a depletion of soil microorganisms to facilitate root uptake and translocation.
However, no growth factors, chelating agents, pesticides nor fertilisers were used in this study. Even if the metal uptake of any species grown on metal contaminated soil should be monitored, the strategy of phytostabilisation of metal contaminants from growing feedstocks into this soil brings eco-system services to marginal areas where the biomass can act a carbon sink.
Even though levels of metal contamination in the above-ground tissues have found to be low under such short periods (months), they would need to be monitored. Such practices still constitute a way to increase the carbon sink by growing renewable biomass on marginal land. Phytoexclusion also participates in the enhancement of soil properties and fight against soil erosion: the eco-system services and advantages of phytoexclusion on marginal land should be studied further to reveal the actual carbon savings and benefits of such processes

Sample	**Analyte** (mg/kg)	Cr	Fe	Ni	Cu	Zn	Cd	Pb
Willow species (*Salix spp.*)	BG1 Control	0.68	48.7	1.65	10.94	138.21	8.22	0.33
	BG1 Stoke	0.48	50.46	1.92	10.76	130.73	6.18	0.31
	Gaston Control	0.88	77.55	0.77	6.99	84.84	1.35	0.15
	Gaston Stoke	0.6	51.31	2.11	13.8	178.19	11.2	0.16
	Rocket Control	0.59	53.55	1.54	5.48	67.97	0.97	0.13
	Rocket Stoke	0.59	33.54	2.07	6.53	100.48	3.89	0.2
Sunflowers (*Helianthus giganteus*)	Sunflower Control	0.31	55.75	2.42	1.52	13.16	0.04	0.18
	Sunflower Stoke	0.53	13.81	10.17	2.34	59.29	0.93	0.24
Tobacco (*Nicotiana tabacum*)	Tobacco Leaves Control	4.79	295.47	4.21	18.10	77.00	1.03	2.29
	Tobacco Leaves Stoke	5.78	227.20	30.14	13.42	134.63	44.26	5.56
	Tobacco Stems Control	1.12	52.69	1.91	9.23	29.97	0.61	1.62
	Tobacco Stems Stoke	0.70	36.07	20.89	8.21	57.60	7.78	0.37

Table 5.5: trace element analysis of the different feedstocks used in pot trials. 'Stoke' indicated biomass samples grown in metal contaminated soil collected from the Stoke Bardolph site in mg/kg. n=number of samples analysed =3, standard deviations omitted for clarity.

.

5.2.2.1 Polish samples, low Pb contamination

The trace element analysis of Polish Miscanthus is shown in Table 5.6. It reveals levels of contamination in the biomass: a content 5.75 mg of Pb per kg of biomass, along with the presence of other contaminants such as Cu, As, Cd and Cr.

	Metal content in mg.kg^{-1}
Pb	5.75 (0.12)
Zn	167.8 (6.4)
Cu	2.23 (0.15)
As	0.12 (0.01)
Cd	0.40 (0.01)
Cr	0.47 (0.01)

Table 5.6: trace element analysis of Miscanthus giganteus grown on lead contaminated land in Poland (Phyto2Energy field trial). The standard deviation is shown between parentheses.

5.2.2.2 Welsh Bwlch samples: high metal content, mainly Pb

Miscanthus sinensis (OPM-10) had performed well in multilocation trials across Europe and was selected for trialling on this exposed mine site because of its demonstrated resilience to cooler environmental conditions at a field trial in Wales.[389–391] Both Reeds and miscanthus yielded very poorly in terms of biomass yield (12.1 g ± 0.29 per plant for miscanthus, 9.1 g ± 0.15 for RCG). The site is highly exposed, with organic matter and pH well below levels required for good productivity, ranging from 0.52 to 0.94 % and 4.32 to 5.67 %, respectively.[392] Portable X-ray fluorimeter readings indicated major metal contaminant concentrations in the unamended spoil, ranging from 5599 to 121261 mg.kg^{-1} for Pb and 1008 to 1744 mg.kg^{-1} for Zn. The EC Directive 86/278/EEC sets the limit for agricultural soil after treatment with sewage sludge to 300 mg.kg^{-1} for Pb, and 200-250 mg.kg^{-1} for Zn (at this pH). 3 different rows of Miscanthus and 6 different rows of Reed Canary Grass (RCG) were analysed for their trace element content, as shown in Figure 5.2.

The main contaminant in quantity found in all the biomass samples is also Pb, reaching 20200 mg.kg^{-1} in RCG H and 6500 mg.kg^{-1} in Miscanthus E. Previously reported excessive Pb contents in top parts of grasses grown on contaminated sites in the literature ranged 63 to 232 mg.kg^{-1} in the UK.[393,394] Anomalous levels Pb have also been observed in Canadian lettuce, which contained as much as 0.15 % Pb; as well as grass shoots with up to 0.27 % Pb.[393,395,396] The presence of Pb at such high levels could be due to surface adherence from windborne or splashed (following rainfall) contamination. It has previously been found that even rigorous

biomass washing would not be able to fully remove such Pb-containing particles entrapped onto the biomass.[397,398,399] However, where the aspiration is to remove and extract metals, such surface adhesion could be advantageous. Other contaminants in smaller quantities include Cr, As and Cd, which are not essential nutrients to the plant but are tolerated by the plant in extreme conditions.

With anomalous contaminant contents usually comes very poor biomass yields, which are observed here. Phytoremediation and stress resistance are a strenuous activity for plants, especially under very high level of metal contamination. Even with species that exhibit large crop yields (e.g., biofuel crops), the biomass yields after harvest can be greatly affected by the presence and uptake of contaminants from the environment.

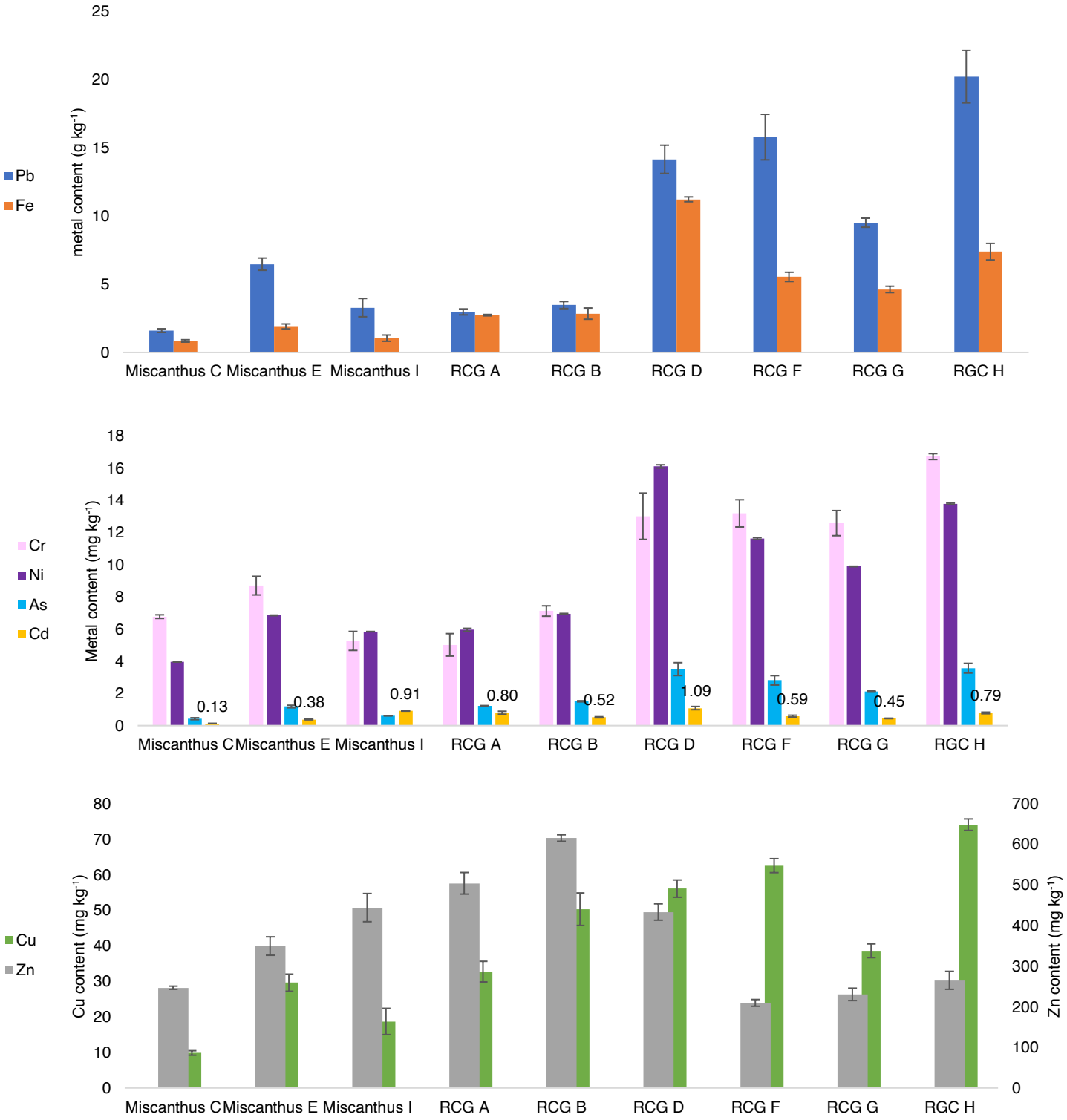


Figure 5.2: trace element analysis of biomass grown on a former mining site in Wales

5.2.3 Biomass loading: an important parameter for process intensification

For any prospective technological process, it is often crucial to work on the process intensification parameters. Researchers often overlook the transition between bench scale experiments, focusing on the purity and characterisation of the product, to up-scale and larger scale experiments. One important factor of the process intensification is the biomass loading, i.e., the amount of biomass used in relation to the amount of solvent (ionic liquid mixture). This plays a role in the techno-economics of the process. This is particularly relevant for feedstocks or processes which suffer from poor economics. Phytoremediation is often discarded as a soil remediation option because of the time needed to remediate the soil and the downstream processes of managing contaminated biomass. Therefore, ashing and burning techniques are mostly used because they are easy to put in place and relatively cheap. Increasing biomass loading has numerous advantages such as reducing the amount of solvent and therefore the cost of IL needed, lower water consumption, reactor size (as the solids loading directly correlates with the size of the reactor).[168] However, high solids loading can also lead to operational and technical challenges such as mixing and higher viscosity. In the context of metal extraction from the ionic liquid pretreatment, increasing the biomass loading could have an impact on the amount of metals in solutions coordinating to the ionic liquid and the purity of the product (metals remaining). In this study, the purity of the cellulose pulp (glucan recovery, enzymatic glucose release and metal extraction) was investigated at 20, 35 and 50 wt% biomass loading (1:5 to 1:2 $g.g^{-1}$ biomass: solvent ratio) using $[C_1Him][Cl]$ (20 wt% water) at 150°C for 1 hour – as shown in Figure 5.3A. The highest glucose release was achieved at 20 wt% loading at 70.8 % and decreased to 58.7 % and 56.1 % for 35 and 50 wt% loading respectively. The decrease in saccharification yield can be attributed to the minor decrease in delignification of the pulp, suffering a 10 % (absolute) decrease from the lowest to the highest biomass loading. The hemicellulose removal remains stable between 20 and 35 wt% loading, while it suffers a slight decrease in hemicellulose extraction at 50 wt% loading. This could be due to the reduced mobility of the ions at higher biomass loadings, making more difficult to extract hemicelluloses in greater quantities, as well as lignin availability. Moreover, we can see a sharp increase in glucan degradation with 79 % glucan recovered to only 60.7 % for 20 and 35 % biomass loading respectively. The pretreatment performance slightly decreases as the solids loading increases. This is expected when the process intensifies and could be due to poor mixing or wetting of the biomass from the ionic liquid as the biomass loading increases; especially when the biomass has a low density, and it is therefore harder to homogenise the solution when vortexing the pretreatment tube.

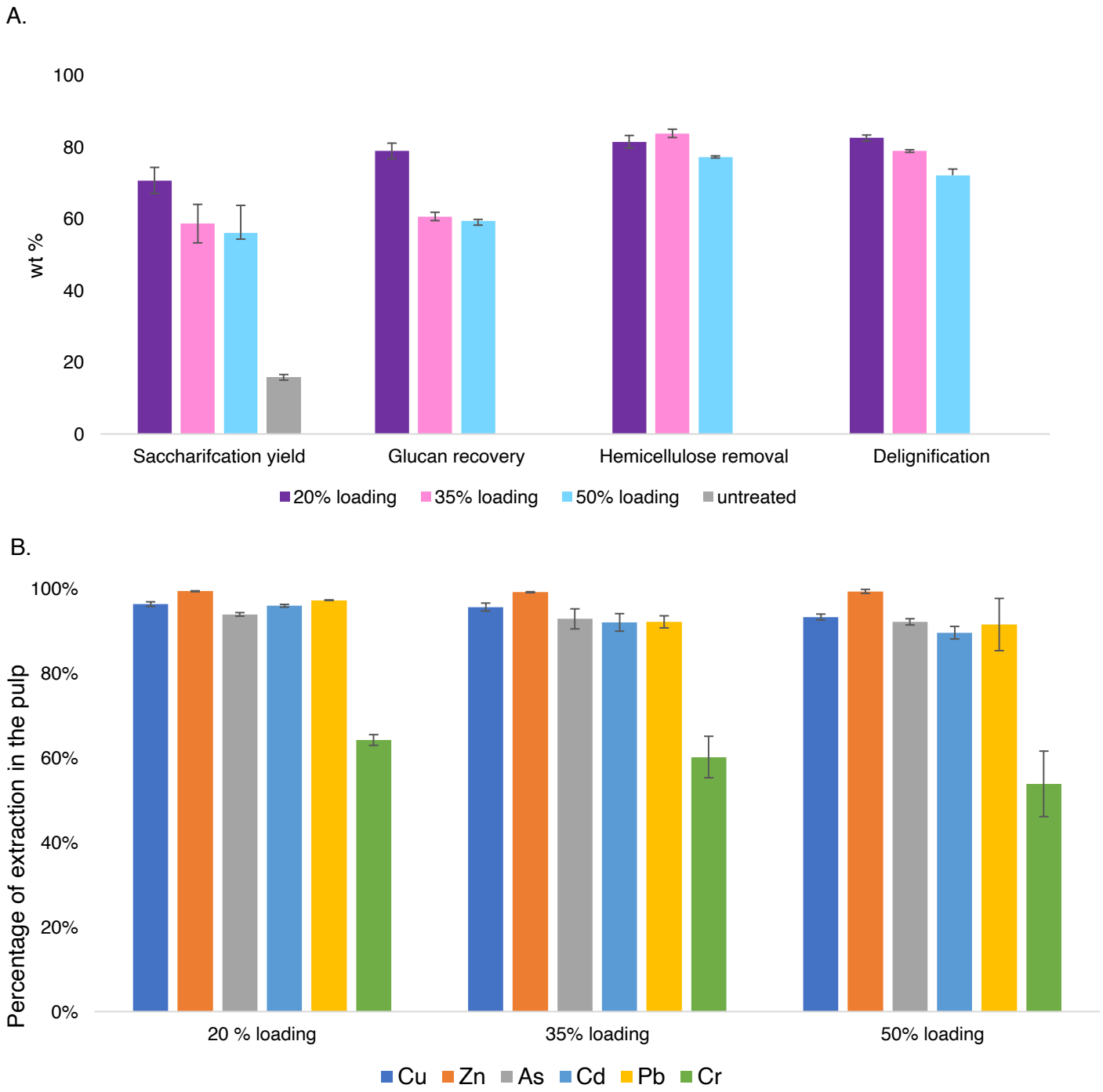


Figure 5.3: A. key indicators of the outcome of the ionSolv process using contaminated Polish Miscanthus at 150°C for 1 hour with [C_1Him][Cl] and increasing biomass loadings and B. metal extractions from the pretreatment of contaminated Polish Miscanthus at 150°C for 1 hour and different biomass loadings

The performance of [C_1Him][Cl] for the extraction of lead and other contaminants was also studied at higher biomass loadings and the results are presented in Figure 5.3B. As expected, the metal extraction performance from the ionic liquid was slightly impacted by the increase in solids loadings (and therefore in metals dissolved). Pb extraction only decreased from 97.2 to

91.5 % with solids loading of 20 to 50 wt% respectively. The extraction of the other contaminants, Cu, Zn, As, Cd and Cr suffered a similar and slight decrease. Rather than metal solubility limitations in the ionic liquid and given the absolute low levels of metal contamination of this phytoremediation feedstock (compared to waste wood previously studied, this change in metal extraction from the increase of the biomass: solvent ratio should be due to lack of wetting of the biomass from the IL. An Alternative explanation could be that waste wood is chemically impregnated with metals (so perhaps more available for chemical extraction), while the metals that were plant-extracted from contaminated soil are likely to be much more integrated into the biomass through biological mechanisms (confined in the vacuole of cells for example).

5.2.4 Interaction of metal contaminants in the biomass and ionic liquids

As we have seen previously, the biomass loading aspect of process intensifications mostly have an impact on the fractionation aspect of the pretreatment (glucan recovery, glucose release from pulp). We have studied in Chapter 4 the metal extraction from CCA wood and the impact of recycling on metal extraction. Cu extraction was very consistent and remained above 90 % along the 6 subsequent recycle of the ionic liquid liquor. Cr and As extractions displayed greater variation. However, some of the possible underlying reasons for this were contamination from stainless steel equipment and shared lab equipment and the troubleshooting of the ICP-OES instrument.

In this chapter, the metal extraction from the ionic liquid pretreatment was assessed using the two most contaminated Welsh feedstock: Miscanthus E and Reed Canary Grass (RCG) H.

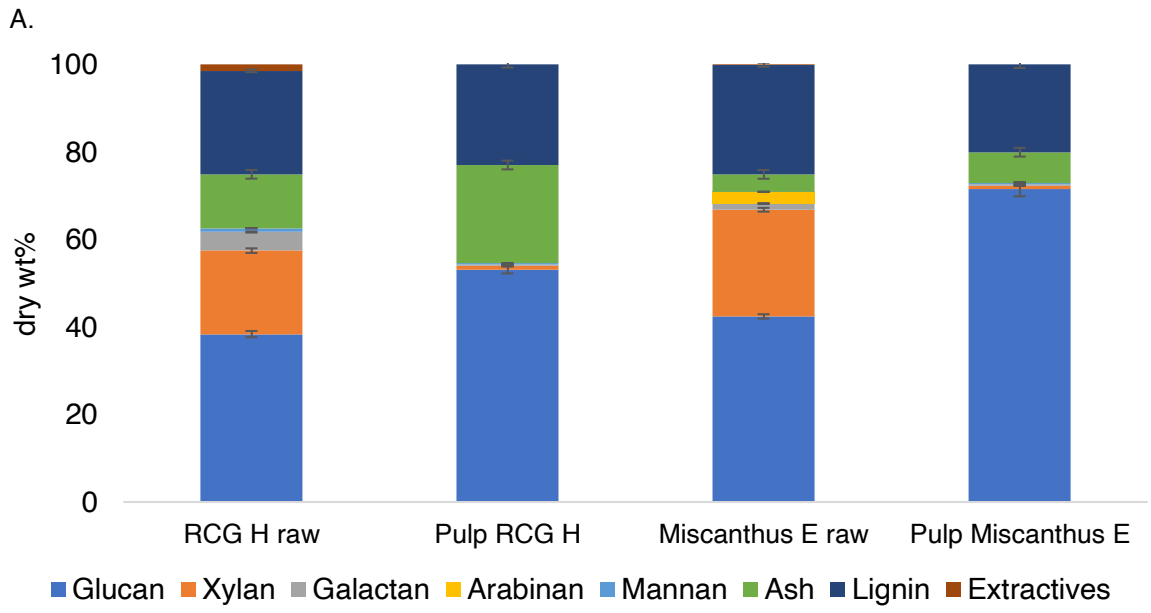
5.2.4.1 Presence of metals and its effect on pretreatment performance between recycling cycles

The biomass was pretreated using a low-cost ionic liquid that has previously been successful in removing a range of metals including Pb, Cu, Cr and As from metal contaminated waste wood. Here we have used the same ionic liquid, 1-methylimidazolium chloride [C_1Him][Cl], for its metal extraction properties. The pretreatment conditions of the biomass were set at 150°C for 1 hour, given the compositional analysis the grassy feedstock shown in Figure 5.4A and previous studies carried out.[103,104] Figure 5.4B shows the key performance indicators of the ionoSolv pretreatment and in this case, the pretreatment exhibits better performance for miscanthus than RCG. A cellulose-rich pulp from miscanthus was produced, with 84 % glucan recovery, while removing 97.5 % of the hemicelluloses and 60 % of lignin. This deconstruction of the biomass from the ionic liquid pretreatment enabled 81.5 % of the theoretical maximum

of glucose to be released through enzymatic saccharification of the pulp, a 3.8-fold increase compared to saccharification of the untreated samples.

However, the pretreatment of RCG using the same conditions produced a pulp with only 53 % glucan with an ash content of 22.5 % ash. The delignification was 52 % and hemicellulose removal remained high at 96.7 %. The pulp was enzymatically hydrolysed to glucose with a saccharification yield of 56.4 %, a 2.6-fold increase compared to the untreated sample. The presence of high ash content has been known to be problematic for pretreatment processes. The ash does not only contain metals such the one studied here, but also silica and alumina, which can also interact with the acidic ionic liquid pretreatment itself.[99,400,401] It should be noted that the chemical analysis of the ash content here reveals only such acid insoluble inorganic matter (e.g. silica), whereas acid soluble ash components are likely to have dissolved in the ionic liquid (i.e. metal contaminants) during the pretreatment (or in the sulfuric acid during the compositional analysis laboratory procedure). A solution would be to perform a prewashing step of the biomass prior to pretreatment, but this would involve creating another potentially contaminated aqueous stream.

After recovery of the pulp, the dissolved lignin in the ionic liquid can be recovered from the ionic liquid liquor by anti-solvent precipitation. Lignin is often valorised for its energy value as a fuel - but lignin analysis was not in the scope for this study.



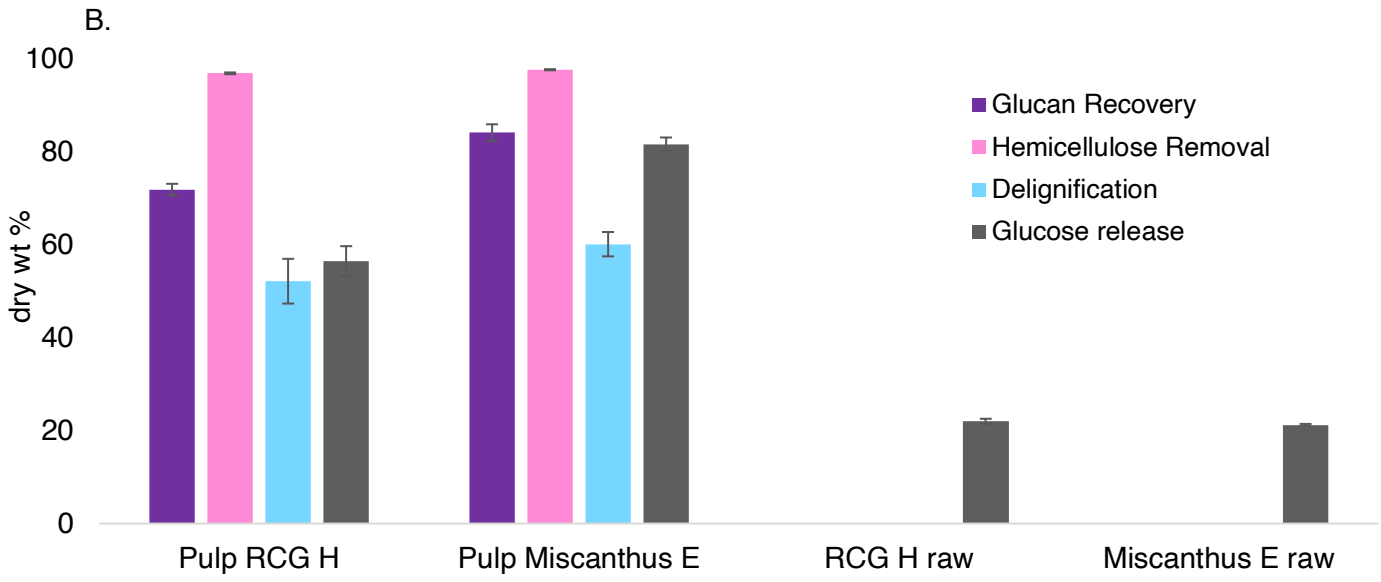


Figure 5.4: A. compositional analysis of the studied untreated biomasses and the pretreated pulps B. outcome of the pretreatment using an aqueous mixture of 80 % [C_1Him][Cl] 20 % water with a 1:5 g/g biomass/solvent loading at 150°C for 1 hour

Recycling of the solvent is an important aspect to take into account for a more sustainable process and integrating such a chemical processes into a circular economy.[86] The results of the pretreament after recycling are shown in Figure 5.5. We observe a noticeable decrease in delignification rate of the biomass from 60 % to 49.2 % from cycle 1 to cycle 2 respectively, whereas the saccharification yield (glucose release) increased from 81.5 % to 90.3 %. In contrast to virgin IL, the IL liquor after pretreatment contains sugar degradation (i.e. HMF, levulinic acid, acetic acid, formic acid) products from the extraction of the hemicelluloses, and to some extent, solubilised lignin fragments, which have not precipitated. Small fragments of lignin are still solubilised in the liquor from the previous cycle, which can recondense back on the pulp in the subsequent pretreatment. Some of these fragments, also called 'pseudo-lignin', can even recombine with sugar degradation products (exhibiting lignin carbohydrates linkages) in solution and inhibit further enzymatic saccharification.[100,402] The changes in lignin structure during the IL pretreatment occur in different stages and take time to reach equilibrium and steady state.[100] Small water-soluble lignin fragments can redeposit onto the pulp during cycle 2, but these fragments had not had enough time to react with sugar degradation products. Longer-chains of extracted, more condensed lignin from cycle 1 and 2 precipitate in the liquor during cycle 2, rather than forming inhibitory pseudo-lignin entities. Overall, the

pretreatment with recycled IL provided sufficient fractionation to give access to the cellulose for the enzymes.

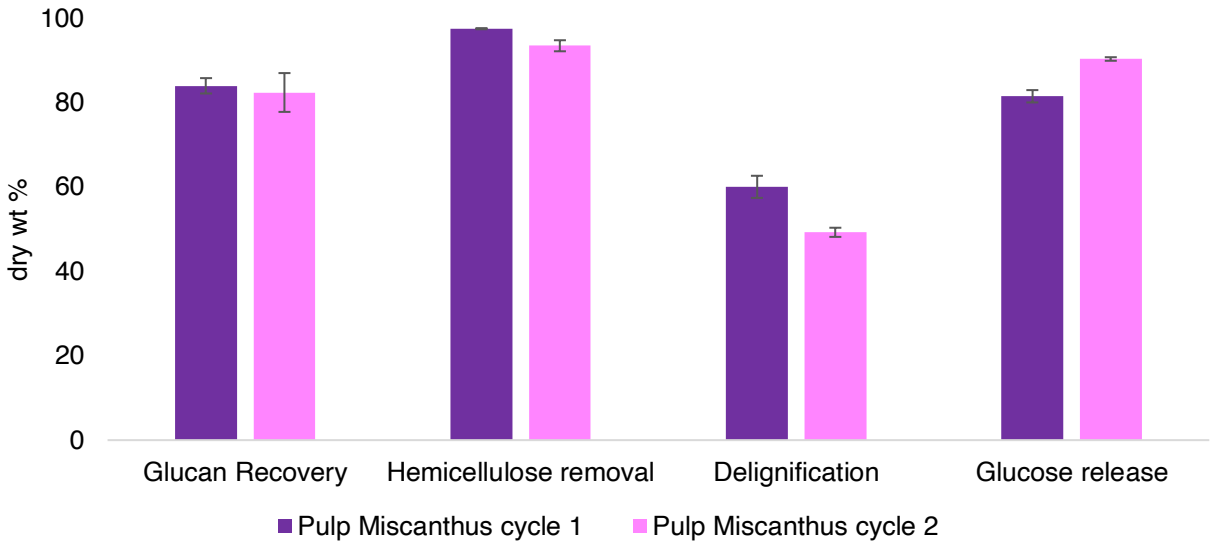


Figure 5.5: comparison of biomass pretreatment using [C_1Him][Cl] for 1 hour at 150°C on metal contaminated miscanthus with virgin ionic liquid (cycle 1) and recycled ionic liquid (cycle 2)

5.2.4.2 Fate of metal contaminants in the IL process

[C_1Him][Cl] not only has the ability to deconstruct lignocellulosic biomass but it is also able to coordinate with metal species present in the biomass. The metal contents in the ionoSolv cellulose rich pulp and precipitated lignin from the liquor were analysed for the two most contaminated feedstocks and the results are displayed in Figure 5.6.

Miscanthus E was the less contaminated of the two feedstocks, and the pretreatment showed the highest metal extractions compared to its RCG analogue. [C_1Him][Cl] pretreatment was able to extract 99.3 % of the major contaminant Pb from both miscanthus product streams, namely the pulp and lignin. The percentages of metal extraction found in the pulp and lignin for Cu, Zn and Cd are also very high, ranging between 97 and 99 %. However, there are some differences in metal extraction for the other metals as 61.5 % of Fe remained in the pulp, while only 29.1 % of As, 28.8 % of Ni and 50.2 % of Cr remained in the cellulose pulp after pretreatment. Based on lignin analysis, the metal extractions are above 99 % for Zn/Cd, around 94-96 % for Fe/As/Ni and 79.8 % for Cr. The Cu content of the lignin is higher than in the pulp, with Cu extraction at 96.3 % in the pulp vs 89.6 % in the lignin.

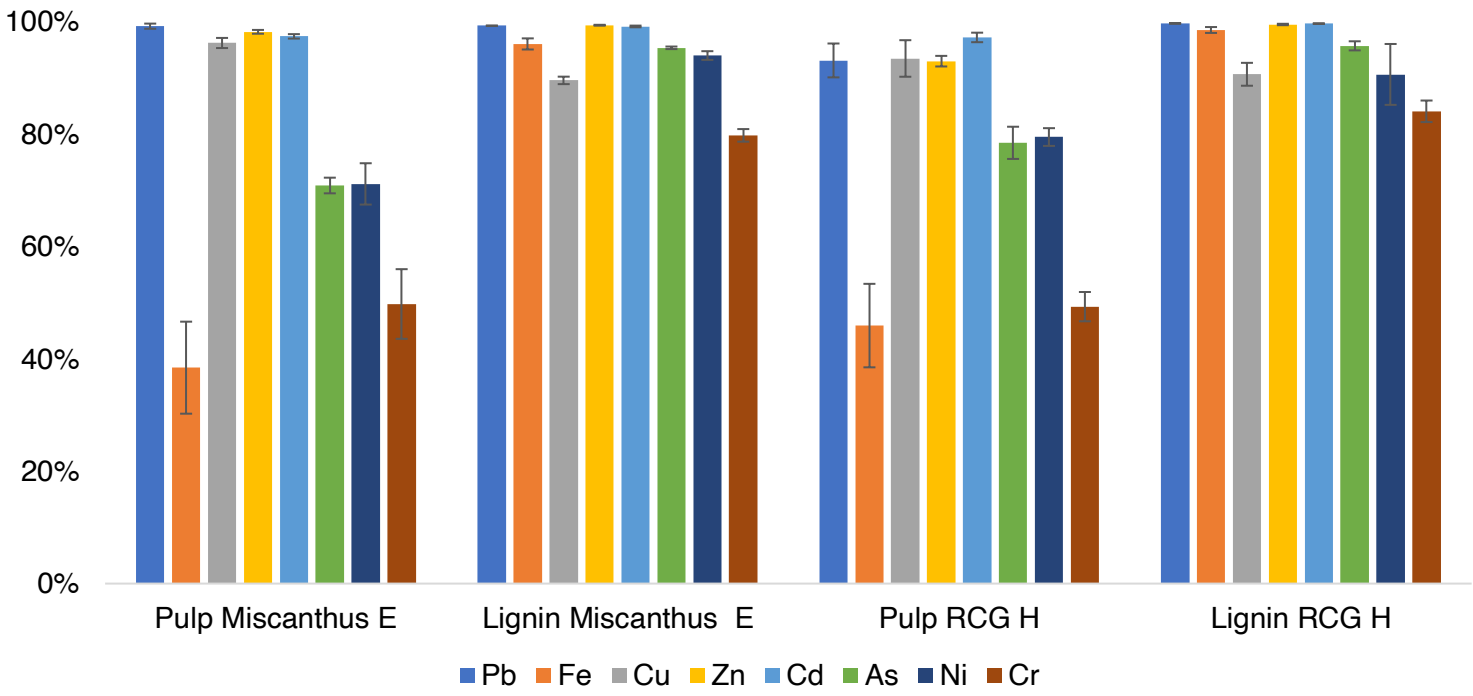
Despite lignin being a potential absorbent for metals, the metal preferably remained in the [H_1Cim][Cl] liquor, and in the pulp to a lesser extent.[345,403] The metal extraction from the ionic liquid occurs during the pretreatment at high temperature, where some metal (Fe, As, Ni, Cr) remain or redeposited onto the pulp. After pulp separation, water is added to the ionic liquid

liquor to precipitate out and recover the lignin from the solvent. During this last stage, the metals stayed in the liquor and the lignin was found to only have a small residual metal content (Cu, Cr).

The overall metal extraction in the RCG pulp is slightly lower that from Miscanthus, One of the reason explaining that difference is the initial higher metal contamination of the feedstock leading to a quicker saturation of the IL. Pb extraction in the pulp was 93.2 %. The metal extraction in the lignin and the pulp follows a similar trend between the two feedstocks, with high Zn and Cd extractions, the lowest extraction observed for Fe. This shows that the metals are located in/on the biomass similarly between the two feedstocks; and that the level of contamination and the affinity of the metals for the Cl anions are likely to be the limiting factors in ionic liquid metal extraction for such highly contaminated biomass.
The high ash content of the RCG pulp observed by compositional analysis (Figure 5.4A) is due to acid insoluble matter (silica and/or alumina), as the ionic liquid removed more than 90 % of Pb, Zn, Cd, 70 % of As and Ni, 50 % of Cr and 39 % of Fe. The remaining ash content of the pulp is not contaminated with components harmful to the environment. Similar ash contents are managed via post hydrolysis solids for agricultural waste for example, and valorised for cement production or wastewater treatment applications.[404]

It is necessary to consider the recovery of metals from the contaminated ionic liquids. Figure 5.5B shows that the ionic liquid liquors exhibit more than 2000 $mg.kg^{-1}$ of Pb, with other metals such as Fe, Zn, Cu, Ni, Cr, As and Cd in smaller quantities. We now discuss the recyclability of the solvent, the potential for metal extraction after re-using the solvent for another round of pretreatment. It should be noted that the following experiments were only performed on the Miscanthus E, as there was not enough biomass material from RCG H to work with.

A.



B.

Sample concentration ($mg.kg^{-1}$)	Pb	Fe	Zn	Cu	Ni	Cr	As	Cd
Ionic Liquid Liquor after pretreatment of Miscanthus E	1477.9 ± 97	172.5 ± 50	80.9 ± 5.1	6.70 ± 0.55	3.11 ± 0.60	0.73 ± 0.01	0.15 ± 0.009	0.09 ± 0.004
Ionic Liquid Liquor after pretreatment from RCG H	2776.05 ± 107	297.59 ± 52	41.82 ± 0.25	14.69 ± 1.7	2.12 ± 0.7	0.94 ± 0.12	0.50 ± 0.07	0.18 ± 0.01

Figure 5.6: A. metal extraction from the pretreatment of Miscanthus E and RCG H using [C_1Him][Cl] at 150°C for 1 hour 20 wt% biomass loading in both cellulose pulp and recovered lignin B. final metal concentrations of the ionic liquid liquor after the pretreatment

5.2.5 Electrochemistry: a way to maintain process performance and recover metals

5.2.5.1 Electrochemical behaviour of Pb^{II}, Cu^{II}, Fe^{II}, Zn^{II} from [C_1Him][Cl] virgin solutions

For the IL to be used in a cyclic manner, the accumulation of metal ions in the IL stream needs to be managed. First, the electrochemical behaviour of Cu^{II}, Pb^{II}, Fe^{II} and Zn^{II} in [C_1Him][Cl], 40 wt% water, was studied with cyclic voltammetry to assess the feasibility of using electrochemical strategies for the removal of metals from the IL stream and to define the electrode potentials for metal deposition.

ILs are very attractive solvents for electrodeposition because of their high electrochemical stability and innate conductivity, that is, no addition of a supporting electrolyte is required.

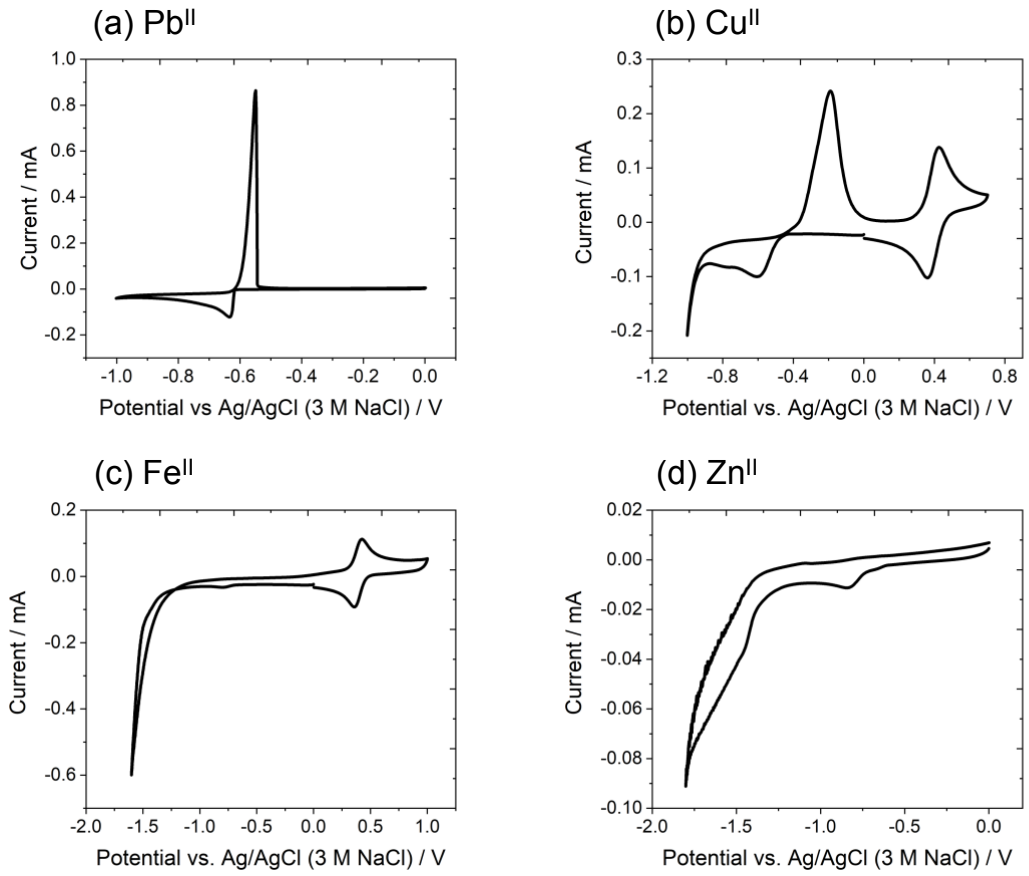


Figure 5.7: cyclic voltammograms showing the potential cycling of a 3 mm-dia. glassy carbon electrode in 1000 mg kg^{-1} (a) Pb^{II}, (b) Cu^{II}, (c) Fe^{II} and (d) Zn^{II} in [C$_1$Him][Cl] (40 wt% water). Scan rate was 50 mV s-1.

Figure 5.7 (a) shows the voltametric behaviour of Pb^{2+} in [C$_1$Him][Cl], 40 wt% water. A negative-going potential scan produced a reduction current wave and stripping peak. This was consistent with the two-electron reduction of Pb^{2+} to deposit Pb^0. The subsequent positive-going potential scan produced a sharp oxidative peak, consistent with the dissolution of deposited Pb^0 from the electrode surface. The formal potential for the $Pb^{II/0}$ redox couple is -0.62 V as previously reported.[405]

Figure 5.7(b) shows the voltametric behaviour of Cu^+ in [C$_1$Him][Cl] (40 wt% water). The initial negative potential scan starts from 0 V to -1.0 V, producing a reduction current and peak at -0.60 V. This is consistent with the reduction of Cu^+ and deposition of Cu^0. At -1.0 V, large reduction currents are observed due to hydrogen evolution reaction catalysed by electrodeposited Cu^0 on the electrode surface. The subsequent positive-going potential scan

produced a sharp oxidative peak at -0.18 V, consistent with the dissolution of deposited Cu^0 from the electrode surface. The potential $E_{I=0}$, at which the current, $I = 0$, on the positive-going potential scan can be used as an estimate of the formal potential for the Cu^0/Cu^+ redox couple and was found to be -0.37 V. At more positive potentials, an oxidative peak is observed at 0.43 V followed by a reductive peak at 0.36 V on the negative going scan. This is consistent with the oxidation and reduction of the $Cu^{+/2+}$ couple. The peak-to-peak separation of 70 mV is close to expected for a reversible redox couple and the formal potential for this redox couple can be estimated from the half-wave potential, $E_{1/2,app}$ = 0.40 V. Stabilisation of the Cu^+ ion species is well known in chloride media as previously reported.[406]

Figure 5.7(c) and (d) show the voltametric behaviour of Fe^{II} and Zn^{II}, respectively, in the ionic liquid aqueous media. Neither of CVs show an oxidising stripping peak for the analytes, which are characteristic of the deposition of the metal onto the electrode. However, we can observe a large and sharp reduction current around -1.5 V. This is the result of mixed solution processes, such as the hydrogen evolution reaction at the cathode from the electrochemical splitting of water. From the CV of Fe^{2+}, the smaller intensity peaks at 0.42 V and 0.36 V correspond to the reversible oxidation and reduction respectively of the Fe^{2+}/Fe^{3+} chloride complexes in the ionic liquid. The cathodic wave observed at -0.75 V from the CV of Zn^{II} (Figure 5.7 (d)) is the bulk reduction of Zn^{II}.

5.2.5.2 Proof of concept: electrodeposition of metals from IL

Electrolysis experiments were carried out for 1 hour at varying potentials for each analyte. The accumulative charge was recorded (Figure 5.8) to calculate the charge efficiency by comparison to the recovery of metal on the working electrode, which was obtained by measuring the analyte content of the main electrolysis solution using ICP-MS. Even though no oxidising stripping peak was observed for Zn and Fe, the ICP-MS measurements confirm that the metals can be deposited using these potentials. From Figure 5.9, it is observed that that 91.5 % of Pb can be deposited after 1-hour electrolysis from this particular media and this electrochemical set-up with a charge efficiency of 0.69; while only 40 % of Cu, 28 % of Fe and 44 % of Zn are removed with 76.1 %, 5 % and 9.6 % efficiencies respectively. Efficiencies for Fe and Zn are low because of the high accumulated charge passed during the electrolysis.

Pb being the main metal contaminant present from the biomass studied here, this shows that the concentration of Pb while recycling the ionic liquid for subsequent pretreatment can be managed in the IL via electrodeposition.

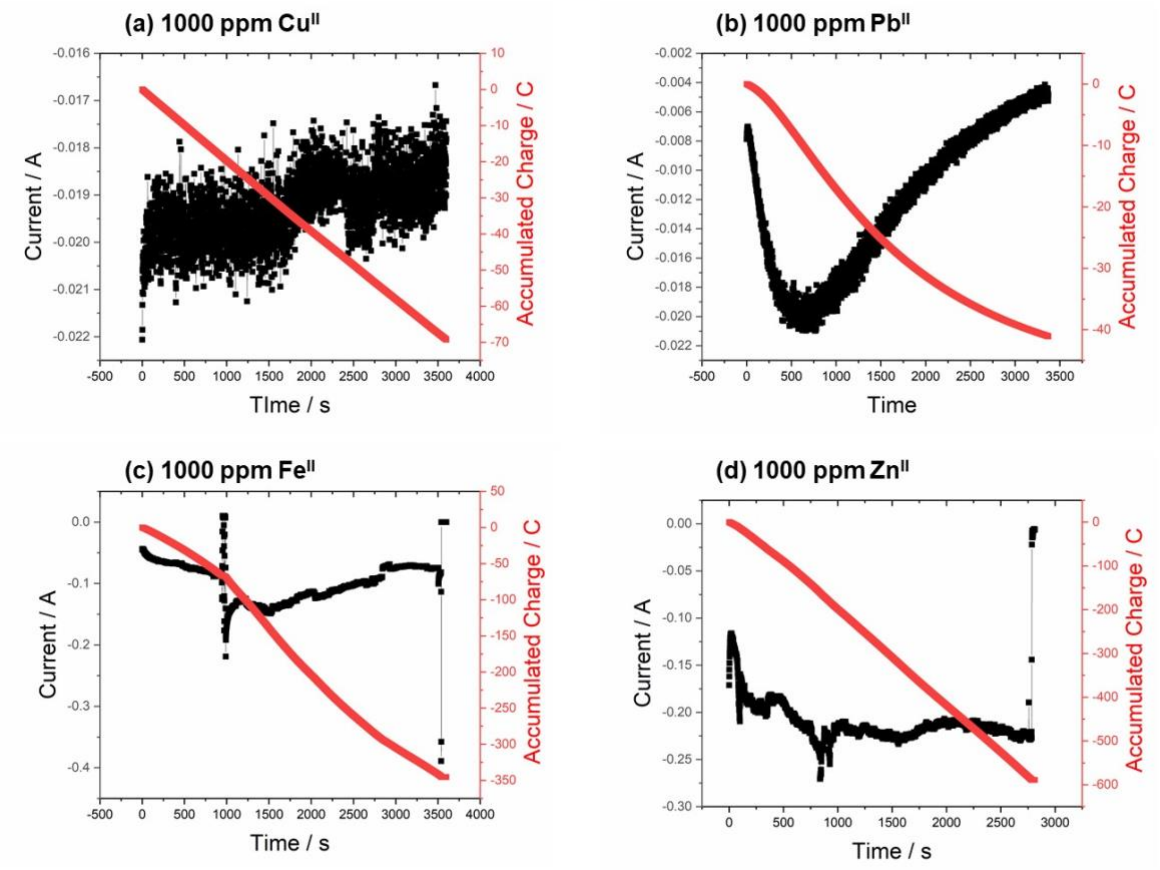


Figure 5.8: accumulative charge over 1 hr for the electrodeposition of 1000 ppm in [C1Him][Cl], 40 wt% H2O of (a) CuII, potential applied was -0.9 V vs. Ag/AgCl, (b) PbII, potential applied was -0.9 V vs. Ag/AgCl (c) FeII, potential applied was -1.2 V vs. Ag/AgCl, (d) ZnII potential applied was -1.4 V vs. Ag/AgCl

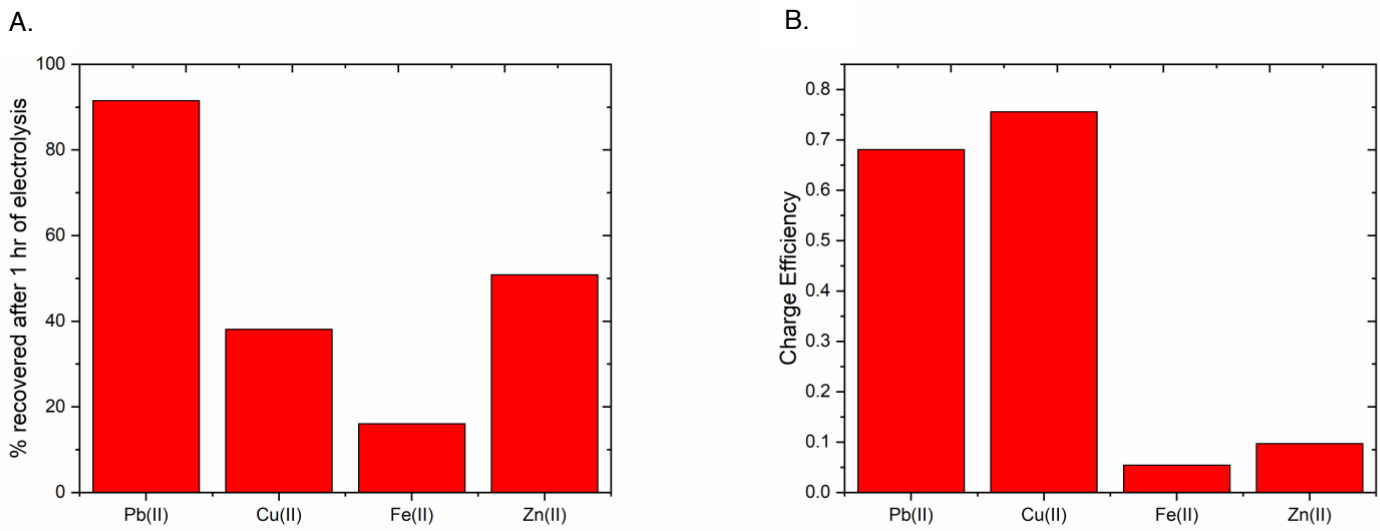


Figure 5.9: A. percentage of recovery by mass and B. charge efficiency of PbII(II), CuII(II), FeII(II) and ZnII(II) recovery from 1000 ppm solutions of [C1Him][Cl], 40 wt% H2O after 1 hr electrolysis with a copper foil electrode. Electrode area = 4.2 cm2. The deposition potential was -0.9 V for Pb and Cu recovery experiments and -1.2 and -1.4 V for Fe and Zn recovery experiments, respectively.

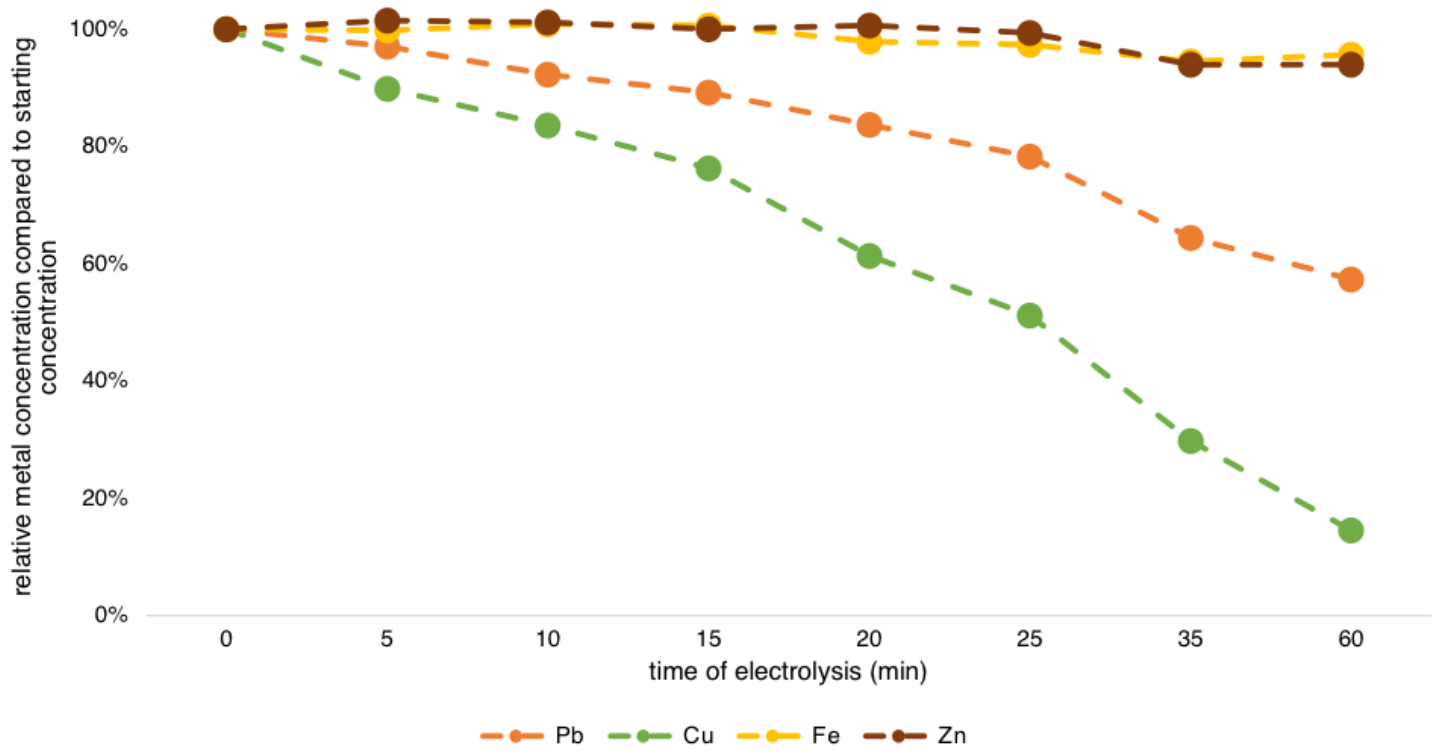
5.2.5.3 Feasibility of electrodeposition of metals from ionic liquid liquors after pretreatment

Based on the results from metal doped-IL solutions, the ionic liquid liquor obtained after the pretreatment of miscanthus was recycled and subject to 1-hour electrolysis at -0.9V to manage metal concentration and recover the metals extracted from cycle 1. As we can see from figure 3.9A, the potential used does not only remove Pb and Cu from the solution as expected, but also Zn and Fe to a lesser extent, as these metals have standard potentials less cathodic than -0.9V.

Figure 5.10B shows the metal extraction efficiency of the IL pretreatment with recycled IL, with and without the electrodeposition of Pb before the second cycle. The overall metal extraction efficiency is increased from 51.5 % to 63.11 % with the extra electrodeposition step, with all metal extractions significantly enhanced from the electrodeposition of Pb. The electrodeposition of Fe from the IL liquor results in observable Fe extraction in the second cycle compared to recycled IL without electrodeposition (where no Fe extraction from the biomass is observed). As and Cr extractions are not affected by the electrodeposition, as the standard potentials of these metals are more cathodic compared to the electrolysis potential used, with similar extractions for both processed samples. Pb extraction increased by a 1.3-fold from the electrodeposition of Pb prior to cycle 2; Cu and Cd extraction also increased when comparing the two recycled ionic liquids used. The metal extraction from the pretreatment with recycled IL does decrease compared to the first cycle for all metals, due to

metal solubility of the metals in the ionic liquid mixture. However, depositing some of the metals prior to recycling via electrodeposition enhances the metal extraction properties of the IL liquor for a subsequent cycle. The competition for ligands to form metal-IL complexes would be a limiting factor at such high concentrations of metals.[407,408] Further recycling studies involving electrodeposition should be investigated. This study has shown the ability of the ionoSolv process to be able to integrate highly contaminated lignocellulosic biomass from MaCL into a sustainable biorefinery to produce clean energy and chemicals; [H_1Cim][Cl]was recycled efficiently without impact on the performance of the pretreatment and is a suitable medium for the recovery of metals from the biomass via electrodeposition.

A.



B.

Metal extraction	Pb	Fe	Cu	Zn	Cd	As	Ni	Cr	Overall
Cycle 1	99.26% (0.46)	38.45 % (8.19)	96.26 % (0.90)	97.45 % (0.34)	97.45% (0.39)	70.89% (1.40)	71.17% (3.68)	49.79% (6.20)	77.69%

Cycle 2 with electrodeposition	83.37% (5.20)	14.09% (0.61)	87.27% (1.85)	95.75% (1.76)	95.19% (1.50)	54.95% (5.55)	53.20% (3.31)	22.42% (1.40)	63.11
Cycle 2 without electrodeposition	67.47% (7.69)	none	73.89% (2.09)	92.20% (1.69)	71.61% (0.39)	51.87% (1.85)	35.3% (0.86)	19.85% (2.67)	51.47

Figure 5.10: A. dissolved metal concentrations determined in IL liquor E during the 1 hour electrolysis of the IL liquor E [C_1Him][Cl] (40 wt% H_20) from the first cycle of pretreatment. Copper foil electrode area = 4.2 cm2, potential applied -0.9V vs Ag/AgCl and B. metal extraction based on pretreated pulps from the ionic liquid pretreatment of metal contaminated miscanthus at 150°C for 1 hr using virgin [C_1Him][Cl] (cycle 1), recycled [H1Cim]Cl and recycled and electrodeposited [C_1Him][Cl] (cycle 2) (standard deviation between parentheses)

5.3 Conclusion: ionic liquids can both deconstruct and decontaminate biomass grown on marginal, contaminated land

Trace element analysis was carried out to study the wide range of metal contents in a variety of plants growing on marginal contaminated land: willow, sunflowers, tobacco, maize, but also hardwoods and softwoods from the *Betulaceae* and *Salicaceae* families. Growing feedstocks constitutes the first step of suppling renewable energy, even without phytoextraction of metals from the soil, and constitutes a valorisation of MaCL.

Combining highly contaminated perennial feedstocks grown on marginal land with a comprehensive low-cost ionic liquid pretreatment process could lead to environmental remediation, clean biofuel production and metal recovery, without the need to incinerate the biomass. After screening of multiple plant species from different phytoremediation contexts, lead contaminated Polish Miscanthus was used as a model crop. It was successfully fractionated and Pb was extracted from the biomass, at biomass loadings up to 50 wt % without a significant impact on the process performances. Such moderately heavy metal containing biomass grown on pernicious metal contaminated areas is an ideal candidate for the ionoSolv pretreatment. It both responds well to the fractionation, and to the metal extraction process at high biomass loadings, enhancing the systems' economics.

Highly contaminated miscanthus from Wales was then fractionated into a clean cellulose pulp, and further saccharified into glucose, extracting 99 % of the main contaminant, Pb, from the feedstock. Lignin was precipitated and successfully recovered from the ionic liquid liquor. After

one cycle of pretreatment, the ionic liquid liquor, which contained more than 1000 mg kg^{-1} of Pb, was used as a medium for the electrodeposition of Pb. After clean up and electrolysis for 1 hour, the ionic liquid liquor was reused on fresh biomass and demonstrated the ability to fractionate the biomass and extract metals for a subsequent cycle. However, the recycle of ionic liquids should be studied over a larger number of cycles to investigate the impact of the electrodeposition and presence of degradation products on the overall ionoSolv process. Extensive contamination, trace metal content and biomass yields of the feedstock should be closely monitored in terms of valorisation and scale-up processing. The risks of transport, handling and processing of such biomass also need to be closely monitored for marginal areas, which are site specific. This study demonstrates a new and innovative way to integrate the properties of ionic liquids into a process for phytoremediation feedstocks. Further life cycle and techno-economics assessments are needed to prove the benefits of this approach in terms of ecosystem services from marginal land and bioenergy production.

6 Analysis and processing of willow from a wastewater remediation irrigation trial for the inoSolv process

6.1 Introduction

Throughout the chapters, we have shown that we can integrate innovative and unconventional feedstocks to the ionoSolv process, with pretreatment performance, production of variable products and management of metals thanks to the unique properties of studied ionic liquids. However, the limitation of these unconventional feedstocks resides in their long term availability: whether they are invasive species, which need eradication, or waste wood, a prohibited waste. Biomass from MaCL can be limited in terms of biomass yields and are very much specific to the nature of the contaminated sites. A possible option to improve biomass yield is to amend the plantation with nutrients, usually in form of synthetic fertilizer. In this last chapter, in the continuity of a sustainable approach, we rather exploited the properties of municipal wastewater, rich in nutrient, to boost the biomass production of a dedicated willow plantation. Willow is wildly acknowledged as a leading biofuel crop and was a good candidate to study the implication of the stress on the composition of the biomass, its recalcitrance to fractionation by the ionoSolv process and potential metal uptake. To further enrich the analysis of this case study and further develop the theme of this thesis to diversify the valuable outcomes for a biorefinery, the profile and production of bioactive phytochemicals was also studied in the context of the phytofiltration of municipal wastewater.

Willow plantations can be a sustainable approach for generating valuable biomass, but also treating primary municipal wastewater, potentially reducing both the environmental and economic burdens associated with conventional treatment. However, there are still unknown implications for the value of biomass as a biofuel crop using phytofiltration plantations, where municipal wastewater is used to irrigate non-food crops, such as fast-growing trees.[257,258,409]

A mature willow phytofiltration field trial was conducted in Quebec, Canada, where trees were either left as controls or irrigated with 29,500,000 L ha^{-1} yr^{-1} primary effluent municipal wastewater. For this PhD research, the impact of the wastewater irrigation on biomass composition, bioenergy potential and persistent phytochemical production from this field trial were investigated to assess the potential of willow irrigated with wastewater to be integrated to the ionoSolv biorefinery.

6.2 Results and discussion

6.2.1 Increased biomass yields and no significant trace element uptake

The impact of wastewater irrigation on aboveground biomass yield was measured at the end of a 3-year coppice cycle of the willow plantation. Stems had a noticeable difference of colour once freshly debarked, with pink spotted stains on wastewater irrigated stems as observed in Figure 6.1. Biomass yields (based on dry matter) significantly increased from 6.7 (±0.4) t ha^{-1} yr^{-1} for control trees to 20.3 (±4.3) t ha^{-1} yr^{-1} for wastewater irrigated trees. Wastewater irrigation substantially increased aerial growth and subsequent biomass yields by 200 % at harvest. The major factors likely to have influenced the development ofthese wastewater irrigated trees were the very high water load of 29.5 million L ha^{-1} yr^{-1}, high macronutrient loads of 1245 N and 121 P kg^{-1} ha^{-1} yr^{-1} and high salt loads of 4.31 t Na ha^{-1} yr^{-1} and 5.63 t Cl ha^{-1} yr^{-1}. Willow is considered to have high nitrogen-use efficiency and nitrogen recycling which allows for high yields from minimal fertilisation.[410,411] However, high water load alone (without macronutrients) is insufficient to induce such higher biomass yields.[258] This emphasises the key role of high macronutrient loads in wastewater. While very high salt loads can be detrimental for tree growth, the large quantities here did not inhibit growth.[412] Moreover, as controls had similar yields to the standard ~ 9 t ha^{-1} yr^{-1} of contemporary willow plantations, wastewater irrigation is likely to be the major contributing factor to the exceptional 200 % biomass yield increase.[413]

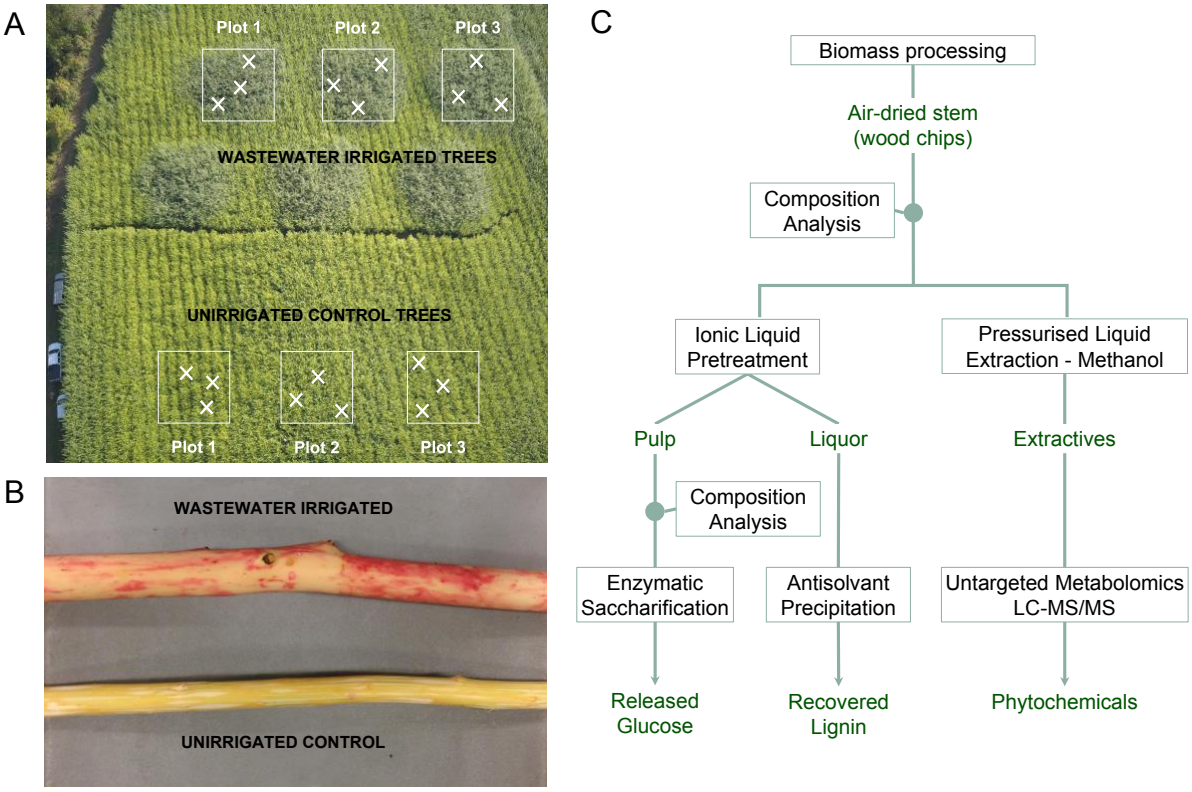


Figure 6.1: A. aerial photograph of the Saint-Roch-de-l'Achigan field trial and experimental design B. representative photograph of a control and a wastewater irrigated debarked willow stem C. diagram of the analytical workflow of biorefinery characteristics used here to compare control and wastewater irrigated trees.

Similarly, trace metal analysis was carried out as heavy metals have the potential to accumulate in biomass and influence downstream bioenergy process. Special care was given to the quantification of metals in biomass, for controls and wastewater irrigated trees. Their presence in the wastewater did not inhibit the growth of willow. Table 6.1 shows the trace element analysis of both the water and the harvested biomass. Metal concentrations in biomass did not significantly vary between control and wastewater irrigated trees for chromium, nickel, arsenic, cadmium, lead, zinc and copper. Iron was significantly higher in wastewater irrigated trees, increasing from 13.14 to 25.72 $mg.kg^{-1}$, the element in the highest concentration in the wastewater compared to the other analytes. The results show that willow exhibits tolerance for metals but did not accumulate toxic contaminants from the wastewater over the period of growth studied. Given the concentration of metals from the wastewater, it could be that the plant simply excluded these compounds to survive from their nutrients uptake (phytoexclusion). Although biomass metal concentrations were low in wastewater irrigated trees and similar to controls, the increased biomass yields represent 3-fold increases in total amounts of extracted metals. Metal uptake should be closely and regularly monitored at scale

over longer period of times to ensure that the plant is still adopting a phytoexclusion strategy in such environments.

Sample	***Municipal Wastewater***	***Control trees***	***Wastewater irrigated trees***
Trace metal / units	$\mu g.L^{-1}$	$mg.kg^{-1}$	
Cr	1.68 ± 0.24	0.31 ± 0.03	0.73 ± 0.43
Ni	3.33 ± 0.47	0.33 ± 0.05	0.70 ± 0.15
As	0.24 ± 0.04	0.01 ± 0.001	0.03 ± 0.01
Cd	0.10 ± 0.02	1.05 ± 0.11	0.85 ± 0.17
Pb	1.44 ± 0.12	0.05 ± 0.001	0.06 ± 0.02
Zn	116.2 ± 7.4	55.58 ± 5.01	44.30 ± 6.48
Fe	187.8 ± 9.7	13.14 ± 0.35	25.72 ± 1.00
Cu	16.72 ± 2.3	3.38 ± 0.24	3.06 ± 0.45

Table 6.1: trace element analysis of the wastewater used for the field trial and the trees harvested used in this study (means of biological replicates, each biological replicate was analysed in triplicate)

6.2.2 Similarities and differences in biomass composition

As wastewater irrigation led to a substantial increase in biomass yields, modification of biomass composition could also be expected. Figure 6.2 shows the compositional analysis from control and wastewater irrigated trees. Changes induced by the wastewater treatment were induced in the structural carbohydrates. Glucan content was significantly higher in wastewater irrigated trees, at 418 mg glucan g^{-1} compared to 386 $mg.g^{-1}$ in control trees. Net cellulose contents can increase in willow from tension wood development, associated with mechanical support to stems and characterised by the production of cellulose rich gelatinous fibres in secondary xylem.[414] However, the minor hemicellulose components arabinose and galactose were significantly lower in wastewater irrigated trees at 15 $mg.g^{-1}$ and 22 $mg.g^{-1}$ respectively compared to 21 $mg.g^{-1}$ and 24 $mg.g^{-1}$ in control trees. Xylose, the major hemicellulose backbone monomer of willow, remained constant (average of 14.5 wt%). Lignification provides mechanical strength to stems and therefore could be predicted to increase in order to support higher biomass weight and nutrient-water transport requirements, potentially impairing biomass pretreatment and enzymatic saccharification.[308,415,416] Interestingly, the lignin content was similar for both treatments at an average of 276 $mg.g^{-1}$ (28 wt%).

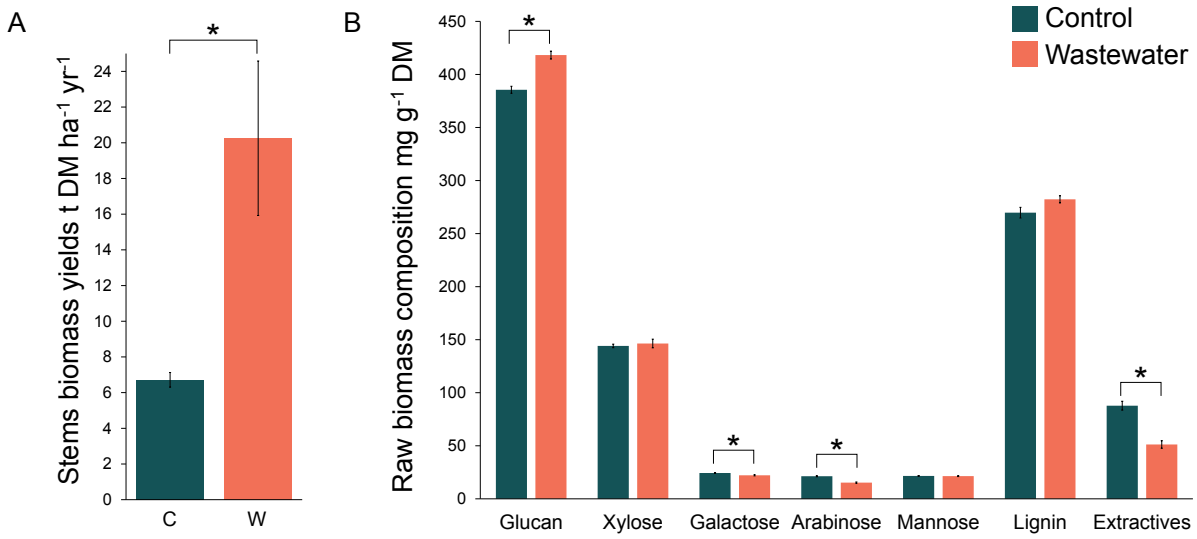


*Figure 6.2: A. harvested stem biomass yields from control C and wastewater irrigated W trees, dry matter tons per hectare per year after a three-year harvest cycle. B. Compositional analysis of raw biomass from control and wastewater irrigated trees. Mean values are based on n =3 trees. Significant differences indicated by * (t-test, p<0.05)*

6.2.3 Impact of stress factor of biomass on the ionoSolv pretreatment

The biomass was pretreated as feedstock for the ionoSolv process and the results are presented in Figure 6.3 (from products recovery yields and compositional analysis of the pulp). The pretreatment led to 526 mg.g^{-1} recovery of biomass in the pulp fraction from control trees, and 573 mg.g^{-1} recovery from wastewater irrigated trees. The resulting pretreated pulp compositions did not significantly vary between treatments (except for higher mannose content in controls compared to wastewater irrigated trees). The ionic liquid pretreatment led to an equivalent fractionation of the biomass from control and wastewater irrigated trees into a cellulose-rich pulp and a lignin-rich liquor, even with a higher glucan content to begin with for wastewater irrigated trees. Specifically, 91–92 % of the glucan was recovered in the pulp while 75–77 % of hemicelluloses and 56–57 % of lignin were removed by the ionic liquid for control and wastewater trees respectively. Lignin recovered by precipitation from the ionic liquid liquor was similar for both treatments, reaching 33–35 % of the initial lignin or 77–79 % of the lignin solubilised by the ionic liquid.

These yields from ionic liquid pretreatment are comparable or better than other pretreatment approaches used in willow, such as hot water pretreatment,[417] acid pretreatment,[418] alkaline pretreatment[419] or Organosolv.[420,421]

Enzymatic saccharification of raw (before pretreatment) biomass performed equally for both control and wastewater irrigated biomass (Figure 6.3), suggesting cell wall structure and

glucose accessibility was not substantially affected by wastewater irrigation and increased growth. This is coherent with stable lignin content, often considered as a key parameter in cell wall recalcitrance to enzymatic deconstruction.[308]

Final glucose release from pretreated biomass was achieved with similar high yields from control and wastewater irrigated trees, corresponding to a glucose release of 92-94 % of the initial glucan in the biomass. This similarity between treatments suggests the pretreatment may have degraded readily accessible, and therefore more vulnerable, glucose from the higher initial glucan in wastewater irrigated trees and could benefit from process optimisation with reduced severity. The severity of the ionic liquid pretreatment condition is a trade-off between the prevention of extensive cellulose degradation and sufficient lignin solubilisation and recovery. Moreover, as sugar degradation compounds, such as HMF, furfural or acetic acid, can inhibit downstream fermentation to biofuels,[422,423] milder severity could potentially better protect sugars within wastewater irrigated trees and further enhance bioenergy yields. At larger scale, recycle of the ionic liquid is also a factor to take into account for the overall ionoSolv pretreatment efficiency, and its impact on the subsequent cycles of the process, e.g. presence and build-up of sugar degradation products, solubilised lignin and trace metals.[97] Both untreated biomass and pulp glucose release yields were similar to the ones reported using willow (Endurance) cultivated without wastewater irrigation treatment in the UK and pretreated with a protic ionic liquid.[104] Although the potential for fermentation inhibition needs to be tested and yields translated to pilot plant biorefinery, these findings suggest wastewater irrigation induced changes in biomass development, but it did not negatively alter willow bioenergy potential at field scale.

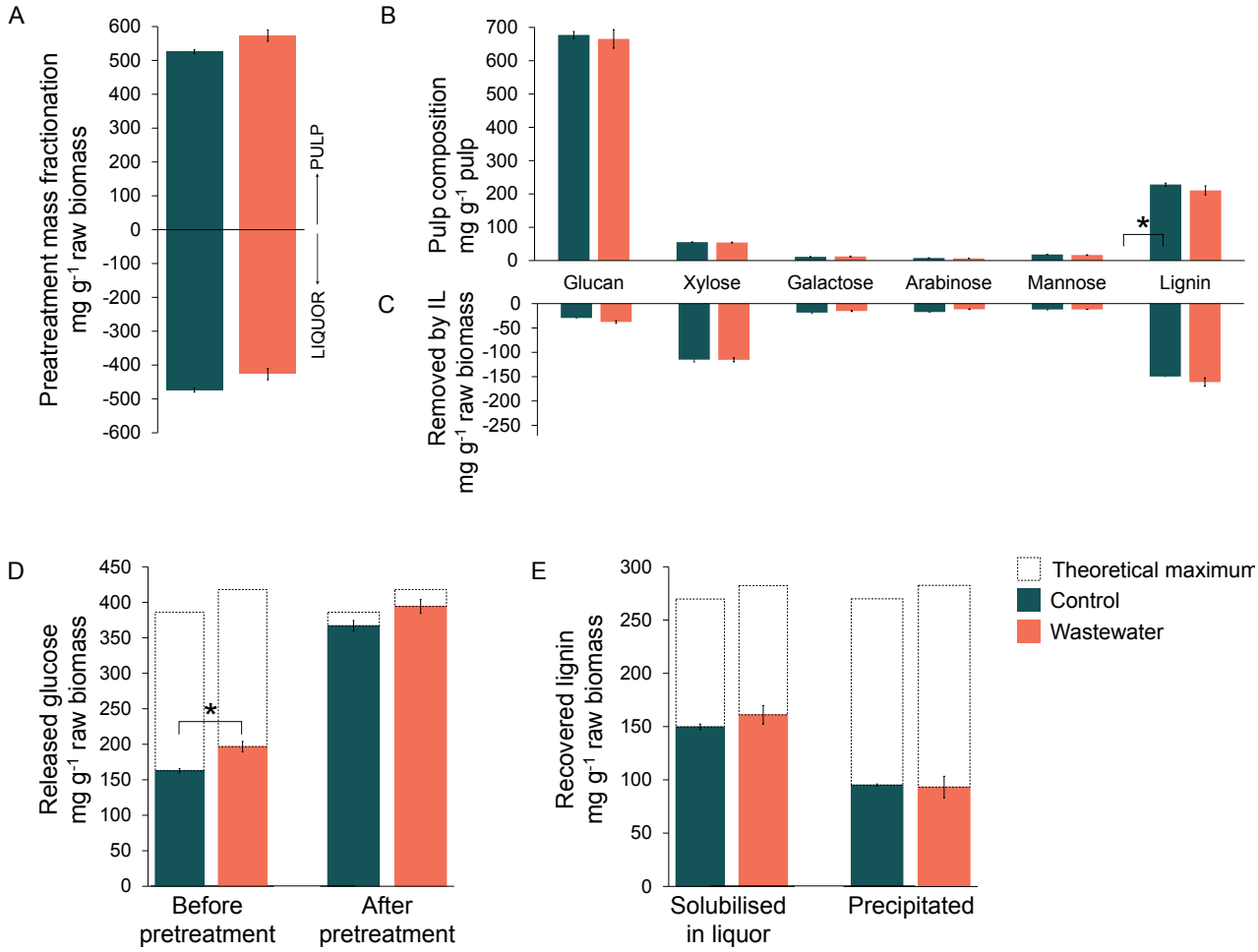


*Figure 6.3: A. Mass proportion between solid (pulp) and liquid (liquor) fractions after ionic liquid pretreatment. B. Pretreated pulp compositional analysis from control and wastewater irrigated trees. C. Inferred biomass composition removed by the ionic liquid pretreatment. D. Glucose release from enzymatic saccharification from control and wastewater irrigated trees untreated samples (before pretreatment) and from the ionoSolv pulps (after pretreatment). E. Lignin solubilised by ionic liquid pretreatment and further precipitated from control and wastewater irrigated trees. Theoretical maximum glucose release and lignin recovery is denoted with dashed lines and are based on initial glucan and lignin content. Significant differences are indicated: * (t-test, p <0.05).*

6.2.4 Impact of stress factor on the structure of lignin

2D HSQC NMR was employed to gain insight on the structure of the ionoSolv lignins obtained from the different treated trees. Since the structure of lignin is altered from the extraction method, HSQC here cannot be used to determine the native structure of the lignin derived from the control and wastewater trees, but it can certainly indicate any differences between the two growth treatment for willow (using the same ionic liquid-based lignin extraction). The S/G ratio of hardwoods has been studied regarding pretreatment and is known to have an

impact on the delignification of the feedstock, as well as hydrolysis of the cellulose and hemicellulose.[306,308–312] From the analysis of the spectra analysed in Figure 6.4; the S/G ratio of the lignin extracted from the ionoSolv is 0.29 and 0.32 for control and wastewater trees respectively. The correlations between plant stress adaptation and lignin biosynthesis at the molecular level are still to be fully understood.[424–427] However, the S/G ratios are consistent with the compositional analysis and response to the pretreatment between the trees. S sub-units are more easily extractible in acidic conditions due to the lability of the β-O-4 linkages.[311] The intensity for such linkages are less important in the wastewater trees than in the control trees' ionoSolv lignin (Figure 6.4). The S-rich lignin from wastewater tress was more easily extracted from the pretreatment and led to smaller fragments from the breakage of ether bonds. This is consistent with the previous results, where the lignin content of the wastewater pulp was lower than for control trees (Figure 6.3B) and lignin solubilised in the liquor was higher for the wastewater pretreated trees than the controls (Figure 6.3E).

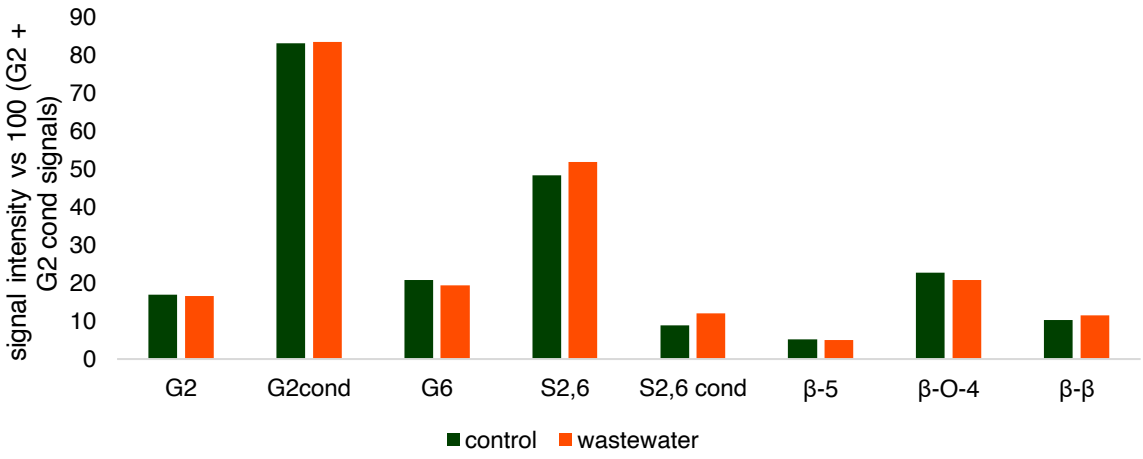


Figure 6.4: HSQC analysis of lignin from the pretreatment of the willow trees

6.2.5 Diversification of products from biomass: valorisation of phytochemicals

Extractable phytochemicals represent another potential valuable bioproduct for biorefinery from wastewater irrigated willow. Willow trees produce highly complex mixtures of phytochemicals in stems to defend against pathogens and herbivory, to protect against abiotic stress as well as for intra and interspecies signalling.[428–430] Because of these essential biological roles, phytochemicals can have diverse and powerful bioactive functions which can make them potentially valuable as extractable bioproducts.[431,432]

In parallel to lignocellulosic biomass characterisation, methanol extraction for persistent phytochemicals was analysed. The total extractives content was significantly lower in

wastewater irrigated trees at 51 $mg.g^{-1}$ compared to 88 $mg.g^{-1}$ respectively, 33 % lower in wastewater irrigated trees compared to controls (Figure 6.2B).

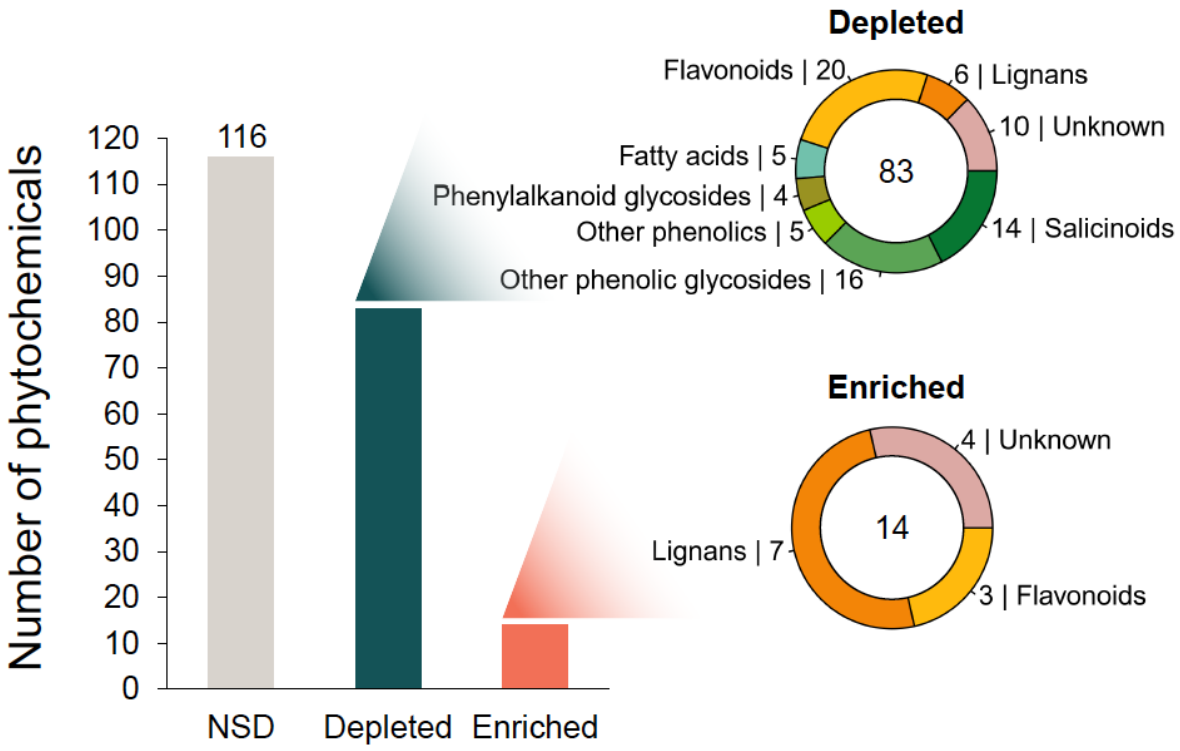
A total of 213 phytochemicals were detected using untargeted metabolite assessment across and shared across multiple trees (biological replicates), as displayed in Figure 6.5. The analysis of these chemicals suggest wastewater irrigation alters extractable phytochemical profile from willow. One theory behind such substantial changes in phytochemical concentrations is the carbon-nutrient hypothesis, proposed by Bryant in 1983, whereby limited nutrient availability leads to a decrease in nutrient concentrations and an increase in carbon-based secondary metabolite concentrations, while greater nutrient availability leads to the converse balance through relatively higher limitation of photo assimilated carbon.[433] Here, the wastewater irrigation provided excess available nitrogen and water, leading to a substantial decrease in carbon-nutrient ratios. The decrease in phytochemicals concentration therefore could correspond to relatively lower carbon ratios.

Molecular networking of features suggested 9 main cluster groups: salicinoids, glycosylated phenolics, glycosylated phenolic acids, glycosylated phenylalkanoids, (7-*O*) glycosylated flavonoids, (3-*O*) glycosylated flavonoids, flavanols, lignans and fatty acids. More detailed analysis of the different phytochemicals is available in the Appendix. 116 of these phytochemicals were not significantly different between controls and wastewater irrigated trees. However, 97 phytochemical features were significantly differently abundant between the control and wastewater irrigated trees (Mann-Whitney U test with Benjamini- Hochberg correction $p < 0.05$). 83 of the phytochemicals were significantly lower (depleted). Within the compounds depleted in wastewater irrigated trees, salicinoids were depleted. The biological function of salicinoids are associated with plant defence, especially against insect herbivory [428,434] Similarly, the reductions in other phenolic glycosides, as well as phenylalkanoid glycosides, observed here may be associated with antioxidant capacity.[435,436] Lipids were also universally depleted in wastewater irrigated trees, including multiple C_{18} fatty acids. The most dominant depleted fatty acid was an oxidised linoleic acid ($C_{18}H_{32}O_3$; see Appendix), the stable precursor of jasmonic acid, one of the major plant hormones associated with defence signalling.[437,438] The lipid azelaic acid, a key-signal molecule that triggers accumulation of salicylic acid and other defence compounds, was also significantly depleted in wastewater irrigated trees.[439] This depletion pattern of diminished carbon investment in phytochemical defence mechanisms in wastewater irrigated trees might be associated with the increased growth and biomass yield in a typical growth-defence trade-off, despite the extremely high nutrient, salt and microbial loads which could have induced stress in the trees.[440] Although the biomass yields were substantially increased over the three-year field trial, longer-term trials

need to be conducted in order to establish whether the reduction in these important phytochemicals can compromise plant defence in the long-term, particularly as short rotation willow plantations are often maintained for continued harvesting for over 20 years.[441,442]

14 phytochemicals were significantly higher in wastewater irrigated trees. The 14 phytochemicals significantly enriched in wastewater treated trees were identified as 6 lignan derivatives and 3 flavonoids. The lignans included salcolin A, ramontoside, quiquesetinerviusin B and three isomers of quiquelignan B; whereas the flavonoids were identified as glabrene, glabraoside A and a procyanidin trimer (Figure 6.5B). Salcolin A ($C_{27}H_{26}O_{11}$) and quiquelignan B ($C_{36}H_{36}O_{13}$) exhibit structured linked to monolignol, potentially acting as nucleation sites for lignin polymerisation.[443–445] More broadly, lignans are characterised for their biotic defence role and antimicrobial activities and could represent a specific type of metabolic investment by willows into defence, particularly in light of very high microbial loads in wastewater. [446,447] Overall, these significantly enriched phytochemicals represent part of the phenotype underpinning the response to primary municipal wastewater irrigation in willow.

A



B

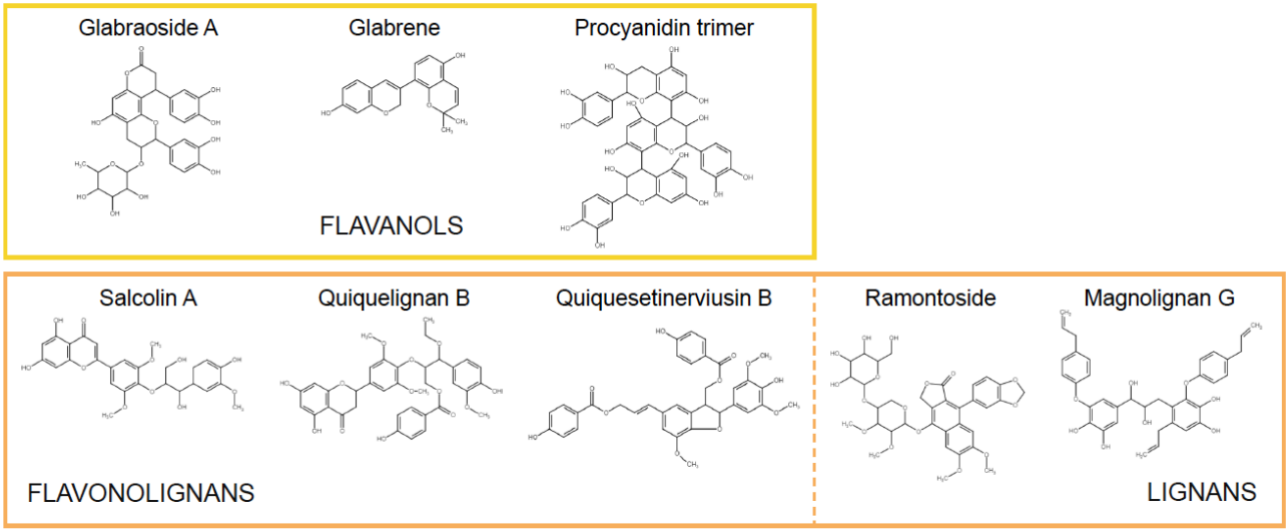


Figure 6.5: A. Number of phytochemicals identified as not significantly different (NSD) between control and wastewater treatment, and those significantly depleted or enriched by wastewater irrigation with chemical classes shown (Mann-Whitney U test followed by BH FDR correction, $p < 0.05$) B. Molecular structures of significantly enriched phytochemicals in wastewater irrigated trees.

6.2.6 Effect of preliminary extractive extraction on ionoSolv pretreatment

The ionoSolv pretreatment conditions at high temperatures (>120°C) degrade the extractives during the reaction. In the context of a biorefinery, phytochemicals of interest would need to be extracted prior to the lignin and hemicellulose extraction from the IL pretreatment. We investigated the impact of the ASE methanol-water extraction prior to the pretreatment of the biomass on both product streams: the pulp and the lignin – as shown in Figure 6.6. Both trees, control (Figure 6.6A-B) and wastewater (Figure 6.6C-D), follow the same trends regarding the impact of the extractives' extraction on the pretreatment, with the exception of glucan recovery between control and wastewater trees, mostly because the wastewater treatment led to a depletion in extractible phytochemicals (Figure 6.5A). The compositional analysis of the pulp after the pretreatment of the extractives free pulps revealed a higher hemicellulose removal and delignification and lower glucose release compared to the trees pretreated with extractives still intact before pretreatment.

Differences were expected as the ASE extraction uses an organic solvent, 75 % of methanol by volume, to extract the extractives from the biomass at 100°C. This extraction step acts a preliminary treatment of the biomass, similar to the Organosolv, a well-known process for its ability to extract high quality lignin and aqueous hemicelluloses from a lignocellulosic feedstocks.[420,421,448] A hybrid ionoSolv-Organosolv fractionation process designed by Chen et al, revealed that this pretreatment produced a more digestible cellulose pulp with higher lignin extraction.[286] However, this was a simultaneous IL-organic solvent pretreatment and hardwoods were not studied. The HSQC lignin analysis of the lignins shown in Figure 6.6 B and D indicates a decrease in the β-*O*-4 linkages, which are more representative of the enhanced lignin extraction; with an increase in S condensed sub-units, which can redeposit onto the pulp and negatively impact the enzymatic hydrolysis of the pulp. The extraction of phytochemicals prior to pretreatment acts as a preliminary organic solvent-based treatment for the biomass, which leads to a harsher subsequent IL pretreatment with enhanced hemicellulose and lignin extraction, but also leads to more condensation of the lignin.

Cellulose digestibility is only one of the possible valorisation routes for the cellulose pulp. In the context of a comprehensive biorefinery, compounds of interest and valorisation routes would need to be defined in order to tune the process for the desired extracted platform chemicals (phytochemicals, high purity pulp, sugar degradation products, chemical structure of lignin etc) pretreatment and process conditions accordingly.

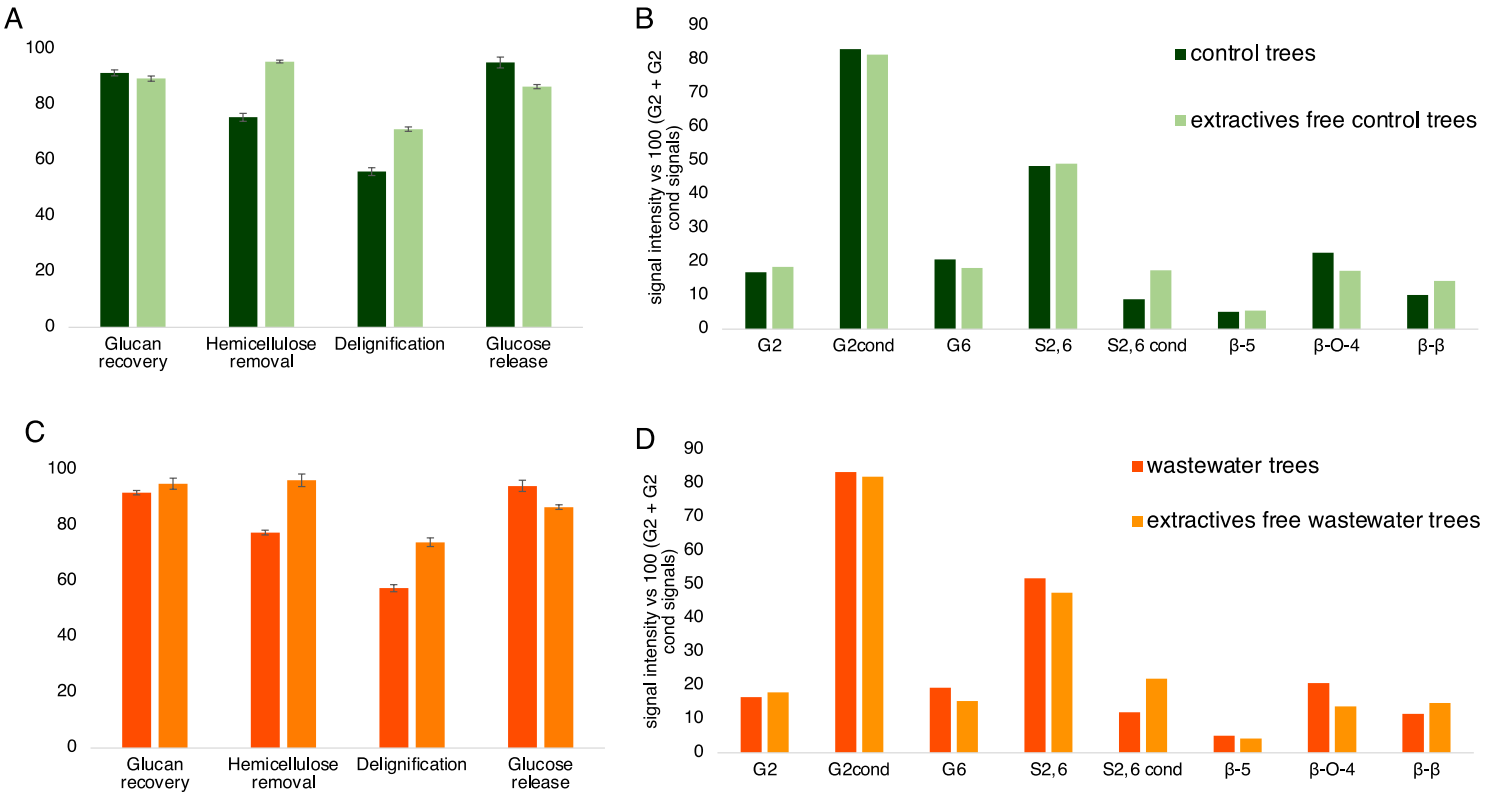


Figure 6.6: Effect of the extractives extraction with methanol-water (75/25 v/v %) prior to ionoSolv pretreatment for both trees A. key outome parameters of the IL pretreatment for the pulp from control trees and B. wastewater trees C. HSQC analysis of ionoSolv lignins for control trees and D. wastewater trees

6.2.7 Large scale predictions: integrated biorefinery projected yields

Willow plantations can provide fundamental environmental services as part of green infrastructure, such as greenhouse gases reduction, soil erosion limitation and biodiversity support.[191,449,450] The integration of wastewater phytofiltration and biomass production within a willow plantation extends this environmental utility with potential economic and social benefits.[451–454]

By combining biomass yield, glucan content and enzymatic saccharification conversion from the ionoSolv pretreatment, projected glucose and ethanol yields per hectare were calculated and compared as seen in Figure 6.7. The yields were significantly increased from 2.73 t glucose ha^{-1} yr^{-1} and 1592 L ethanol ha^{-1} yr^{-1} from control trees, to 8.89 t glucose ha^{-1} yr^{-1} and 5186 L ethanol ha^{-1} yr^{-1} from wastewater irrigated trees. The projected ionoSolv lignin yields per hectare also significantly increased from 0.64 t lignin ha^{-1} yr^{-1} for control trees to

1.89 t lignin ha^{-1} yr^{-1} for wastewater irrigated trees. The total extractives yield is projected at 0.66 t extractives ha^{-1} yr^{-1} from control trees and was significantly higher from wastewater irrigated trees, at 1.40 t extractives ha^{-1} yr^{-1}. Purified standards were used to precisely quantify absolute amounts of catechin $C_{15}H_{14}O_6$ and salicin $C_{13}H_{18}O_7$ as examples of phytochemicals. Catechin yield was projected to 10.2 kg ha^{-1} yr^{-1} from control trees and 23.7 kg ha^{-1} yr^{-1} from wastewater irrigated trees, whereas salicin yield was projected to 12.1 kg ha^{-1} yr^{-1} from control trees and 25.2 kg ha^{-1} yr^{-1} from wastewater irrigated trees. These yields are likely meet the minimum thresholds estimated in recent technoeconomic assessment of >0.6 mg g^{-1} for cost-effective extraction of a single compound valued at > \$10 kg^{-1} for a biorefinery.[455]

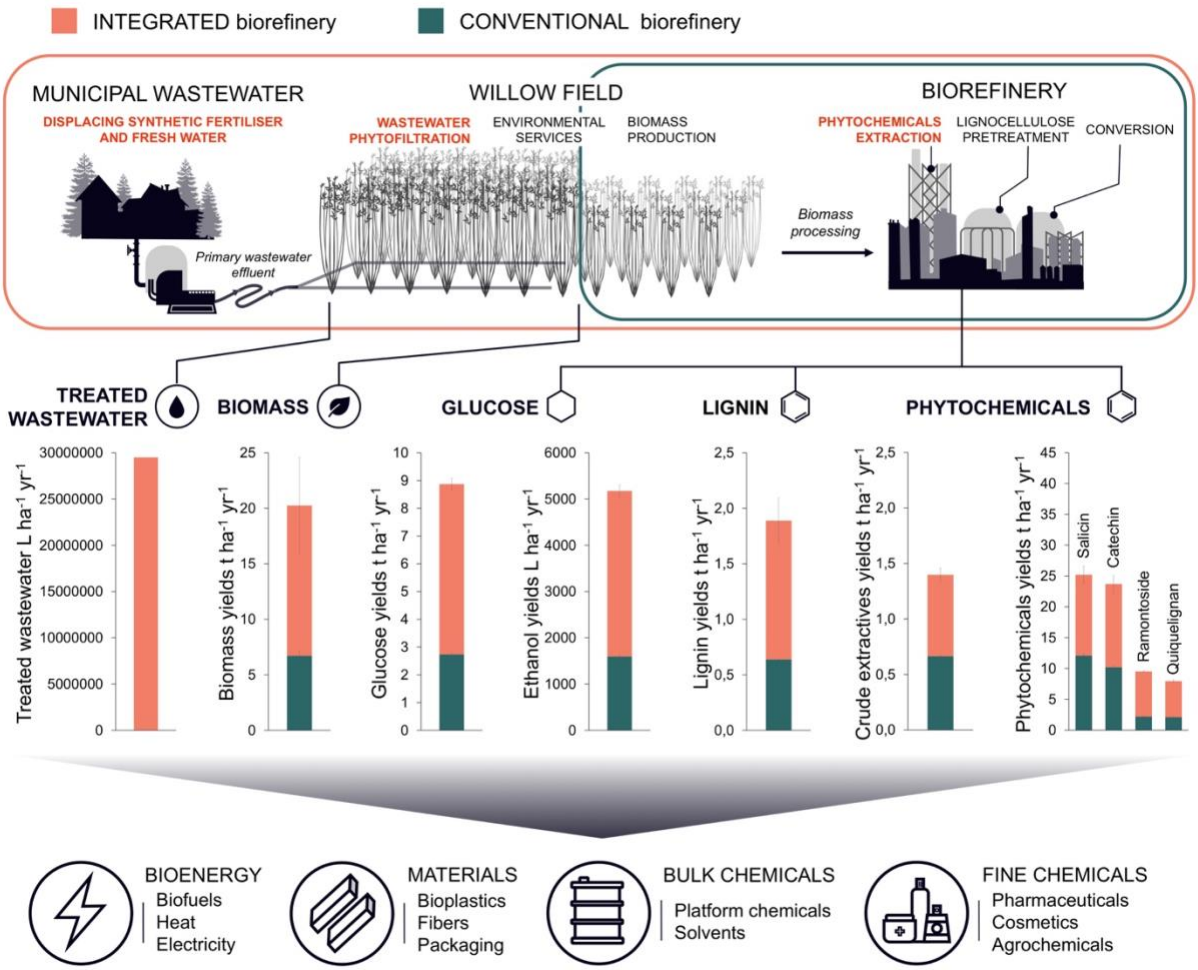


Figure 6.7: willow wastewater treatment integrated biorefinery illustration and projected yields, illustrating a proposed biorefinery integrating willow wastewater treatment by phytofiltration, biomass production, lignocellulosic bioenergy and phytochemicals extraction

6.3 Conclusion: willow as a stable and sustainable biomass feed under stress condition

Biomass availability is one of the crucial parameters to the feasibility of a biorefinery feedstock. The high biomass willow yields of over 20 t ha^{-1} yr^{-1} from wastewater irrigation could be influenced by multiple factors (willow genotype, site soil and climate, and plantation management practices,[456–460]), but similar yields of up to 22 t ha^{-1} yr^{-1} have been reported in the literature in willow plantations with high nitrogen fertilisation.[411,461] This system takes advantage of nutrient loads in wastewater to displace the use of synthetic fertiliser, and its associated economic and environmental costs, together with removing freshwater use and the associated environmental costs in traditional agriculture.[462–466] Furthermore, those results of stable quality of biomass in increased yields demonstrate that the ionoSolv could take advantage from such phytoremediation trials and as a long term biomass supply, as opposed to their short to medium term availabilities investigated in previous chapters.

An integrated ionoSolv biorefinery is able to produce bioenergy, lignin, as well as high-value specialised phytochemicals from willow. These findings and diversification of phyto-extractives outcomes could also be applied to other types of biomass, such as waste wood and invasives species studied previously. Such synergies could help improve the economic feasibility of a biorefinery as a closer cost-competitive analogue of petroleum refinery, but with the advantage of a reliance on renewable inputs instead of fossil fuels. The complementary benefits of integrating wastewater treatment with the production of sustainable bioproducts illustrate the potential of multifunctional biotechnologies to address environmental challenges caused by human activities. Finally, as land-use is an important consideration when growing bioenergy crops, the capability of willows to grow on marginal lands,[467,468] combined with the use of municipal wastewater to provide high water and nutrient loads, could help to unlock new valorisation for MaCL. Nevertheless, the long-term impact of wastewater irrigation, in particular the accumulation of trace metals and salts, should be assessed before the ecological benefits and ecosystem benefits can be asserted.

7 Conclusions: ionoSolv process flexibility towards a wide-ranging biorefinery

7.1 Key messages

This PhD research has demonstrated the flexibility and versatility of an ionic-liquid based technology, the ionoSolv fractionation process, which allows the sourcing of innovative supplies of biomass and the production of sustainable bioenergy and bioproducts. These unconventional feedstocks explored here are terrestrial invasive species - knotweed and rhododendron – CCA waste wood, biomass grown on marginal land and willow irrigated with wastewater, as illustrated in Figure 7.1.

To evaluate their potential, two main fraction streams were used: the first one based on glucose release of the resulted fractionated cellulose rich pulp after pretreament, the second is the isolated lignin recovered from the ionic liquid liquor. The sugar obtained from each feedstock ranges from 289 to 443 $kg.t^{-1}$ and ionoSolv lignin yields from 91 to 258 $kg.t^{-1}$ (Figure 7.1). Different values are due to natural variations between the feedstock themselves (species, type of feedstock, growth conditions) and pretreatment conditions used (IL, inherent chemical nature of lignin and its solubility in IL). A previous life cycle assessment (LCA) of the environmental and economic sustainability of willow bioethanol in the UK proposed a minimum 70 % conversion of biomass glucan to ethanol (i.e. 0.3 ton of glucose per ton of biomass) in an optimised process system using dilute acid pretreatment.[469] In comparison, the ionoSolv pretreatment resulted in almost complete availability of cellulose from lignocellulosic biomass, allowing for nearly all feedstocks studied to reach this threshold of 0.3 ton of glucose per ton of biomass (truly indicative, as the LCA was carried out using different boundaries and parameters than this study). Protic ionic liquid pretreatment consistently and robustly fractionated these unconventional feedstocks into cellulose and lignin streams. Moreover, these results from unconventional biomass could serve as references for new feedstocks to handle, predict their response to the ionoSolv process and feed future life cycle assessment studies.

This ionic liquid based process was also designed to demonstrate the dual property of some protic ionic liquids, which are able to both fractionate the biomass and extract metal species present in the plant. Adding to the upgrading of an underutilised, potentially cheap, biomass (invasive species), this further extends the use of ionic liquid for metal enriched biomass. This approach constitutes an alternative to conventional burning or ashing of metal contaminated

biomass; an opportunity to generate revenue from clean metal-free renewable chemicals and energy. Such promising results can provide a roadmap for possible inroads to the circular bio-economy by rehabilitating toxic waste material, diverting such materials from polluting landfills and incineration and the utilisation and valorisation of marginal land.

After process optimisation, these unconventional feedstocks revealed to be suitable for the ionoSolv process, with short reaction time (30-60 mins) and high temperatures (150-170°C). However, the use of unconventional feedstock could bring new challenges, especially when they contain trace elements, which had until now understudied interaction with the ionic liquid based process, as well as on the following transformation steps, such as fermentation. Here, we showed that the ionic liquid extracts a wide range of metal contaminants present in biomass, including multiple trace elements (Cu, Zn, As, Cd, Pb, Ce, Fe and Ni) and different levels of contamination (ranging from 0.1 $mg.kg^{-1}$ to 20 $g.kg^{-1}$). Further intensification of process conditions was also researched, such as biomass loading and recycling of the solvent. Contaminated waste wood was pretreated with the ionic liquid solvent being recycled up to 6 times, retaining efficiency for deconstruction of biomass and metal extraction (99%).

Finally, this research demonstrates that valuable products can be obtained from ionic-liquid based pretreatment, beyond the binarity of glucose and lignin, and usually exclusive from each other (optimised for one or the other). Downstream processes were used in combination with the ionoSolv process to produce fermented bioethanol and pyrolysis products from post-hydrolysis residues (a waste stream from saccharification). The electrodeposition of metals from the ionic liquid liquor from highly contaminated biomass (Welsh Miscanthus) showed to be a suitable way to recover metals from the solvent, but also to manage the concentration of metals in the liquor. The metal extraction efficiency was found to be improved by 20 % by removing the metals before subsequent pretreatment with recycled ionic liquid liquor. Willow phytochemicals were also studied to show an even wider range of bio-active compounds. Extractives were recovered from biomass (before pretreatment) with an organic solvent extraction. This extra step could help mitigating softer pretreatment conditions, the organic solvent acting as a first pretreatment.

Moving away from imported, standardised American timber wood pellets for Drax co-firing power generation plant for example, this coherent body of work shows the importance of multi-disciplinary research to engineer and tailor solutions for marginal landowners and bioenergy suppliers. The experimental boundary of this research was set at bench scale, but it is a first step towards understanding and scaling-up ionic liquid-based technologies for sustainable bioenergy and bioproducts. For a scale-up of this technology, we showed that the biomass

input for an ionoSolv biorefinery could be made of a myriad of different feedstocks, allowing to secure the supply chain with different short / medium / long term supplies, and to make it financially attractive from producing different and simultaneously biochemicals and bioenergy: e.g. high purity cellulose, bioethanol, lignin, bioheat, bio-oils, deposited lead. A techno-economical assessment of the ionoSolv process carried out in 2017 estimated the ionoSolv plant size input at 770 000 tons of biomass per year.[97] If this biomass input would be largely covered by the estimated 4.5 million tons of the UK's waste wood,[367] biomass supply could still be supplemented and/ or supported with other unconventional feedstocks such as invasive species and crops grown in unconventional environments. The flexibility of the ionoSolv technology supports the idea of the implementation of regional biorefinery plants, using on the same ionic liquid process but supplied with locally available biomass. In fact, the reduction of distances needed for transport could facilitate the logistics and mitigate the economic and environmental impact of the whole biorefinery system.

This body of work represents significant innovation into the sourcing, processing and characterisation of bioenergy feedstocks grown / obtained from marginal contaminated areas with multiple benefits for both the energy and environmental sectors:

- in combination with plant management practises, invasive species could be controlled, transformed into biochemicals to generate revenue and eventually restore biodiversity balance,
- marginal land can be used and valorised using a second generation pretreatment technology to produce for clean energy production and strive for environmental remediation,
- contaminated waste can be diverted from landfill and decontaminated to produce clean bioproducts,
- wastewater can act as a fertiliser and freshwater replacement to enhance and deliver a qualitative biofuel crop.

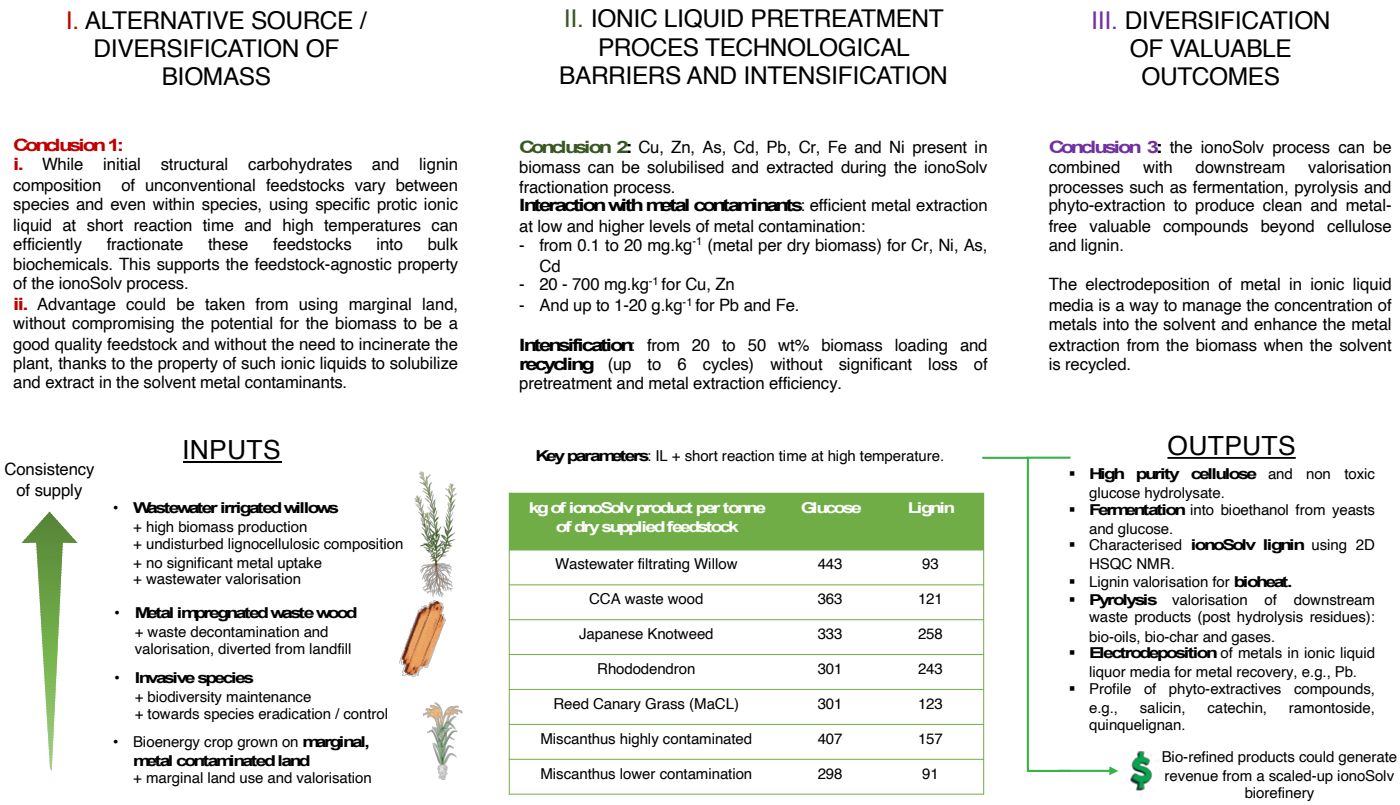


Figure 7.1: illustrative conclusion of 3 axes of the research objectives: alternative inputs, design of chemical ionoSolv process and diversification of outputs

7.2 Future work

The very detailed experimental results presented in this thesis should be used and feed other research projects. The collaboration with modelling experts could generate estimation of feedstock availability and supply, biomass yields and marginal land mapping and analysis. For each unconventional feedstock studied, having an estimated biomass yield and feedstock availability (land) would be of great importance to assess the range of biomass, which could enter a scaled-up ionoSolv integrated local biorefinery. Techno-economic assessments and lifecycle analysis of combined technologies and associated supply chains need to be carried out for each bioenergy case study. In particular, short, medium and long term availability of these feedstocks need to be obtained and integrated with the concept of a large scale ionic liquid based biorefinery; as well as their associated greenhouse gas emissions compared to conventional feedstocks to assess their sustainability. Moreover, this thesis aimed to

investigate the chemical engineering aspects of the ionoSolv process: economic and ecological aspects must be investigated by others to provide a holistic examination of the sustainability of the ionoSolv biorefinery.

How many feedstocks can we pretreat with protic ionic liquids to say for certain that the ionoSolv is feedstock independent? Perhaps many more, there are always alternative sources of biomass to pretreat: e.g., agricultural waste, hydrocarbons contaminated biomass, 3rd generation feedstock such as algae. One straight-forward experimental next step for the unconventional feedstock ionic liquid pretreatment would be to mix the different feedstocks and study the fractionation, purity of outputs and metal extraction process. Would the feedstocks have to be sorted by species, lignin content or even level of contamination when entering the ionoSolv biorefinery?

One of the barrier to commercialisation of ionic liquids is the cost of the solvent. Economic and environmental assessments of chloride-based ILs should be carried out, similarly to the study performed for $[HSO_4]^-$ based protic ILs. Even if pilots have been carried out at larger scale, the methodology for washing of the cellulose pulp and lignin is still based on lab scale, unknowns remain regarding the rheological properties of produced ionic liquid-based slurries, product separation and the possible technologies used for the removal of water between cycles. Recycling of the ionic liquid solvent needs to further investigated, especially regarding the fate of the metal-enriched ionic liquid liquor, possible ionic liquid degradation, in depth chemical characterisation of IL-metals complexes, as well as metal solubility in the ionic liquid used. Further study of the recovery of the metals from the liquor should be studied, via electrodeposition, the analysis of the metals electrodeposited; or investigating other metal recovery process from the liquor (e.g. membrane filtration). The addition of the electrodeposition step to the process could hinder the development of the ionoSolv technology at scale.

Furthermore, the ionoSolv process optimisation has focused on the production of bioethanol as an end product for the cellulose pulp, as a proof of concept for biofuels. However, more research is needed on the factors inhibiting both saccharification and fermentation from ionic liquid-based pretreatment and impact of residual ILs in product streams. In depth characterisation of the cellulose pulp valorisation should be expanded towards the production of cellulose-based end-use markets, such as nanocellulose. Similarly, the characterised lignin was studied for its heating value as a fuel but characterised lignin can also be a starting chemical for high value products. Lignin is by nature environmentally benign and constitutes one of the few renewable sources of aromatic molecules. Ionic liquids have been used as

solvent media for chemical modifications of cellulose and lignin to obtain specialty chemicals: plastics from lignin monomers, composite materials, additives, films, fibres; with biomedical applications as well as constituents for electronics and batteries. The upstream extraction of bio-active compounds could also be extended to other feedstocks, such as the invasive species, some of them also known for their medicinal properties. Extractable phytochemicals have potential as bioproducts due to antioxidant, anticancer, anti-inflammatory and antimicrobial functions with high social, environmental and economic value within the medical (pharmaceuticals), agricultural (biopesticides and biostimulants), commercial (cosmetics, nutraceuticals and household chemicals) and industrial (lubricants and resins) sectors.[470,471]

Finally, a lot of the work presented for phytoremediation potential of biomass is limited and could have been improved upon in a number of ways, in collaboration with Biology and Plants experts. The methodologies for plant selection and environmental sampling should be improved, incorporating design of experiments, further characterisation of biomass with longer growth periods in controlled environments, plant tissue metal staining experiments and estimation of extraction metal phytoextraction kinetics. Complex spectroscopy techniques can be employed to study metal speciation and bonding within the plant, as well as microscopy analysis for metal spatial distribution. We could envision biological engineering of plants to enhance metal extraction and/or tolerance to contaminants for phytoremediation and phytomining. Some research has been done on how to improve the bioavailability of the metal and therefore, a better metal uptake of the plant. Soil pH adjustments, adding fertilisers (P, N, K or S) to increase biomass yields, bacterial inoculation or even adding chelating agents such as ethylenediaminetetraacetic acid (EDTA) have been tried - but their toxicity and leaching of some of these chelating agents into the environment is controversial. More environmentally friendly alternatives are being investigated to increase the metal availability of the metals, such as citric acid addition. Many studies have tried to unlock the interactions between the microorganisms of the soil and the root system, which plays a crucial role in metal uptake.[472–474] Plant associated microorganisms can be added to the soil to enhance the process of phytoremediation: mycorrhizal fungi (AMF) and plant growth promoting rhizobacteria (PGPR). However, if the results are promising for understanding of the role of the rhizosphere community, the practicality of this technique seems to be a major obstacle on large scales of contaminated sites.

As we have seen in this thesis, innovative multi-disciplinary solutions are complex, often context specific and therefore knowledge from different fields are needed to investigate their system scaling, pilots and demonstration schemes for such sustainable biorefineries to make sure the solutions are towards economically viable environmental remediation. Moreover, research is often triggered and pushed by environment and energy policy: there is a need to accompany scientific research and advances with transparent and innovative environment and energy policies to meet the Paris Agreement Targets and do so in an economically viable manner.

8 Bibliography

1. International Energy Agency. IEA Statistics - United Kingdom [Internet]. 2020 [cited 2021 Nov 14]. Available from: https://www.iea.org/countries/united-kingdom
2. Miller J. Limiting Global Warming to 1.5°C. Parliam Sci Technol. 2019;(594):1–4.
3. IPCC. Global Warming of 1.5°C. An IPCC Special Report on the impacts of global warming of 1.5°C above pre-industrial levels and related global greenhouse gas emission pathways, in the context of strengthening the global response to the threat of climate change. Masson-Delmotte V, Zhai P, Pörtner H, Roberts D, Skea J, Shukla P, et al., editors. Cambrige, UK and New York, NY: Cambridge University Press; 2018.
4. Department for Business Energy & Industrial Strategy. 2018 UK greenhouse gas emissions, provisional figures [Internet]. National Statistics. 2019 [cited 2021 Aug 13]. Available from: https://assets.publishing.service.gov.uk/government/uploads/system/uploads/attachment_data/file/790626/2018-provisional-emissions-statistics-report.pdf
5. Gummer RHJ, Brown B, Bell K, Chater N, Forster P, Heaton R, et al. Net Zero: The UK's contribution to stopping global warming Committee on Climate Change [Internet]. Committee on Climate Change. 2019 [cited 2021 Aug 13]. p. 1–275. Available from: https://www.theccc.org.uk/wp-content/uploads/2019/05/Net-Zero-The-UKs-contribution-to-stopping-global-warming.pdf
6. The Royal Society. Greenhouse Gas Removal Technologies [Internet]. London, England; 2018 [cited 2021 Aug 13]. Available from: https://royalsociety.org/-/media/policy/projects/greenhouse-gas-removal/royal-society-greenhouse-gas-removal-report-2018.pdf
7. IPCC. Climate Change 2013: The Physical Science Basis. Contribution of Working Group I to the Fifth Assessment Report of the Intergovernmental Panel on Climate Change. Qin D, Plattner G, Tignor M, Allen S, Boschung J, Nauels A, et al., editors. Cambrige, UK and New York, NY: Cambridge University Press; 2013. 741–866 p.
8. European Academies Science Advisory Council. Commentary on Forest Bioenergy and Carbon Neutrality [Internet]. 2018 [cited 2021 Aug 16]. Available from: https://easac.eu/publications/details/commentary-on-forest-bioenergy-and-carbon-neutrality/
9. Chatham House International Affairs Think Tank. Woody Biomass for Power and Heat [Internet]. [cited 2021 Aug 16]. Available from: https://www.chathamhouse.org/2017/02/woody-biomass-power-and-heat
10. Kuhlmann W, Putt P. Are Forests the New Coal ? A Global Threat Map of Biomass

Energy Development. Environ Pap Netw [Internet]. 2018;1–6. Available from: https://environmentalpaper.org/wp-content/uploads/2018/11/Threat-Map-Briefing-Are-Forests-the-New-Coal-01.pdf

11. Welfle A, Thornley P, Röder M. A review of the role of bioenergy modelling in renewable energy research & policy development. Biomass and Bioenergy. 2020;136.
12. Smith P, Gregory PJ, Van Vuuren D, Obersteiner M, Havlík P, Rounsevell M, et al. Competition for land. Philos Trans R Soc B Biol Sci. 2010;365(1554):2941–57.
13. Ni Y, Mwabonje ON, Richter GM, Qi A, Yeung K, Patel M, et al. Assessing availability and greenhouse gas emissions of lignocellulosic biomass feedstock supply – case study for a catchment in England. Biofuels, Bioprod Biorefining. 2019;13(3):568–81.
14. IPCC. Renewable energy sources and climate change mitigation: Special report of the intergovernmental panel on climate change [Internet]. Edenhofer O, Madruga RP, Sokona Y, Seyboth K, Matschoss P, Kadner S, et al., editors. Cambridge: Cambridge University Press; 2011 [cited 2020 Dec 4]. Available from: https://www.ipcc.ch/report/renewable-energy-sources-and-climate-change-mitigation/
15. International Energy Agency. IEA Data overview [Internet]. CO2 Emissions from Fuel Combustion 2018: Overview. 2018 [cited 2021 Aug 16]. Available from: https://www.iea.org/data-and-statistics
16. United Nations. Gathering a body of global agreements: Our Common Future- Report of the World Commission on Environment and Development [Internet]. Conference of NGO: United Nations web sites. 2000 [cited 2021 Aug 16]. Available from: http://www.un-documents.net/ocf-09.htm#I.1
17. Wentworth J. Seeking sustainability. Parliam Off Sci Technol. 2012;(408):1–4.
18. European Academies Science Advisory Counci. Multi-functionality and sustainability in the European Union's forests [Internet]. EASAC Policy Report: Volume 32. 2017 [cited 2021 Aug 16]. Available from: https://easac.eu/publications/details/multi-functionality-and-sustainability-in-the-european-unions-forests/
19. Harvey C, Heikkinen N. Congress Says Biomass Is Carbon-Neutral, but Scientists Disagree: Using wood as fuel source could actually increase CO2 emissions. Sci Am. 2018;
20. Royal Society. The role of land carbon sinks in mitigating global climate change [Internet]. London, England; 2001 [cited 2021 Aug 16]. Available from: https://royalsociety.org/~/media/royal_society_content/policy/publications/2001/9996.pdf
21. International Energy Agency. IEA Bioenergy - Carbon neutrality [Internet]. IEA Publications. 2018 [cited 2021 Nov 14]. Available from: https://www.ieabioenergy.com/iea-publications/faq/woodybiomass/carbon-neutrality/

22. Global Bioenergy Partnership. Sustainability Indicators for Bioenergy [Internet]. 2011 [cited 2021 Nov 14]. Available from: http://www.globalbioenergy.org/programmeofwork/task-force-on-sustainability/gbep-report-on-sustainability-indicators-for-bioenergy/en/
23. International Energy Agency. Technology Roadmap: Delivering Sustainable Bioenergy [Internet]. IEA Publications. 2017 [cited 2021 Aug 16]. Available from: https://www.iea.org/reports/technology-roadmap-delivering-sustainable-bioenergy
24. Wentworth J. Bioenergy. Parliam Off Sci Technol. 2012;(410):1–4.
25. Gough C, Upham P. Biomass energy with carbon capture and storage (BECCS or Bio-CCS). Greenh Gases Sci Technol. 2011;1(4):324–34.
26. Committee on Climate Change. Biomass in a low-carbon economy [Internet]. 2018 [cited 2021 Nov 5]. Available from: https://www.theccc.org.uk/publication/biomass-in-a-low-carbon-economy/
27. Stafford W, Lotter A, Brent A, Von Maltitz G. Biofuels technology: A look forward. Unu-Wider. 2017;(87):1–25.
28. Welfle A, Gilbert P, Thornley P. Securing a bioenergy future without imports. Energy Policy. 2014 May 1;68:1–14.
29. Röder M, Thornley P. Waste wood as bioenergy feedstock. Climate change impacts and related emission uncertainties from waste wood based energy systems in the UK. Waste Manag. 2018;74:241–52.
30. International Energy Agency. Transport biofuels [Internet]. Renewables 2019. Analysis and forecast to 2024. 2019 [cited 2021 Nov 15]. p. 107–28. Available from: https://www.iea.org/reports/transport-biofuels
31. Cherubini F, Strømman AH. Principles of Biorefining. Biofuels Altern Feed Convers Process. 2011;3–24.
32. Valin H, Peters D, Van der Berg M, Frank S, Havlik P, Forsell N, et al. The land use change impact of biofuels in the EU: Quantification of area and greenhouse gas impacts [Internet]. 2015 [cited 2016 Aug 17]. Available from: https://ec.europa.eu/energy/sites/ener/files/documents/Final Report_GLOBIOM_publication.pdf
33. Kline KL, Msangi S, Dale VH, Woods J, Souza GM, Osseweijer P, et al. Reconciling food security and bioenergy: priorities for action. GCB Bioenergy. 2017;9(3):557–76.
34. Whitaker J, Field JL, Bernacchi CJ, Cerri CEP, Ceulemans R, Davies CA, et al. Consensus, uncertainties and challenges for perennial bioenergy crops and land use. GCB Bioenergy. 2018;10(3):150–64.
35. Brandt A, Gräsvik J, Hallett JP, Welton T. Deconstruction of lignocellulosic biomass with ionic liquids. Green Chem. 2013;15(3):550–83.

36. Mood S, Golfeshan A, Tabatabaei M, Jouzani G, Najafi G, Gholami M, et al. Lignocellulosic biomass to bioethanol, a comprehensive review with a focus on pretreatment. Renew Sustain Energy Rev. 2013;27:77–93.
37. Ray MJ, Brereton NJB, Shield I, Karp A, Murphy RJ. Variation in Cell Wall Composition and Accessibility in Relation to Biofuel Potential of Short Rotation Coppice Willows. Bioenergy Res. 2012 Sep 12;5(3):685–98.
38. Karp A, Hanley SJ, Trybush SO, Macalpine W, Pei M, Shield I. Genetic Improvement of Willow for Bioenergy and Biofuels. J Integr Plant Biol. 2011 Feb 1;53(2):151–65.
39. Samson R, Mani S, Boddey R, Sokhansanj S, Quesada D, Urquiaga S, et al. The potential of C4 perennial grasses for developing a global Bioheat Industry. CRC Crit Rev Plant Sci. 2005 Sep;24(5–6):461–95.
40. Henniges U, Schiehser S, Rosenau T, Potthast A. Cellulose solubility: Dissolution and analysis of “problematic” cellulose pulps in the solvent system DMAc/LiCl. ACS Symp Ser. 2010;1033:165–77.
41. De Gregorio GF, Weber CC, Gräsvik J, Welton T, Brandt A, Hallett JP. Mechanistic insights into lignin depolymerisation in acidic ionic liquids. Green Chem. 2016;18(20):5456–65.
42. Tao L, Aden A, Elander RT, Pallapolu VR, Lee YY, Garlock RJ, et al. Process and technoeconomic analysis of leading pretreatment technologies for lignocellulosic ethanol production using switchgrass. Bioresour Technol. 2011;102(24):11105–14.
43. Siqueira G, Bras J, Dufresne A. Cellulosic bionanocomposites: A review of preparation, properties and applications. Polymers (Basel). 2010;2(4):728–65.
44. Eminov S, Brandt A, Wilton-Ely JDET, Hallett JP. The highly selective and near-quantitative conversion of glucose to 5-hydroxymethylfurfural using ionic liquids. PLoS One. 2016;11(10).
45. Ragauskas AJ, Beckham GT, Biddy MJ, Chandra R, Chen F, Davis MF, et al. Lignin valorization: Improving lignin processing in the biorefinery. Science. 2014;344(6185).
46. Van Putten RJ, Van Der Waal JC, De Jong E, Rasrendra CB, Heeres HJ, De Vries JG. Hydroxymethylfurfural, a versatile platform chemical made from renewable resources. Chem Rev. 2013;113(3):1499–597.
47. Brandt A, Chen L, Van Dongen BE, Welton T, Hallett JP. Structural changes in lignins isolated using an acidic ionic liquid water mixture. Green Chem. 2015;17(11):5019–34.
48. Lange JP, Van Der Heide E, Van Buijtenen J, Price R. Furfural-A promising platform for lignocellulosic biofuels. ChemSusChem. 2012;5:150–66.
49. Mainka H, Täger O, Körner E, Hilfert L, Busse S, Edelmann FT, et al. Lignin - An alternative precursor for sustainable and cost-effective automotive carbon fiber. J

Mater Res Technol. 2015;4(3):283–96.
50. Xu C, Arancon RAD, Labidi J, Luque R. Lignin depolymerisation strategies: Towards valuable chemicals and fuels. Chem Soc Rev. 2014 Oct 20;43(22):7485–500.
51. De Wild PJ, Huijgen WJJ, Gosselink RJA. Lignin pyrolysis for profitable lignocellulosic biorefineries. Biofuels, Bioprod Biorefining. 2014 Sep 1;8(5):645–57.
52. Alvira P, Tomás-Pejó E, Ballesteros M, Negro MJ. Pretreatment technologies for an efficient bioethanol production process based on enzymatic hydrolysis: A review. Bioresour Technol. 2010 Jul;101(13):4851–61.
53. Boerjan W, Ralph J, Baucher M. Lignin Biosynthesis. Annu Rev Plant Biol. 2003;54:519–46.
54. Sorek N, Yeats TH, Szemenyei H, Youngs H, Somerville CR. The implications of lignocellulosic biomass chemical composition for the production of advanced biofuels. Bioscience. 2014 Mar 1;64(3):192–201.
55. Chaturvedi V, Verma P. An overview of key pretreatment processes employed for bioconversion of lignocellulosic biomass into biofuels and value added products. 3 Biotech. 2013 Oct 5;3(5):415–31.
56. Kumari D, Singh R. Pretreatment of lignocellulosic wastes for biofuel production: A critical review. Renew Sustain Energy Rev. 2018;90:877–91.
57. Amin FR, Khalid H, Zhang H, Rahman S, Zhang R, Liu G, et al. Pretreatment methods of lignocellulosic biomass for anaerobic digestion. AMB Express. 2017;7(1):72.
58. Putro JN, Soetaredjo FE, Lin SY, Ju YH, Ismadji S. Pretreatment and conversion of lignocellulose biomass into valuable chemicals. RSC Adv. 2016;6(52):46834–52.
59. Singh R, Shukla A, Tiwari S, Srivastava M. A review on delignification of lignocellulosic biomass for enhancement of ethanol production potential. Renew Sustain Energy Rev. 2014;32:713–28.
60. Michelin M, Teixeira JA. Liquid hot water pretreatment of multi feedstocks and enzymatic hydrolysis of solids obtained thereof. Bioresour Technol. 2016;216:862–9.
61. Steinbach D, Kruse A, Sauer J. Pretreatment technologies of lignocellulosic biomass in water in view of furfural and 5-hydroxymethylfurfural production- A review. Biomass Convers Biorefinery. 2017;7(2):247–74.
62. Singh J, Suhag M, Dhaka A. Augmented digestion of lignocellulose by steam explosion, acid and alkaline pretreatment methods: A review. Carbohydr Polym. 2015;117:624–31.
63. Jacquet N, Maniet G, Vanderghem C, Delvigne F, Richel A. Application of Steam Explosion as Pretreatment on Lignocellulosic Material: A Review. Ind Eng Chem Res. 2015;54(10):2593–8.

64. Mathew AK, Parameshwaran B, Sukumaran RK, Pandey A. An evaluation of dilute acid and ammonia fiber explosion pretreatment for cellulosic ethanol production. Bioresour Technol. 2016;199:13–20.
65. Zhao C, Shao Q, Chundawat SPS. Recent advances on ammonia-based pretreatments of lignocellulosic biomass. Bioresour Technol. 2020;298:122446.
66. Kim JS, Lee YY, Kim TH. A review on alkaline pretreatment technology for bioconversion of lignocellulosic biomass. Bioresour Technol. 2016;199:42–8.
67. Yang B, Wyman CE. Pretreatment: The key to unlocking low-cost cellulosic ethanol. Biofuels, Bioprod Biorefining. 2008 Jan;2:26–40.
68. da Costa Sousa L, Chundawat SP, Balan V, Dale BE. “Cradle-to-grave” assessment of existing lignocellulose pretreatment technologies. Curr Opin Biotechnol. 2009;20(3):339–47.
69. Treasure T, Gonzalez R, Jameel H, Phillips RB, Park S, Kelley S. Integrated conversion, financial, and risk modeling of cellulosic ethanol from woody and non-woody biomass via dilute acid pre-treatment. Biofuels, Bioprod Biorefining. 2014 Nov;8(6):755–69.
70. Bozell JJ, Petersen GR. Technology development for the production of biobased products from biorefinery carbohydrates—the US Department of Energy’s “top 10” revisited. Green Chem. 2010;12(4):539–55.
71. Chiappe C, Pieraccini D. Ionic liquids: Solvent properties and organic reactivity. J Phys Org Chem. 2005;18(4):275–97.
72. Plechkova N, Seddon K. Applications of ionic liquids in the chemical industry. Chem Soc Rev. 2008;37(1):123–50.
73. Brandt A, Hallett JP, Leak DJ, Murphy RJ, Welton T. The effect of the ionic liquid anion in the pretreatment of pine wood chips. Green Chem. 2010;12(4):672–67.
74. Ovejero-Pérez A, Rigual V, Domínguez JC, Alonso MV, Oliet M, Rodriguez F. Acidic depolymerization vs ionic liquid solubilization in lignin extraction from eucalyptus wood using the protic ionic liquid 1-methylimidazolium chloride. Int J Biol Macromol. 2020 Aug;157:461–9.
75. Hossain MM, Rawal A, Aldous L. Aprotic vs protic ionic liquids for lignocellulosic biomass pretreatment: Anion effects, enzymatic hydrolysis, solid-state NMR, distillation, and recycle. ACS Sustain Chem Eng. 2019;7(14):11928–36.
76. Kuroda K, Kunimura H, Fukaya Y, Ohno H. 1H NMR analysis of cellulose dissolved in non-deuterated ionic liquids. Cellulose. 2014 May;21(4):2199–206.
77. Hauru LKJ, Hummel M, King AWT, Kilpeläinen I, Sixta H. Role of solvent parameters in the regeneration of cellulose from ionic liquid solutions. Biomacromolecules. 2012;13(9):2896–905.

78. Gschwend FJV, Hallett JP, Brandt-Talbot A. Exploring the effect of water content and anion on the pretreatment of poplar with three 1-Ethyl-3-methylimidazolium ionic liquids. Molecules. 2020;25(10).
79. Ab Rani MA, Brant A, Crowhurst L, Dolan A, Lui M, Hassan NH, et al. Understanding the polarity of ionic liquids. Phys Chem Chem Phys. 2011;13(37):16831–40.
80. Doherty T V., Mora-Pale M, Foley SE, Linhardt RJ, Dordick JS. Ionic liquid solvent properties as predictors of lignocellulose pretreatment efficacy. Green Chem. 2010;12(11):1967–75.
81. Rigual V, Ovejero-Pérez A, Rivas S, Domínguez JC, Alonso MV, Oliet M, et al. Protic, Aprotic, and Choline-Derived Ionic Liquids: Toward Enhancing the Accessibility of Hardwood and Softwood. ACS Sustain Chem Eng. 2020 Jan;8(3):1362–70.
82. Magalhães Da Silva SP, Da Costa Lopes AM, Roseiro LB, Bogel-Łukasik R. Novel pre-treatment and fractionation method for lignocellulosic biomass using ionic liquids. RSC Adv. 2013;3(36):16040–50.
83. Sathitsuksanoh N, Holtman KM, Yelle DJ, Morgan T, Stavila V, Pelton J, et al. Lignin fate and characterization during ionic liquid biomass pretreatment for renewable chemicals and fuels production. Green Chem. 2014 Feb 25;16(3):1236–47.
84. da Costa Lopes AM, João KG, Rubik DF, Bogel-Łukasik E, Duarte LC, Andreaus J, et al. Pre-treatment of lignocellulosic biomass using ionic liquids: Wheat straw fractionation. Bioresour Technol. 2013;142:198–208.
85. Kamlet MJ, Taft RW. The Solvatochromic Comparison Method. I. The β-Scale Of Solvent Hydrogen-Bond Acceptor (HBA) Basicities. J Am Chem Soc. 1976 Jan;98(2):377–83.
86. Abouelela AR, Gschwend F V., Malaret F, Hallett JP. Commercial Aspects of Biomass Deconstruction with Ionic Liquids. In: Commercial Applications of Ionic Liquids. Switzerland: Springer; 2020. p. 87–127.
87. Li W, Sun N, Stoner B, Jiang X, Lu X, Rogers RD. Rapid dissolution of lignocellulosic biomass in ionic liquids using temperatures above the glass transition of lignin. Green Chem. 2011 Jan;13(8):2038–47.
88. Sun N, Rahman M, Qin Y, Maxim ML, Rodríguez H, Rogers RD. Complete dissolution and partial delignification of wood in the ionic liquid 1-ethyl-3-methylimidazolium acetate. Green Chem. 2009 May;11(5):646–65.
89. Viell J, Marquardt W. Concentration measurements in ionic liquid-water mixtures by mid-infrared spectroscopy and indirect hard modeling. Appl Spectrosc. 2012 Feb;66(2):208–17.
90. Fort DA, Remsing RC, Swatloski RP, Moyna P, Moyna G, Rogers RD. Can ionic liquids dissolve wood? Processing and analysis of lignocellulosic materials with 1-n-

butyl-3-methylimidazolium chloride. Green Chem. 2007;9(1):63–9.
91. Wang X, Li H, Cao Y, Tang Q. Cellulose extraction from wood chip in an ionic liquid 1-allyl-3-methylimidazolium chloride (AmimCl). Bioresour Technol. 2011 Sep;102(17):7959–65.
92. Kilpeläinen I, Xie H, King A, Granstrom M, Heikkinen S, Argyropoulos DS. Dissolution of wood in ionic liquids. J Agric Food Chem. 2007 Oct;55(22):9142–8.
93. Leskinen T, King AWT, Kilpeläinen I, Argyropoulos DS. Fractionation of lignocellulosic materials with ionic liquids. Part 1. Effect of mechanical treatment. Ind Eng Chem Res. 2011 Nov;50(22):12349–57.
94. Li Q, He YC, Xian M, Jun G, Xu X, Yang JM, et al. Improving enzymatic hydrolysis of wheat straw using ionic liquid 1-ethyl-3-methyl imidazolium diethyl phosphate pretreatment. Bioresour Technol. 2009 Jul;100(14):3570–5.
95. García-Verdugo E, Altava B, Burguete MI, Lozano P, Luis S V. Ionic liquids and continuous flow processes: A good marriage to design sustainable processes. Green Chem. 2015 May;17(5):2693–713.
96. Tan SSY, MacFarlane DR, Upfal J, Edye LA, Doherty WOS, Patti AF, et al. Extraction of lignin from lignocellulose at atmospheric pressure using alkylbenzenesulfonate ionic liquid. Green Chem. 2009 Mar;11(3):339–34.
97. Brandt-Talbot A, Gschwend FJV, Fennell PS, Lammens TM, Tan B, Weale J, et al. An economically viable ionic liquid for the fractionation of lignocellulosic biomass. Green Chem. 2017;19(13):3078–102.
98. Brandt A, Ray MJ, To TQ, Leak DJ, Murphy RJ, Welton T. Ionic liquid pretreatment of lignocellulosic biomass with ionic liquid–water mixtures. Green Chem. 2011;13(9):2489–99.
99. Chambon CL, Chen M, Fennell PS, Hallett JP. Efficient fractionation of lignin- and ash-rich agricultural residues following treatment with a low-cost protic ionic liquid. Front Chem. 2019 Apr 17;7.
100. Gschwend FJV, Malaret F, Shinde S, Brandt-Talbot A, Hallett JP. Rapid pretreatment of: Miscanthus using the low-cost ionic liquid triethylammonium hydrogen sulfate at elevated temperatures. Green Chem. 2018 Jul 30;20(15):3486–98.
101. Chambon CL, Mkhize TY, Reddy P, Brandt-Talbot A, Deenadayalu N, Fennell PS, et al. Pretreatment of south african sugarcane bagasse using a low-cost protic ionic liquid: A comparison of whole, depithed, fibrous and pith bagasse fractions. Biotechnol Biofuels. 2018 Dec;11:1–16.
102. Malaret F, Gschwend FJV, Lopes JM, Tu WC, Hallett JP. Eucalyptus red grandis pretreatment with protic ionic liquids: Effect of severity and influence of sub/super-critical CO2 atmosphere on pretreatment performance. RSC Adv. 2020 Apr

22;10(27):16050–60.
103. Gschwend FJV, Chambon CL, Biedka M, Brandt-Talbot A, Fennell PS, Hallett JP. Quantitative glucose release from softwood after pretreatment with low-cost ionic liquids. Green Chem. 2019;21(3):692–703.
104. Weigand L, Mostame S, Brandt-Talbot A, Welton T, Hallett JP. Effect of pretreatment severity on the cellulose and lignin isolated from: Salix using ionoSolv pretreatment. Faraday Discuss. 2017 Sep 20;202:331–49.
105. Chambon CL, Fitriyanti V, Verdía P, Yang SM, Hérou S, Titirici MM, et al. Fractionation by Sequential Antisolvent Precipitation of Grass, Softwood, and Hardwood Lignins Isolated Using Low-Cost Ionic Liquids and Water. ACS Sustain Chem Eng. 2020;8(9):3751–61.
106. Tu WC, Weigand L, Hummel M, Sixta H, Brandt-Talbot A, Hallett JP. Characterisation of cellulose pulps isolated from Miscanthus using a low-cost acidic ionic liquid. Cellulose. 2020;27(8):4745–61.
107. Chambon CL, Verdía P, Fennell PS, Hallett JP. Process intensification of the ionoSolv pretreatment: effects of biomass loading, particle size and scale-up from 10 mL to 1 L. Sci Rep. 2021 Jul 28;11(1):1–15.
108. Nakasu PYS, Verdía Barbará P, Firth AEJ, Hallett JP. Pretreatment of biomass with protic ionic liquids. Trends Chem. 2022;4(3):175–8.
109. Chen L, Sharifzadeh M, Mac Dowell N, Welton T, Shah N, Hallett JP. Inexpensive ionic liquids: [HSO4]--based solvent production at bulk scale. Green Chem. 2014 May;16(6):3098–106.
110. Baaqel H, Díaz I, Tulus V, Chachuat B, Guillén-Gosálbez G, Hallett JP. Role of life-cycle externalities in the valuation of protic ionic liquids-a case study in biomass pretreatment solvents. Green Chem. 2020 May 21;22(10):3132–40.
111. George A, Brandt A, Tran K, Zahari SMSNS, Klein-Marcuschamer D, Sun N, et al. Design of low-cost ionic liquids for lignocellulosic biomass pretreatment. Green Chem. 2015 Dec;17(3):1728–34.
112. Verdía P, Brandt A, Hallett JP, Ray MJ, Welton T. Fractionation of lignocellulosic biomass with the ionic liquid 1-butylimidazolium hydrogen sulfate. Green Chem. 2014;16(3):1617–27.
113. Sun J, Konda NVSNM, Parthasarathi R, Dutta T, Valiev M, Xu F, et al. One-pot integrated biofuel production using low-cost biocompatible protic ionic liquids. Green Chem. 2017;19(13):3152–63.
114. Cox BJ, Ekerdt JG. Pretreatment of yellow pine in an acidic ionic liquid: Extraction of hemicellulose and lignin to facilitate enzymatic digestion. Bioresour Technol. 2013 Apr;134:59–65.

115. Pin TC, Nakasu PYS, Mattedi S, Rabelo SC, Costa AC. Screening of protic ionic liquids for sugarcane bagasse pretreatment. Fuel. 2019 Jan;235:1506–14.
116. Miranda R, Neta JV, Romanholo Ferreira LF, Gomes WA, do Nascimento CS, Gomes E, et al. Pineapple crown delignification using low-cost ionic liquid based on ethanolamine and organic acids. Carbohydr Polym. 2019 Feb;206:302–8.
117. Rocha EGA, Pin TC, Rabelo SC, Costa AC. Evaluation of the use of protic ionic liquids on biomass fractionation. Fuel. 2017;206:145–54.
118. Nakasu PYS, Nakasu PYS, Clarke CJ, Rabelo SC, Costa AC, Brandt-Talbot A, et al. Interplay of Acid-Base Ratio and Recycling on the Pretreatment Performance of the Protic Ionic Liquid Monoethanolammonium Acetate. ACS Sustain Chem Eng. 2020;8(21):7952–61.
119. Achinivu EC, Howard RM, Li G, Gracz H, Henderson WA. Lignin extraction from biomass with protic ionic liquids. Green Chem. 2014;16(3):1114–9.
120. Xia S, Baker GA, Li H, Ravula S, Zhao H. Aqueous ionic liquids and deep eutectic solvents for cellulosic biomass pretreatment and saccharification. RSC Adv. 2014 Feb;4(21):10586–96.
121. Kamiya N, Matsushita Y, Hanaki M, Nakashima K, Narita M, Goto M, et al. Enzymatic in situ saccharification of cellulose in aqueous-ionic liquid media. Biotechnol Lett. 2008;30(6):1037–40.
122. Xu J, He B, Wu B, Wang B, Wang C, Hu L. An ionic liquid tolerant cellulase derived from chemically polluted microhabitats and its application in in situ saccharification of rice straw. Bioresour Technol. 2014;157:166–73.
123. Ninomiya K, Kohori A, Tatsumi M, Osawa K, Endo T, Kakuchi R, et al. Ionic liquid/ultrasound pretreatment and in situ enzymatic saccharification of bagasse using biocompatible cholinium ionic liquid. Bioresour Technol. 2015;176:169–74.
124. Shi J, Gladden JM, Sathitsuksanoh N, Kambam P, Sandoval L, Mitra D, et al. One-pot ionic liquid pretreatment and saccharification of switchgrass. Green Chem. 2013;15(9):2579–89.
125. Grewal J, Ahmad R, Khare SK. Development of cellulase-nanoconjugates with enhanced ionic liquid and thermal stability for in situ lignocellulose saccharification. Bioresour Technol. 2017;242:236–43.
126. Ben Hmad I, Gargouri A. Ionic liquid-tolerant cellulase system of Stachybotrys microspora exploited in the in situ saccharification of lignocellulosic biomass. J Mol Liq. 2020;310.
127. Xu J, Wu B, Hu L, Wu Z, Xu N, Dai B, et al. Enzymatic in situ saccharification of lignocellulose in a compatible ionic liquid-cellulase system. Chem Eng J. 2015;267:163–9.

128. Nargotra P, Vaid S, Bajaj BK. Cellulase Production from Bacillus subtilis SV1 and Its Application Potential for Saccharification of Ionic Liquid Pretreated Pine Needle Biomass under One Pot Consolidated Bioprocess. Fermentation. 2016;2(4).
129. Grewal J, Khare SK. One-pot bioprocess for lactic acid production from lignocellulosic agro-wastes by using ionic liquid stable Lactobacillus brevis. Bioresour Technol. 2018;251:268–73.
130. Liu L, Li Z, Hou W, Shen H. Direct conversion of lignocellulose to levulinic acid catalyzed by ionic liquid. Carbohydr Polym. 2018;181:778–84.
131. Khan AS, Man Z, Bustam MA, Nasrullah A, Ullah Z, Sarwono A, et al. Efficient conversion of lignocellulosic biomass to levulinic acid using acidic ionic liquids. Carbohydr Polym. 2018;181:208–14.
132. Ramli NAS, Amin NAS. Optimization of Biomass Conversion to Levulinic Acid in Acidic Ionic Liquid and Upgrading of Levulinic Acid to Ethyl Levulinate. Bioenergy Res. 2017;10(1):50–63.
133. Amoah J, Ogura K, Schmetz Q, Kondo A, Ogino C. Co-fermentation of xylose and glucose from ionic liquid pretreated sugar cane bagasse for bioethanol production using engineered xylose assimilating yeast. Biomass and Bioenergy. 2019;128.
134. Yamada R, Nakashima K, Asai-Nakashima N, Tokuhara W, Ishida N, Katahira S, et al. Direct Ethanol Production from Ionic Liquid-Pretreated Lignocellulosic Biomass by Cellulase-Displaying Yeasts. Appl Biochem Biotechnol. 2017;182(1):229–37.
135. Carrozza CF, Papa G, Citterio A, Sebastiano R, Simmons BA, Singh S. One-pot bio-derived ionic liquid conversion followed by hydrogenolysis reaction for biomass valorization: A promising approach affecting the morphology and quality of lignin of switchgrass and poplar. Bioresour Technol. 2019 Dec 1;294.
136. Liszka MJ, Kang A, Konda NVSNM, Tran K, Gladden JM, Singh S, et al. Switchable ionic liquids based on di-carboxylic acids for one-pot conversion of biomass to an advanced biofuel. Green Chem. 2016;18(14):4012–21.
137. Xu F, Sun J, Konda NVSNM, Shi J, Dutta T, Scown CD, et al. Transforming biomass conversion with ionic liquids: Process intensification and the development of a high-gravity, one-pot process for the production of cellulosic ethanol. Energy Environ Sci. 2016 Mar 1;9(3):1042–9.
138. Rigual V, Papa G, Rodriguez A, Wehrs M, Kim KH, Oliet M, et al. Evaluating Protic Ionic Liquid for Woody Biomass One-Pot Pretreatment + Saccharification, Followed by Rhodosporidium toruloides Cultivation. ACS Sustain Chem Eng. 2020;8(2):782–91.
139. Sundstrom E, Yaegashi J, Yan J, Masson F, Papa G, Rodriguez A, et al. Demonstrating a separation-free process coupling ionic liquid pretreatment,

saccharification, and fermentation with: Rhodosporidium toruloides to produce advanced biofuels. Green Chem. 2018;20(12):2870–9.

140. Park JI, Steen EJ, Burd H, Evans SS, Redding-Johnson AM, Batth T, et al. A thermophilic ionic liquid-tolerant cellulase cocktail for the production of cellulosic biofuels. PLoS One. 2012;7(5).
141. Yan J, Liang L, He Q, Li C, Xu F, Sun J, et al. Methyl Ketones from Municipal Solid Waste Blends by One-Pot Ionic-Liquid Pretreatment, Saccharification, and Fermentation. ChemSusChem. 2019;12(18):4313–22.
142. Matsagar BM, Hossain SA, Islam T, Alamri HR, Alothman ZA, Yamauchi Y, et al. Direct Production of Furfural in One-pot Fashion from Raw Biomass Using Brønsted Acidic Ionic Liquids. Sci Rep. 2017;7(1):1–7.
143. Yu H, Hu J, Fan J, Chang J. One-pot conversion of sugars and lignin in ionic liquid and recycling of ionic liquid. Ind Eng Chem Res. 2012;51(8):3452–7.
144. Imteyaz Alam M, De S, Dutta S, Saha B. Solid-acid and ionic-liquid catalyzed one-pot transformation of biorenewable substrates into a platform chemical and a promising biofuel. RSC Adv. 2012;2(17):6890–6.
145. Li M, Jiang H, Zhang L, Yu X, Liu H, Yagoub AEGA, et al. Synthesis of 5-HMF from an ultrasound-ionic liquid pretreated sugarcane bagasse by using a microwave-solid acid/ionic liquid system. Ind Crops Prod. 2020;149:112361.
146. Li Y, Zhang X, Li Z, Song J, Wang X. Full Utilization of Lignocellulose with Ionic Liquid Polyoxometalates in a One-Pot Three-Step Conversion. ChemSusChem. 2019;12(22):4936–45.
147. Shi N, Liu D, Huang Q, Guo Z, Jiang R, Wang F, et al. Product-oriented decomposition of lignocellulose catalyzed by novel polyoxometalates-ionic liquid mixture. Bioresour Technol. 2019;283:174–83.
148. Trivedi N, Gupta V, Reddy CRK, Jha B. Detection of ionic liquid stable cellulase produced by the marine bacterium Pseudoalteromonas sp. isolated from brown alga Sargassum polycystum C. Agardh. Bioresour Technol. 2013;132:313–9.
149. Vaid S, Mishra T, Bajaj BK. Ionic-liquid-mediated pretreatment and enzymatic saccharification of Prosopis sp. biomass in a consolidated bioprocess for potential bioethanol fuel production. Energy, Ecol Environ. 2018;3(4):216–28.
150. Vaid S, Bajaj BK. Production of Ionic Liquid Tolerant Cellulase from Bacillus subtilis G2 Using Agroindustrial Residues with Application Potential for Saccharification of Biomass Under One Pot Consolidated Bioprocess. Waste and Biomass Valorization. 2017;8(3):949–64.
151. Gladden JM, Allgaier M, Miller CS, Hazen TC, VanderGheynst JS, Hugenholtz P, et al. Glycoside hydrolase activities of thermophilic bacterial consortia adapted to

switchgrass. Appl Environ Microbiol. 2011;77(16):5804–12.
152. Frederix M, Mingardon F, Hu M, Sun N, Pray T, Singh S, et al. Development of an: E. coli strain for one-pot biofuel production from ionic liquid pretreated cellulose and switchgrass. Green Chem. 2016;18(15):4189–97.
153. Sitepu I, Enriquez L, Nguyen V, Fry R, Simmons B, Singer S, et al. Ionic Liquid Tolerance of Yeasts in Family Dipodascaceae and Genus Wickerhamomyces. Appl Biochem Biotechnol. 2020;191(4):1580–93.
154. Sitepu IR, Enriquez LL, Nguyen V, Doyle C, Simmons BA, Singer SW, et al. Ethanol production in switchgrass hydrolysate by ionic liquid-tolerant yeasts. Bioresour Technol Reports. 2019;7.
155. Mehmood N, Alayoubi R, Husson E, Jacquard C, Büchs J, Sarazin C, et al. Kluyveromyces marxianus, an attractive yeast for ethanolic fermentation in the presence of imidazolium ionic liquids. Int J Mol Sci. 2018;19(3).
156. Yadav N, Pranaw K, Khare SK. Screening of lactic acid bacteria stable in ionic liquids and lignocellulosic by-products for bio-based lactic acid production. Bioresour Technol Reports. 2020;11.
157. Douglas J. Conceptual Design of Chemical Processes. Clark B, Bradley J, editors. Singapore: McGraw-Hill Book Company; 1988.
158. Stojanovic A, Keppler BK. Ionic Liquids as Extracting Agents for Heavy Metals. Sep Sci Technol. 2012 Jan 15;47(2):189–203.
159. Janssen CHC, Macías-Ruvalcaba NA, Aguilar-Martínez M, Kobrak MN. Copper extraction using protic ionic liquids: Evidence of the Hofmeister effect. Sep Purif Technol. 2016 Aug;168:275–83.
160. Yao JG, Tan SY, Metcalfe PI, Fennell PS, Kelsall GH, Hallett JP. Demetallization of Sewage Sludge Using Low-Cost Ionic Liquids. Environ Sci Technol. 2021;55(8):5291–300.
161. Suryanto BHR, Gunawan CA, Lu X, Zhao C. Tuning the electrodeposition parameters of silver to yield micro/nano structures from room temperature protic ionic liquids. Electrochim Acta. 2012 Oct;81:98–105.
162. Gunawan CA, Suryanto BHR, Zhao C. Electrochemical Study of Copper in Room Temperature Protic Ionic Liquids Ethylammonium Nitrate and Triethylammonium Methylsulfonate. J Electrochem Soc. 2012;159(10).
163. El Abedin SZ, Pölleth M, Meiss SA, Janek J, Endres F. Ionic liquids as green electrolytes for the electrodeposition of nanomaterials. Green Chem. 2007;9(6):549–55.
164. Liu Z, Abedin SZ El, Endres F. Electrodeposition of zinc films from ionic liquids and ionic liquid/water mixtures. Electrochim Acta. 2013;89:635–43.

165. Abbott AP, El Ttaib K, Ryder KS, Smith EL. Electrodeposition of nickel using eutectic based ionic liquids. Trans Inst Met Finish. 2008;86(4):234–40.
166. Endres F, MacFarlane D, Abbott A. Electrodeposition from Ionic Liquids. Weinheim, Germany: Wiley-VCH Verlag GmbH & Co. KGaA; 2008.
167. Chan CP, Lam H, Surya C. Preparation of Cu2ZnSnS4 films by electrodeposition using ionic liquids. Sol Energy Mater Sol Cells. 2010 Feb;94(2):207–11.
168. Klein-Marcuschamer D, Simmons BA, Blanch HW. Techno-economic analysis of a lignocellulosic ethanol biorefinery with ionic liquid pre-treatment. Biofuels, Bioprod Biorefining. 2011 Sep 1;5(5):562–9.
169. Auxenfans T, Buchoux S, Larcher D, Husson G, Husson E, Sarazin C. Enzymatic saccharification and structural properties of industrial wood sawdust: Recycled ionic liquids pretreatments. Energy Convers Manag. 2014 Dec;88(1):1094–103.
170. Qiu Z, Aita GM. Pretreatment of energy cane bagasse with recycled ionic liquid for enzymatic hydrolysis. Bioresour Technol. 2013 Feb;129:532–7.
171. Coulon, F Jiang, Y Longhurst, P Shaw, H Harries, N Bone, B Earl, N Moreby S. Examination of contaminated land sector activity in England - SP101 [Internet]. 2014. Available from: http://randd.defra.gov.uk
172. Kibble, A Harold P. Contaminated Land and Human Health. Harrison R, editor. Environmental Pollutant Exposures and Public Health. Croydon: Royal Society of Chemistry; 2020.
173. Van Liedekerke M, Prokop G, Rabl-Berger S, Kibblewhite M, Louwagie G. Progress in the management of Contaminated Sites in Europe [Internet]. JRC Reference Reports. Elsevier; 2014 [cited 2016 Aug 17]. Available from: http://www.eea.europa.eu/data-and-maps/indicators/progress-in-management-of-contaminated-sites-3/assessment#toc-0
174. European Commission. In Depth Report - Soil Contamination : Impacts on Human Health. Science for Environmental Policy. 2013.
175. Khalid S, Shahid M, Natasha, Bibi I, Sarwar T, Shah AH, et al. A review of environmental contamination and health risk assessment of wastewater use for crop irrigation with a focus on low and high-income countries. Int J Environ Res Public Health. 2018;15(5).
176. Dar SA, Lone FA, Dar SA, Bhat RA, Bashir I, Mir SA, et al. Bioremediation and Biotechnology, Vol 2. Bioremediation Biotechnol Vol 2. 2020;2:207–19.
177. Smith, B Rawlins, BG Ferguson, AJ Fordyce, F Hutchins, MG FInnamore, JR Barr D. Information on Land Quality in England - R&D Technical Report. Environment Agency. 2002.
178. Dealing with Contaminated land in England: A review of progress from April 2000 to

December 2013 with Part 2A of the Environmental Protection Act 1990. Environment Agency. Bristol; 2016.
179. Dealing with contaminated land in England and Wales: A review of progress from 2000-2007 with Part 2A of the Environmental Protection Act. Environment Agency. Bristol; 2009.
180. Hakeem K, Ṣābir M, Öztürk M, Mermut A. Phytoremediation of Soils: Prospects and Challenges. In: Hakeem K, editor. Soil Remediation and Plants: Prospects and Challenges. Amsterdam: Elsevier/AP; 2015. p. 1–36.
181. Tangahu BV, Sheikh Abdullah SR, Basri H, Idris M, Anuar N, Mukhlisin M. A review on heavy metals (As, Pb, and Hg) uptake by plants through phytoremediation. Int J Chem Eng. 2011;2011:1–31.
182. Jankong P, Visoottiviseth P, Khokiattiwong S. Enhanced phytoremediation of arsenic contaminated land. Chemosphere. 2007 Aug;68(10):1906–12.
183. Vamerali T, Bandiera M, Mosca G. In situ phytoremediation of arsenic- and metal-polluted pyrite waste with field crops: Effects of soil management. Chemosphere. 2011 May;83(9):1241–8.
184. Reeves RD, Baker AJM, Jaffré T, Erskine PD, Echevarria G, van der Ent A. A global database for plants that hyperaccumulate metal and metalloid trace elements. New Phytol. 2018 Apr 1;218(2):407–11.
185. Clemens S, Palmgren MG, Krämer U. A long way ahead: Understanding and engineering plant metal accumulation. Trends Plant Sci. 2002;7(7):309–15.
186. IPCC. Climate Change and Land: an IPCC special report on climate change, desertification, land degradation, sustainable land management, food security, and greenhouse gas fluxes in terrestrial ecosystems [Internet]. Shukla P, Skea J, Calvo Buendia E, Masson-Delmotte V, Pörtner HO, Roberts D, et al., editors. In Press; 2019 [cited 2020 Dec 4]. Available from: https://www.ipcc.ch/srccl/
187. Verma M. Ecotoxicology of Heavy Metals: Sources, Effects and Toxicity. In: Bioremediation and Biotechnology, Vol 2. Cham, Switzerland: Springer; 2020. p. 13–23.
188. Chaney R, Angle J, Broadhurst C, Peters C, Tappero R, Sparks D. Improved Understanding of Hyperaccumulation Yields Commercial Phytoextraction and Phytomining Technologies. J Environ Qual. 2007;36(5):1429–43.
189. Sheoran V, Sheoran AS, Poonia P. Phytomining: A review. Miner Eng. 2009;22(12):1007–19.
190. Brooks R, Chambers M, Nicks L, Robinson B. Phytomining. Trends Plant Sci. 1998;3(9):359–62.
191. van der Ent A, Reeves RD. Foliar metal accumulation in plants from copper-rich

ultramafic outcrops: case studies from Malaysia and Brazil. Plant Soil. 2015;389(1–2):401–18.

192. Robinson BH, Chiarucci A, Brooks RR, Petit D, Kirkman JH, Gregg PEH, et al. The nickel hyperaccumulator plant Alyssum bertolonii as a potential agent for phytoremediation and phytomining of nickel. J Geochemical Explor. 1997 Jun;59(2):75–86.
193. Liang HM, Lin TH, Chiou JM, Yeh KC. Model evaluation of the phytoextraction potential of heavy metal hyperaccumulators and non-hyperaccumulators. Environ Pollut. 2009;157(6):1945–52.
194. Niu Z xin, Sun L na, Sun T heng, Li Y shuang, Wang H. Evaluation of phytoextracting cadmium and lead by sunflower, ricinus, alfalfa and mustard in hydroponic culture. J Environ Sci. 2007;19(8):961–7.
195. Tariq SR, Ashraf A. Comparative evaluation of phytoremediation of metal contaminated soil of firing range by four different plant species. Arab J Chem. 2016 Nov 1;9(6):806–14.
196. Pulford ID, Watson C. Phytoremediation of heavy metal-contaminated land by trees - A review. Environ Int. 2003;29(4):529–40.
197. Lone MI, He ZL, Stoffella PJ, Yang XE. Phytoremediation of heavy metal polluted soils and water: Progresses and perspectives. J Zhejiang Univ Sci B. 2008;9(3):210–20.
198. Stewart J, Toma Y, Fernàndez F, Nishikawi A, Yamada T, Bollero G. The ecology and agronomy of Miscanthus sinensis , a species important to bioenergy crop development, in its native range in Japan: a review. GCB Bioenergy. 2009 Apr 1;1(2):126–53.
199. Chou CH. Miscanthus plants used as an alternative biofuel material: The basic studies on ecology and molecular evolution. Renew Energy. 2009 Aug 1;34(8):1908–12.
200. Huang LS, Flavell R, Donnison IS, Chiang YC, Hastings A, Hayes C, et al. Collecting wild Miscanthus germplasm in Asia for crop improvement and conservation in Europe whilst adhering to the guidelines of the United Nations' convention on biological diversity. Ann Bot. 2019 Sep 13;124(4):591–604.
201. Mahar A, Wang P, Ali A, Awasthi MK, Lahori AH, Wang Q, et al. Challenges and opportunities in the phytoremediation of heavy metals contaminated soils: A review. Ecotoxicol Environ Saf. 2016;126:111–21.
202. Nsanganwimana F, Pourrut B, Mench M, Douay F. Suitability of Miscanthus species for managing inorganic and organic contaminated land and restoring ecosystem services. A review. J Environ Manage. 2014 Oct 1;143:123–34.

203. Pogrzeba M, Krzyżak J, Rusinowski S, McCalmont JP, Jensen E. Energy crop at heavy metal-contaminated arable land as an alternative for food and feed production: Biomass quantity and quality. Plant Met Funct Omi A Syst Perspect. 2019 Jan 1;1–21.
204. Rusinowski S, Krzyżak J, Clifton-Brown J, Jensen E, Mos M, Webster R, et al. New Miscanthus hybrids cultivated at a Polish metal-contaminated site demonstrate high stomatal regulation and reduced shoot Pb and Cd concentrations. Environ Pollut. 2019 Sep 1;252:1377–87.
205. Clifton-Brown J, Hastings A, Mos M, McCalmont JP, Ashman C, Awty-Carroll D, et al. Progress in upscaling Miscanthus biomass production for the European bio-economy with seed-based hybrids. GCB Bioenergy. 2017 Jan 1;9:6–17.
206. Clifton-Brown J, Schwarz KU, Awty-Carroll D, Iurato A, Meyer H, Greef J, et al. Breeding strategies to improve Miscanthus as a sustainable source of biomass for bioenergy and biorenewable products. Agronomy. 2019 Oct 24;9(11):673.
207. Krzyżak J, Pogrzeba M, Rusinowski S, Clifton-Brown J, McCalmont JP, Kiesel A, et al. Heavy Metal Uptake by Novel Miscanthus Seed-Based Hybrids Cultivated in Heavy Metal Contaminated Soil. Civ Environ Eng Reports. 2017 Sep 26;26(3):121–32.
208. Kacálková L, Tlustoš P, Száková J. Phytoextraction of Risk Elements by Willow and Poplar Trees. Int J Phytoremediation. 2015 May 4;17(5):414–21.
209. Wieshammer G, Unterbrunner R, García TB, Zivkovic MF, Puschenreiter M, Wenzel WW. Phytoextraction of Cd and Zn from agricultural soils by Salix ssp. and intercropping of Salix caprea and Arabidopsis halleri. Plant Soil. 2007 Sep 12;298(1–2):255–64.
210. Subhashini V, Swamy AVVS, Krishna RH. Pot Experiment: To Study the Uptake of Zinc by Different Plant Species in Artificially Contaminated Soil. World J Environ Eng. 2013;1(2):27–33.
211. Wuana RA, Okieimen FE. Heavy Metals in Contaminated Soils: A Review of Sources, Chemistry, Risks and Best Available Strategies for Remediation. ISRN Ecol. 2011 Oct 24;1–20.
212. Wei S, Teixeira da Silva JA, Zhou Q. Agro-improving method of phytoextracting heavy metal contaminated soil. J Hazard Mater. 2008;150(3):662–8.
213. Wood JL, Tang C, Franks AE. Microbial associated plant growth and heavy metal accumulation to improve phytoextraction of contaminated soils. Soil Biol Biochem. 2016;103:131–7.
214. Rascio N, Navari-Izzo F. Heavy metal hyperaccumulating plants: How and why do they do it? And what makes them so interesting? Plant Sci. 2011;180(2):169–81.
215. Bhargava A, Carmona FF, Bhargava M, Srivastava S. Approaches for enhanced

phytoextraction of heavy metals. J Environ Manage. 2012;105:103–20.
216. Souza LA, Piotto FA, Nogueirol RC, Azevedo RA. Use of non-hyperaccumulator plant species for the phytoextraction of heavy metals using chelating agents. Sci Agric. 2013;70(4):290–5.
217. Chaney RL, Baker AJM, Morel JL. The Long Road to Developing Agromining/Phytomining. In: Agromining: Farming for Metals. Cham: Springer; 2021. p. 1–22.
218. Zhang X, Houzelot V, Plasari E, Barbaroux R, Laubie B, Mercier G, et al. Phytomining : a Win-Win Partnership Between Agronomy and Chemical Engineering To Recycle Metals Dispersed in Soils. In: GPE – 4th International Congress on Green Process Engineering. 2014.
219. Kidd P, Mench M, Álvarez-López V, Bert V, Dimitriou I, Friesl-Hanl W, et al. Agronomic Practices for Improving Gentle Remediation of Trace Element-Contaminated Soils. Int J Phytoremediation. 2015;17(11):1005–37.
220. Bani A, Echevarria G, Sulçe S, Morel JL. Improving the Agronomy of Alyssum murale for Extensive Phytomining: A Five-Year Field Study. Int J Phytoremediation. 2015;17(2):117–27.
221. Bani A, Echevarria G, Sulçe S, Morel JL, Mullai A. In-situ phytoextraction of Ni by a native population of Alyssum murale on an ultramafic site (Albania). Plant Soil. 2007;293(1–2):79–89.
222. Ghosh M, Singh S. A Review on Phytoremediation of Heavy Metals And Utilization of its Byproducts. Appl Ecol Environ Res. 2005;3(1):153–79.
223. Morel JL, Simonnot MO, Echevarria G, van der Ent A, Baker AJM. Conclusions and Outlook for Agromining. In: Agromining : farming for metals :extracting unconventional resources using plants. 2nd ed. Cham: Springer; 2021. p. 485–9.
224. Van der Ent A, Echevarria G, Baker AJM, Morel JL. Agromining: Farming for Metals. Agromining: Farming for Metals. Cham: Springer; 2018.
225. Jiang Y, Ameh A, Lei M, Duan L, Longhurst P. Solid–gaseous phase transformation of elemental contaminants during the gasification of biomass. Sci Total Environ. 2016 Sep 1;563–564:724–30.
226. Koppolu L, Agblevor FA, Clements LD. Pyrolysis as a technique for separating heavy metals from hyperaccumulators. Part II: Lab-scale pyrolysis of synthetic hyperaccumulator biomass. Biomass and Bioenergy. 2003 Dec 1;25(6):651–63.
227. Asad M, Menana Z, Ziegler-Devin I, Bert V, Chalot M, Herzig R, et al. Pretreatment of trace element-enriched biomasses grown on phytomanaged soils for bioethanol production. Ind Crops Prod. 2017 Nov 15;107:63–72.
228. Bert V, Neub S, Zdanevitch I, Friesl-Hanl W, Collet S, Gaucher R, et al. How to

manage plant biomass originated from phytotechnologies? Gathering perceptions from end-users. Int J Phytoremediation. 2017;19(10):947–54.
229. Nzihou A, Stanmore B. The fate of heavy metals during combustion and gasification of contaminated biomass: A brief review. J Hazard Mater. 2013;256–257:56–66.
230. van Ginneken L, Meers E, Guisson R, Ruttens A, Elst K, Tack MG, et al. Phytoremediation for heavy metal - contaminated soils combined with bioenergy production. J Environ Eng Landsc Manag. 2010;15(4):227–36.
231. Vigil M, Marey-Pérez MF, Martinez Huerta G, Álvarez Cabal V. Is phytoremediation without biomass valorization sustainable? Comparative LCA of landfilling vs. anaerobic co-digestion. Sci Total Environ. 2015;505:844–50.
232. Lord RA. Reed canarygrass (Phalaris arundinacea) outperforms Miscanthus or willow on marginal soils, brownfield and non-agricultural sites for local, sustainable energy crop production. Biomass and Bioenergy. 2015 Jul 1;78:110–25.
233. Laubie B, Vaughan J, Simonnot MO. Processing of Hyperaccumulator Plants to Nickel Products. In: Agromining: Farming for Metals. Cham: Springer; 2021. p. 47–61.
234. Chaney R, Angle J, Baker A. Method for phytomining of nickel, cobalt and other metals from soil. United States Patent. United-States; Patent 5944872, 1999.
235. Barbaroux R, Mercier G, Blais JF, Morel JL, Simonnot MO. A new method for obtaining nickel metal from the hyperaccumulator plant Alyssum murale. Sep Purif Technol. 2011 Nov 15;83(1):57–65.
236. Zhang X. Procédé hyrométallurgique pour la valorisation du nickel contenu dans les plantes hyperaccumulatrices. PhD Thesis. Université de Lorraine; 2014.
237. Li YM, Chaney R, Reeves R, Angle J, Baker A. Thlaspi caerulescens subspecies for cadmium and zinc recovery. United-States; Patent 0038334 A1, 2007.
238. Jally B, Laubie B, Tang YT, Simonnot MO. Processing of Plants to Products: Gold, REEs and Other Elements. In: Agromining: Farming for Metals. Cham: Springer; 2021. p. 63–74.
239. Oh K, Li T, Cheng H, Hu X, He C, Yan L, et al. Development of Profitable Phytoremediation of Contaminated Soils with Biofuel Crops. J Environ Prot (Irvine, Calif). 2013;04(04):58–64.
240. Burges A, Alkorta I, Epelde L, Garbisu C. From phytoremediation of soil contaminants to phytomanagement of ecosystem services in metal contaminated sites. Int J Phytoremediation. 2018;20(4):384–97.
241. Van Ginneken L, Meers E, Guisson R, Ruttens A, Elst K, Tack FMG, et al. Phytoremediation for heavy metal-contaminated soils combined with bioenergy production. J Environ Eng Landsc Manag. 2007;15(4):227–36.
242. Kocoń A, Matyka M. Phytoextractive potential of Miscanthus giganteus and Sida

hermaphrodita growing under moderate pollution of soil with Zn and Pb. J Food, Agric Environ. 2012;10(2):1253–6.

243. Vamerali T, Bandiera M, Mosca G. Field crops for phytoremediation of metal-contaminated land. A review. Environ Chem Lett. 2010;8:1–17.
244. Pandey S, Pandey A. Capability Development and Technology Transfer Essential for Economic Transformation. Green Chem Environ Remediat. 2012;137–51.
245. Abhilash PC, Yunus M. Can we use biomass produced from phytoremediation? Biomass and Bioenergy. 2011;35(3):1371–2.
246. Jiang Y, Lei M, Duan L, Longhurst P. Integrating phytoremediation with biomass valorisation and critical element recovery: A UK contaminated land perspective. Biomass and Bioenergy. 2015;83:328–39.
247. Gomes HI. Phytoremediation for bioenergy: challenges and opportunities. Environ Technol Rev. 2012;59–66.
248. Dastyar W, Zhao M, Yuan W, Li H, Ting ZJ, Ghaedi H, et al. Effective Pretreatment of Heavy Metal-Contaminated Biomass Using a Low-Cost Ionic Liquid (Triethylammonium Hydrogen Sulfate): Optimization by Response Surface Methodology-Box Behnken Design. ACS Sustain Chem Eng. 2019 May 15;7(13):11571–81.
249. Tripathi V, Edrisi SA, Abhilash PC. Towards the coupling of phytoremediation with bioenergy production. Renew Sustain Energy Rev. 2016;57:1386–9.
250. Sotenko M, Coles S, Barker G, Song L, Jiang Y, Longhurst P, et al. Phytoremediation-biorefinery tandem for effective clean-up of metal contaminated soil and biomass valorisation. Int J Phytoremediation. 2017;19(11):965–75.
251. Dastyar W, Raheem A, He J, Zhao M. Biofuel Production Using Thermochemical Conversion of Heavy Metal-Contaminated Biomass (HMCB) Harvested from Phytoextraction Process. Chem Eng J. 2019 Feb 15;358:759–85.
252. Koppolu L, Clements LD. Pyrolysis as a technique for separation heavy metals from hyperaccumulators. Part I: Preparation of synthetic hyperaccumulator biomass. Biomass and Bioenergy. 2003;24:67–79.
253. Sas-Nowosielska A, Kucharski R, Małkowski E, Pogrzeba M, Kuperberg JM, Kryński K. Phytoextraction crop disposal - An unsolved problem. Environ Pollut. 2004;128(3):373–9.
254. Tian Y, Zhang H. Producing biogas from agricultural residues generated during phytoremediation process: Possibility, threshold, and challenges. Int J Green Energy. 2016;13(15):1556–63.
255. Bwlch Glas Mine, Talybont, Ceulanymaesmawr, Ceredigion, Wales, UK [Internet]. [cited 2021 May 29]. Available from: https://www.mindat.org/loc-4265.html

256. Miscanthus for Contaminated and Marginal Lands PLUS [Internet]. [cited 2021 Jun 18]. Available from: https://www.miscomar.eu/
257. Lachapelle-T. X, Labrecque M, Comeau Y. Treatment and valorization of a primary municipal wastewater by a short rotation willow coppice vegetation filter. Ecol Eng. 2019;130:32–44.
258. Jerbi A, Brereton NJB, Sas E, Amiot S, Lachapelle-T. X, Comeau Y, et al. High biomass yield increases in a primary effluent wastewater phytofiltration are associated to altered leaf morphology and stomatal size in Salix miyabeana. Sci Total Environ. 2020;738.
259. Sluiter A, Hames B, Hyman D, Payne C, Ruiz R, Scarlata C, et al. Determination of total solids in biomass and total dissolved solids in liquid process samples. Natl Renew Energy Lab. 2008;(TP-510-42621).
260. Carney PM. Record of Determination of Cinderhill (Acid Tar Pits), Kilburn , Derbyshire as Contaminated Land. [Internet]. 2007. Available from: https://info.ambervalley.gov.uk/docarc/docviewer.aspx?docGuid=305a00eca8924587b87e8b4ef4b1b4a4
261. Amber Valley Borough Council. Cinderhill Tar Pits, Kilburn – Determination of Contaminated Land and Designation as a 'Special Site.' [Internet]. 2007. Available from: https://info.ambervalley.gov.uk/docarc/docviewer.aspx?docGuid=381ce1b9729f48888eefcceba06033d8
262. Dohrmann R. Cation exchange capacity methodology II: A modified silver-thiourea method. Appl Clay Sci. 2006 Oct 1;34(1–4):38–46.
263. Soil Survey Staff. Kellogg Soil Survey Laboratory Methods Manual. U.S. Department of Agriculture, Natural Resources Conservation Service. 2014;(5):42.
264. A. Sluiter, R. Ruiz, C. Scarlata, J. Sluiter A. Determination of Extractives in Biomass - Technical Report. Natl Renew Energy Lab. 2008;(TP-510-42619).
265. Sluiter A, Hames B, Ruiz RO, Scarlata C, Sluiter J, Templeton D, et al. Determination of Structural Carbohydrates and Lignin in Biomass. Natl Renew Energy Lab. 2011;(TP-510-42618).
266. Pluskal T, Castillo S, Villar-Briones A, Orešič M. MZmine 2: Modular framework for processing, visualizing, and analyzing mass spectrometry-based molecular profile data. BMC Bioinformatics. 2010;11(1):395.
267. Schmid R, Petras D, Nothias LF, Wang M, Aron A, Jagels A, et al. Ion Identity Molecular Networking in the GNPS Environment. bioRxiv. 2020.
268. Chong J, Wishart DS, Xia J. Using MetaboAnalyst 4.0 for Comprehensive and Integrative Metabolomics Data Analysis. Curr Protoc Bioinforma. 2019;68.

269. Xia J, Psychogios N, Young N, Wishart DS. MetaboAnalyst: A web server for metabolomic data analysis and interpretation. Nucleic Acids Res. 2009;37.
270. Oksanen AJ, Blanchet FG, Kindt R, Legen- P, Minchin PR, Hara RBO, et al. Community Ecology Package [Internet]. version 2. Ecology Package. https://CRAN.R-project.org/package=vegan; 2012. p. 263. Available from: http://mirror.bjtu.edu.cn/cran/web/packages/vegan/vegan.pdf
271. Gil de la Fuente A, Godzien J, Fernández López M, Rupérez FJ, Barbas C, Otero A. Knowledge-based metabolite annotation tool: CEU Mass Mediator. J Pharm Biomed Anal. 2018;154:138–49.
272. Caspi R, Billington R, Keseler IM, Kothari A, Krummenacker M, Midford PE, et al. The MetaCyc database of metabolic pathways and enzymes-a 2019 update. Nucleic Acids Res. 2020;48(D1):D455–D453.
273. Nothias, Petras, Schmid, Sarvepalli. Feature-based Molecular Networking in the GNPS Analysis Environment. Nat Methods. 2019;17(9):905–8.
274. Dührkop K, Fleischauer M, Ludwig M, Aksenov AA, Melnik A V., Meusel M, et al. SIRIUS 4: a rapid tool for turning tandem mass spectra into metabolite structure information. Nat Methods. 2019;16(4):299–302.
275. Dührkop K, Nothias LF, Fleischauer M, Reher R, Ludwig M, Hoffmann MA, et al. Systematic classification of unknown metabolites using high-resolution fragmentation mass spectra. Nat Biotechnol. 2021;39(4):462–71.
276. Sumner LW, Amberg A, Barrett D, Beale MH, Beger R, Daykin CA, et al. Proposed minimum reporting standards for chemical analysis: Chemical Analysis Working Group (CAWG) Metabolomics Standards Initiative (MSI). Metabolomics. 2007;3(3):211–21.
277. Djoumbou Feunang Y, Eisner R, Knox C, Chepelev L, Hastings J, Owen G, et al. ClassyFire: automated chemical classification with a comprehensive, computable taxonomy. J Cheminform. 2016;8(1):1–20.
278. Gschwend FJV, Brandt A, Chambon CL, Tu WC, Weigand L, Hallett JP. Pretreatment of lignocellulosic biomass with low-cost Ionic liquids. J Vis Exp [Internet]. 2016 Aug 10 [cited 2016 Aug 19];(114). Available from: http://www.jove.com/video/54246/pretreatment-of-lignocellulosic-biomass-with-low-cost-ionic-liquids
279. Fernandes Diniz JMB, Gil MH, Castro JAAM. Hornification - Its origin and interpretation in wood pulps. Wood Sci Technol. 2004;37(6):489–94.
280. Iwamoto S, Abe K, Yano H. The effect of hemicelluloses on wood pulp nanofibrillation and nanofiber network characteristics. Biomacromolecules. 2008;9(3):1022–6.
281. Luo XL, Zhu JY, Gleisner R, Zhan HY. Effects of wet-pressing-induced fiber

hornification on enzymatic saccharification of lignocelluloses. Cellulose. 2011;18(4):1055–62.
282. Resch MG, Baker JO, Decker SR. Low Solids Enzymatic Saccharification of Lignocellulosic Biomass. Natl Renew Energy Lab. 2015;(TP-510-42629):1–9.
283. Wen JL, Sun SL, Xue BL, Sun RC. Recent advances in characterization of lignin polymer by solution-state nuclear magnetic resonance (NMR) methodology. Materials (Basel). 2013;6(1):359–91.
284. Del Río JC, Prinsen P, Rencoret J, Nieto L, Jiménez-Barbero J, Ralph J, et al. Structural characterization of the lignin in the cortex and pith of elephant grass (Pennisetum purpureum) stems. J Agric Food Chem. 2012;60(14):3619–34.
285. Savy D, Nebbioso A, Mazzei P, Drosos M, Piccolo A. Molecular composition of water-soluble lignins separated from different non-food biomasses. Fuel Process Technol. 2015 Mar 1;131:175–81.
286. Chen M, Malaret F, Firth AEJ, Verdía P, Abouelela AR, Chen Y, et al. Design of a combined ionosolv-organosolv biomass fractionation process for biofuel production and high value-added lignin valorisation. Green Chem. 2020 Aug 7;22(15):5161–78.
287. Demirbaş A. Calculation of higher heating values of biomass fuels. Fuel. 1997 Apr;76(5):431–4.
288. Kazi FK, Fortman J, Anex R. Techno-Economic Analysis of Biochemical Scenarios for Production of Cellulosic Ethanol Techno-Economic Analysis of Biochemical Scenarios for Production of Cellulosic Ethanol. Natl Renew Energy Lab. 2010;102.
289. Davis R, Grundl N, Tao L, Biddy MJ, Tan ECD, Beckham GT, et al. Process Design and Economics for the Conversion of Lignocellulosic Biomass to Hydrocarbon Fuels and Coproducts: 2018 Biochemical Design Case Update. Natl Renew Energy Lab. 2018.
290. Boot-handford ME. The Utilisation of Biomass as a fuel for Chemical Looping Combustion. PhD thesis. Imperial College London; 2015.
291. Boateng AA, Daugaard DE, Goldberg NM, Hicks KB. Bench-scale fluidized-bed pyrolysis of switchgrass for bio-oil production. Ind Eng Chem Res. 2007;46(7):1891–7.
292. Emons H. Certificate of analysis ERM®- EC681k [Internet]. Sigma-Aldrich. 2007. Available from: https://publications.jrc.ec.europa.eu
293. International Atomic Energy Agency. Reference Material IAEA 413: Major, Minor and Trace Elements in Algae [Internet]. Vol. 14, IAEA Analytical Quality in Nuclear Applications. 2010. Available from: https://www.iaea.org/publications/8169/reference-material-iaea-413-major-minor-and-trace-elements-in-algae
294. Environment Audit Committee. Invasive species - First Report of Session 2019.

House of Commons. 2019.
295. Souza GM, Victoria RL, Joly CA, Verdade LM. In: Bioenergy & Sustainability: bridging the gaps. São Paulo: Scientific Committee on Problems of the Environment (SCOPE); 2015.
296. Quinn LD, Endres AB, Voigt TB. Why not harvest existing invaders for bioethanol? Biol Invasions. 2014 Nov 20;16(8):1559–66.
297. Lewis KC, Porter RD. Global approaches to addressing biofuel-related invasive species risks and incorporation into U.S. laws and policies. Ecol Monogr. 2014 May 1;84(2):171–201.
298. Witt ABR. Biofuels and invasive species from an African perspective - a review. GCB Bioenergy. 2010 Dec 1;2(6):321–9.
299. Borah AJ, Agarwal M, Poudyal M, Goyal A, Moholkar VS. Mechanistic investigation in ultrasound induced enhancement of enzymatic hydrolysis of invasive biomass species. Bioresour Technol. 2016 Jan 2;213:342–9.
300. Bauer S, Sorek H, Mitchell VD, Ibáñez AB, Wemmer DE. Characterization of Miscanthus giganteus lignin isolated by ethanol organosolv process under reflux condition. J Agric Food Chem. 2012 Aug 22;60(33):8203–12.
301. Rasmussen H, Sørensen HR, Meyer AS. Formation of degradation compounds from lignocellulosic biomass in the biorefinery: Sugar reaction mechanisms. Carbohydr Res. 2014;385:45–57.
302. Jönsson LJ, Martín C. Pretreatment of lignocellulose: Formation of inhibitory by-products and strategies for minimizing their effects. Bioresour Technol. 2016;199:103–12.
303. Zhang Q, Wei Y, Han H, Weng C. Enhancing bioethanol production from water hyacinth by new combined pretreatment methods. Bioresour Technol. 2018 Mar 1;251:358–63.
304. Klinke HB, Thomsen AB, Ahring BK. Inhibition of ethanol-producing yeast and bacteria by degradation products produced during pre-treatment of biomass. Appl Microbiol Biotechnol. 2004;66(1):10–26.
305. Del Río JC, Rencoret J, Prinsen P, Martínez ÁT, Ralph J, Gutiérrez A. Structural characterization of wheat straw lignin as revealed by analytical pyrolysis, 2D-NMR, and reductive cleavage methods. J Agric Food Chem. 2012 Jun 13;60(23):5922–35.
306. Happs RM, Addison B, Doeppke C, Donohoe BS, Davis MF, Harman-Ware AE. Comparison of methodologies used to determine aromatic lignin unit ratios in lignocellulosic biomass. Biotechnol Biofuels. 2021 Mar 6;14:1–16.
307. Dutta T, Isern NG, Sun J, Wang E, Hull S, Cort JR, et al. Survey of Lignin-Structure Changes and Depolymerization during Ionic Liquid Pretreatment. ACS Sustain Chem

Eng. 2017 Nov 6;5(11):10116–27.
308. Studer MH, DeMartini JD, Davis MF, Sykes RW, Davison B, Keller M, et al. Lignin content in natural populus variants affects sugar release. PNAS. 2011;108(15);6300-5.
309. Davison BH, Drescher SR, Tuskan GA, Davis MF, Nghiem NP. Variation of S/G ratio and lignin content in a Populus family influences the release of xylose by dilute acid hydrolysis. Appl Biochem Biotechnol. 2006;130:427–35.
310. Ventorim G, Alves EF, Penna LS, Francis RC. Effect of S/G ratio on kraft pulping and ECF bleaching of some poplars and eucalyptus. Cellul Chem Technol. 2014;48(3–4):365–73.
311. Anderson EM, Stone ML, Katahira R, Reed M, Muchero W, Ramirez KJ, et al. Differences in S/G ratio in natural poplar variants do not predict catalytic depolymerization monomer yields. Nat Commun. 2019 Dec 1;10:1–10.
312. Yoo CG, Meng X, Pu Y, Ragauskas AJ. The critical role of lignin in lignocellulosic biomass conversion and recent pretreatment strategies: A comprehensive review. Bioresour Technol. 2020 Apr 1;301.
313. Tolbert A, Akinosho H, Khunsupat R, Naskar AK, Ragauskas AJ. Characterization and analysis of the molecular weight of lignin for biorefining studies. Biofuels, Bioprod Biorefining. 2014;8(6):836–56.
314. Hosseinaei O, Harper DP, Bozell JJ, Rials TG. Improving processing and performance of pure lignin carbon fibers through hardwood and herbaceous lignin blends. Int J Mol Sci. 2017 Jul 1;18(7).
315. Xin J, Li M, Li R, Wolcott MP, Zhang J. Green Epoxy Resin System Based on Lignin and Tung Oil and Its Application in Epoxy Asphalt. ACS Sustain Chem Eng. 2016 May 2;4(5):2754–61.
316. Hennequin LM, Levers O, Hallett JP. Ionic Liquids as Solvents for the Production of Materials from Biomass. In: Encyclopedia of Ionic Liquids. Singapore: Springer; 2019.
317. Abdelaziz OY, Brink DP, Prothmann J, Ravi K, Sun M, García-Hidalgo J, et al. Biological valorization of low molecular weight lignin. Biotechnol Adv. 2016 Dec 1;34(8):1318–46.
318. Holladay JE, Bozell JJ, White JF JD. Top value added chemicals from biomass Volume II: Results of Screening for Potential Candidates from Biorefinery Lignin Produced. 2007.
319. Guo D, Wu S, Lyu G, Guo H. Effect of molecular weight on the pyrolysis characteristics of alkali lignin. Fuel. 2017;193:45–53.
320. Kim JY, Shin EJ, Eom IY, Won K, Kim YH, Choi D, et al. Structural features of lignin macromolecules extracted with ionic liquid from poplar wood. Bioresour Technol.

2011 Oct;102(19):9020–5.

321. Sun R, Tomkinson J, Sun XF, Wang NJ. Fractional isolation and physico-chemical characterization of alkali- soluble lignins from fast-growing poplar wood. Polymer. 2000;41(23):8409–17.
322. Zhang Q, Chang J, Wang T, Xu Y. Review of biomass pyrolysis oil properties and upgrading research. Energy Convers Manag. 2007 Jan 1;48(1):87–92.
323. Demirbas A. Higher heating values of lignin types from wood and non-wood lignocellulosic biomasses. Energy Sources, Part A Recover Util Environ Eff. 2017;39(6):592–8.
324. Demirbas A. Relationships between heating value and lignin, moisture, ash and extractive contents of biomass fuels. Energy Explor Exploit. 2002;20:105–11.
325. Demirbaş A. Relationships between lignin contents and heating values of biomass. Energy Convers Manag. 2001 Jan 1;42(2):183–8.
326. Narron RH, Kim H, Chang HM, Jameel H, Park S. Biomass pretreatments capable of enabling lignin valorization in a biorefinery process. Curr Opin Biotechnol. 2016;38:39–46.
327. Williams F, Eschen R, Harris A, Djeddour D, Pratt C, Shaw RS, et al. The economic cost of invasive non-native species on Great Britain: Technical report. Surrey; 2010.
328. Fasham M, Trumper K. Review of non-native species legislation and guidance. Department of Environment of Food and Rural Affairs. 2001.
329. Scottish Environnent Protection Agency. Manual eradication of rhododendron - light, medium or difficult [Internet]. 2015 [cited 2019 Jun 27]. Available from: https://www.ruralpayments.org/publicsite/futures/topics/all-schemes/agri-environment-climate-scheme/management-options-and-capital-items/manual-eradication-of-rhododendron---light--medium-or-difficult/
330. Department for Environment Food & Rural Affairs. How to stop invasive non-native plants from spreading [Internet]. 2014 [cited 2019 Jun 27]. Available from: https://www.gov.uk/guidance/prevent-the-spread-of-harmful-invasive-and-non-native-plants
331. Environment Agency. Managing Japanese Knotweed on Development Sites: the knotweed Code of Practice [Internet]. Version 3. 2013 [cited 2019 Jul 10]. Available from: https://www.gov.uk/government/uploads/system/uploads/attachment_data/file/296930/LIT_2695_df1209.pdf
332. Scottish Environnent Protection Agency. Invasive non–native species [Internet]. 2014 [cited 2019 Jun 27]. Available from: https://www.sepa.org.uk/environment/biodiversity/invasive-non-native-species/

333. Brewer A. NFI preliminary estimates of the presence and extent of rhododendron in British woodlands. 2016.
334. Mercer TG, Frostick LE. Leaching characteristics of CCA-treated wood waste: A UK study. Sci Total Environ. 2012;427–428:165–74.
335. Jambeck J, Weitz K, Solo-Gabriele H, Townsend T, Thorneloe S. CCA-Treated wood disposed in landfills and life-cycle trade-offs with waste-to-energy and MSW landfill disposal. Waste Manag. 2007;27(8):21–8.
336. Ohgami N, Yamanoshita O, Thang ND, Yajima I, Nakano C, Wenting W, et al. Carcinogenic risk of chromium, copper and arsenic in CCA-treated wood. Environ Pollut. 2015;206:456–60.
337. Augustsson A, Sörme L, Karlsson A, Amneklev J. Persistent Hazardous Waste and the Quest Toward a Circular Economy: The Example of Arsenic in Chromated Copper Arsenate–Treated Wood. J Ind Ecol. 2017 Dec;21(3):689–99.
338. Bomparola R, Caporali S, Lavacchi A, Bardi U. Silver electrodeposition from air and water-stable ionic liquid: An environmentally friendly alternative to cyanide baths. Surf Coatings Technol. 2007 Oct;201(24):9485–90.
339. Vaughan J, Tu J, Dreisinger D. Ionic liquid electrodeposition of reactive metals. Miner Process Extr Metall Trans Institutions Min Metall Sect C. 2008;117(2):113–7.
340. Endres F. Ionic liquids: Solvents for the electrodeposition of metals and semiconductors. ChemPhysChem. 2002 Feb;3(2):144–54.
341. Zhang Q, Wang Q, Zhang S, Lu X, Zhang X. Electrodeposition in Ionic Liquids. ChemPhysChem. 2016;17(3):335–51.
342. Janssen CHC, Macías-Ruvalcaba NA, Aguilar-Martínez M, Kobrak MN. Metal extraction to ionic liquids: the relationship between structure, mechanism and application. Int Rev Phys Chem. 2015 Oct 2;34(4):591–622.
343. Shinde SD, Meng X, Kumar R, Ragauskas AJ. Recent advances in understanding the pseudo-lignin formation in a lignocellulosic biorefinery. Green Chem. 2018;20(10):2192–205.
344. Labbé S, Zhu Z, Thiele DJ. Copper-specific transcriptional repression of yeast genes encoding critical components in the copper transport pathway. J Biol Chem. 1997;272(25):15951–8.
345. Verma KVR, Subrahmanyam T, Subrahmanyam PVR. Heavy metal removal with lignin. J Environ Sci Heal. 1990 Apr;25(3):243–65.
346. Moon SJ, Eom IY, Kim JY, Kim TS, Lee SM, Choi IG, et al. Characterization of lignin-rich residues remaining after continuous super-critical water hydrolysis of poplar wood (Populus albaglandulosa) for conversion to fermentable sugars. Bioresour Technol. 2011 May 1;102(10):5912–6.

347. Kim JY, Hwang H, Oh S, Choi JW. Structural features of lignin-rich solid residues obtained from two-step acid-hydrolysis of Miscanthus biomass (Miscanthus sacchariflorus Benth.). J Ind Eng Chem. 2015 Oct 25;30:302–8.
348. Troiano M, Cammarota A, Tregambi C, Chirone R, Salatino P, Solimene R. Fluidized bed combustion of solid lignin-rich residues from bioethanol production. Powder Technol. 2020 Jun 30;371:170–9.
349. Nowakowski DJ, Bridgwater A V., Elliott DC, Meier D, de Wild P. Lignin fast pyrolysis: Results from an international collaboration. J Anal Appl Pyrolysis. 2010 May;88(1):53–72.
350. Scott DS, Piskorz J. The flash pyrolysis of aspen-poplar wood. Can J Chem Eng. 1982;60(5):666–74.
351. Scott DS, Piskorz J. The continuous flash pyrolysis of biomass. Can J Chem Eng. 1984;62(3):404–12.
352. Scott DS, Plskorz J, Radleln D. Liquid Products from the Continuous Flash Pyrolysis of Biomass. Ind Eng Chem Process Des Dev. 1985;24(3):581–8.
353. Scott DS, Piskorz J, Bergougnou MA, Graham R, Overend RP. The Role of Temperature in the Fast Pyrolysis of Cellulose and Wood. Ind Eng Chem Res. 1988;27(1):8–15.
354. Bridgwater A V. Principles and practice of biomass fast pyrolysis processes for liquids. J Anal Appl Pyrolysis. 1999 Jul;51(1):3–22.
355. Ji-lu Z. Bio-oil from fast pyrolysis of rice husk: Yields and related properties and improvement of the pyrolysis system. J Anal Appl Pyrolysis. 2007;80(1):30–5.
356. Mohan D, Pittman CU, Steele PH. Pyrolysis of wood/biomass for bio-oil: A critical review. Energy and Fuels. 2006 May;20(3):848–89.
357. Oasmaa A, Solantausta Y, Arpiainen V, Kuoppala E, Sipilä K. Fast pyrolysis bio-oils from wood and agricultural residues. Energy and Fuels. 2010;24(2):1380–8.
358. Huang Y, Wei Z, Yin X, Wu C. Pyrolytic characteristics of biomass acid hydrolysis residue rich in lignin. Bioresour Technol. 2012 Jan 1;103(1):470–6.
359. Mullen CA, Boateng AA. Chemical composition of bio-oils produced by fast pyrolysis of two energy crops. Energy and Fuels. 2008 May;22(3):2104–9.
360. Mullen CA, Strahan GD, Boateng AA. Characterization of various fast-pyrolysis bio-oils by NMR spectroscopy. Energy and Fuels. 2009 May 21;23(5):2707–18.
361. Mullen CA, Strahan GD, Boateng AA. Characterization of Biomass Pyrolysis Oils by Diffusion Ordered NMR Spectroscopy. ACS Sustain Chem Eng. 2019 Dec 16;7(24):19951–60.
362. Kosa M, Ben H, Theliander H, Ragauskas AJ. Pyrolysis oils from CO2 precipitated Kraft lignin. Green Chem. 2011;13(11):3196–202.

363. Vali N, Åmand LE, Combres A, Richards T, Pettersson A. Pyrolysis of municipal sewage sludge to investigate char and phosphorous yield together with heavy-metal removal—experimental and by thermodynamic calculations. Energies. 2021;14(5):1477.
364. Liu Y, Wang B, Cao X. Transformation of Heavy Metals during Pyrolysis of Predried Dyeing Sludge. Energy and Fuels. 2020 Jan 16;34:879–89.
365. Yuan H, Lu T, Zhao D, Huang H, Noriyuki K, Chen Y. Influence of temperature on product distribution and biochar properties by municipal sludge pyrolysis. J Mater Cycles Waste Manag. 2013 Sep 1;15(3):357–61.
366. Phoungthong K, Zhang H, Shao LM, He PJ. Leaching characteristics and phytotoxic effects of sewage sludge biochar. J Mater Cycles Waste Manag. 2018 Oct 1;20(4):2089–99.
367. Department of Environment of Food and Rural Affairs. Wood waste : A short review of recent research [Internet]. London, England; 2012. Available from: https://www.gov.uk/government/uploads/system/uploads/attachment_data/file/82571/consult-wood-waste-researchreview-20120731.pdf
368. Singh RP, Agrawal M. Potential benefits and risks of land application of sewage sludge. Waste Manag. 2008 Jan 1;28(2):347–58.
369. Heaven FW. Detailed Investigation of Heavy Metal and Agricultural Nutrient Content of Soils - Stoke Bardolph Estate. 2004.
370. Bünemann EK, Bongiorno G, Bai Z, Creamer RE, De Deyn G, de Goede R, et al. Soil quality – A critical review. Soil Biol Biochem. 2018;120:105–25.
371. Jolly YN, Islam A, Akbar S. Transfer of metals from soil to vegetables and possible health risk assessment. Springerplus. 2013 Aug 15;2:1–8.
372. Okereafor U, Makhatha M, Mekuto L, Uche-Okereafor N, Sebola T, Mavumengwana V. Toxic metal implications on agricultural soils, plants, animals, aquatic life and human health. Int J Environ Res Public Health. 2020 Mar 25;17(7).
373. Hutchings TR. The opportunities for woodland on contaminated land [Internet]. Forest Commission Research. Edinburgh, Scotland; 2002. Available from: https://www.forestresearch.gov.uk/publications/archive-the-opportunities-for-woodland-on-contaminated-land/
374. Koptsik GN. Modern approaches to remediation of heavy metal polluted soils: A review. Eurasian Soil Sci. 2014;47(7):707–22.
375. Hoffman DJ, Rattner BA, Burton GA, Cairns J. Heavy Metals. In: Handbook of Ecotoxicology, Second Edition. 2nd ed. Boca Raton, FL: CRC Press; 2002. p. 543–69.
376. United States Environmental Protection Agency. Introduction to Phytoremediation.

Washington, D.C.; 2000; EPA/600/R-99/107.
377. Syam N, Wardiyati T, Maghfoer MD, Handayanto E, Ibrahim B, Muchdar A. Effect of Accumulator Plants on Growth and Nickel Accumulation of Soybean on Metal-contaminated Soil. Agric Agric Sci Procedia. 2016;9:13–9.
378. Greger M, Landberg T. Use of willow in phytoexfraction. Int J Phytoremediation. 1999;1(2):115–23.
379. Fischerová Z, Tlustoš P, Jiřina Száková, Kornelie Šichorová. A comparison of phytoremediation capability of selected plant species for given trace elements. Environ Pollut. 2006;144(1):93–100.
380. Pleguezuelo CRR, Zuazo VHD, Bielders C, Bocanegra JAJ, PereaTorres F, Martínez JRF. Bioenergy farming using woody crops. A review. Agron Sustain Dev. 2015;35(1):95–119.
381. Nehnevajova E, Herzig R, Federer G, Erismann KH, Schwitzguébel JP. Screening of sunflower cultivars for metal phytoextraction in a contaminated field prior to mutagenesis. Int J Phytoremediation. 2005;7(4):337–49.
382. Zalewska M, Nogalska A. Phytoextraction potential of sunflower and white mustard plants in zinc-contaminated soil. Chil J Agric Res. 2014;74(4):485–9.
383. Lin C, Liu J, Liu L, Zhu T, Sheng L, Wang D. Soil amendment application frequency contributes to phytoextraction of lead by sunflower at different nutrient levels. Environ Exp Bot. 2009;65(2–3):410–6.
384. Chaney RL, Angle JS, McIntosh MS, Reeves RD, Li YM, Brewer EP, et al. Using hyperaccumulator plants to phytoextract soil Ni and Cd. Z Naturforsch C J Biosci. 2005;60(3–4):190–8.
385. Fritz C, Palacios-Rojas N, Feil R, Stitt M. Regulation of secondary metabolism by the carbon-nitrogen status in tobacco: Nitrate inhibits large sectors of phenylpropanoid metabolism. Plant J. 2006;46(4):533–48.
386. Lodenius M, Maarala L, Mukheerje B. Occurence and turnover of cadmium in Finnish forest ecosystem. In: Cadmium in the Environment - Ecological and Analytical Problems. 1999.
387. Welch RM, Cary EE. Concentration of Chromium, Nickel, and Vanadium in Plant Materials. J Agric Food Chem. 1975 May 1;23(3):479–82.
388. Cataldo DA, Garland TR, Wildung RE, Drucker H. Nickel in Plants. Plant Physiol. 1978 Oct 1;62(4):566–70.
389. Holder AJ, McCalmont JP, Rowe R, McNamara NP, Elias D, Donnison IS. Soil N 2 O emissions with different reduced tillage methods during the establishment of Miscanthus in temperate grassland. GCB Bioenergy. 2019 Mar 1;11(3):539–49.
390. Nunn C, Hastings AFSJ, Kalinina O, Özgüven M, Schüle H, Tarakanov IG, et al.

Environmental influences on the growing season duration and ripening of diverse Miscanthus germplasm grown in six countries. Front Plant Sci. 2017 May 30;8.
391. Lewandowski I, Clifton-Brown J, Trindade LM, Van Der Linden GC, Schwarz KU, Müller-Sämann K, et al. Progress on optimizing miscanthus biomass production for the european bioeconomy: Results of the EU FP7 project OPTIMISC. Front Plant Sci. 2016 Nov 18;7.
392. Egendorf SP, Groffman P, Moore G, Cheng Z. The limits of lead (Pb) phytoextraction and possibilities of phytostabilization in contaminated soil: a critical review. Int J Phytoremediation. 2020;916–30.
393. Davies BE. Heavy metal pollution of British agricultural soils with special reference to the role of lead and copper mining. In: International seminar on soil environment and fertility management in intensive agriculture. 1977.
394. Roberts TM, Gizyn W, Hutchinson TC. Lead contamination of air, soil, vegetation and people in the vicinity of secondary lead smelters. In: Annual conference on trace substances in environmental health. Univeristy of Missouri, Columbia, MO; 1974.
395. Roberts RD, Johnson MS, Firth JNM. Predator-prey relationship in the food chain transfer of heavy metals. In: Annual conference on trace substances in environmental health. Univeristy of Missouri, Columbia, MO; 1979.
396. De Koning HW. Lead and cadmium contamination in the area immediately surrounding a lead smelter. Water Air Soil Pollut. 1974 Mar;3(1):63–70.
397. van der Ent A, Baker AJM, Reeves RD, Pollard AJ, Schat H. Hyperaccumulators of metal and metalloid trace elements: Facts and fiction. Plant Soil. 2013 May 22;362(1–2):319–34.
398. Attard TM, McElroy CR, Gammons RJ, Slattery JM, Supanchaiyamat N, Kamei CLA, et al. Supercritical CO2 extraction as an effective pretreatment step for wax extraction in a miscanthus biorefinery. ACS Sustain Chem Eng. 2016 Nov 7;4(11):5979–88.
399. Jensen E, Robson P, Farrar K, Thomas Jones S, Clifton-Brown J, Payne R, et al. Towards Miscanthus combustion quality improvement: the role of flowering and senescence. GCB Bioenergy. 2017 May 1;9(5):891–908.
400. Huang C, Lai C, Wu X, Huang Y, He J, Huang C, et al. An integrated process to produce bio-ethanol and xylooligosaccharides rich in xylobiose and xylotriose from high ash content waste wheat straw. Bioresour Technol. 2017 Oct 1;241:228–35.
401. Zhang J, Zou D, Singh S, Cheng G. Recent developments in ionic liquid pretreatment of lignocellulosic biomass for enhanced bioconversion. Sustain Energy Fuels. 2021 Mar 23;5(6):1655–67.
402. Yuan TQ, Sun SN, Xu F, Sun RC. Characterization of lignin structures and lignin-carbohydrate complex (LCC) linkages by quantitative 13C and 2D HSQC NMR

spectroscopy. J Agric Food Chem. 2011;59(19):10604–14.
403. Abdelaziz OY, Hulteberg CP. Physicochemical Characterisation of Technical Lignins for Their Potential Valorisation. Waste and Biomass Valorization. 2017;8(3):859–69.
404. Foo KY, Hameed BH. Utilization of rice husk ash as novel adsorbent: A judicious recycling of the colloidal agricultural waste. Adv Colloid Interface Sci. 2009 Nov 30;152(1–2):39–47.
405. Abouelela AR, Tan SY, Kelsall GH, Hallett JP. Toward a Circular Economy: Decontamination and Valorization of Postconsumer Waste Wood Using the ionoSolv Process. ACS Sustain Chem Eng. 2020;8(38):14441–61.
406. Popescu AM, Cojocaru A, Donath C, Constantin V. Electrochemical study and electrodeposition of copper(I) in ionic liquid-reline. Chem Res Chinese Univ. 2013;29(5):991–7.
407. He W, Shi Z, Liu F, Yang S. Electrodeposition of copper metal from the 1-ethyl-3-methylimidazolium fluoride ([EMIM]F)-urea-H2O system containing Cu2O. Electrochemistry. 2020;88(4):253–5.
408. Moustafa EM, Mann O, Furbeth W, Schuster R. Electrochemical behaviour of iron in a third-generation ionic liquid: Cyclic voltammetry and micromachining investigations. ChemPhysChem. 2009;10(17):3090–6.
409. Wang M, Zhang D, Dong J, Tan SK. Application of constructed wetlands for treating agricultural runoff and agro-industrial wastewater: a review. Hydrobiologia. 2018 Jan 1;805(1):1–31.
410. Brereton NJB, Pitre FE, Shield I, Hanley SJ, Ray MJ, Murphy RJ, et al. Insights into nitrogen allocation and recycling from nitrogen elemental analysis and 15N isotope labelling in 14 genotypes of willow. Tree Physiol. 2014;34(11):1252–62.
411. Fabio ES, Smart LB. Effects of nitrogen fertilization in shrub willow short rotation coppice production – a quantitative review. GCB Bioenergy. 2018;10(8):548–64.
412. Hangs RD, Schoenau JJ, Van Rees KCJ, Steppuhn H. Examining the salt tolerance of willow (Salix spp.) bioenergy species for use on salt-affected agricultural lands. Can J Plant Sci. 2011;91(3):509–17.
413. Gouker FE, Fabio ES, Serapiglia MJ, Smart LB. Yield and biomass quality of shrub willow hybrids in differing rotation lengths and spacing designs. Biomass and Bioenergy. 2021;146.
414. Brereton NJB, Pitre FE, Ray MJ, Karp A, Murphy RJ. Investigation of tension wood formation and 2,6-dichlorbenzonitrile application in short rotation coppice willow composition and enzymatic saccharification. Biotechnol Biofuels. 2011;4(1).
415. Li M, Pu Y, Ragauskas AJ. Current understanding of the correlation of lignin structure with biomass recalcitrance. Front Chem. 2016;4.

416. Meng X, Pu Y, Yoo CG, Li M, Bali G, Park DY, et al. An In-Depth Understanding of Biomass Recalcitrance Using Natural Poplar Variants as the Feedstock. ChemSusChem. 2017;10(1):139–50.
417. Serapiglia MJ, Humiston MC, Xu H, Hogsett DA, de Orduña RM, Stipanovic AJ, et al. Enzymatic saccharification of shrub willow genotypes with differing biomass composition for biofuel production. Front Plant Sci. 2013.
418. Eklund R, Galbe M, Zacchi G. The influence of SO2 and H2SO4 impregnation of willow prior to steam pretreatment. Bioresour Technol. 1995;52(3):225–9.
419. Zhong L, Yang L, Wang C, Ji X, Yang G, Chen J, et al. NaOH-Aided Sulfolane Pretreatment for Effective Fractionation and Utilization of Willow (Salix matsudana cv. Zhuliu). Ind Eng Chem Res. 2020;59(39):17546–53.
420. Huijgen WJJ, Smit AT, Reith JH, Uil H Den. Catalytic organosolv fractionation of willow wood and wheat straw as pretreatment for enzymatic cellulose hydrolysis. J Chem Technol Biotechnol. 2011;86(11):1428–38.
421. Zhao X, Li S, Wu R, Liu D. Organosolv fractionating pre-treatment of lignocellulosic biomass for efficient enzymatic saccharification: chemistry, kinetics, and substrate structures. Biofuels, Bioprod Biorefining. 2017;11(3):567–90.
422. Larsson S, Palmqvist E, Hahn-Hägerdal B, Tengborg C, Stenberg K, Zacchi G, et al. The generation of fermentation inhibitors during dilute acid hydrolysis of softwood. Enzyme Microb Technol. 1999;24(3–4):151–9.
423. Palmqvist E, Hahn-Hägerdal B, Galbe M, Zacchi G. The effect of water-soluble inhibitors from steam-pretreated willow on enzymatic hydrolysis and ethanol fermentation. Enzyme Microb Technol. 1996;19(6):470–6.
424. Herrero J, Fernández-Pérez F, Yebra T, Novo-Uzal E, Pomar F, Pedreño MÁ, et al. Bioinformatic and functional characterization of the basic peroxidase 72 from Arabidopsis thaliana involved in lignin biosynthesis. Planta. 2013 Jun;237(6):1599–612.
425. Liu Q, Luo L, Zheng L. Lignins: Biosynthesis and biological functions in plants. Int J Mol Sci. 2018;19(2).
426. Moura JCMS, Bonine CAV, de Oliveira Fernandes Viana J, Dornelas MC, Mazzafera P. Abiotic and biotic stresses and changes in the lignin content and composition in plants. J Integr Plant Biol. 2010 Apr;52(4):360–76.
427. Ohlsson JA, Hallingbäck HR, Jebrane M, Harman-Ware AE, Shollenberger T, Decker SR, et al. Genetic variation of biomass recalcitrance in a natural Salix viminalis (L.) population. Biotechnol Biofuels. 2019.
428. Boeckler GA, Gershenzon J, Unsicker SB. Phenolic glycosides of the Salicaceae and their role as anti-herbivore defenses. Phytochemistry. 2011;72(13):1497–509.

429. Chen F, Liu CJ, Tschaplinski TJ, Zhao N. Genomics of secondary metabolism in populus: Interactions with biotic and abiotic environments. CRC Crit Rev Plant Sci. 2009;28(5):375–92.
430. Tegelberg R, Julkunen-Tiitto R. Quantitative changes in secondary metabolites of dark-leaved willow (Salix myrsinifolia) exposed to enhanced ultraviolet-B radiation. Physiol Plant. 2001;113(4):541–7.
431. Brereton NJB, Berthod N, Lafleur B, Pedneault K, Pitre FE, Labrecque M. Extractable phenolic yield variation in five cultivars of mature short rotation coppice willow from four plantations in Quebec. Ind Crops Prod. 2017;97:525–35.
432. Tyśkiewicz K, Konkol M, Kowalski R, Rój E, Warmiński K, Krzyżaniak M, et al. Characterization of bioactive compounds in the biomass of black locust, poplar and willow. Trees. 2019;33:1235–63.
433. Bryant JP, Chapin FS, Klein DR. Carbon/Nutrient Balance of Boreal Plants in Relation to Vertebrate Herbivory. Oikos. 1983;40(3):357.
434. Abreu IN, Ahnlund M, Moritz T, Albrectsen BR. UHPLC-ESI/TOFMS Determination of Salicylate-like Phenolic Gycosides in Populus tremula Leaves. J Chem Ecol. 2011;37(8):857–70.
435. Noleto-Dias C, Wu Y, Bellisai A, Macalpine W, Beale MH, Ward JL. Phenylalkanoid glycosides (non-salicinoids) from wood chips of Salix triandra × dasyclados Hybrid Willow. Molecules. 2019;24(6):1152.
436. Si CL, Xu J, Kim JK, Bae YS, Liu PT, Liu Z. Antioxidant properties and structural analysis of phenolic glucosides from bark of Populus ussuriensis Kom. Wood Sci Technol. 2011;45(1):5–13.
437. Gfeller A, Dubugnon L, Liechti R, Farmer EE. Jasmonate biochemical pathway. Sci Signal. 2010;3(109).
438. Vick BA, Zimmerman DC. Biosynthesis of Jasmonic Acid by Several Plant Species. Plant Physiol. 1984;75(2):458–61.
439. Jung HW, Tschaplinski TJ, Wang L, Glazebrook J, Greenberg JT. Priming in systemic plant immunity. Science. 2009;324(5923):89–91.
440. Huot B, Yao J, Montgomery BL, He SY. Growth-defense tradeoffs in plants: A balancing act to optimize fitness. Mol Plant. 2014;7(8):1267–87.
441. Ericsson K, Rosenqvist H, Ganko E, Pisarek M, Nilsson L. An agro-economic analysis of willow cultivation in Poland. Biomass and Bioenergy. 2006;30(1):16–27.
442. González-García S, Mola-Yudego B, Dimitriou I, Aronsson P, Murphy R. Environmental assessment of energy production based on long term commercial willow plantations in Sweden. Sci Total Environ. 2012;421–422:210–9.
443. Lan W, Lu F, Regner M, Zhu Y, Rencoret J, Ralph SA, et al. Tricin, a flavonoid

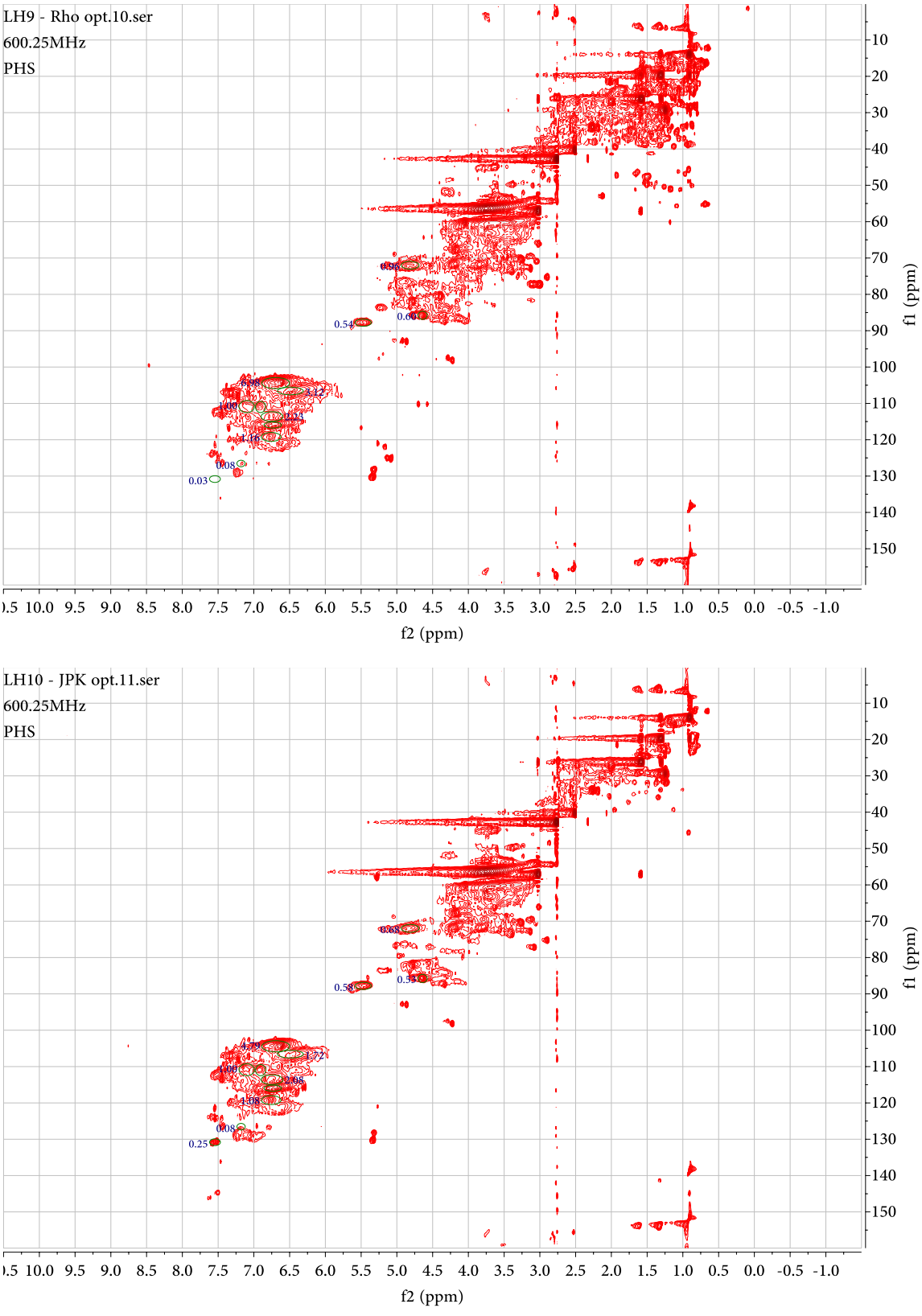
monomer in monocot lignification. Plant Physiol. 2015;167(4):1284–95.
444. Li M, Pu Y, Yoo CG, Ragauskas AJ. The occurrence of tricin and its derivatives in plants. Green Chem. 2016;18(6):1439–54.
445. Vanholme R, De Meester B, Ralph J, Boerjan W. Lignin biosynthesis and its integration into metabolism. Curr Opin Biotechnol. 2019;56:230–9.
446. Ni H fan, Cai X, Qiu X, Liu L, Ma X, Wan L, et al. Biphenyl-type neolignans from stem bark of Magnolia officinalis with potential anti-tumor activity. Fitoterapia. 2020;147.
447. Xiao X, Huang H, Ge Z, Rounge TB, Shi J, Xu X, et al. A pair of chiral flavonolignans as novel anti-cyanobacterial allelochemicals derived from barley straw (Hordeum vulgare): Characterization and comparison of their anti-cyanobacterial activities. Environ Microbiol. 2014;16(5):1238–51.
448. Galbe M, Wallberg O. Pretreatment for biorefineries: A review of common methods for efficient utilisation of lignocellulosic materials. Biotechnol Biofuels. 2019 Dec 23;12.
449. Livingstone D, Smyth BM, Foley AM, Murray ST, Lyons G, Johnston C. Willow coppice in intensive agricultural applications to reduce strain on the food-energy-water nexus. Biomass and Bioenergy. 2021;144.
450. Dauber J, Jones MB, Stout JC. The impact of biomass crop cultivation on temperate biodiversity. GCB Bioenergy. 2010;2(6):289–309.
451. Börjesson P, Berndes G. The prospects for willow plantations for wastewater treatment in Sweden. Biomass and Bioenergy. 2006;30(5):428–38.
452. Dimitriou I, Rosenqvist H. Sewage sludge and wastewater fertilisation of Short Rotation Coppice (SRC) for increased bioenergy production-Biological and economic potential. Biomass and Bioenergy. 2011;35(2):835–42.
453. Englund O, Dimitriou I, Dale VH, Kline KL, Mola-Yudego B, Murphy F, et al. Multifunctional perennial production systems for bioenergy: performance and progress. Wiley Interdiscip Rev Energy Environ. 2020;9(5).
454. Zalesny RS, Berndes G, Dimitriou I, Fritsche U, Miller C, Eisenbies M, et al. Positive water linkages of producing short rotation poplars and willows for bioenergy and phytotechnologies. Wiley Interdiscip Rev Energy Environ. 2019;8(5).
455. Yang M, Baral NR, Simmons BA, Mortimer JC, Shih PM, Scown CD. Accumulation of high-value bioproducts in planta can improve the economics of advanced biofuels. In: Proceedings of the National Academy of Sciences of the United States of America. 2020.
456. Labrecque M, Teodorescu TI. Field performance and biomass production of 12 willow and poplar clones in short-rotation coppice in southern Quebec (Canada). Biomass and Bioenergy. 2005;29(1):1–9.
457. Serapiglia MJ, Gouker FE, Smart LB. Early selection of novel triploid hybrids of shrub

willow with improved biomass yield relative to diploids. BMC Plant Biol. 2014;14(1):74.
458. Stolarski MJ, Szczukowski S, Tworkowski J, Klasa A. Yield, energy parameters and chemical composition of short-rotation willow biomass. Ind Crops Prod. 2013;46:60–5.
459. Lindegaard KN, Parfitt RI, Donaldson G, Hunter T, Dawson WM, Forbes EGA, et al. Comparative trials of elite Swedish and UK biomass willow varieties. Asp Appl Biol. 2001;65:183–92.
460. Volk T, Abrahamson L, Cameron K, Castellano P, Corbin T, Fabio E, et al. Yields of willow biomass crops across a range of sites in North America. Asp Appl Biol. 2011;112(6):67–74.
461. Quaye AK, Volk TA. Biomass production and soil nutrients in organic and inorganic fertilized willow biomass production systems. Biomass and Bioenergy. 2013;57:113–25.
462. Aronsson P, Perttu K. Willow vegetation filters for wastewater treatment and soil remediation combined with biomass production. For Chron. 2011;87(6):797.
463. Aronsson P, Rosenqvist H, Dimitriou I. Impact of Nitrogen Fertilization to Short-Rotation Willow Coppice Plantations Grown in Sweden on Yield and Economy. Bioenergy Res. 2014;7(3):993–1001.
464. Heller MC, Keoleian GA, Volk TA. Life cycle assessment of a willow bioenergy cropping system. Biomass and Bioenergy. 2003;25(2):147–65.
465. Fedoroff N V., Battisti DS, Beachy RN, Cooper PJM, Fischhoff DA, Hodges CN, et al. Radically rethinking agriculture for the 21st century. Science. 2010;327(5967):833–4.
466. Budsberg E, Rastogi M, Puettmann ME, Caputo J, Balogh S, Volk TA, et al. Life-cycle assessment for the production of bioethanol from willow biomass crops via biochemical conversion. For Prod J. 2012;62(4):305–13.
467. Matyka M, Radzikowski P. Productivity and biometric characteristics of 11 varieties of willow cultivated on marginal soil. Agric. 2020;10(12):1–10.
468. Stolarski MJ, Szczukowski S, Tworkowski J, Klasa A. Willow biomass production under conditions of low-input agriculture on marginal soils. For Ecol Manage. 2011;262(8):1558–66.
469. Stephenson AL, Dupree P, Scott SA, Dennis JS. The environmental and economic sustainability of potential bioethanol from willow in the UK. Bioresour Technol. 2010;101(24):9612–23.
470. Devappa RK, Rakshit SK, Dekker RFH. Forest biorefinery: Potential of poplar phytochemicals as value-added co-products. Biotechnol Adv. 2015;33(6):681–716.
471. Devappa RK, Rakshit SK, Dekker RFH. Potential of Poplar Bark Phytochemicals as Value-Added Co-products from the Wood and Cellulosic Bioethanol Industry. Bioenergy Res. 2015;8(3):1235–51.

472. Majumder A, Jha S. Hairy Roots: A Promising Tool for Phytoremediation. In: Satyanarayana S, editor. Microorganisms in Environmental Management: Microbes and Environment. Dordrecht: Springer; 2012. p. 607–29.
473. Soussou. Adaptation de la symbiose Fabacées-rhizobium aux sites miniers : Absorption du zinc par Anthyllis vulneraria et analyse de la diversité des bactéries symbiotiques d'Hedysarum coronarium. PhD Thesis. Montpellier Supagro; 2013.
474. Frérot H, Vidal C, Mahieu S, Escarré J, Maure L. Phytostabilisation de déchets miniers utilisant les interactions spécifiques entre des plantes méditerranéennes métallicoles et la symbiose Rhizobium / Fabaceae. In: Conférence du Centre d'Ecologie Fonctionnelle & Evolutive. 2009.

9 Appendix

Figure S0.1: HSQC spectra of lignin from RHDN (top) and JPK (bottom)



	Temperature	Time	C (%)	N (%)	H (%)	S (%)	O (%)
JPK	150	0	45.9	0.8	5.9	0.0	47.4
		0.25	-	-	-	-	-
		0.5	61.0	1.5	6.1	1.1	30.3
		0.75	60.8	1.7	6.0	1.5	30.0
		1	58.9	2.3	6.0	2.9	30.0
		1.25	61.4	1.9	5.8	1.7	29.2
	170	1.5	59.9	2.0	5.9	2.6	29.5
		0	45.9	0.8	5.9	0.0	47.4
		0.25	59.9	1.7	6.1	1.4	30.9
		0.5	58.0	2.3	6.1	3.2	30.5
		0.75	57.7	2.5	6.1	3.6	30.2
		1	58.9	2.3	6.0	2.9	30.0
RHDN	150	1.25	58.0	2.5	6.0	3.7	29.8
		0	44.7	0.6	6.2	0.1	48.4
		0.25	-	-	-	-	-
		0.5	60.5	1.2	6.7	1.1	30.4
		0.75	57.2	2.0	6.9	2.8	31.0
		1	57.3	2.0	6.7	3.0	31.0
	170	1.25	56.5	2.3	6.9	3.5	30.8
		1.5	55.6	2.6	7.0	4.0	30.8
		0	44.7	0.6	6.2	0.1	48.4
		0.25	61.2	1.2	7.0	0.6	30.0
		0.5	60.6	1.3	6.4	1.5	30.3
		0.75	60.2	1.6	6.5	2.2	29.6
		1	62.0	1.3	6.3	1.5	28.9
		1.25	61.1	1.5	6.5	2.0	28.9

Table S0.1: Elemental analysis of lignin from the time course pretreatment of JPK and RHDN

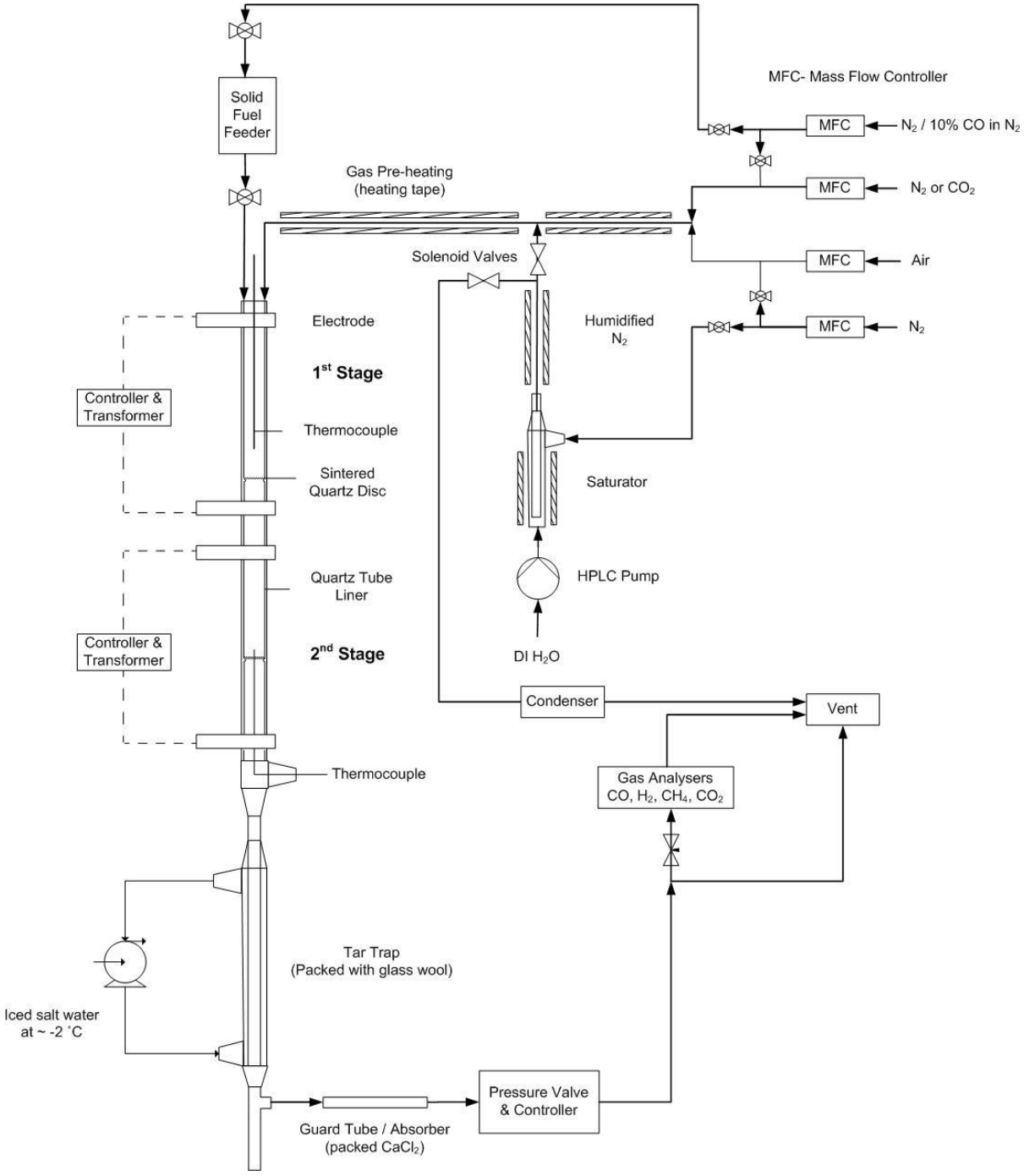


Figure S0.2: schematic of experimental set-up for fast pyrolysis experiments using a single-stage fixed-bed reactor; shown here in two-stage configuration though the second stage was not used during experiments

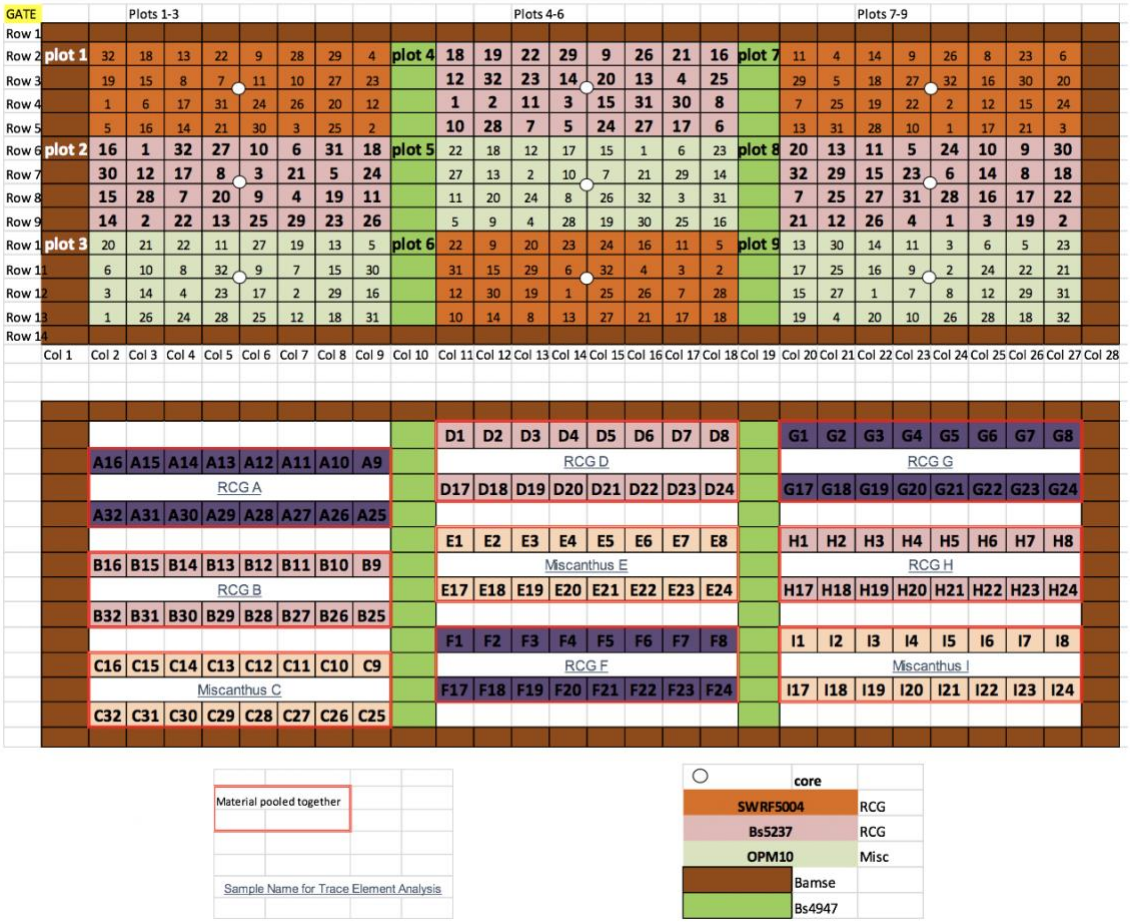
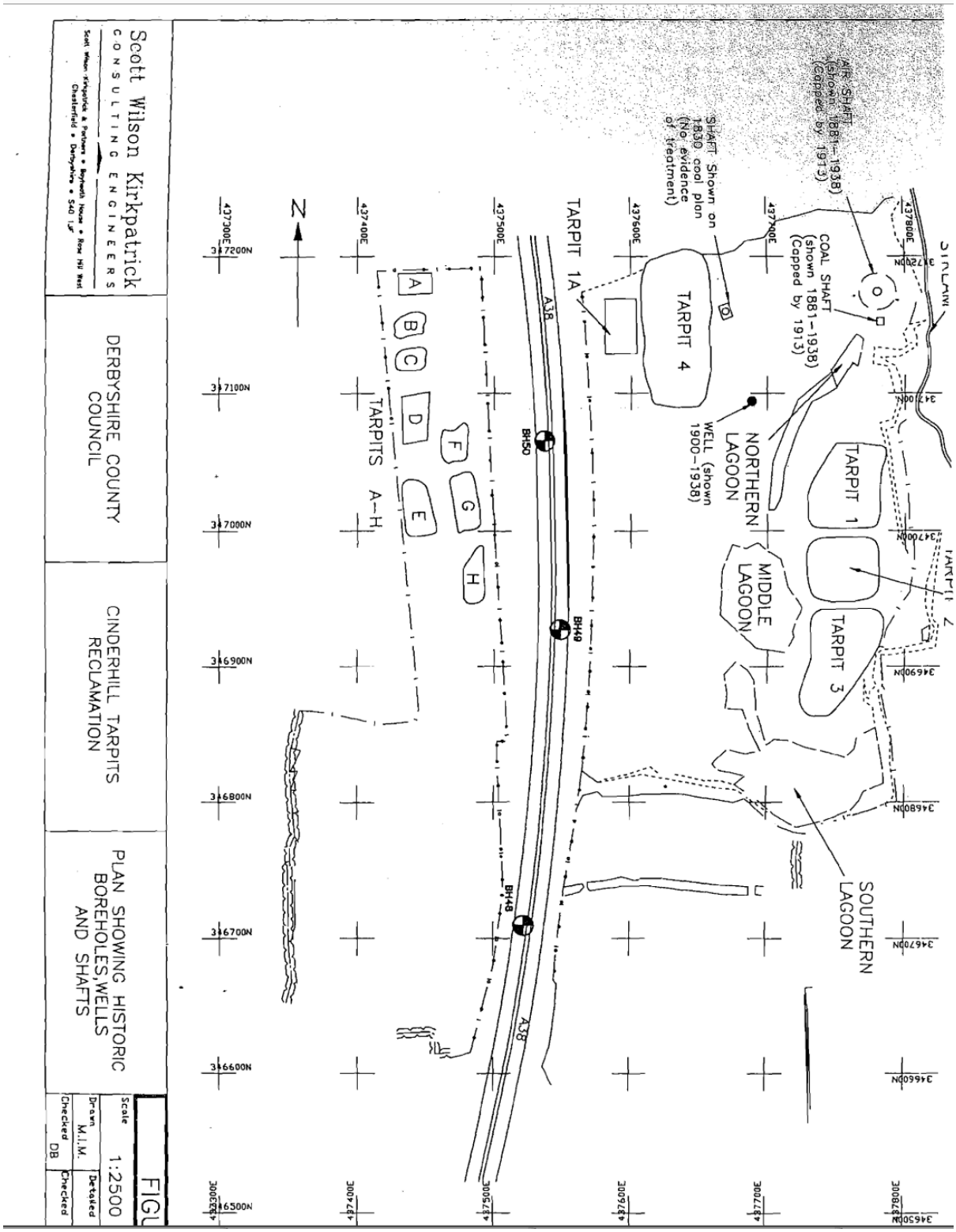
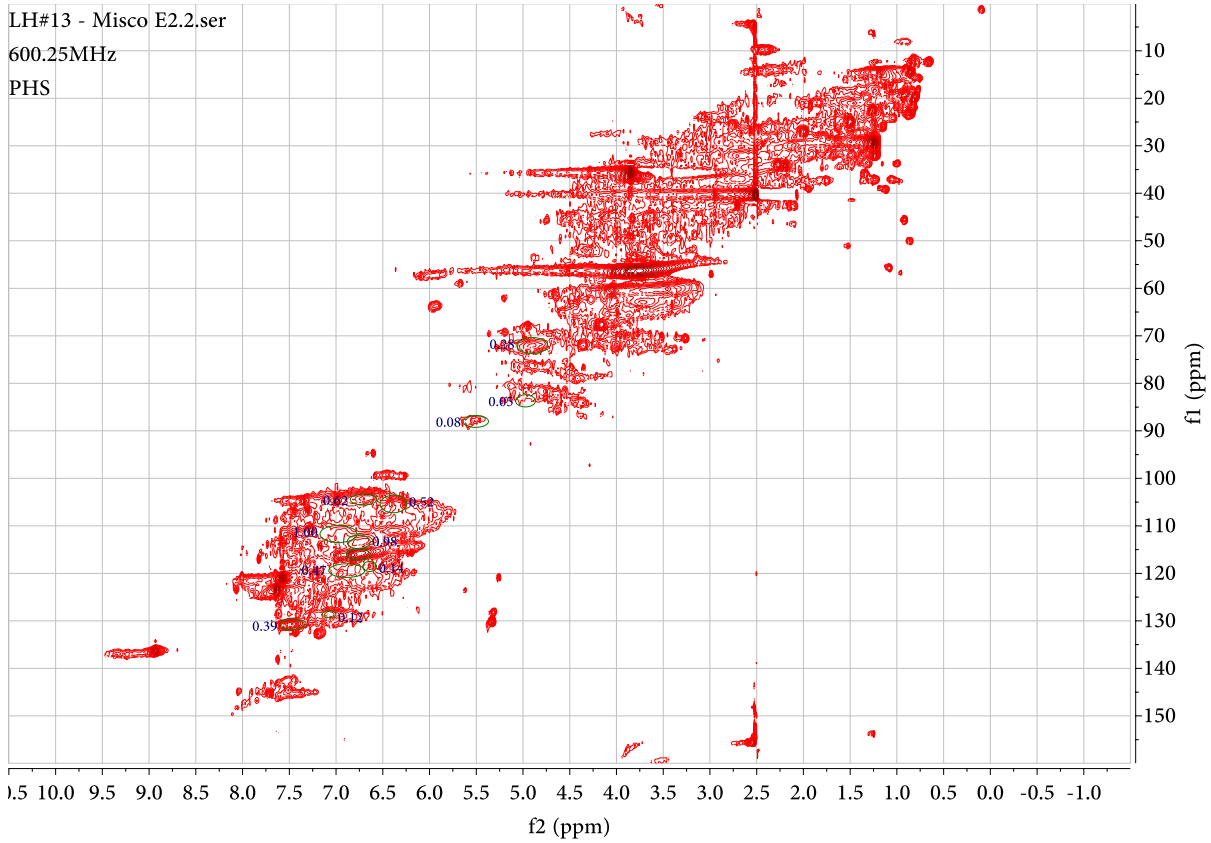


Figure S0.3: plant trial block design at Bwlch glas mine

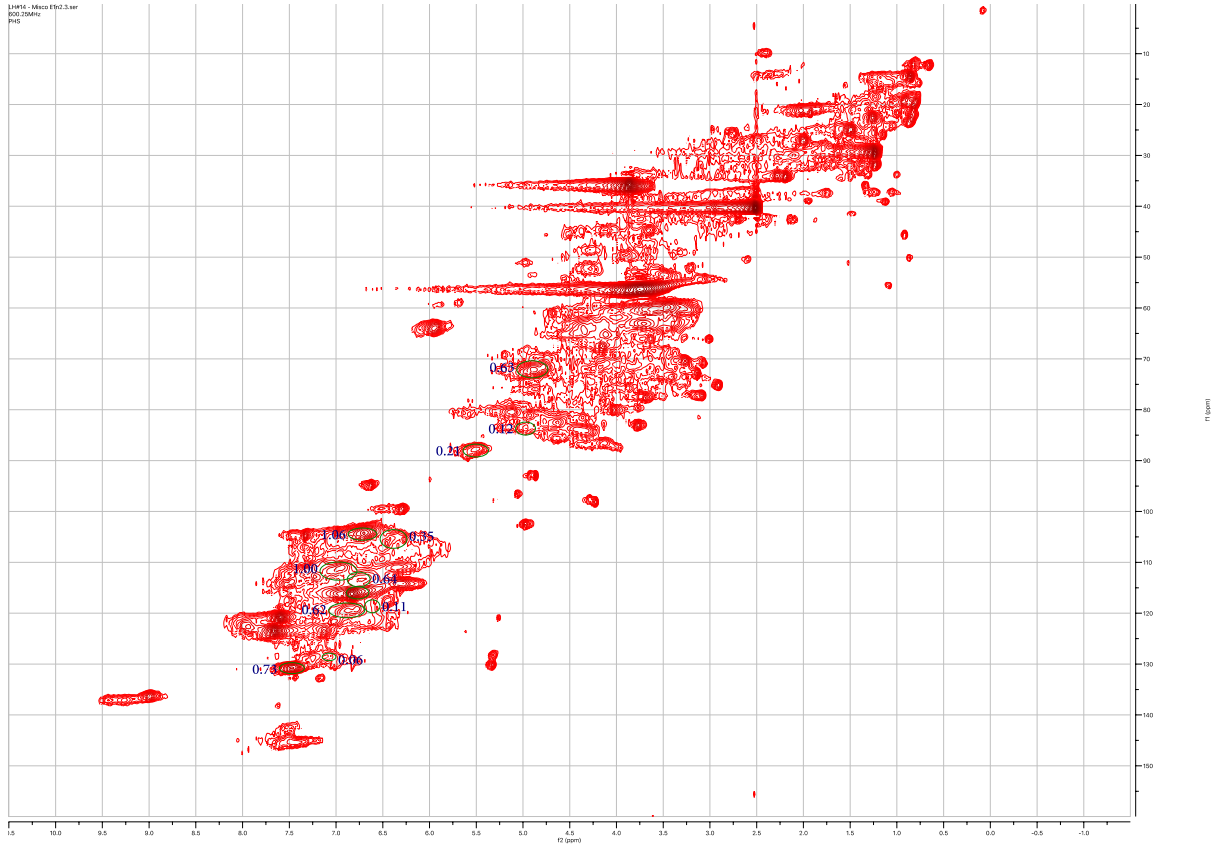
Figure S0.4: area of interest from CinderHill



A.



B.



C.

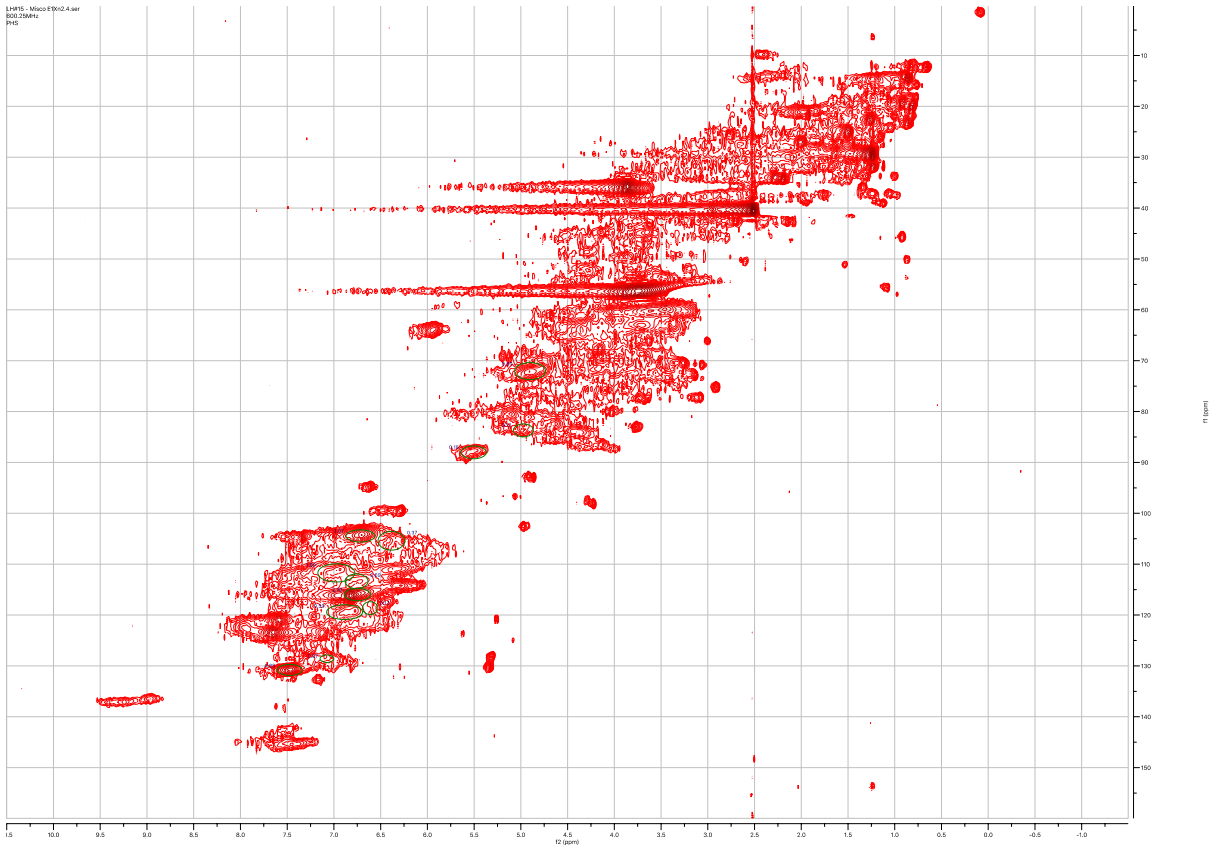
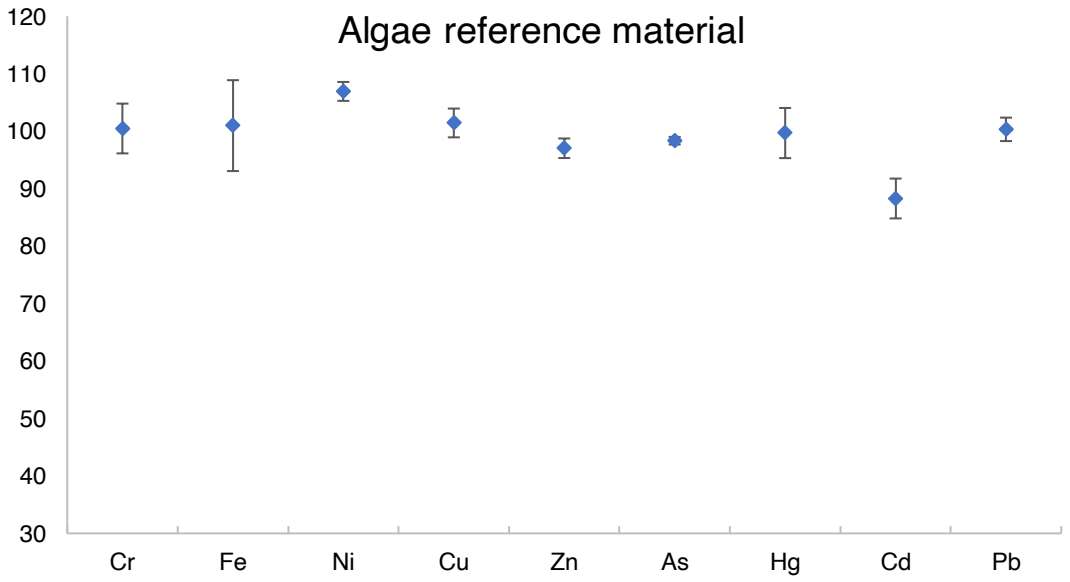


Figure S0.5: NMR HSQC spectra of Miscanthus ionoSolv lignin samples A. Miscanthus cycle 1, B. Miscanthus cycle 2 without electrodeposition, C. Miscanthus cycle 2 with electrodeposition

A.



B.

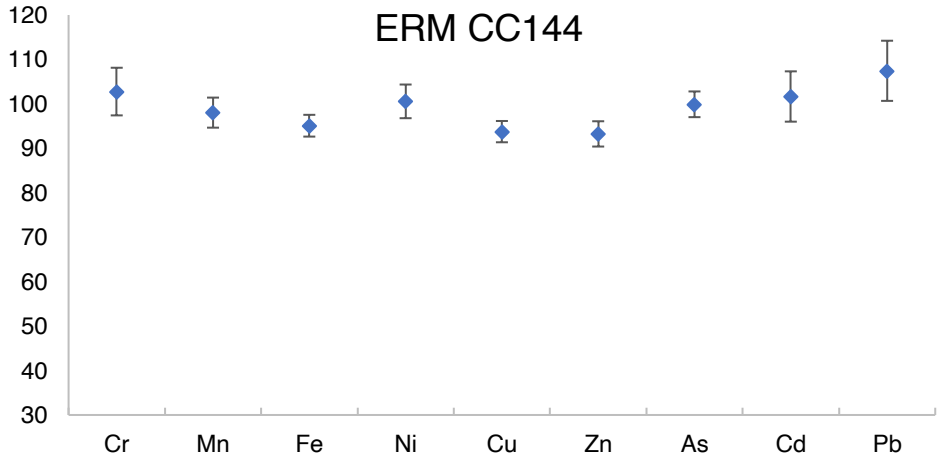


Figure S0.6: percentage recovery of certified trace element reference materials after acid digestion A. algae IAEA 413 B. sludge ERM® CC-144.

Mass	Element	Integration Time / Mass (sec)	Gas Mode used (Stabilisation time 7s H_2 / 5s He)	Internal Standard used
52	Cr	1.0	He	Ge
56	Fe	0.3	H_2	Ge
60	Ni	1.0	He	Ge
63	Cu	1.0	He	Ge
66	Zn	0.3	He	Ge
75	As	1.0	He	Y
78	Se	3.0	H_2	Y
111	Cd	3.0	He	Ir
201	Hg	3.0	He	In/Bi
208	Pb	3.0	He	In/BI

Table S0.2: details of the method developed for ICP-MS analysis. 4 replicates of 100 sweeps for each sample, 2 rinses of 60 seconds between each sample, nebulizer pump speed 0.1/0.3 rps

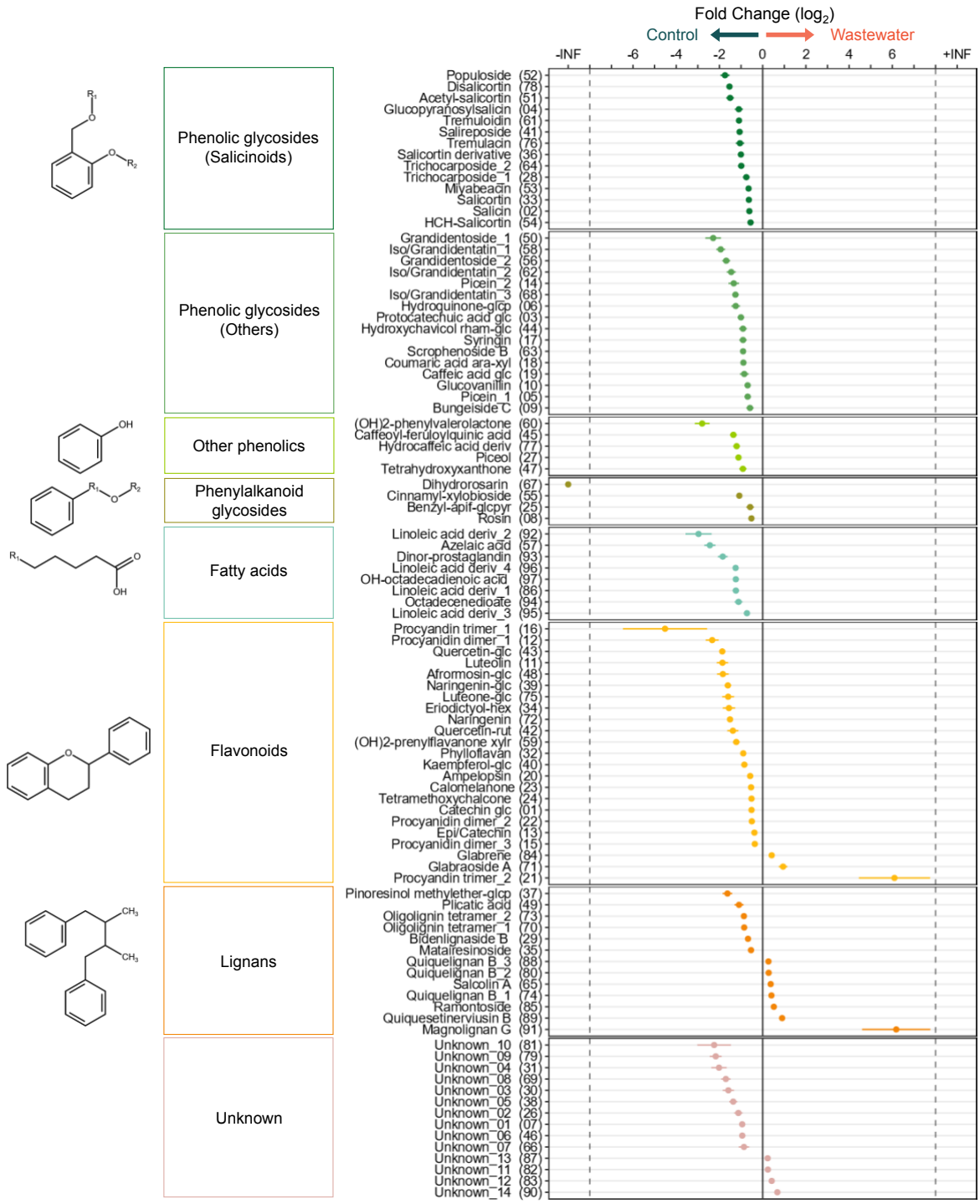


Figure S0.7: Differentially abundant phytochemicals between control and wastewater irrigated willows. Differentially abundant phytochemicals between control and wastewater irrigated trees were annotated and grouped by putative phytochemical classes.

Mann-Whitney U test was used followed by Benjamini-Hochberg false discovery rate (FDR) correction ($p < 0.05$). Fold change (FC log2) of mean peak intensities from significantly each),

standard error is shown. The dashed line indicates “infinite” fold change, where the phytochemical had detectable signal in trees from only one condition.

ID	Annotation	Formula	Compound class	Compound subclass	Cluster group
1	Catechin glucose	$C_{21}H_{26}O_{12}$	Flavonoids	Flavan-3-ol	Flavanols
2	Salicin	$C_{13}H_{18}O_7$	Phenolic glycosides (Salicinoids)	Salicinoid	Salicinoids
3	Protocatechuic acid 3-glucoside	$C_{13}H_{16}O_9$	Phenolic glycosides (Others)	Phenolic acid (glycosilated)	Glycosilated phenolic acids
4	2'-O-β-D-Glucopyranosylsalicin	$C_{19}H_{28}O_{12}$	Phenolic glycosides (Salicinoids)	Salicinoid	Phenylalkanoid glycosides
5	Picein_1	$C_{14}H_{18}O_7$	Phenolic glycosides (Others)	Phenolic cetone (glycosilated)	Phenolic glycosides
6	Hydroquinone-O-β-L-glucopyranoside	$C_{12}H_{16}O_7$	Phenolic glycosides (Others)	Simple phenol (glycosilated)	Glycosilated phenolic acids
7	Unknown_01	Unknown	Unknown	Unknown	N/A
8	Rosin	$C_{15}H_{20}O_6$	Phenylalkanoid glycosides	N/A	Phenolic glycosides
9	Bungeiside C	$C_{19}H_{26}O_{11}$	Phenolic glycosides (Others)	Phenolic cetone (glycosilated)	Phenylalkanoid glycosides
10	Glucovanillin	$C_{14}H_{18}O_8$	Phenolic glycosides (Others)	Phenolic aldehyde (glycosilated)	Glycosilated phenolic acids
11	Luteolin	$C_{13}H_{18}O_7$	Flavonoids	Flavone	N/A
12	Procyanidin dimer_1	$C_{30}H_{24}O_{12}$	Flavonoids	Flavan-3-ol (polymer)	Flavanols
13	Catechin	$C_{15}H_{14}O_6$	Flavonoids	Flavan-3-ol	Flavanols
14	Picein_2	$C_{14}H_{18}O_7$	Phenolic glycosides (Others)	Phenolic cetone (glycosilated)	N/A
15	Procyanidin dimer_3	$C_{30}H_{26}O_{12}$	Flavonoids	Flavan-3-ol (polymer)	Flavanols
16	Procyandin trimer_1	$C_{45}H_{38}O_{18}$	Flavonoids	Flavan-3-ol (polymer)	Flavanols
17	Syringin	$C_{17}H_{24}O_9$	Phenolic glycosides (Others)	Phenolic alcohol (glycosilated)	Phenylalkanoid glycosides
18	p-Coumaric acid arabinoxylan	$C_{20}H_{26}O_{12}$	Phenolic glycosides (Others)	Phenolic acid (glycosilated)	Phenolic glycosides
19	Caffeic acid 3-glucoside	$C_{15}H_{18}O_9$	Phenolic glycosides (Others)	Phenolic acid (glycosilated)	N/A
20	Ampelopsin	$C_{15}H_{12}O_8$	Flavonoids	Flavanonol	N/A
21	Procyandin trimer_2	$C_{45}H_{38}O_{18}$	Flavonoids	Flavan-3-ol (polymer)	N/A
22	Procyanidin dimer_2	$C_{30}H_{26}O_{12}$	Flavonoids	Flavan-3-ol (polymer)	Flavanols
23	Calomelanone	$C_{17}H_{18}O_5$	Flavonoids	Chalcone	N/A
24	2,3,4,6-Tetramethoxychalcone	$C_{19}H_{20}O_5$	Flavonoids	Chalcone	N/A
25	Benzyl-β-D-apiofuranosyl-(1→6)-β-D-glucopyranoside	$C_{18}H_{26}O_{10}$	Phenylalkanoid glycosides	N/A	Phenylalkanoid glycosides
26	Unknown_02	Unknown	Unknown	Unknown	N/A
27	Piceol	$C_8H_8O_2$	Other phenolics	Phenolic cetone	N/A
28	Trichocarposide_1	$C_{22}H_{24}O_9$	Phenolic glycosides (Salicinoids)	Salicinoid	Phenylalkanoid glycosides
29	Bidenlignaside B	$C_{26}H_{34}O_{12}$	Lignans	Neolignan	N/A
30	Unknown_03	Unknown	Unknown	Unknown	Flavanols
31	Unknown_04	Unknown	Unknown	Unknown	Salicinoids

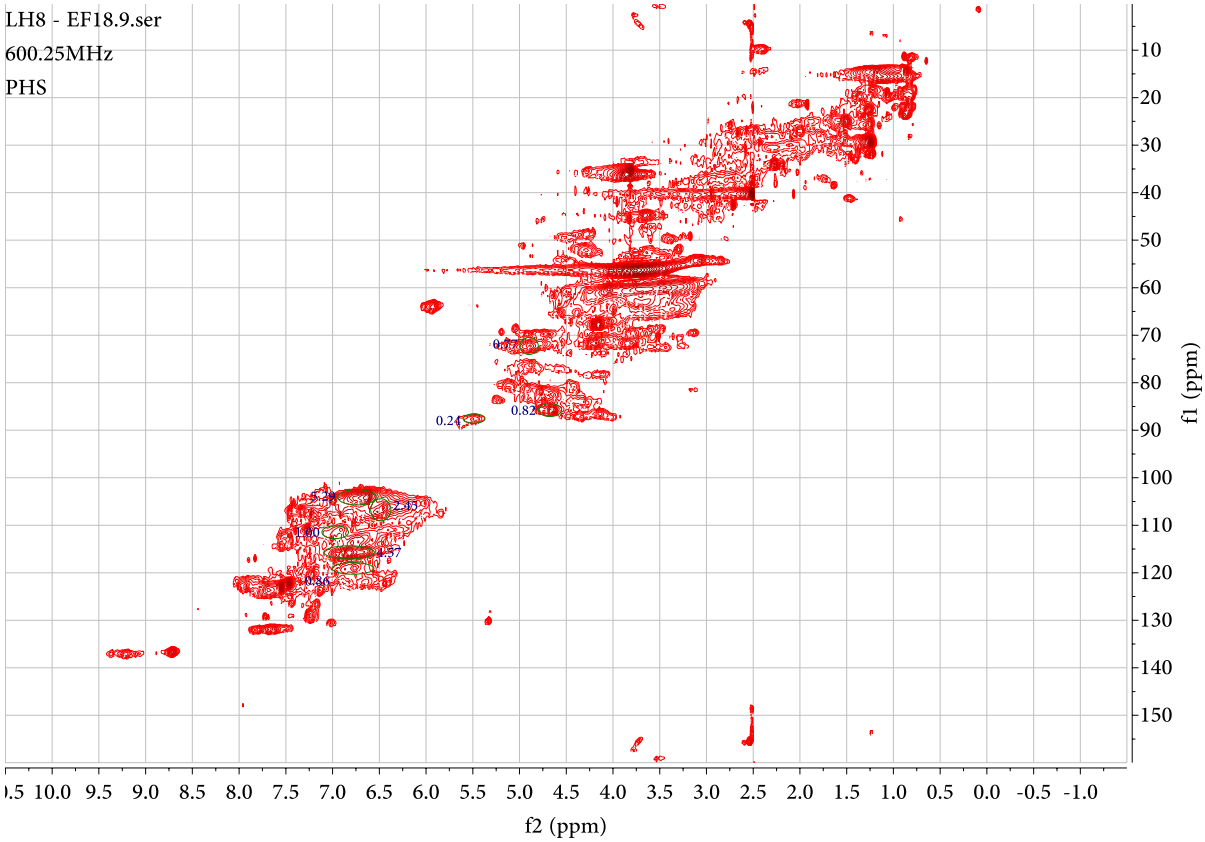
32	Phylloflavan	$C_{26}H_{26}O_{10}$	Flavonoids	Flavan-3-ol (glycoside)	Flavanols
33	Salicortin	$C_{20}H_{24}O_{10}$	Phenolic glycosides (Salicinoids)	Salicinoid	Salicinoids
34	Eriodictyol-O-hexoside	$C_{21}H_{22}O_{11}$	Flavonoids	Flavanone (glycoside)	(7-O) glycosilated flavonoids
35	Matairesinoside	$C_{26}H_{32}O_{11}$	Lignans	Glycosilated lignan	N/A
36	Salicortin derivative	$C_{20}H_{24}O_{11}$	Phenolic glycosides (Salicinoids)	Salicinoid	Salicinoids
37	Pinoresinol monomethyl ether-O-β-d-glucopyranoside	$C_{27}H_{34}O_{11}$	Lignans	N/A	N/A
38	Unknown_05	Unknown	Unknown	Unknown	Phenylalkanoid glycosides
39	Naringenin-7-glucoside	$C_{21}H_{22}O_{10}$	Flavonoids	Flavanone (glycoside)	(7-O) glycosilated flavonoids
40	Kaempferol-3-O-glucoside	$C_{21}H_{20}O_{11}$	Flavonoids	Flavonol (glycoside)	(3-O) glycosilated flavonoids
41	Salireposide	$C_{20}H_{22}O_{9}$	Phenolic glycosides (Salicinoids)	Salicinoid	Salicinoids
42	Quercetin-3-rutinoside	$C_{27}H_{30}O_{16}$	Flavonoids	Flavonol (glycoside)	(3-O) glycosilated flavonoids
43	Quercetin-3-O-glucoside	$C_{21}H_{20}O_{12}$	Flavonoids	Flavonol (glycoside)	(3-O) glycosilated flavonoids
44	3-Hydroxychavicol 1-[rhamnosyl-(1->6)-glucoside]	$C_{21}H_{30}O_{11}$	Phenolic glycosides (Others)	Phenylpropane	Phenylalkanoid glycosides
45	1-Caffeoyl-5-feruloylquinic acid	$C_{26}H_{26}O_{12}$	Other phenolics	Hydroxycinnamic acid	N/A
46	Unknown_06	Unknown	Unknown	Unknown	N/A
47	1,3,6,7-Tetrahydroxyxanthone	$C_{13}H_{8}O_{6}$	Other phenolics	Xanthone	N/A
48	Afrormosin-7-O-glucoside	$C_{23}H_{24}O_{10}$	Flavonoids	Isoflavone (glycoside)	(7-O) glycosilated flavonoids
49	Plicatic acid	$C_{20}H_{22}O_{10}$	Lignans	N/A	Lignans
50	Grandidentoside_1	$C_{21}H_{28}O_{10}$	Phenolic glycosides (Others)	Hydroxycinnamic ester (glycosilated)	Phenolic glycosides
51	2'-O-Acetyl-salicortin	$C_{22}H_{26}O_{11}$	Phenolic glycosides (Salicinoids)	Salicinoid	N/A
52	Populoside (A)	$C_{22}H_{24}O_{10}$	Phenolic glycosides (Salicinoids)	Salicinoid	Phenolic glycosides
53	Miyabeacin	$C_{40}H_{44}O_{20}$	Phenolic glycosides (Salicinoids)	Salicinoid	N/A
54	HCH-Salicortin	$C_{27}H_{30}O_{13}$	Phenolic glycosides (Salicinoids)	Salicinoid	Salicinoids
55	Cinnamyl-β-D-xylobioside	$C_{19}H_{26}O_{9}$	Phenylalkanoid glycosides	N/A	N/A
56	Grandidentoside_2	$C_{21}H_{28}O_{10}$	Phenolic glycosides (Others)	Hydroxycinnamic ester (glycosilated)	Phenolic glycosides
57	Azelaic acid	$C_{9}H_{16}O_{4}$	Fatty acids	Dicarboxylic acid	N/A
58	Iso/Grandidentatin_1	$C_{21}H_{28}O_{9}$	Phenolic glycosides (Others)	Hydroxycinnamic ester (glycosilated)	Phenolic glycosides
59	5,4-Dihydroxy-6-C-prenylflavanone 4-xylosyl-(1-2)-rhamnoside	$C_{31}H_{38}O_{12}$	Flavonoids	Flavanone (glycoside)	N/A

60	5-(Dihydroxyphenyl)-gamma-valerolactone	$C_{11}H_{12}O_4$	Other phenolics	Lactone	N/A
61	Tremuloidin	$C_{20}H_{22}O_8$	Phenolic glycosides (Salicinoids)	Salicinoid	Salicinoids
62	Iso/Grandidentatin_2	$C_{21}H_{28}O_9$	Phenolic glycosides (Others)	Hydroxycinnamic ester (glycosilated)	Phenolic glycosides
63	Scrophenoside B	$C_{23}H_{24}O_9$	Phenolic glycosides (Others)	Hydroxycinnamic ester (glycosilated)	Phenolic glycosides
64	Trichocarposide_2	$C_{22}H_{24}O_9$	Phenolic glycosides (Salicinoids)	Salicinoid	Phenolic glycosides
65	Salcolin A	$C_{27}H_{26}O_{11}$	Lignans	Flavanolignan	Lignans
66	Unknown_07	Unknown	Unknown	Unknown	N/A
67	Dihydrorosarin	$C_{20}H_{30}O_{10}$	Phenylalkanoid glycosides	N/A	Phenylalkanoid glycosides
68	Iso/Grandidentatin_3	$C_{21}H_{28}O_9$	Phenolic glycosides (Others)	Hydroxycinnamic ester (glycosilated)	Phenolic glycosides
69	Unknown_08	Unknown	Unknown	Unknown	N/A
70	Oligolignin tetramer_1	$C_{42}H_{50}O_{16}$	Lignans	Oligolignin	N/A
71	Glabraoside A	$C_{30}H_{30}O_{13}$	Flavonoids	Flavan-3-ol	N/A
72	Naringenin	$C_{15}H_{12}O_5$	Flavonoids	Flavanone	N/A
73	Oligolignin tetramer_2	$C_{42}H_{50}O_{16}$	Lignans	Oligolignin	N/A
74	Quiquelignan B	$C_{36}H_{36}O_{13}$	Lignans	Flavanolignan	Lignans
75	Luteone 7-glucoside	$C_{26}H_{28}O_{11}$	Flavonoids	Isoflavone (glycoside)	N/A
76	Tremulacin	$C_{27}H_{28}O_{11}$	Phenolic glycosides (Salicinoids)	Salicinoid	Salicinoids
77	Disynapoyl-hydro feruloyl-feruloyl-hydrocaffeic acid	$C_{40}H_{52}O_{26}$	Other phenolics	Hydroxycinnamic acid	N/A
78	Disalicortin	$C_{40}H_{48}O_{20}$	Phenolic glycosides (Salicinoids)	Salicinoid	Salicinoids
79	Unknown_09	Unknown	Unknown	Unknown	Salicinoids
80	Quiquelignan B	$C_{36}H_{36}O_{13}$	Lignans	Flavanolignan	Lignans
81	Unknown_10	Unknown	Unknown	Unknown	N/A
82	Unknown_11	Unknown	Unknown	Unknown	N/A
83	Unknown_12	Unknown	Unknown	Unknown	Lignans
84	Glabrene	$C_{20}H_{18}O_4$	Flavonoids	Isoflavan (pterocarptan)	N/A
85	Ramontoside	$C_{34}H_{38}O_{16}$	Lignans	Butyrolactone lignan	Lignans
86	Linoleic acid derivative (pinellic acid)	$C_{18}H_{34}O_5$	Fatty acids	Linoleic acid	Fatty acids
87	Unknown_13	Unknown	Unknown	Unknown	N/A
88	Quiquelignan B	$C_{36}H_{36}O_{13}$	Lignans	Flavanolignan	Lignans
89	Quiquesetinerviusin B	$C_{35}H_{32}O_{11}$	Lignans	Flavanolignan derivatives	Lignans
90	Unknown_14	Unknown	Unknown	Unknown	N/A
91	Unknown_15	Unknown	Unknown	Unknown	N/A
92	Linoleic acid derivative (pinellic acid)	$C_{18}H_{34}O_5$	Fatty acids	Linoleic acid	Fatty acids
93	2,3-Dinor-8-iso prostaglandin F1 α	$C_{18}H_{32}O_5$	Fatty acids	Prostaglandin	Fatty acids
94	alpha,omega-9Z-Octadecenedioate	$C_{18}H_{30}O_4$	Fatty acids	Linoleic acid	N/A

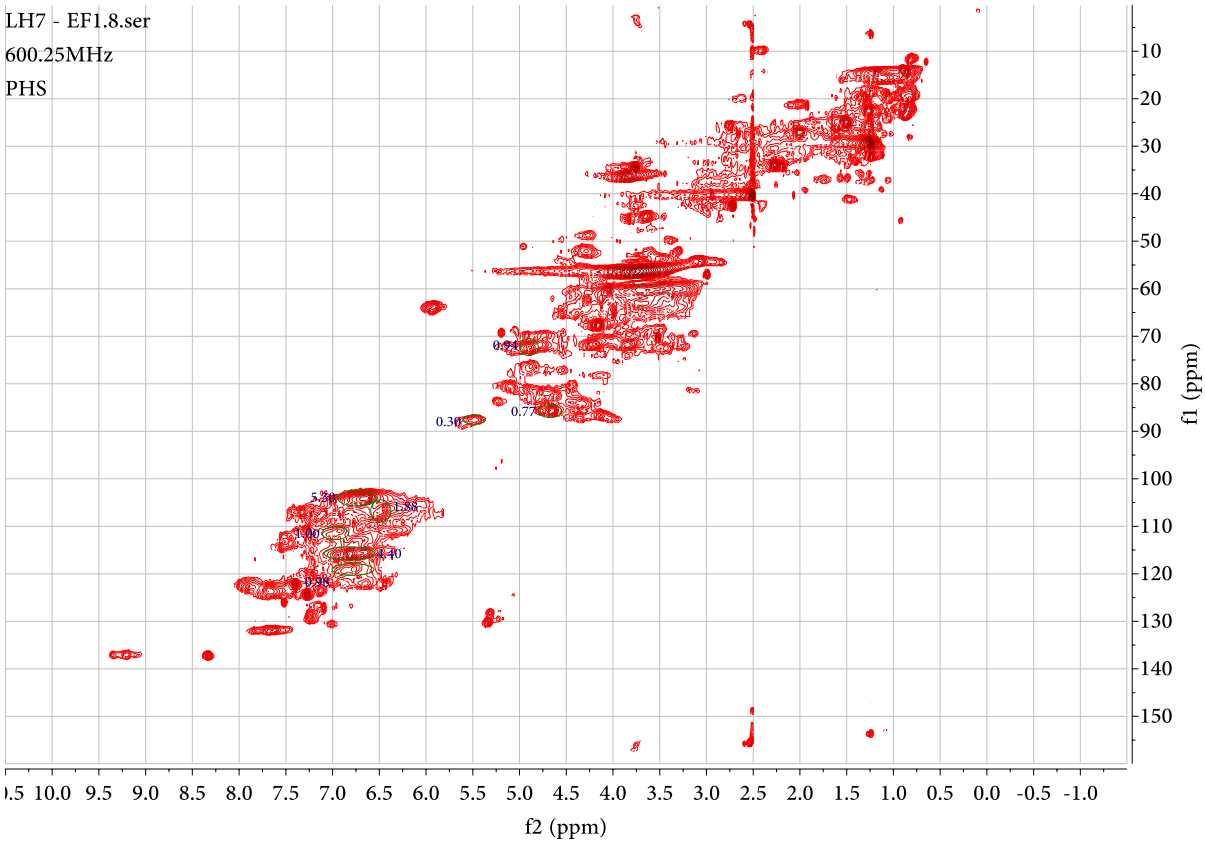
95	Linoleic acid derivative (octadecenedioic acid)	$C_{18}H_{32}O_4$	Fatty acids	Linoleic acid	N/A
96	Linoleic acid derivative (octadecenedioic acid)	$C_{18}H_{32}O_4$	Fatty acids	Linoleic acid	N/A
97	Hydroxy-octadecadienoic acid	$C_{18}H_{32}O_3$	Fatty acids	Linoleic acid	N/A

Table S0.3: phytochemicals annotations, formulas and classes associated.

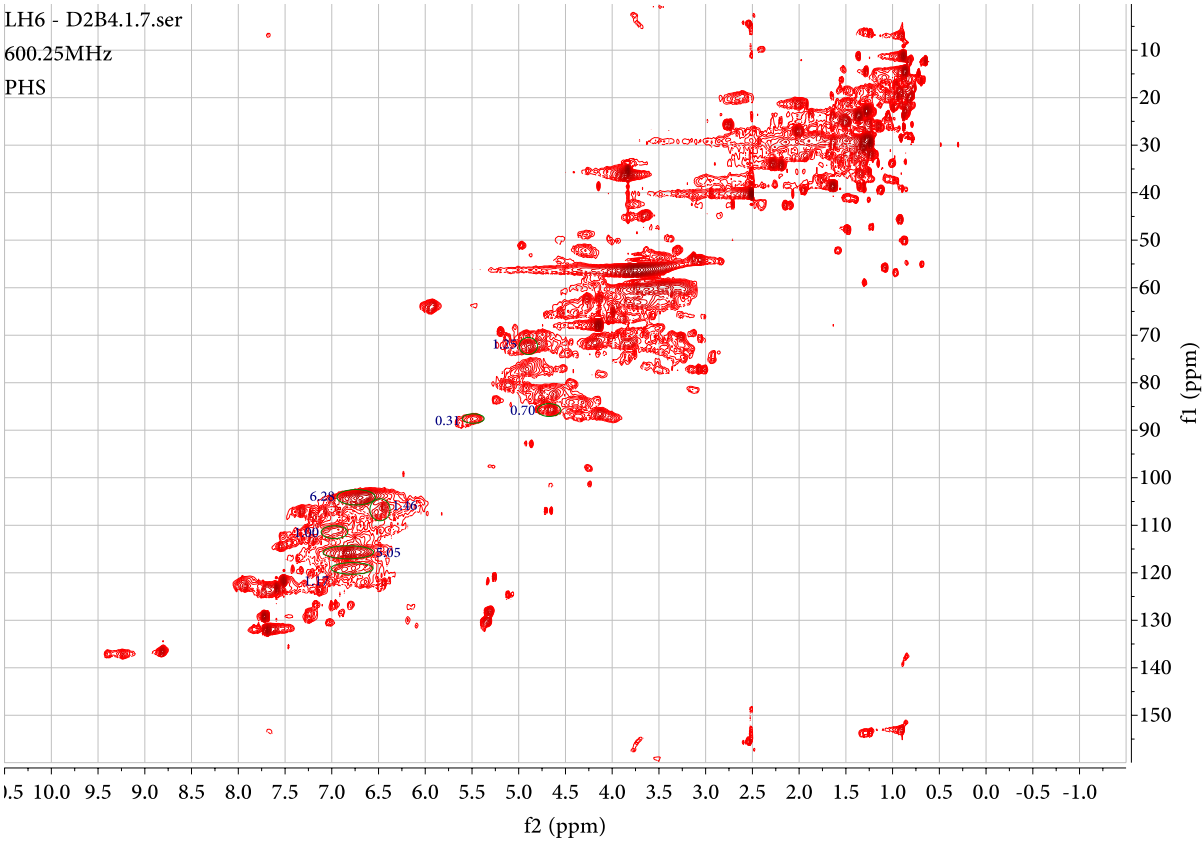
A.


LH8 - EF18.9.ser
600.25MHz
PHS
f1 (ppm)
f2 (ppm)

B.


LH7 - EF1.8.ser
600.25MHz
PHS
f1 (ppm)
f2 (ppm)

C.



D.

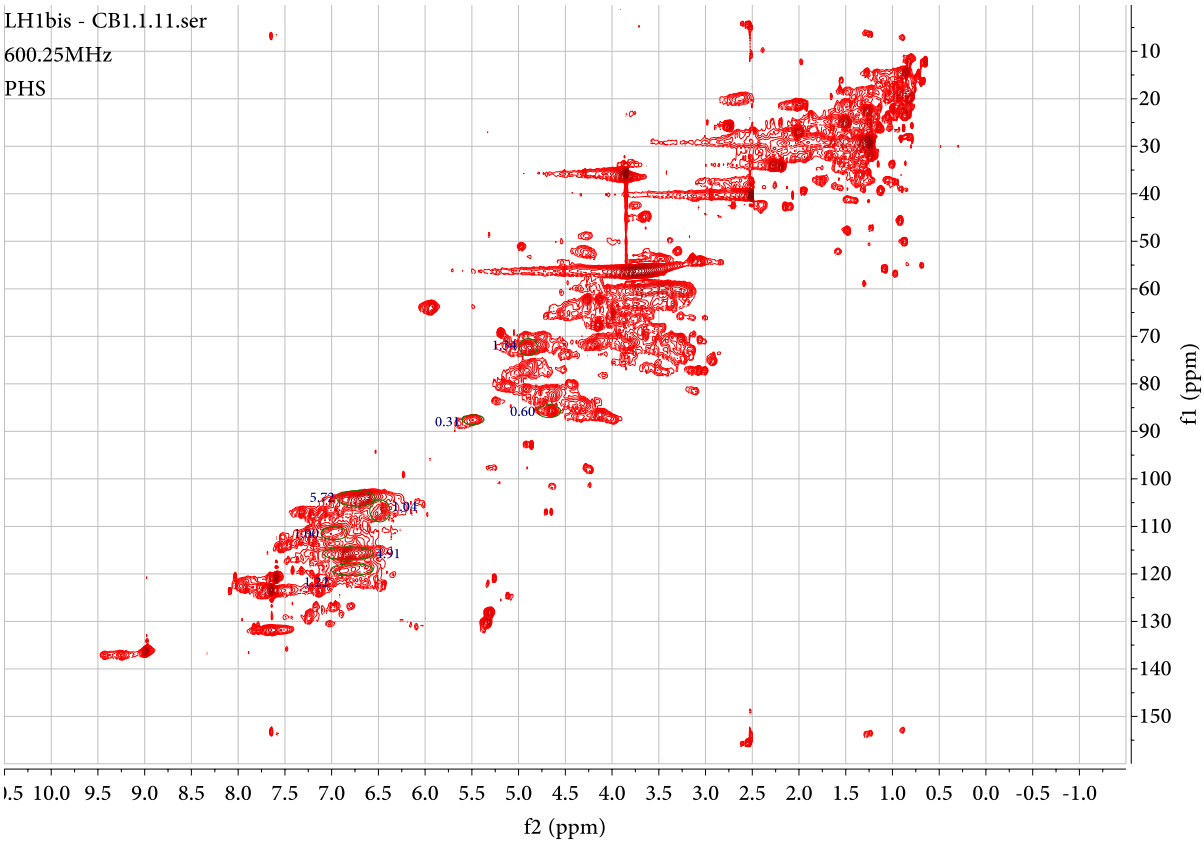


Figure S0.8: NMR HSQC spectra of ionoSolv lignin from Canadian willow A. wastewater extractives-free, B. controls extractives free, C. wastewater with extractives, D. control with extractives

10 The use of an algae-flow way for consistent biomass production and utilisation of compromised waters

10.1 Introduction

The Salton Sea is a large, landlocked body of water with a tumultuous ecological history. It was formed in 1905 when the Colorado river overflowed a manmade canal and filled the Salton Sink, an endorheic basin separating the Imperial and Coachella valleys in California's Colorado Desert.[1] While the basin had held standing water many times throughout North America's geological history, it had only been for brief periods of time in the last 3000 years prior to this overflow, which created the large sea that exists today. Since its formation, the Salton Sea and its tributaries from the Colorado river have played a critical economic and ecological role in Riverside and Imperial Counties. Furthermore, the sea itself has become a highly trafficked stop for many migratory birds along the Pacific Flyway, and the tributaries to the sea, namely the Alamo, New, and Whitefish rivers, have supported a large agricultural presence in the Imperial valley.[2]

Water has become an increasingly constrained resource in the Imperial Valley in recent years due to growing metropolitan areas in the Southwest desert and reduced snowpack in the Colorado River Watershed.[3] The reduction of water flowing to the Colorado River has inadvertently affected the amount of water flowing into the Salton Sea[4]; in the period of 15 years from 2004 to 2019, the surface depth has dropped by more than three meters.[5] Beyond the severe health and economic impacts of the rapidly receding shoreline and exposed playa, the decrease in total water volume has significantly increased salinity levels in the Salton Sea.[6,7] This increasing hyper-salinity has strained the local aquatic ecosystem with cascading impacts across the food chain. Of particular concern is the health of the bird populations that rely on the Salton Sea during migration.

The Imperial Valley produced roughly $1.5 billion worth of field crops in 2018.[8] Water usage for agriculture in the region creates significant nutrient runoff, which coupled to reduced total water inputs leads to growing concerns around eutrophication and more serious biological instability of the Salton Sea. In addition to nutrients and salinity, weathering of minerals accumulated along the Colorado River basin has led to increased heavy metal concentrations (As, Cr, Cd, Pb, Zn, Ni, Fe, Mo, Mn, etc.) in soil and water systems. [9] Furthermore, common agricultural and industrial effluents contribute to elevated total organics loading, as indicated by biological oxygen demand (BOD). Increased agricultural demand and increasing

populations in the imperial valley are expected to further exacerbate these issues in the coming decades.

In addition to ecological challenges from eutrophication and increasing salinity, the Salton Sea is a terminal destination for Selenium salts leached from soil in crustaceous formations in the upper regions of the Colorado River watershed.[10,11] Selenium (Se) is a known biological toxicant to both fish and birds when bioaccumulated.

While there have been many proposals to address the water scarcity and salinity issues of the Salton Sea, very few solutions have been proposed to remedy the impacts of trace element accumulation and eutrophication. Several previous studies have reported on the performance of algae flow-way systems using a variety of source waters; the Alamo River tributary to the Salton Sea provides a unique opportunity to evaluate the application of periphytic algae flow-way systems to bioaccumulate a range of contaminants together.[12–14] In principle, phototrophic algae have the potential to address these challenges. Algae are widely known to rapidly uptake N/P during growth and have also been demonstrated to bioaccumulate contaminants, such as Se.[15–18] However, the scale of the installation, required flow rates, capital cost, and biological stability make traditional open raceway pond algae cultivation solutions untenable for this application. To investigate the potential for algae cultivation to address the Se and eutrophication issues, we investigated the use of an autotrophic biofilm cultivation system which propagates naturally abundant (i.e. periphytic) algae biomass. The system and biomass that is produced are generally referred to as “Algae Turf” because of resemblance to open field agriculture. For this study, we investigated the major properties of the biomass and metals accumulation resulting from cultivation and weekly harvesting of the algae biofilm using untreated Alamo River water. Through the use of the Algae Turf system, we were able to simultaneously intercept dilute N, P, BOD, Se, and other persistent contaminants from the runoff. During the full 2-years of operation, turf algae biomass production was continuous, demonstrating resiliency and high nutrient utilization efficiencies at low nutrient loadings, indicating the potential of attached algae systems to address significant environmental challenges facing the Salton Sea.

10.2 Materials and methods

10.2.1 Algae flow-way deployment location and operations

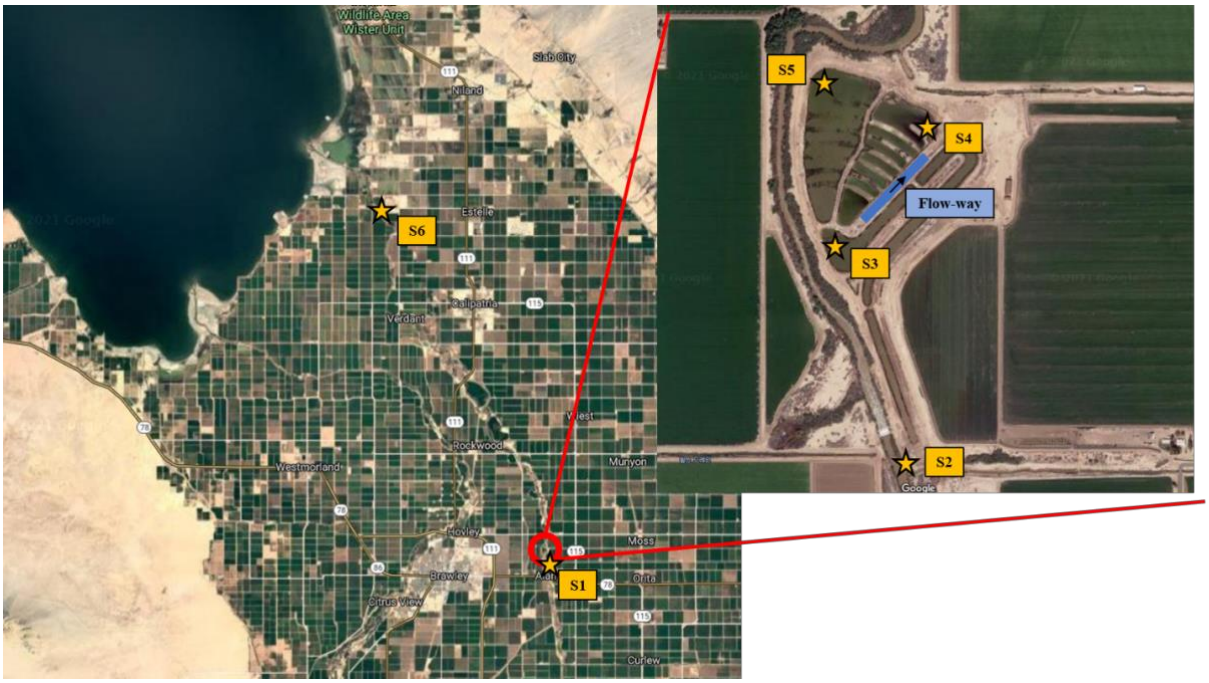


Figure S6.1: satellite image of study area of the attached algae flow-way deployment at around the Alamo River, a tributary of the Salton Sea in Brawley, CA.

The site of the field trial was adjacent to the Alamo River, one of two southern tributaries to Salton Sea; more precisely as a feature of the Alamo River Wetland (Figure S6.1), operated by the Imperial Irrigation District. On Figure S6.1, S1 indicates upstream of the Alamo River; S2 indicates upstream of the wetland, where the water is diverted into the Alamo River Wetlands; S3 indicates the end of the settling basin of the Shank Road wetland, where the water is split between the West Cell and the East Cell and where the inlet of the algae flow-way is located; S4 indicates that the outlet of the Shank Road wetland East Cell, where the outlet of the algae flow-way is located, S5 indicates the outlet of the Shank Road wetland West Cell, where the water is not diverted into the algae flow-way; and S6 indicates Alamo River Downstream, bank of the river very close to the delta where the river flows into the Salton Sea. The algae flow-way used in this study was acquired from Hydromentia Inc and was 0.3m wide and 275 m long. A black nylon 3D mesh, the same model used by Hydromentia Inc, was used as the substrate in this study and was laid on the 245m(l) x 0.3(w) flow-way. The Hydromentia Inc system included a headwork unit to provide a pulsed flow with an adjustable interval. A Grundfos SQF-40 well pump was used to supply water to the surge tank from the terminus of the settling basin, labelled as location S3 in Figure S6.1. The pump speed was set so that the flowrate going into the surge box of the flow-way was at approximately 35-40 L min^{-1} with an

interval between surges of approximately 1 minute. The flow-way was constructed using stilted support for a 0.5 % slope over its 270 m length. Pumping of water from the settling basin was provided by a PV - battery bank.

The algae biomass was manually harvested on a 7-day cycle using squeegees to scrape the filamentous algae into collection pans which were then transferred to fish baskets lined with mesh screen for dewatering. The harvested algae was allowed to sit for 24 hours to before being weighed. Biomass was harvested sequentially in 30 m sections along the total 270 m of length, so for each harvest nine fish baskets were filled, and the tared weight taken. From this dewatered material three different samples were taken from the top, middle, and bottom of the basket and combined to fill a 1L container. These samples were then shipped on ice to Sandia National Laboratories in Livermore, CA for additional analysis.

10.2.2 Ash-free biomass productivity and its compositional analysis

Dried biomass was ground into a fine powder using a hammer mill (Model CF198, Chippewa Falls, WI) and mixed to be homogeneous. Ash content measurement method was essentially the same method conducted in the previous study, which is the standard measurement method of ash content in biomass reported by NREL.[19,20] Proximate analysis was completed via EPA method XYZ by New Jersey Feed Lab (NJFL) in BLANK, New Jersey. Calories, Phosphorus, crude fat, crude carbohydrate, crude protein, and crude fibre contents were analysed from New Jersey Feed Lab (1686 5th St, Ewing Township, NJ). Nitrogen content was calculated by dividing protein content by 4.8.[21]

10.2.3 Microbial analysis

Microbial analysis data were derived from samples collected in the flow-ways during regular biomass harvests. Replicate samples collected at each location were treated as independent samples to assess the validity and reproducibility of the results. Pair-end sequencing was performed using Illumina MiSeq protocol resulting in 300 base pair reads which were converted into demultiplexed fastq files. The periphytic biofilms are diverse and bioinformatic challenges were expected. To overcome these expected challenges we employed the DADA2 pipeline to produce exact amplicon sequence variants (ASVs).[22] Low-quality reads were trimmed (approximately 100-150 bp) and Illumina adapters were removed prior to performing downstream analysis. A database containing the taxonomic assignment, the ASV table, and sample information was generated using the R package phyloseq.[23] Normalization and rarefying (less than 1,000 ASVs) of the dataset was performed before calculating the proportion of the microbial community within the flow way.

10.2.4 Environmental sampling for trace elements

Water samples were collected in clean 250 mL plastic containers and neutralized with Nitric Acid Trace Metal Grade for preservation from VWR based on the EPA 200.8 method.[24]
Algae samples were collected using plastic spatulas and buckets. The algae was then air dried for 24 hours, further oven dried at 100°C and placed in sealed clean plastic bags for analysis. Sediment samples were collected in 250 mL plastic containers then further freeze-dried for further analysis using a LabConco FreezeDry Benchtop.

10.2.5 Calculations of environmental factors

Enrichment and contamination factors were calculated according to the following equations:

$$Contamination\ Factor = CF = C_{metal}/C_{background}$$

$$Enrichment\ Factor = EF = \frac{(\frac{C_{metal}}{C_{Fe}})_{sample}}{(\frac{C_{metal}}{C_{Fe}})_{background}}$$

where C_{metal} is the concentration of the metal in the sample (mg kg^{-1}), $C_{background}$ is the background reference value of the same metal and the subscript *Fe* refers to the iron concentration (mg kg^{-1}). The background values for the sediments are available from the 'Distribution of the Elements in Some Major Units of the Earth's Crust' for North America.[25]
The evaluation criteria were as described in the table below:

Environmental Index	Criteria	References
EF	EF > 1.5 (human influence) 1.5 < EF < 3 (minor modification) 3 < EF < 5 (moderate modification) 5 < EF < 10 (severe modification) EF > 10 (very severe modification)	[26,27]
CF	CF < 1 (low contamination) 1 < CF < 3 (moderate contamination) 3 < CF < 6 (considerable contamination) CF > 6 (high contamination)	

The bioconcentration factor (BCF) was calculated at the inlet and the outlet of the flow-way, according to the equation:

$$Bioconcentration\ Factor = BCF = \frac{C_{algae}}{C_{water}}$$

$$BCF_{inlet} = \frac{C_{algae\ 100\ ft}}{C_{water\ inlet}}$$

$$BCF_{oulet} = \frac{C_{algae\ 900\ ft}}{C_{water\ oulet}}$$

where *C* is the concentration of a trace element in mg kg^{-1} in the algae or the water at a given time point. *100 ft* and *900 ft* refer to algae sampled at this exact distance of the flow-way, corresponding to inlet and outlet respectively.

The evaluation criteria for the BCF are described in the table below (established for animal species):

Factor	Criteria	References
BCF	BCF < 1000 species non accumulative 5000 > BCF > 1000 species accumulative BCF > 5000 species very accumulative	[28–33]

10.2.6 Trace element analysis

All reagents used are trace element pure grade from Fisher Scientific and all equipment was soaked into 2 % nitric acid overnight. All trace element experiments were carried out in a designated laboratory at Imperial College of London, designed for safety and to avoid any trace element contamination.

Samples were digested in concentrated acids for trace metal analysis from Fisher Scientific based on the Environmental Protection Agency Method 3051a.[34] In brief, 500 mg of sample was weighed into iWave EasyPrep digestion vessels. A mixture of concentrated acids was added to the solids: 9 mL of 69 % HNO_3 and 3 mL of 37 % HCl; and the vessels were fully

tightened. The vessels were placed in CEM Mars™ 6 microwave temperature and power-controlled reactor. The digestion program had 3 stages: 5.5 minutes at 175°C, followed by 10 minutes at 100°C and finally cooling down for 15 minutes. After the digestion, the samples were allowed to further cool down for a minimum of 3 hours at room temperature. The vessels were carefully opened and diluted in 100 mL plastic volumetric flasks with ultra-purified water (18.2 $\Omega.cm^{-1}$). The samples were shaken and 10 mL aliquots were filtered (0.22 μm) and used for IPC-MS analysis. All samples were done in triplicates, with blanks for each run from the digestion vessels. Diluted samples were through an Agilent 7900 ICP-MS. Multi-element standard ICP solutions were made from Inorganic Ventures™ stock solutions in the same matrix as the microwave digested filtered samples. A mixture of different internal standards was used to match the different ionization potentials of the analytes and internal standard recoveries were monitored for each run.

To assess the digestion and ICP methods used, reference standard materials were also analysed: Sewage Sludge reference material ERM CC144 from Sigma Aldrich and Algae reference material 413 from the International Atomic Energy Agency.

10.2.7 Water quality data

Water samples were collected at the beginning and end of the flow-ways, filtered through a 0.2 um filter, and stored at 4°C for analysis. As required, samples were stored with additional preservation reagents as outlined by the EPA method used for analysis.[24] Samples were analysed for BOD via EPA within 24 hours of collection by ATS Laboratories, located in Brawley, CA. Samples were measured for chemical oxygen demand (COD), nitrate and nitrite as nitrogen, total Kjeldahl nitrogen, and total nitrogen by Anatek Laboratories in San Diego, CA.

10.2.8 Weather data

Daily weather data including solar irradiation on horizontal surface (MJ/m^2/day), air temperature (°C), dew point (°C), wind speed (m/s), relative humidity (%), and precipitation (mm/day) were obtained from the National Aeronautics and Space Administration (NASA) Langley Research Centre (LaRC) Prediction of Worldwide Energy Resource (POWER) Project funded through the NASA Earth Science/Applied Science Program. Average, maximum and minimum of each environmental factors during the cultivation period between each harvesting day were than calculated and used for further analysis.

10.2.9 Principal Component Analysis (PCA)

PCA was conducted using an add-on Microsoft Excel-based software (Addinsoft XLSTAT statistical and data analysis solution. Boston, USA). Total 30 independent variables were used with 80 data points. The type of PCA was Pearson correlation. The minimum total variability of the PCA was set to be 60%. Independent variables (environmental factors) were average, maximum, and minimum value of weather data including air temperature (T-Avg, T-Max, T-Min), dew point (DP-Avg, DP-Max, DP-Min), wind speed (WS-Avg, WS-Max, WS-Min), solar irradiation (Ins-Avg, Ins-Max, Ins-Min), relative humidity (RH-Avg, RH-Max, RH-Min), precipitation (Prec-Avg, Prec-Max, Prec-Min), total precipitation (Prec-Total), and water quality data including chemical oxygen demand (COD), nitrate/nitrite as nitrogen, total Kjeldahl nitrogen, total nitrogen, total phosphorus, Water N/P, total dissolved solids (TDS), pH, conductivity, water temperature, and dissolved oxygen (DO). Dependent variables were biomass productivity (BP), ash content (Ash), crude protein content, crude fat content, crude carbohydrate content, crude fibre content, calories of biomass, nitrogen content, phosphorus content, N/P ratio of biomass, N removal rate, and P removal rate.

10.2.10 Anaerobic digestion

The anaerobic digestion experiments were carried out using an Automatic Methane Potential Test System (AMPTS®) from Bioprocess Control[35], and according to an existing method.[36,37] Biomethane potential was evaluated by following the methane produced during 10 days under mesophilic conditions (35°C). The inoculum was an industrial sludge sampled in a UASB (Upflow Anaerobic Sludge Blanket) process treating sugar factory effluent. The test was performed on 500 mL flask with a working volume of 400 mL. Each flask contained a reactive medium composed of substrate sample (5 g), inoculum (187.5 mL), bicarbonate buffer (1 g), 113 mL of microelements and trace elements solution (NH_4Cl, 26.6 g L^{-1}; KH_2PO_4, 10 g L^{-1}; $MgCl_2$, 6 g L^{-1}; $CaCl_2$, 3 g L^{-1}; $FeCl_2$, 2 g L^{-1}; $CoCl_2$, 0.5 g L^{-1}; $MnCl_2$, 0.1 g L^{-1}; $NiCl_2$, 0.1 g L^{-1}; $ZnCl_2$, 0.05 g L^{-1}; H_3BO_3, 0.05 g L^{-1}; Na_2SeO_3, 0.05 g L^{-1}; $CuCl_2$, 0.04 g L^{-1}; Na_2MoO_4, 0.01 g L^{-1}) and water to adjust the volume to 400 mL. The pH was measured using a pH probe before and after the experiment; and adjusted to 7 before the experiment using 1 M of HCl. Samples with algae and blanks were carried out. The concentration of biogas measured was measured using the AMTPS II Bioprocess Control process software. Each sample and blank were done in triplicate.

10.2.11 Washing protocols

Water washing protocols of the algae was performed using an algae:purified water ratio of 1:10 g g^{-1}. The solution was stirred overnight with sonication and finally centrifuged. The ash content was measured as previously described. Samples were run in triplicate.

EDTA washing protocol was carried out using 0.05 M of ethylenediaminetetraacetic acid (EDTA) solution (prepared from EDTA powder from Sigma Aldrich). 1 g of algae was mixed with 10 mL of 0.05 M EDTA solution and shaken for 1 hour. The mixed solution was then centrifuged and rinsed with 10 mL of deionized water. After centrifugation, the supernatant was analysed via ICP-MS.

10.3 Results and discussion

10.3.1 Trace elements in the Alamo River tributary of the Salton Sea

The environmental monitoring of aquatic ecosystems is complex and often multi-faceted. To investigate the level of contamination of the site, namely the presence of heavy metal and selenium contaminants, it is important to take a holistic approach and look at various components of the ecosystem. Here we have selected the resident biota (terrestrial plant and algae biofilm), the water and the sediments. The values were compared to US quality standards and guidelines, as well as samples from a non-compromised riverine area – the Santa Ana River, which acted as a control.

10.3.1.1 Assessment of trace elements in the sediments

Previous studies have shown the presence of contaminants such as pesticides, organic contaminants and metals in the sediments in the Alamo River and New River, down into the Salton Sea.[38,39] Heavy metals and contaminants are known to accumulate in river sediments, as they can act as potential sink or source of such contaminants into the environment and transfer to the water column. The dynamics of such contaminants depend on many factors such redox conditions, pH, salinity of the water etc.[40,41] However, the trace element analysis of sediments can be indicators of anthropogenic contamination of water systems.[42–44] Here we hope that the measurement of such contaminants in the area would help shape decisions in ecosystem management of the Salton Sea area and highlight differences in the Alamo River tributary that feeds the Algae Turf System (ATS).

In this study, 8 metals and metalloids as well as selenium were analysed via ICP-MS, along the Alamo River, upstream and downstream and where the ATS is located – the Shank Road Wetland. The results are shown in Table S6.1 and compared to Sediments Quality Guidelines (SQGs), namely the Threshold Effect Concentration (TEC) established by MacDonald et al.[43]

Along with the comparison with SQGs, environmental indexes were calculated to exhibit potential contamination of the area: the Enrichment and Contamination Factors, EF and CF respectively.

The metal and selenium contents follow a trend regarding the orientation of the flow of the water: they are higher upstream of the Alamo River than downstream. Lower values downstream or at the outlets, suggests the metals are more likely to be trapped in the sediments earlier along the river flow way, as a result of lower salinity upstream.[16] This has been reported elsewhere where the values along the Salton Sea tributaries are higher than in the Salton Sea itself.[4,10,45]

The West Cell is one of the two cells from the Shank Road wetland, where no water was diverted to feed the ATS system. The Outlet West Cell exhibits 2 values above the TEC Value (SQGs) for Cr, Ci. These heavy metals are often found in agricultural run-off.[46,47] On the other hand, the Outlet of the East Cell, where the ATS is situated, exhibits the lowest concentration of metals across all sites. We can only suggest the hypothesis that the presence of the ATS in the East cell has a remediation effect for trace metals; explaining why the outlet of the 'control' West cell exhibits much higher metal concentration in its sediments. However, sediments samples were not taken before the implementation of the ATS system or periodically throughout the study.

Even though the trace elements assessments did not exceed the TECs in the other sites, the trace elements in the Alamo River are significantly higher than those found the Santa Ana River (a non-compromised area from agricultural and wastewater runoff), especially for As, Cd, and Se. On average across the Alamo River sediment samples, there is a 14-fold increase in Se content compared to the Santa Ana sediment sample.

Metal content (mg kg^{-1})	As	Cd	Cu	Cr	Ni	Pb	Se	Zn
Upstream Alamo River - S1	5.52	0.39	21.92	32.09	19.52	14.93	0.72	68.39
Upstream Shank Road Wetland - S2	6.29	0.33	20.14	30.21	22.51	16.98	0.71	65.71
Inlet of Shank Road Wetland (Inlet ATS) - S3	6.53	0.24	15.07	25.08	14.71	16.73	0.87	54.88
Outlet East Cell (Outlet ATS) - S4	1.74	0.06	3.32	6.37	6.18	5.68	0.14	21.02
Outlet West Cell (no ATS) - S5	9.01	0.42	22.62	48.22*	32.04*	30.61	1.17	87.52
Downstream Alamo River - S6	2.41	0.17	6.65	13.54	7.35	4.89	0.18	30.41
Santa Ana River	1.32	0.04	10.88	20.36	11.77	8.99	0.09	51.5
TEC	9.79	0.99	31.6	43.4	22.7	35.8	2	121

*Table S6.1: trace elements in the sediments in the Alamo river tributary. TEC= Threshold Effect Concentration from the Sediment Quality Guidelines. * indicates values above the TEC.*

Furthermore, based on the trace element assessment of the sediments, environmental indexes were calculated to investigate the enrichment and extent of contamination of these elements in the area of study. Figure S6.2 shows that the enrichment factor for Cd, Pb, Se and Zn are above 1.5 for all sites, except Site 6 (downstream for Pb only). This exhibits that there has been human influence in the heavy metal and selenium contents of the area, with a minor but significant modification for Cd (S1, S6) and Se (S3, S4). The contamination factor data shows that a significant number of sites exhibit moderate contamination from Cd (S1, S2, S5), Pb (S5) and Se (S1, S2, S3, S5). This is clear evidence that this particular tributary of the Salton Sea, the Alamo River, is suffering from anthropogenic activities, to the extent that the area is contaminated with certain metals, namely Cd, Pb and Se.

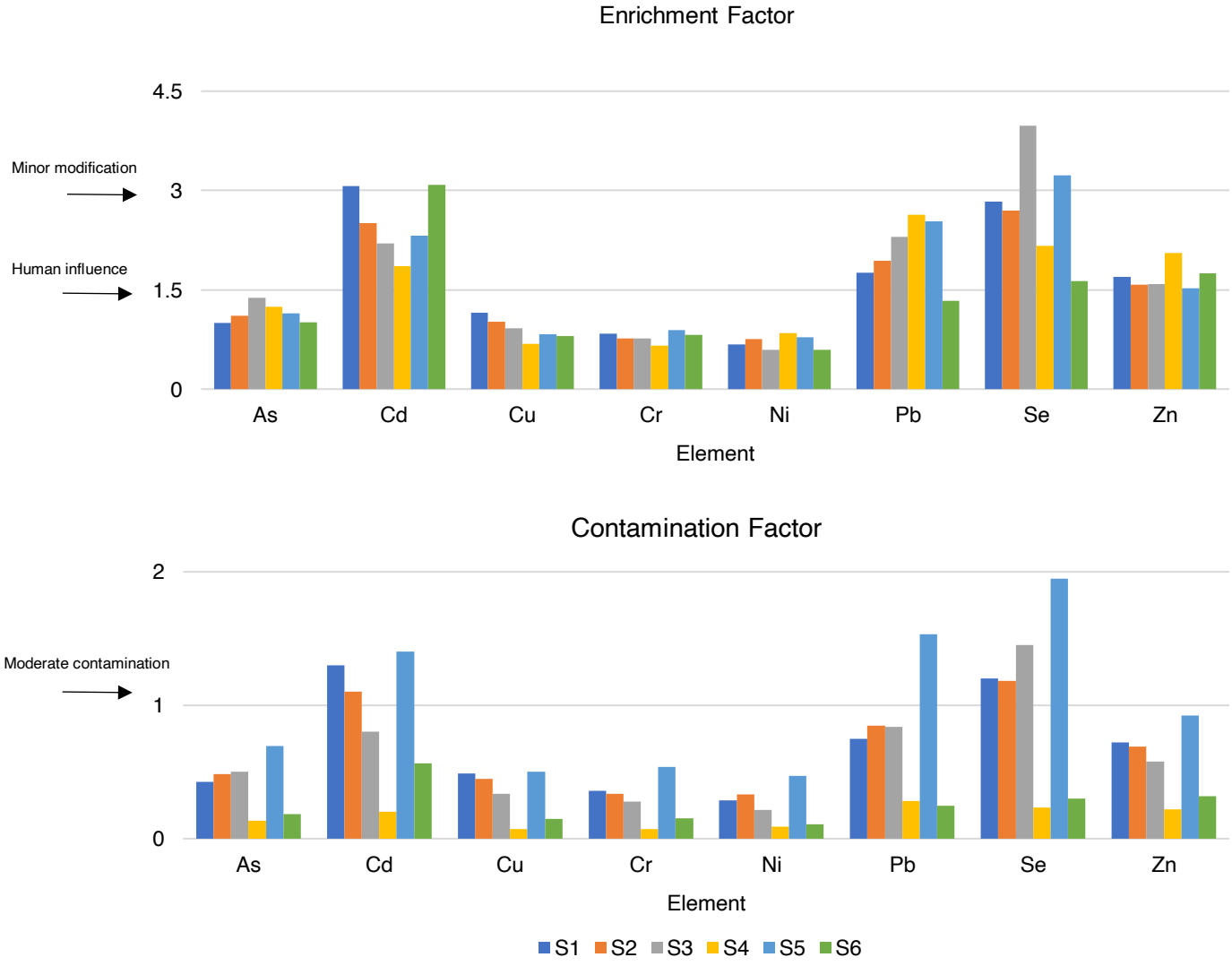


Figure S6.2: enrichment (top) and contamination factors (bottom) of the sediments at the different points of interest.

S1: Upstream Alamo River; S2: Upstream Shank Road Wetland; S3: Inlet of Shank Road Wetland (Inlet ATS); S4: Outlet East Cell (Outlet ATS); S5: Outlet West Cell (no ATS); S6: Downstream Alamo River.

10.3.1.2 Quality of the water in the Alamo tributary

Previous studies have shown the presence of contaminants including pesticides, organic contaminants and metals in the sediments in the Alamo River and New River, which feed into the Salton Sea.[38,39,45] The trace element content of the water was also sampled along the flow of water in the same upstream and downstream locations as the sediments. They were compared to samples taken in the Santa Ana River in California, as well as current federally promulgated Water Quality Standards for the State of California (Environment Protection Agency §131.37). The trace element analysis of the water samples are shown in Table S6.2. All samples exceed the criteria for priority toxic pollutant for Se in freshwater at 5 μg mL^{-1}. The average concentration for all different sites is 6.441 μg L^{-1}, a 10.3-fold increase from the Se content found in the Santa Ana river. This assessment is coherent with the sediment samples reported in this study. The latest value for Se reported by the USGS in June 2017 in the water from the Alamo River is 4.490 μg L^{-1}. This value is lower than any of the values reported across the 6 sites studied here in 2018 in the same tributary of the Salton Sea; confirming that selenium contamination is an increasing environmental concern for the area of the Salton Sea. In addition, Cu water concentration upstream of the Shank Road Wetland (S2) is above the criterion for continuous concentration of this pollutant. Values upstream (S1) and downstream (S6) of the Alamo river show levels of Cu above both criterion for maximum and continuous of saltwater (4.8 and 3.1 μg L^{-1} respectively). Finally, the Pb concentration downstream of the river (S6) is above the criterion for continuous concentration of the metal in freshwater (2.5 μg L^{-1}). Additionally, observed As and Cd values, even being within the federal quality standards, indicate levels more than 10 times higher than the water samples in the Santa Ana River. These may represent emerging contaminants in the future if they were to rise with the intensification of agriculture and wastewater-generating activities upstream.[46,47]

Element content (μg.L^{-1})	As	Cd	Cr	Cu	Ni	Pb	Se	Zn
Upstream Alamo River - S1	7.680	0.138	1.030	5.746*	2.568	2.640*	6.565*	6.895
Upstream Shank Road Wetland - S2	7.163	0.074	0.424	3.535*	1.724	0.968	7.840*	2.888

Inlet of Shank Road Wetland (Inlet ATS)- S3	6.212	0.039	0.218	2.639	1.390	0.022	6.150*	5.842
Outlet East Cell (Outlet ATS) - S4	5.645	0.034	0.139	2.498	1.219	0.020	6.386*	3.392
Outlet West Cell (no ATS) - S5	5.583	0.031	0.174	2.306	1.400	0.194	5.898*	6.491
Downstream Alamo River - S6	6.578	0.118	0.704	4.805*	2.101	2.245	5.804*	7.646
Water Santa Ana	0.976	0.015	1.805	1.555	0.683	2.294	0.626	9.982

*Table S6.2: trace element analysis of water samples along the Alamo River tributary and Shank Road wetland. * indicates that the value is above the toxicity water quality criteria.*

10.3.2 Quantitative and qualitative analysis on biomass production of the flow-way

During the operation of the system between 2017-2019 (Figure S6.3), periphytic algal biomass was produced and harvested on a weekly basis and analysed for ash content to obtain ash free dry weight (AFDW) of the biomass. Weekly and monthly average AFDW biomass productivity along with ash content are plotted and shown in Figure S6.4.



Figure S6.3: pictures of the 900 feet long ATS flow way

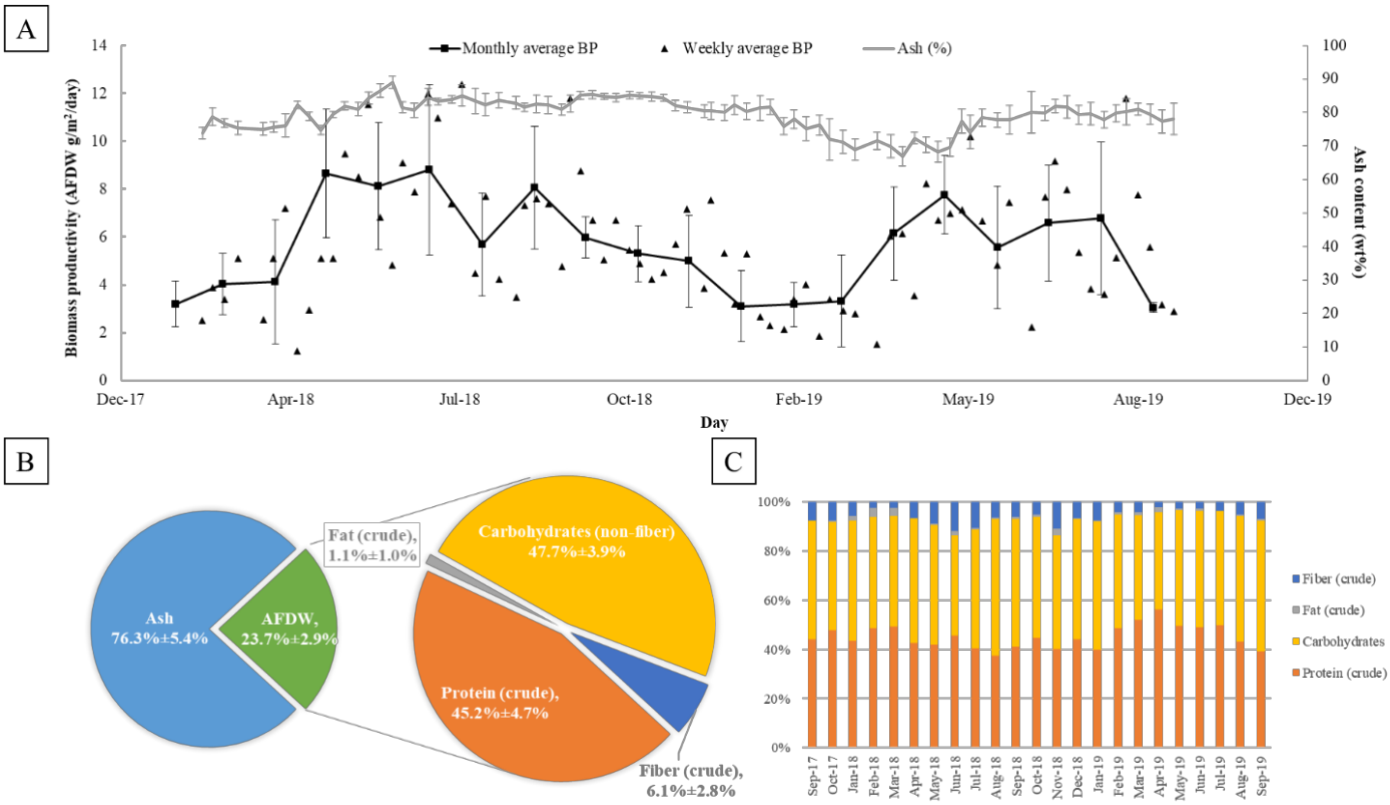


Figure S6.4: A. Change in biomass productivity and its ash content over the course of entire cultivation period, B. overall average biomass composition, C. Change in biomass composition on a monthly basis.

	N (wt%)	P (wt%)	N/P	N removal rate (mg/m^2/day)	P removal rate (mg/m^2/day)	BOD removal rate (%)
Feb-18	10.2%	0.33%	30.8	325.0	10.6	-
Mar-18	10.3%	0.32%	32.1	414.5	12.9	-
Apr-18	8.8%	0.25%	35.4	364.7	10.3	-
May-18	8.8%	0.27%	32.4	758.2	23.4	-
Jun-18	9.5%	0.22%	43.2	772.6	17.9	-
Jul-18	8.5%	0.18%	47.0	745.1	15.9	-
Aug-18	7.8%	0.16%	48.8	444.0	9.1	-
Sep-18	8.5%	0.21%	40.7	689.6	16.9	19.5%
Oct-18	9.3%	0.22%	42.2	555.0	13.2	74.3%
Nov-18	8.4%	0.20%	41.9	444.1	10.6	92.2%

Dec-18	9.2%	0.23%	40.0	458.5	11.5	91.4%
Jan-19	8.3%	0.18%	46.0	256.6	5.6	78.5%
Feb-19	10.1%	0.33%	30.7	321.4	10.5	75.1%
Mar-19	10.9%	0.42%	25.8	360.9	14.0	-
Apr-19	11.7%	0.48%	24.3	718.3	29.5	76.7%
May-19	10.3%	0.26%	39.7	799.4	20.2	-
Jun-19	10.2%	0.22%	46.3	565.5	12.2	-
Jul-19	10.4%	0.31%	33.5	682.9	20.4	-
Aug-19	9.0%	0.21%	42.9	610.6	14.2	-
Sep-19	8.2%	0.16%	51.1	248.5	4.9	-
Average	**9.4±1.0%**	**0.26±0.08%**	**38.7±7.7**	**526.8±185.1**	**14.2±6.0**	**72.5±24.6%**

Table S6.3: monthly change in nitrogen and phosphorus content of the biomass, N/P ratio, N removal rate, P removal rate, and BOD removal rate.

Overall, the average AFDW biomass productivity was 5.8±2.7 g/m^2/day with the highest at 12.4 g/m^2/day in July 2018 and the lowest at 1.2 g/m^2/day in April 2018. Ash content in general was around 70 % to 90 % and was trending down over the cultivation period. Monthly average biomass productivity showed that the productivity was generally high in summer with an average around 7 to 9 g/m^2/day and low in winter with an average around 3 to 4 g/m^2/day. Although the general seasonal oscillating trend of biomass productivity was similar to what has been reported in the previous similar studies, the average productivity was slightly lower than what has been reported in the previous study on attached algae flow-way deployment at Corpus Christi, TX, and higher than those reported by Mulbry et al. and Kangas et al.[20,48,49] The average ash content in the present study was the highest yet among the reported values, presumably due to high total suspended solids of the inlet water, which was 76±55 ppm. High TSS has been reported as one of the major cause of high ash content of harvested algal biomass.[50] Harvested biomass in general consisted of about 30 % of diatoms, including *Bacillaria, Gomphonema, Navicula, Nitzschia*, and *Pleurosira*, and about 70 % of green algae, including *Chlamydomonas*, *Chlorella, Desmodesmus, Mychonastes, Oocystis,* and *Tetranephris*. In addition to entrainment of suspended solids in the biomass, the major abundance of diatomaceous cohorts also contributes significantly to ash accumulation in the biomass. Composition of the ash-free biomass (protein, total lipid, carbohydrates, and fibre content) was measured on a monthly basis and their values with overall average are shown in Figure S6.4C and B, respectively. The average non-fibrous carbohydrates, crude fibre, crude protein, and crude lipid content of the ash-free biomass were 47.7±3.9 %, 6.1±2.8 %,

45.2±4.7 %, and 1.1±1.0 %, respectively. Relatively high ash and low lipid contents have been reported as a typical characteristic of periphyton.[20,49] The monthly change in nitrogen and phosphorus content, nitrogen to phosphorus ratio, nitrogen and phosphorus removal rates, and BOD removal rate are listed in Table 6.3. The average nitrogen and phosphorus content of the biomass was 9.4±1.0 % and 0.26±0.08 %, respectively, corresponding to an N:P ratio 38.7±7.7, significantly larger than the Redfield ratio, indicating likelihood of P-limiting conditions. Relatively higher nitrogen content (or protein content) of the biomass was identified, presumably due to relatively higher concentration of total nitrogen of the source water. Similar results has been reported for biomass with excessive nitrogen input, which can be attributed to an increase in protein content associated with photosystem biosynthesis.[51] The average of total nitrogen and total phosphorus concentration of the source water were 7.73±1.83 mg L^{-1} and 0.52±0.30 mg L^{-1}, respectively, and removal rate of respective nutrients were 543.9±248.7 mg/m^2/day and 14.5±7.4 mg/m^2/day. The highest major N/P nutrient removal rates were observed in summer at ~1000 mg of N/m^2/day and ~40 mg of P/m^2/day. The average removal rate is equivalent to approximately 25 % and 10 % of nitrogen and phosphorus removal from the source water, respectively, with the highest during the summer (50 to 60 % of N and 20 to 30 % of P) and the lowest during the winter (10 to 20 % of N and 3 to 5 % of P). Additionally, the attached algae biofilm showed substantial effectiveness in BOD removal rate, which an average reduction of 72.5±24.6 % from the source water.[52–54] Highly effective BOD removal is also reported in algae-based wastewater treatment process, especially where there is symbiotic reaction between photoautotrophic algae and heterotrophic bacteria. High BOD removal by the attached algae biofilm is believed to be possible by the favourable environment for the coexistence of bacteria and algae provided by the substrate-line flow-way design.

10.3.3 Effects of the length of the flow-way

Spatial variations in biomass productivity, biomass composition, and nutrient removal rates over the length of the flow-way were investigated by harvesting biomass separately in every 30 m sections of the flow-way. Over the entire cultivation period, total of 774 sectional biomass productivity data were generated and corresponding biomass samples were analysed to investigate spatial variations in biomass productivity, biomass composition, and nutrient removal rate and shown in Figure S6.5. In order to diminish the effect of seasonal variation in overall biomass productivity, three different ranges of the biomass productivity, high productivity in top 20 % (T20), low productivity in bottom 20 % (B20), and the productivity in between top 20 % and bottom 20 % (Med), were analysed separately for their spatial variations. Figure S6.5A shows spatial variation in average sectional biomass productivities in

cases of T20, B20, and Avg. In general, all three cases, T20, B20, and Med, showed decreasing trend as the distance from the inlet of the flow-way increases with the highest and the lowest sectional biomass productivities at around 24 g/m^2/day and 0.1 g/m^2/day, respectively. In case of T20, the average of sectional biomass productivity in 30 m section was at the highest (12.9±2.4 g/m^2/day) and decreased to around 8.8±1.9 g/m^2/day in 210 m section then increased back to around 10.4±3.3 g/m^2/day at the end of the flow-way. In both case of B20 and Med, the average sectional biomass productivity gradually decreased as the distance increases from the inlet. The case of B20 showed the average sectional biomass productivity decrease from 2.5±0.4 g/m^2/day to 1.4±0.4 g/m^2/day and the case of Med showed the productivity decrease from 6.3±1.8 g/m^2/day to 4.4±1.0 g/m^2/day over the length of the flow-way. In Figure S6.5B and C, average ash contents of the harvested biomass as well as both nitrogen and phosphorus removal rates show a decreasing trend as the distance increases from the inlet, concomitant with increase in carbohydrate and protein contents of biomass, while total lipid content decreasing over the distance (Figure S6.5D). Average ash contents decreased from 82.5±3.6 % to 75.7±7.5 % over the length of the flow-way likely due to the more potential of TSS to be caught up at the initial part of the flow-way than at the terminus. Nitrogen and phosphorus removal rates were analysed separately for each case of T20, B20, and Med in the same context of the analysis in sectional biomass productivity. Overall, nitrogen and phosphorus removal rate decreased from 1000~200 to 900~100 mg N/m^2/day and 26~5 to 20~3 mg P/m^2/day, respectively, over the length of the flow-way. In average (Med), nitrogen removal rate and phosphorus removal rate decreased from ~500±150 to ~400±90 mg N/m^2/day and ~13±4 to ~8±2 mg P/m^2/day, respectively, as the distance of the flow-way increased. In the present study, nitrogen and phosphorus contents of the biomass initially increased by ~10 %, but subsequently decreased by ~5 %, which led to increase in N:P ratio of the biomass by ~17 % between the extrema at the top and bottom of the flow-way. The flow-way also showed noticeable decrease in water flow velocity at the terminus of the flow-way, which resulted in increased water depth in this section. We also observed a steady increase in pH from ~8 to >9 over the 270 m of distance of the flow-way presumably due to reduction of the dissolved CO_2/bicarbonate from the cumulative photosynthetic activity along the residence time of the flow-way

A previous study reported a similar decrease in biomass productivity along the distance of an attached algae system. D'Aiuto et al. suggested that this is due to the decrease in phosphorus in the source water as it processes down the flow-way. This was based on the fact that the P content of biomass harvested from the downstream section was 15 % lower, while N content was only reduced by 5 % as compared to those from the upstream.[55] Adey et al also documented that precipitation of phosphorus can occur in a longer flow-way due to higher pH at the terminus, further driving P-limitation for biomass production.

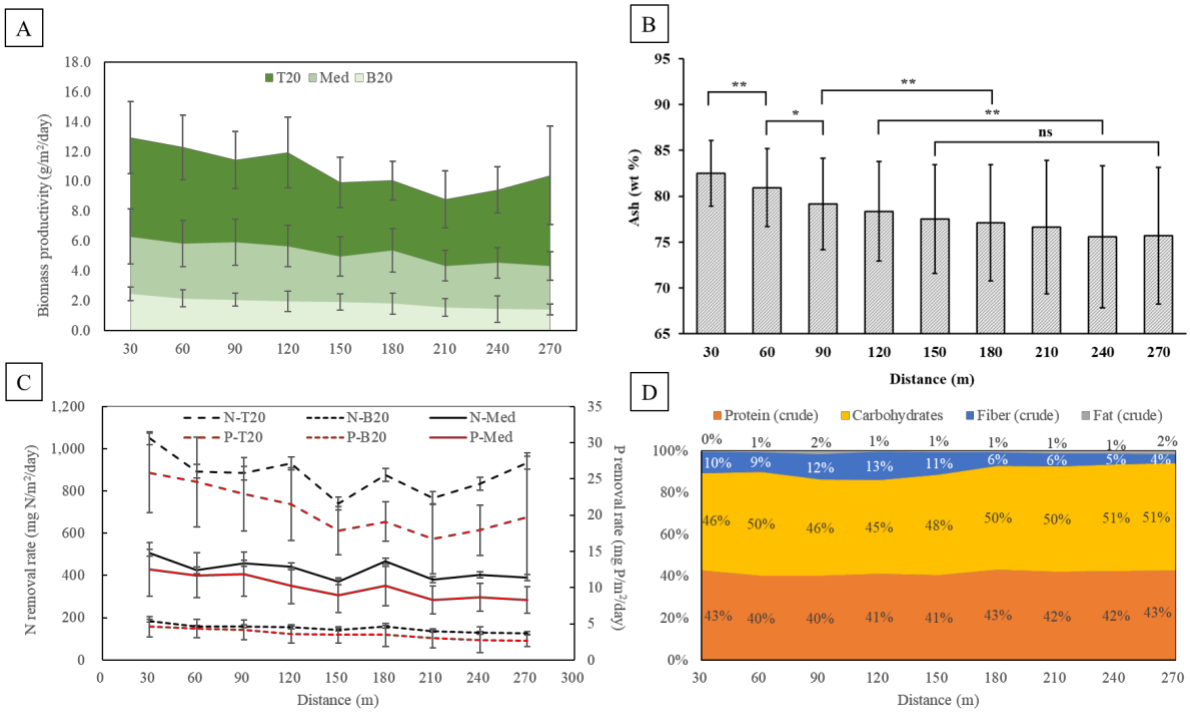


*Figure S6.5: Spatial variations in every 30m over the length of the flow-way including: A. biomass productivity in case of the high productivity in top 20 % (T20, dark green), the low productivity in bottom 20 % (B20, light green), and the productivity in between T20 and B20 (Med, green), B. ash content, C. nitrogen (black) and phosphorus (red) removal rate in case of the T20 (dashed), B20 (dotted), and Med (solid), D. composition of the biomass including crude protein (orange), crude carbohydrate (yellow), crude fiber (blue), and total lipid (grey). (Statistical significance in differences in sectional biomass productivities are listed in Table S2, * = $p < 0.05$, ** = $p < 0.01$, ns = not significant)*

10.3.4 Environmental impact assessment through Principal Components Analysis

Correlation between various key environmental factors and dependent variables including biomass productivity and its composition was assessed through principal component analysis (PCA). A biplot explaining 60.33 % of total variance based on two principal components, PC1 and PC2, which explained 37.68 % and 22.64 % of total variance, respectively, was generated and is shown in Figure S6.6.

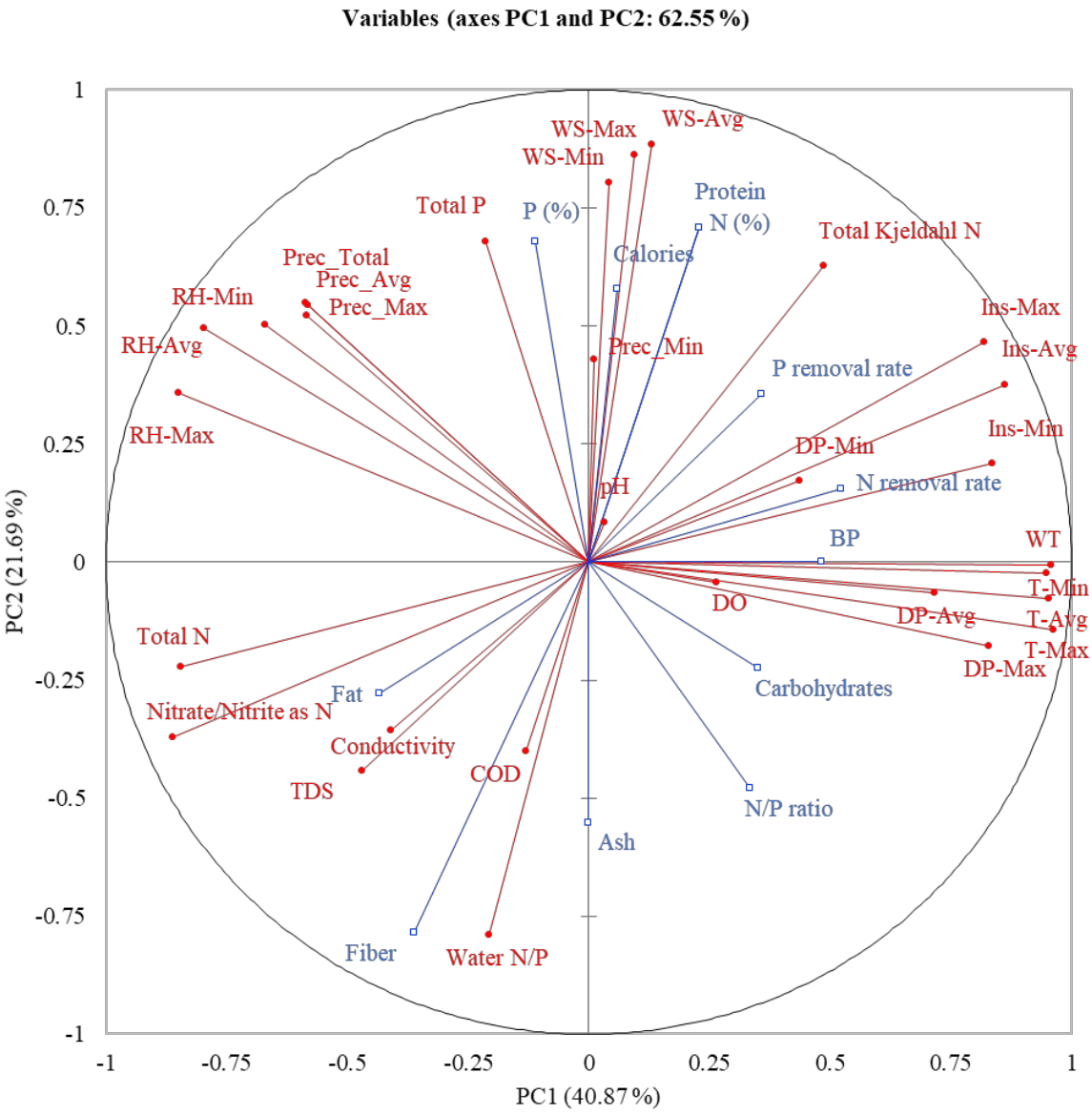


Figure S6.6: biplot generated through principle components analysis (PCA) with environmental factors (red) and various dependent variables (blue)

Biomass productivity, along with nitrogen and phosphorus removal rates, show positive correlation with PC1, which consists of major positive contributors including air temperature (T_Avg, T_Min, and T_Max), insolation (Ins_Avg, Ins_Min, and Ins_Max), dew points (DP_Max and DP_Avg), and water temperature (WT). Positive correlations for biomass productivity with insolation and temperature are well reported.[13] Generally, variations in nutrient removal rates followed the oscillating trends of biomass productivity throughout the year. Mulbry et al reported that the nutrient removal rate at the Patuxent river site was at the

highest during summer and early fall but dropped by more than 10-fold during the winter period, mainly due to significant drop of biomass productivity.

Negative correlation of biomass productivity with relative humidity and precipitation is due to the unique characteristics of the Salton Sea region deployment location, where most of precipitation occurs during the winter and the rest of the year is mostly dry. No significant correlation between biomass productivity and precipitation was observed in this case due to lack of detailed information. An insignificant correlation was also found between the nutrient concentration of the water and algae turf biomass productivity, indicating the biofilm's ability to stably uptake nutrients from the source water, even at a low nutrient concentrations, as previously reported.[14,56] As an example, a recent study on nutrient recovery from oyster aquaculture effluent achieved the highest yet reported biomass productivity, despite TN and TP concentrations in the source water that were similar or relatively lower than those reported elsewhere. Another previous, long-term study to investigate the effect of reducing nitrogen input on eutrophication of lakes, discovered that phytoplankton biomass remained unchanged regardless of nitrogen inputs as long as phosphorus input kept consistent.[57] In this study, both total nitrogen and nitrate/nitrite concentration of the source waters show strong negative correlations with biomass productivity. This negative correlation is, however, presumably due to the spike in total nitrogen and nitrate/nitrite concentration of the source water during the winter season, when biomass productivity was lowest due to less favourable seasonal temperature and light regimes, as seen in Figure S6.7. On the other hand, nitrogen and phosphorus content of the biomass show positive correlation with total Kjeldahl nitrogen and total phosphorus concentration of the source water, respectively, which can be attributed to the metabolism of the periphyton in the biofilm.[58]

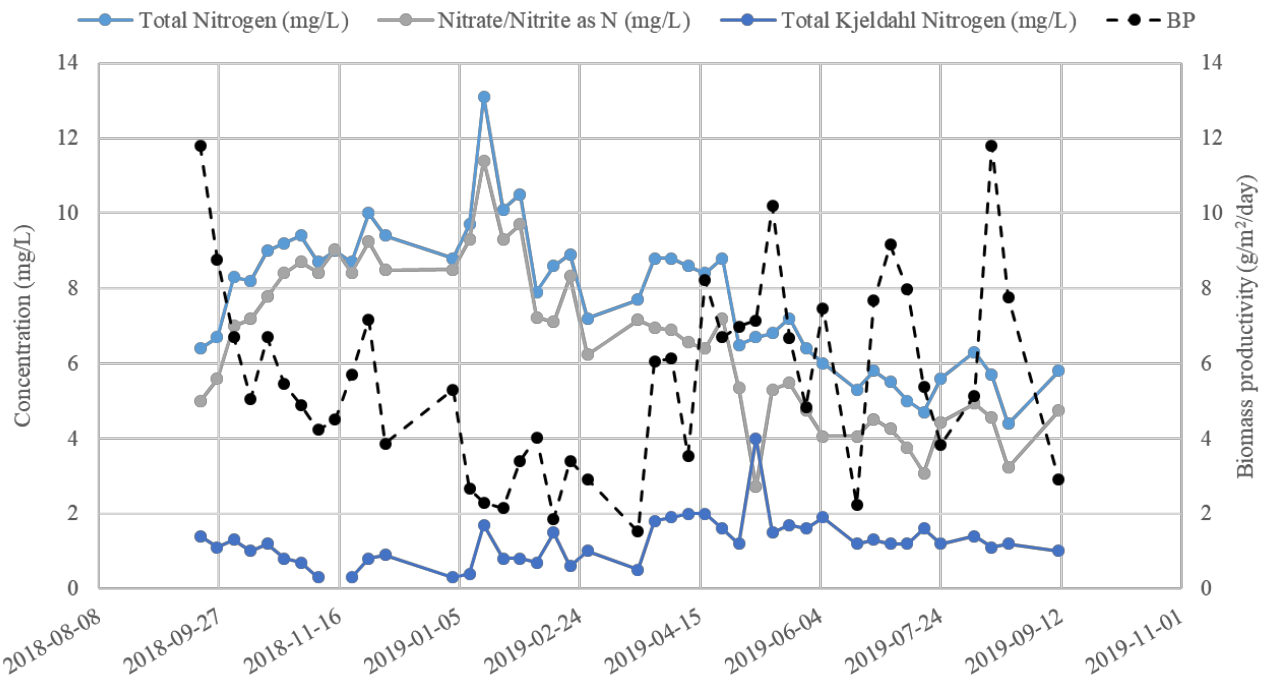


Figure S6.7: comparison between change in biomass productivity, concentration total nitrogen, nitrate/nitrite as nitrogen and total Kjeldahl nitrogen (mg L^{-1})

10.3.5 Trace element analysis of the biofilm: metal contaminants removal

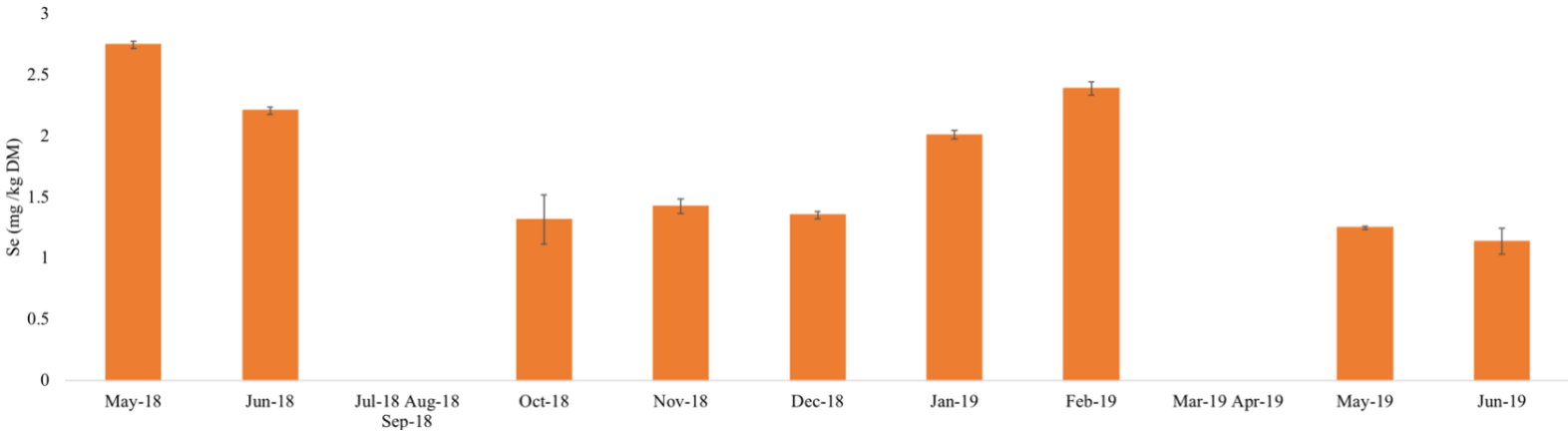
10.3.5.1 Se content of the biomass from the ATS

Selenium is an essential micronutrient for many animals, including fish. However, the window between being a nutrient and a contaminant in organisms is narrow, which makes the monitoring of this element in aquatic ecosystems crucial.[16] Normal weathering and intensive agricultural and industrial activities trigger solubilization of Se from geological sources. Bioaccumulation of Se in the aquatic food chain is a concern, as fish accumulate Se by eating contaminated foods from their surroundings. The toxicity of Se on fish embryos has been studied; although the EPA is not promulgating human health criteria for this contaminant.[11,59] Figure S6.8A shows the Se content of the harvested algae at different time intervals, indicating that the attached algae biofilm is able to intercept Se from the environment (i.e. water, sediments). However, Se uptake from the biofilm was not constant throughout the field trial. Between summer 2018 and 2019, the Se content of the biofilm was observed to decline from 2.21 to 1.14 mg kg^{-1}, with a peak at 2.39 mg kg^{-1} at the beginning of the year in 2019. The fluctuations in Se content can be due to the algae tissues reaching Se toxicity, or variations in Se content of the water itself feeding the algae flow-way. In fact, levels of water contaminants can be influenced by precipitation levels, seasons and intensity of anthropogenic activities

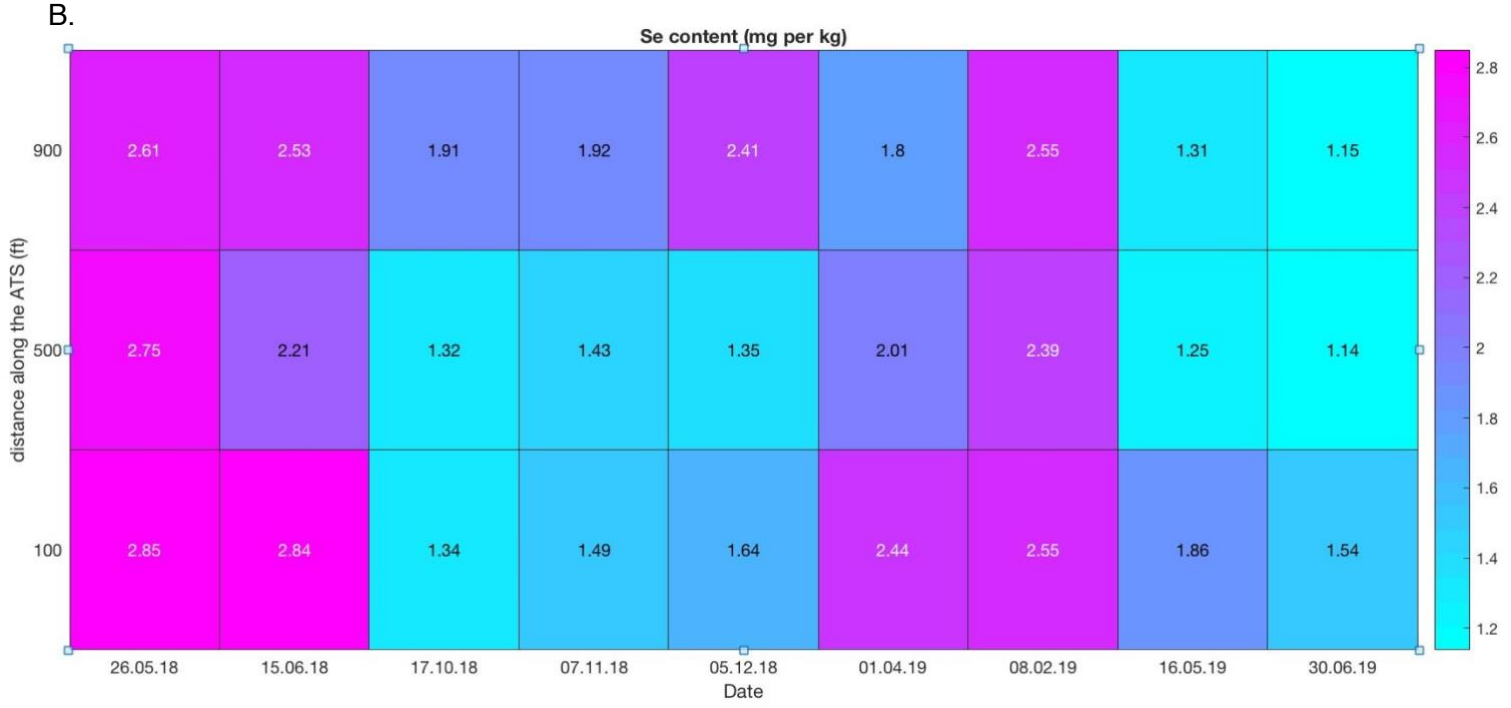
(e.g. industry and agriculture).[41] The potential for metals uptake could also be linked to the start-up and stop cycles of specific algal species, some of which might have higher tolerance for contaminants.[20]

In order to investigate a possible pattern in the Se uptake along the flow-way, samples at 100 (inlet), 500 and 900 ft (outlet) were sampled for trace element analysis and their bioconcentration factor (BCF) was calculated (Figure S6.8B and C). The BCF values do not seem to follow any pattern depending on the inlet/outlet along the flow-way, nor could a clear trend between inlet/outlet be interpreted from the data. The BCF values are below 1000, this is described as 'non bioaccumulative' according to the USEPA regulations.

A.



B.



C.

Se content (µg L^{-1})			BCF inlet	BCF outlet
Date	Water inlet	Water outlet		
17/10/2018	6.072	5.994	**220**	**318**
07/11/2018	5.417	5.343	**275**	**360**
05/12/2018	5.024	5.344	**326**	**451**
01/04/2019	5.258	5.130	**465**	**351**
08/02/2019	5.130	4.887	**497**	**522**
16/05/2019	5.157	4.993	**361**	**262**
30/06/2019	4.601	4.411	**335**	**260**

Figure S6.8: A. Se content of the resident algae biofilm from the ATS taken at 500 ft, B. Heatmap of the Se content in the biofilm along the flow-way taken at 100, 500 and 900 ft and C. Se content in the water sampled from the inlet and outlet and calculated BCF Se factor

10.3.6 Essential trace element content of the biomass from the ATS

Similarly to Selenium, Ni, Cu and Zn are essential nutrients, which can become toxic at higher levels.[33] The environmental analysis showed that the concentration of Ni in some of the sediments of the area was above the TEC in one of the site; as well as the concentration of Cu in the water sampled above toxicity criteria. Figure S6.9 shows the content of these metals in the algae biomass harvested from the flow-way. The concentration of the essential metals in the algae are within the same order of magnitude that the concentration of the surrounding sediment sampled. This is consistent with the fact that such filamentous biofilms can retrain suspended solids from the stream of water, participating to the formation of biogenic sediments. The fate of such algae is closely linked to their environment, i.e. water and sediments.

It is interesting to observe that each of the essential metals follows one similar trend over the time of analysis, with a drop in metal content in June 2018 and peak in concentration in winter 2018 (November – December) for all three metals. However, the attached algae flow-way system was clearly capable of intercepting metals of concern, such as Cu, at a level of ~8 mg kg^{-1} of biomass harvested on average over the course of the study (2018-2019). Paired with biomass production and valorisation at scale, this could lead to significant toxic pollutant removal from the water effluent.

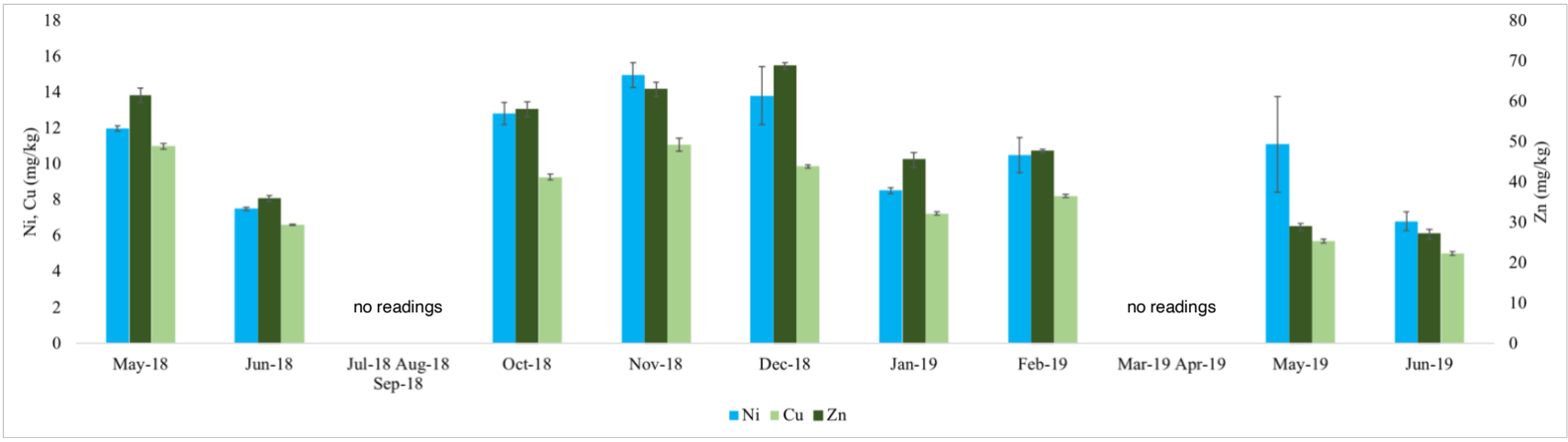


Figure S6.9: essential metal content of the algae biofilm from the ATS taken at 500 ft

10.3.7 Non-essential trace element content of the biomass from the ATS

Beyond Se, Cu, Ni, and Zn, Cr, As, Pb and Cd can be taken up by living organisms in a contaminated environment, provided that the levels of contaminants are below toxicity levels. Algae Turf systems and their resident algal biofilms have been extensively studied for tolerance to such contaminants.[18,41,60] The content of the metals in the attached algae from the system are shown in Figure S6.10. We observe that non-essential and essential metal contents of the algae follow a similar pattern over the time of the study, suggesting that the potential of metal removal from the algae flow-way is not metal specific. Among the non-essential metals detected in the biofilm, Pb was a specific concern, as its concentration in the water is above the federal regulations. Pb levels reached a maximum of 16.2 mg per kg of dried biomass in November 2018. Generally, the concentrations of non-essential metals, Pb, Cr and As in the biomass are higher than the ones of essential metals.

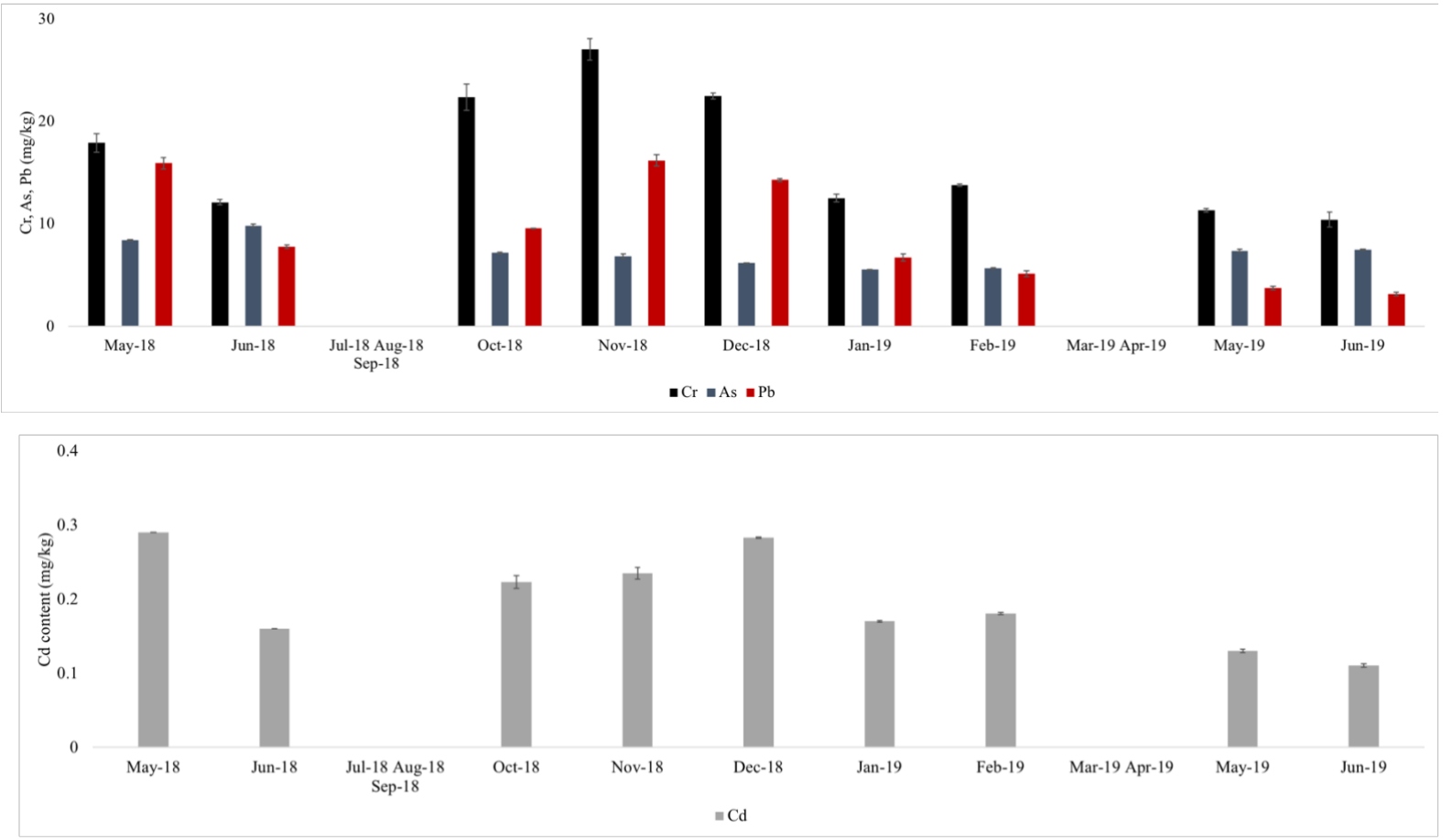


Figure S6.10: non-essential metal content of the algae biofilm from the ATS taken at 500 ft. Cr, As, Pb (top) and Cd (bottom).

The presence of trace elements in the biomass, even in small quantities, testifies that the ATS system has a water remediation potential. This study suggests that this type of system can be producing renewable biomass, using a compromised effluent, with very little input (energy of the pump, maintenance), for environmental remediation of an endangered ecosystem in the Salton Sea.

10.3.8 Bioconcentration factor

The bioconcentration factor was calculated at the inlet and outlet for one time point on the 5th of December 2018, the peak in concentration in the algae. The thresholds for bioaccumulation are described in the method section, taken from the USEPA Toxic Substances Control Act (TSCA) and Toxic Release Inventory (TRI) programs. The results are shown in the Figure S6.11 The values show that the algae population from the algae flow-way is bioaccumulative for Cu, Zn and As, while being very bioaccumulative for Ni, Cr, Cd and Pb. These results verify

that operation of an attached algae flow-way has significant water remediation potential. Furthermore, we show that the system can be used to produce biomass using compromised, runoff-laded surface-waters, with relatively little input (water pumping, harvesting), supporting goals for environmental remediation in the Salton Sea region.

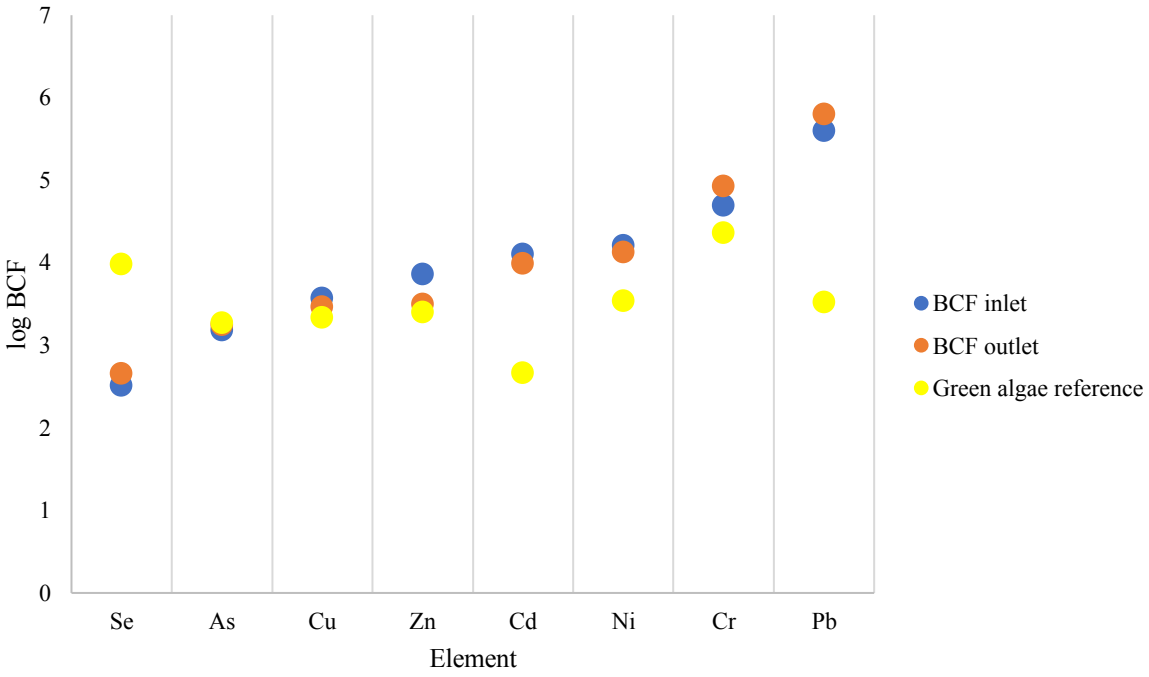


Figure S6.11: BCF for each trace element along the flow way (05.12.2018). log BCF<3: non accumulative, 3< log BCF<3.7: accumulative, 3.7<log BCF: very accumulative. Green algae reference was taken from Lopez i Losada (2020)

Based on the values from the metal content along the flow way (30, 150 and 270 m) and the productivity of the flow-way for the specific dates related to trace element sampling, the average metal uptake from the biofilm was calculated for each trace element. The results are shown in Figure S6.12. Over 2 mg of Zn per square meter per day can be harvested from the algae, 0.3-0.4 mg of Ni, Cu, As and Pb, 0.6 mg of Cr. These data show the potential of a pilot-scale flow-way system (83.6 m^2) to intercept a wide range of contaminants from environment, including water and sediments.[29,41,61–63] However, valorisation of the filamentous biomass is currently limited by the very high ash content (Figure S6.5) and presence of potentially toxic metals. Therefore, biomass utilization options will likely be limited to those that support efficient pre-concentration and disposal of the metals.

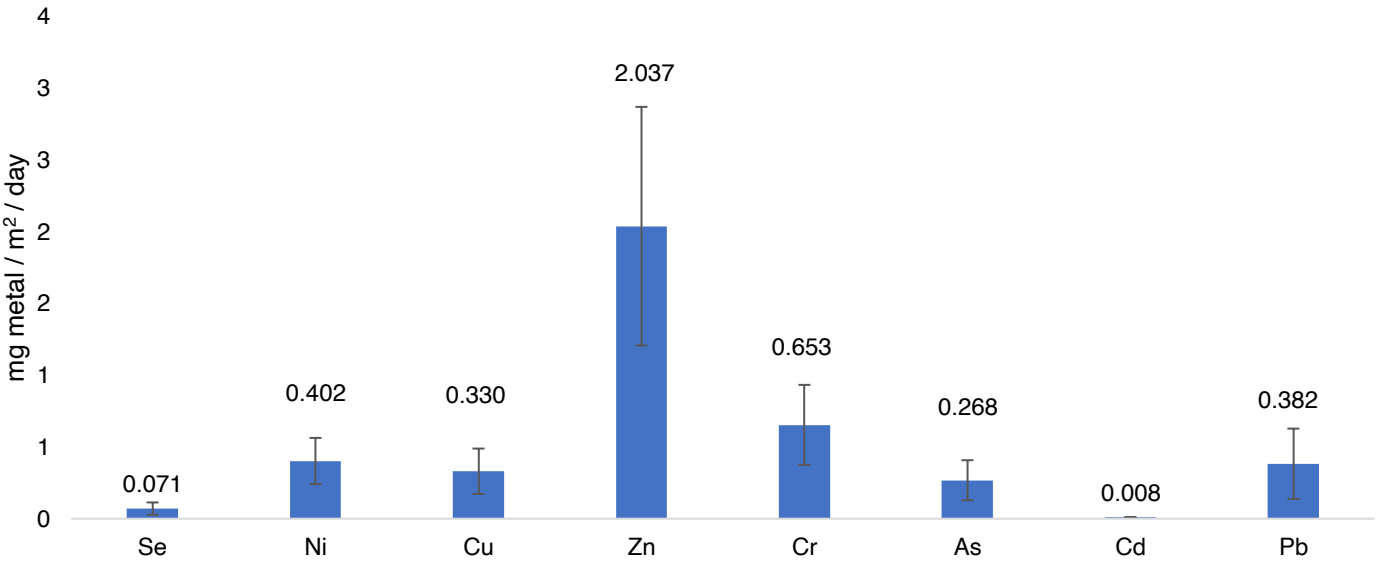


Figure S6.12: Average metal uptake along the flow way between spring 2018 and summer 2019 based on metal content and biomass productivity.

10.3.9 Valorisation of the biomass harvested

A simple deashing technique was used: washing with water, followed by sonication and centrifugation to remove some of the ash of the biomass. Unfortunately, the ash content of the algae did not decrease but increased from the water washing of the algae: from 85 % to 89-90 %; due to the fact that some of the organic content (sugars) is water soluble and dissolved into the wash.

EDTA liquid extraction was performed on the algae using 0.05 M EDTA solution. The purpose of the experiment was to see if the trace elements were bound to the surface of the algae was intracellular. The algae samples were digested for trace element analysis before and after EDTA extraction. The results revealed that no extraction was observed for Cr and Se. These two elements are accumulating in the algae and confined in the cell wall. Less than 40 % of Ni, Cu and As were extracted using EDTA with 20.1 % 24.7 and 35.8 % extraction respectively. 77.4 % of Cd was extracted from the algae sample using this EDTA washing, while only 9.9 % of Zn and 7.5 % of Pb were extracted.

Given the high ash content of the biomass above 70 wt%, its low lipid content and the presence of a range of metal contaminants (some of them being absorbed onto the surface of the algae, others bound to the cell wall of the organism), anaerobic digestion was performed on the algae as mean to valorise the small organic content of the turf algae. The anaerobic digestion was carried out using an AMTPS II and revealed the biomethane potential of the

substrate: 251.8 (+/- 5.7) NmL of CH_4 per g of volatile suspended solids (VSS). This is the first step into the valorisation of this algae and potential valorisation of the metal concentrated sludge afterwards, perhaps using ionic liquid extraction.

10.4 Conclusion

The Salton Sea and surrounding region is one example among many of the effects of growing population, diminishing water levels, and increasing environmental contaminants. Our approach to address eutrophication and metals accumulation in this environmental setting was to install and evaluate a 270 m attached algae flow-way system on the Alamo River tributary to the Salton Sea for coupling algae biomass production with remediation of major nutrients, metals, and organic contaminants. Our results suggest that attached algae cultivation promotes simultaneous biological removal of each of these contaminants. Furthermore, persistent biomass production achieved from this study provides an opportunity for significant value-addition, e.g. for bioenergy applications, in addition to reducing the likelihood of harmful algal blooms that typically form in nutrient laden surface waters. However, means for efficient valorisation of the algae biomass obtained from attached algae cultivation in compromised surface waters should be further investigated, focusing on technoeconomic and lifecycle implications of conversion technologies that are suitable for contaminated biomass utilization, and including geographic assessment of high impact deployment options, system scaling, and waste management.

References

1. California Department of Water Resources. Salton Sea History [Internet]. [cited 2021 Feb 4]. Available from: https://water.ca.gov
2. U.S. Fish and Wildlife Service. ServCat - Geospatial Dataset [Internet]. 2019 [cited 2021 Feb 4]. Available from: https://ecos.fws.gov
3. Hobbins M, Barsugli J. Threatening the vigor of the Colorado River. Science (New York, NY). 2020;367(6483):1192–3.
4. Imperial Irrigation Ditrict, Ch2m Hill. Salton Sea Hydrology Development: Technical Report [Internet]. San Diego, USA; 2018. Available from: https://www.iid.com
5. USGS Water Resources. Current Conditions for Salton Sea NR Westmorland CA [Internet]. [cited 2021 Feb 4]. Available from: https://nwis.waterdata.usgs.gov
6. Jones BA, Fleck J. Shrinking lakes, air pollution, and human health: Evidence from California's Salton Sea. Sci Total Environ. 2020 Apr 10;712.

7. Doede AL, DeGuzman PB. The Disappearing Lake: A Historical Analysis of Drought and the Salton Sea in the Context of the GeoHealth Framework. GeoHealth. 2020 Sep 23;4(9).
8. Kothe E, Varma A, editors. Bio-Geo Interactions in Metal-Contaminated Soils. Vol. 31, Journal of Physics A: Mathematical and Theoretical. Heidelberg, Germany: Springer; 2012.
9. Mishra S, Bharagava RN, More N, Yadav A, Zainith S, Mani S, et al. Heavy Metal Contamination: An Alarming Threat to Environment and Human Health. Environ Biotechnol Sustain Futur. 2019;103–25.
10. Radtke D, Kepner W, Effertz R. Reconnaissance Investigation of Water Quality , Bottom Sediment , and Biota Associated With Irrigation Drainage in the Lower Colorado River Valley , Arizona , California, And Nevada. Water-Resources Investigations Report. 1988.
11. Presser TS, Sylvester MA, Low WH. Bioaccumulation of selenium from natural geologic sources in western states and its potential consequences. Environ Manage. 1994 May;18(3):423–36.
12. Mulbry W, Kondrad S, Pizarro C, Kebede-Westhead E. Treatment of dairy manure effluent using freshwater algae: Algal productivity and recovery of manure nutrients using pilot-scale algal turf scrubbers. Bioresour Technol. 2008 Nov 1;99(17):8137–42.
13. Liu J, Danneels B, Vanormelingen P, Vyverman W. Nutrient removal from horticultural wastewater by benthic filamentous algae Klebsormidium sp., Stigeoclonium spp. and their communities: From laboratory flask to outdoor Algal Turf Scrubber (ATS). Water Res. 2016 ;92:61–8.
14. Ray NE, Terlizzi DE, Kangas PC. Nitrogen and phosphorus removal by the Algal Turf Scrubber at an oyster aquaculture facility. Ecol Eng. 2015 May 1;78:27–32.
15. Haritonidis S, Malea P. Bioaccumulation of metals by the green alga Ulva rigida from Thermaikos Gulf, Greece. Environ Pollut. 1999 Mar 1;104(3):365–72.
16. Schiavon M, Pilon-Smits EAH. The fascinating facets of plant selenium accumulation – biochemistry, physiology, evolution and ecology. New Phytol. 2017;213(4):1582–96.
17. Schiavon M, Ertani A, Parrasia S, Vecchia FD. Selenium accumulation and metabolism in algae. Aquat Toxicol. 2017;189:1–8.
18. Al Ketife AMD, Al Momani F, Judd S. A bioassimilation and bioaccumulation model for the removal of heavy metals from wastewater using algae: New strategy. Process Saf Environ Prot. 2020 Dec 1;144:52–64.

19. Van Wychen S, Laurens LML. Determination of Total Solids and Ash in Algal Biomass. Natl Renew Energy Lab . 2016;(TP-5100-60957).
20. Kim S, Quiroz-Arita C, Monroe EA, Siccardi A, Mitchell J, Huysman N, et al. Application of attached algae flow-ways for coupling biomass production with the utilization of dilute non-point source nutrients in the Upper Laguna Madre, TX. Water Res. 2021;191.
21. Templeton DW, Laurens LML. Nitrogen-to-protein conversion factors revisited for applications of microalgal biomass conversion to food, feed and fuel. Algal Res. 2015 Sep 1;11:359–67.
22. Callahan BJ, McMurdie PJ, Rosen MJ, Han AW, Johnson AJA, Holmes SP. DADA2: High-resolution sample inference from Illumina amplicon data. Nat Methods. 2016 May 23;13(7):581–3.
23. McMurdie PJ, Holmes S. Phyloseq: An R Package for Reproducible Interactive Analysis and Graphics of Microbiome Census Data. PLoS One. 2013 Apr 22;8(4).
24. Creed JT, Brockhoff CA, Martin TD. EPA Method 200.8: Determination of Trace Elements in Waters and Wastes by Inductively Coupled Plasma-Mass Spectrometry [Internet]. U.S. Epa. 1994 [cited 2021 Feb 12]. Available from: https://www.epa.gov
25. Turekian KK, Wedepohl KH. Distribution of the elements in some major units of the earth's crust. Bull Geol Soc Am. 1961;72(2):175–92.
26. Hakanson L. An ecological risk index for aquatic pollution control.a sedimentological approach. Water Res. 1980 Jan 1;14(8):975–1001.
27. Algül F, Beyhan M. Concentrations and sources of heavy metals in shallow sediments in Lake Bafa, Turkey. Sci Rep. 2020;10(1):1–12.
28. Arnot JA, Gobas FAPC. A review of bioconcentration factor (BCF) and bioaccumulation factor (BAF) assessments for organic chemicals in aquatic organisms. Environ Rev. 2006;14(4):257–97.
29. Arini A, Baudrimont M, Feurtet-Mazel A, Coynel A, Blanc G, Coste M, et al. Comparison of periphytic biofilm and filter-feeding bivalve metal bioaccumulation (Cd and Zn) to monitor hydrosystem restoration after industrial remediation: A year of biomonitoring. J Environ Monit. 2011;13(12):3386–98.
30. Jang A, Kim SM, Kim SY, Lee SG, Kim IS. Effects of heavy metals (Cu, Pb, and Ni) on the compositions of EPS in biofilms. Water Sci Technol. 2001;43(6):41–8.
31. Karlsson S, Meili M, Bergström U. Bioaccumulation factors in aquatic ecosystems: A critical review [Internet]. 2002 [cited 2022 Oct 18]. Available from: https://www.osti.gov/etdeweb/servlets/purl/20293388
32. Doucette WJ, Shunthirasingham C, Dettenmaier EM, Zaleski RT, Fantke P, Arnot JA. A review of measured bioaccumulation data on terrestrial plants for organic

chemicals: Metrics, variability, and the need for standardized measurement protocols. Environ Toxicol Chem. 2018;37(1):21–33.

33. Verma M. Ecotoxicology of Heavy Metals: Sources, Effects and Toxicity. In: Bioremediation and Biotechnology, Vol 2. Cham, Switzerland: Springer; 2020. p. 13–23.
34. U. S Environment Protection Agency. Method 3051A: Microwave assisted acid digestion of sediments, sludges, soils, and oils [Internet]. Test Methods for Evaluating Solid Waste,. 2007 [cited 2021 Feb 12]. Available from: http://www.epa.gov/osw/hazard/testmethods/sw846/pdfs/3051a.pdf
35. Bioprocess Control. AMPTS II -An evolution in methane potential analysis [Internet]. 2014 [cited 2020 Sep 15]. Available from: http://www.bioprocesscontrol.com/products/ampts/overview.aspx
36. Motte JC, Escudié R, Beaufils N, Steyer JP, Bernet N, Delgenès JP, et al. Morphological structures of wheat straw strongly impacts its anaerobic digestion. Ind Crops Prod. 2014 Jan;52:695–701.
37. Riggio S, Torrijos M, Debord R, Esposito G, van Hullebusch ED, Steyer JP, et al. Mesophilic anaerobic digestion of several types of spent livestock bedding in a batch leach-bed reactor: substrate characterization and process performance. Waste Manag. 2017 Jan 1;59:129–39.
38. Vogl RA, Henry RN. Characteristics and contaminants of the Salton Sea sediments. Hydrobiologia. 2002;473:47–54.
39. Orlando JL, Smalling KL, Kuivila KM. Pesticides in water and suspended sediments of the Alamo and New Rivers, Imperial Valley/Salton Sea Basin, California, 2006-2007 [Internet]. U.S. Geological Survey Data Series. 2008 [cited 2021 Feb 18]. Available from: https://pubs.usgs.gov/ds/365/
40. Charriau A, Lesven L, Gao Y, Leermakers M, Baeyens W, Ouddane B, et al. Trace metal behaviour in riverine sediments: Role of organic matter and sulfides. Appl Geochemistry. 2011;26(1):80–90.
41. Tien CJ, Chen CS. Patterns of metal accumulation by natural river biofilms during their growth and seasonal succession. Arch Environ Contam Toxicol. 2013;64(4):605–16.
42. de Deckere E, de Cooman W, Leloup V, Meire P, Schmitt C, von der Ohe PC. Development of sediment quality guidelines for freshwater ecosystems. J Soils Sediments. 2011;11(3):504–17.
43. Long ER, MacDonald DD. Recommended uses of empirically derived, sediment quality guidelines for marine and estuarine ecosystems. Hum Ecol Risk Assess. 1998;4(5):1019–39.

44. Burton GA. Sediment quality criteria in use around the world. Limnology. 2002;3(2):65–75.
45. Xu EG, Bui C, Lamerdin C, Schlenk D. Spatial and temporal assessment of environmental contaminants in water, sediments and fish of the Salton Sea and its two primary tributaries, California, USA, from 2002 to 2012. Sci Total Environ. 2016;559:130–40.
46. Cohn JP. Saving the Salton Sea: Researchers work to understand its poblems and provide possible solutions. Bioscience. 2000 Apr 1;50(4):295–301.
47. Cohen MJ, Hyun KH. Hazard : the future of the Salton Sea with no restoration project [Internet]. Oakland, USA; 2006. Available from: https://pacinst.org/publication/restoration-project-critical-to-salton-seas-future/
48. Kangas P, Mulbry W. Nutrient removal from agricultural drainage water using algal turf scrubbers and solar power. Bioresour Technol. 2014 Jan 1;152:484–9.
49. Mulbry W, Kangas P, Kondrad S. Toward scrubbing the bay: Nutrient removal using small algal turf scrubbers on Chesapeake Bay tributaries. Ecol Eng. 2010 Apr 1;36(4):536–41.
50. Aston JE, Wahlen BD, Davis RW, Siccardi AJ, Wendt LM. Application of aqueous alkaline extraction to remove ash from algae harvested from an algal turf scrubber. Algal Res. 2018 Nov 1;35:370–7.
51. Schindler DW, Hecky RE, Findlay DL, Stainton MP, Parker BR, Paterson MJ, et al. Eutrophication of lakes cannot be controlled by reducing nitrogen input: Results of a 37-year whole-ecosystem experiment. In: Proceedings of the National Academy of Sciences of the United States of America. National Academy of Sciences; 2008. p. 11254–8.
52. Nirmalakhandan N, Selvaratnam T, Henkanatte-Gedera SM, Tchinda D, Abeysiriwardana-Arachchige ISA, Delanka-Pedige HMK, et al. Algal wastewater treatment: Photoautotrophic vs. mixotrophic processes. Algal Res. 2019;41.
53. Henkanatte-Gedera SM, Selvaratnam T, Caskan N, Nirmalakhandan N, Van Voorhies W, Lammers PJ. Algal-based, single-step treatment of urban wastewaters. Bioresour Technol. 2015 Aug 1;189:273–8.
54. McGriff EC, McKinney RE. The removal of nutrients and organics by activated algae. Water Res. 1972 Oct 1;6(10):1155–64.
55. D'Aiuto PE, Patt JM, Albano JP, Shatters RG, Evens TJ. Algal turf scrubbers: Periphyton production and nutrient recovery on a South Florida citrus farm. Ecol Eng. 2015 Feb 1;75:404–12.

56. Apel AC, Pfaffinger CE, Basedahl N, Mittwollen N, Göbel J, Sauter J, et al. Open thin-layer cascade reactors for saline microalgae production evaluated in a physically simulated Mediterranean summer climate. Algal Res. 2017 Jul 1;25:381–90.
57. Conley DJ, Paerl HW, Howarth RW, Boesch DF, Seitzinger SP, Havens KE, et al. Ecology - Controlling eutrophication: Nitrogen and phosphorus. Science. 2009;323(5917):1014–5.
58. Zimmo OR, Al Sa'ed R, Gijzen H. Comparison between algae-based and duckweed-based wastewater treatment: Differences in environmental conditions and nitrogen transformations. Water Sci Technol. 2000;42(10–11):215–22.
59. Hamilton SJ. Review of selenium toxicity in the aquatic food chain. Sci Total Environ. 2004;326(1–3):1–31.
60. Sekabira K, Origa HO, Basamba TA, Mutumba G, Kakudidi E. Application of algae in biomonitoring and phytoextraction of heavy metals contamination in urban stream water. Int J Environ Sci Technol. 2011;8(1):115–28.
61. Bradac P, Navarro E, Odzak N, Behra R, Sigg L. Kinetics of cadmium accumulation in periphyton under freshwater conditions. Environ Toxicol Chem. 2009;28(10):2108–16.
62. Wang M, Zhang D, Dong J, Tan SK. Application of constructed wetlands for treating agricultural runoff and agro-industrial wastewater: a review. Hydrobiologia. 2018 Jan 1;805(1):1–31.
63. Saiki MK, Martin BA, May TW. Selenium in aquatic biota inhabiting agricultural drains in the Salton Sea Basin, California. Environ Monit Assess. 2012 Sep;184(9):5623–40.